

**THE FATE OF ANTIBIOTIC RESISTANCE GENES DURING
TREATMENT AND DISPOSAL OF RESIDUAL MUNICIPAL
WASTEWATER SOLIDS**

A DISSERTATION SUBMITTED TO THE FACULTY OF THE UNIVERSITY OF
MINNESOTA BY

TUCKER RAMSEY BURCH

IN PARTIAL FULFILLMENT OF THE REQUIREMENTS FOR THE DEGREE OF
DOCTOR OF PHILOSOPHY

Timothy M. LaPara, Advisor

December 2013

© Tucker R. Burch 2013

Acknowledgements

This work would not have been possible without the contributions of many individuals who provided me with their time, energy, and thoughts.

I must thank my committee members, all of whom have provided valuable insight and suggestions that have improved the overall quality of my thesis. I must also thank the numerous fellow graduate students and other colleagues that have attended classes, shared offices, and shared lab space with me. Among these, Patrick McNamara (now at Marquette University, Milwaukee, WI) deserves special mention. He has always had great questions that forced me to confront my own thinking regarding my research, and he was also a frequent voice of reason that helped keep me on the straight and narrow when I became frustrated with my work.

My advisor, Tim LaPara, has both challenged and supported me. He has always been personally invested in my success, and he has been a unique and irreplaceable influence on my professional development. Tim taught me two valuable lessons: 1) always spend time with my family and 2) do everything in triplicate.

My mom and dad have supported me in all ways imaginable, and I appreciate all the hard work they have put into placing me in a position to succeed.

Finally, I must thank my lovely wife, Jennifer. Her love, patience, and grace have seemed inexhaustible for the nearly 10 years that I have known her. Recently, she has put up with some very long nights and me neglecting to shave for most of the month of November. She has also shouted timely and much appreciated updates on football games from the other room while I have been writing.

This work was supported by National Science Foundation Award 0967176, a University of Minnesota Sommerfeld Fellowship, and the Minnesota Environment and Natural Resources Trust Fund.

Dedication

This work is dedicated to great teachers and mentors. Tom Zimmerman (Columbus Catholic High School, Marshfield, WI) taught me to appreciate details and solve problems. John Katers (University of Wisconsin – Green Bay, Green Bay, WI) inspired me to solve environmental problems, gave me my first job in research, and told me I should be an engineer. Daniel Zitomer (Marquette University, Milwaukee, WI) gave me my second job in research and seemed to be a great example of someone who thoroughly enjoyed what he did for a living. The opportunity he provided me heavily influenced my decision to pursue graduate education. Finally, Tim LaPara has been completely candid with me from the first time we spoke. The fact that I can ask him any question, no matter how stupid it sounds in my head beforehand, has been a defining feature of our relationship. Without these individuals, I would probably be handling manure instead of sewage for a living, and I would be far less qualified to do so.

It is also dedicated to my family, for their inexhaustible patience and support and the countless ways in which they have shaped my life: Mom, Dad, Grandma and Grandpa Mallo, Grandma and Grandpa Burch, and my lovely wife Jennifer. Without these people, I simply would not be me.

Abstract

The development of resistance to antibiotics among pathogens is a global public health dilemma with significant consequences for the length and quality of human life. As a result, the bacterial antibiotic resistance genes (ARGs) that confer resistance are increasingly regarded as environmental contaminants. A significant body of knowledge has been generated that catalogues the occurrence of ARGs in numerous environmental reservoirs, among which residual municipal wastewater solids are one of the largest. Only a handful of studies, however, make the critical paradigm shift to considering treatment technologies and management strategies intended to reduce the quantities of ARGs in those reservoirs. The objective of the work presented here was to evaluate various treatment technologies and management strategies for reducing the quantity of ARGs discharged from the municipal wastewater treatment process during treatment and disposal of residual solids. Aerobic digestion, air drying, and hyperthermophilic ($\geq 60^{\circ}\text{C}$) anaerobic digestion were evaluated for their abilities to reduce ARG quantities in residual municipal wastewater solids using laboratory-scale treatment units. The technologies were compared among each other and to mesophilic (40°C) and thermophilic (56°C) anaerobic digestion on the basis of the kinetics of ARG removal from residual solids. While all technologies were effective, hyperthermophilic anaerobic digestion tended to exhibit the fastest kinetics. In addition, class 1 integrons were identified as a candidate design gene, and batch or semi-batch flow configurations were demonstrated to be a potential means of optimizing the removal of ARGs from residual solids during aerobic digestion, thermophilic anaerobic digestion, and hyperthermophilic

anaerobic digestion. The fate of ARGs in soil following simulated disposal was also investigated by applying treated residual solids from full-scale treatment facilities and from numerous laboratory-scale treatment units to soil microcosms. ARGs from residual solids treated at typical full-scale treatment facilities persisted in soil at high concentrations for relatively long periods of time, with half-lives on the order of months. Alkali stabilization, thermophilic anaerobic digestion, hyperthermophilic anaerobic digestion, and pasteurization, however, caused drastic decreases in ARG quantities in soil within one month. The results presented here can be used to optimize and design the residual municipal wastewater solids treatment and disposal process to remove ARGs.

Table of Contents

Acknowledgements	i
Dedication	iii
Abstract	iv
Table of Contents	vi
List of Tables	viii
List of Figures	xii
Chapter 1: Introduction	1
Chapter 2: The Role of Municipal Wastewater Treatment in Mitigating the Spread of Antibiotic Resistance	5
2.1 Antibiotics	5
2.2 Antibiotic Resistance.....	14
2.3 Antibiotic Resistance Genes as Environmental Contaminants	26
2.4 Treatment of Residual Municipal Wastewater Solids as an Opportunity to Mitigate the Spread of Antibiotic Resistance.....	30
Chapter 3: Aerobic Digestion Reduces the Quantity of Antibiotic Resistance Genes in Residual Municipal Wastewater Solids	34
3.1 Introduction	36
3.2 Materials and Methods	38
3.3 Results	42
3.4 Discussion	54
Chapter 4: Air-Drying Beds Reduce the Quantities of Antibiotic Resistance Genes and Class 1 Integrons in Residual Municipal Wastewater Solids	58
4.1 Introduction	60
4.2 Materials and Methods	62
4.3 Results	66
4.4 Discussion	83

Chapter 5: The Kinetics of Declining Antibiotic Resistance Gene and Class 1 Integron Quantities During Hyperthermophilic Anaerobic Digestion of Residual Municipal Wastewater Solids.....	87
5.1 Introduction	89
5.2 Materials and Methods	92
5.3 Results	98
5.4 Discussion	136
Chapter 6: The Fate of Antibiotic Resistance Genes and Class 1 Integrons in Soil Microcosms Following the Application of Treated Residual Municipal Wastewater Solids from Full-Scale Treatment Facilities	142
6.1 Introduction	144
6.2 Materials and Methods	146
6.3 Results	150
6.4 Discussion	177
Chapter 7: Effects of Several Processes to Significantly Reduce Pathogens and Processes to Further Reduce Pathogens on the Fate of Antibiotic Resistance Genes and Class 1 Integrons in Soil Microcosms Following the Application of Treated Residual Municipal Wastewater Solids.....	182
7.1 Introduction	184
7.2 Materials and Methods	186
7.3 Results	189
7.4 Discussion	216
Chapter 8: Conclusions and Recommendations	220
Bibliography	225
Appendix A: Supporting Information for Chapter 3.....	247
Appendix B: Supporting Information for Chapter 4.....	253
Appendix C: Supporting Information for Chapter 5.....	256
Appendix D: Supporting Information for Chapter 6.....	315
Appendix E: Supporting Information for Chapter 7	330

List of Tables

Table 2.1. A timeline detailing the development and/or discovery of important antibiotic compounds. Data are compiled from Reference 34 and references noted in right-most column.....	10
Table 2.2. Median minimum inhibitory concentrations (MIC) of major antibiotic classes for a model gram-negative microorganism (<i>Escherichia coli</i>) and a model gram-positive microorganism (<i>Staphylococcus aureus</i>).	16
Table 2.3. A timeline outlining the development of antibiotic resistance. Data are adapted and compiled from References 61 and 65. Microorganisms were not identified for Reference 61.....	23
Table 3.1. Operating variables during operation in semi-continuous-flow mode.	43
Table 3.2. Summary of first-order degradation kinetic model parameter estimates for the 16S rRNA gene, fecal indicator bacteria as measured by 16S rRNA genes of all <i>Bacteroides</i> spp., fecal indicator bacteria as measured by 16S rRNA genes of human-specific <i>Bacteroides</i> spp., <i>erm</i> (B), <i>intI1</i> , <i>sulI</i> , <i>tet</i> (A), <i>tet</i> (W), and <i>tet</i> (X) during batch mode operation. All rates were regressed from 10 data points (except human-specific <i>Bacteroides</i> spp., $n = 6$) and are statistically significant ($P < 0.05$).	53
Table 4.1. First-order kinetic coefficients (k) ^a , half-lives ($t_{1/2}$), r^2 , and lack-of-fit P from monophasic first-order kinetic models of gene target concentrations in 3 replicate drying beds.	75
Table 4.2. First-order kinetic coefficients (k) ^a , half-lives ($t_{1/2}$), r^2 , P , and lack-of-fit P from biphasic first-order kinetic models of gene target concentrations in 3 replicate drying beds.....	77
Table 4.3. First-order kinetic coefficients (k) ^a , half-lives ($t_{1/2}$), r^2 , P , and lack-of-fit P from biphasic first-order kinetic models of gene target to 16S rRNA gene ratios in 3 replicate drying beds.	81
Table 5.1. Fitted values of k and calculated half-lives ($t_{1/2}$) from an ordinary least squares fit of the first-order kinetic model to each time series of gene target quantities or ratios of gene target quantities to 16S rRNA genes. Error terms represent the standard error of the mean.....	122

Table 5.2. Fitted values of k and b from an ordinary least squares fit of the modified Collins-Selleck kinetic model to each time series of gene target quantities or ratios of gene target quantities to 16S rRNA genes. Error terms represent the standard error of the mean.	129
Table 6.1. Net evaporation rates and the total mass of water lost to evaporation (expressed as the fraction of the initial mass of soil and residual solids present in each microcosm) for sets of three replicate microcosms at all loading rates for each experiment. Error terms represent the standard error of the mean.	151
Table 6.2. The quantities of all gene targets in both residual solids sources. Values are the arithmetic mean of triplicate samples; error terms represent one standard deviation.	152
Table 6.3. The number of data points with quantifiable values (n) and quantities for AllBac, HF183, ARGs, and <i>intI1</i> in triplicate experimental negative control microcosms for both experiments. Values are the arithmetic mean of n data points; error terms represent one standard deviation.	154
Table 6.4. First-order kinetic coefficients (k), P , number of data points (n), lack-of-fit P (LOF P), r^2 , and half-lives ($t_{1/2}$) from first-order kinetic models of gene target quantities in three replicate soil microcosms at all loading rates (LR, g treated residual municipal wastewater solids kg^{-1} soil) for both experiments.	164
Table 6.5. First-order kinetic coefficients (k), P , number of data points (n), lack-of-fit P (LOF P), r^2 , and half-lives ($t_{1/2}$) from first-order kinetic models of ratios of ARGs and <i>intI1</i> to 16S rRNA genes in three replicate soil microcosms at all loading rates (LR, g treated residual municipal wastewater solids kg^{-1} soil) for both experiments.	170
Table A.1. Gene targets, resistance mechanisms, primer sequences, amplicon sizes, and annealing temperatures for real-time PCR assays.	247
Table A.2. Values of P for comparing the relative statistical significance of different kinetic coefficients determined using Welch's t-test for unequal n and unequal sample variance.	251
Table B.1. The primer sequences, expected amplicon size, and annealing temperature for each gene target considered in this work.	253
Table C.1. The primer sequences, expected amplicon size, and annealing temperature for each real-time PCR method used in this work.	256

Table C.2. The number of standards (n), slope, intercept, amplification efficiency determined from a dilution series of standards, r^2 , and quantification limit (QL, copies μL^{-1} template) for each real-time PCR assay conducted to generate the data presented in this work.....	258
Table C.3. The number of data points (n), r^2 , analysis of variance (ANOVA) P , lack-of-fit (LOF) P , and non-constant variance (NCV) P for an ordinary least squares fit of the first-order kinetic model to each time series of gene target quantities or ratios of gene target quantities to 16S rRNA gene quantities.....	287
Table C.4. The number of data points (n), r^2 , analysis of variance (ANOVA) P , lack-of-fit (LOF) P , and non-constant variance (NCV) P for an ordinary least squares fit of the second-order kinetic model to each time series of gene target quantities or ratios of gene target quantities to 16S rRNA gene quantities.....	294
Table C.5. The number of data points (n), r^2 , analysis of variance (ANOVA) P , lack-of-fit (LOF) P , and non-constant variance (NCV) P for an ordinary least squares fit of the modified Collins-Selleck kinetic model to each time series of gene target quantities or ratios of gene target quantities to 16S rRNA gene quantities.....	301
Table C.6. Fitted values of k and calculated initial half-lives ($t_{1/2}$) from an ordinary least squares fit of the second-order kinetic model to each time series of gene target quantities or ratios of gene target quantities to 16S rRNA genes. Error terms represent the standard error of the mean.	308
Table D.1. The primer sequences, expected amplicon size, and annealing temperature for each real-time PCR method used in this work.....	315
Table D.2. The number of standards (n), slope, intercept, amplification efficiency determined from a dilution series of standards, r^2 , and quantification limit (QL, copies μL^{-1} template) for each real-time PCR assay conducted to generate the data presented in this work.....	318
Table E.1. The temperatures, hydraulic residence times (HRT), total solids (TS) destruction, volatile solids (VS) destruction, gas methane content, and dissolved oxygen (DO) concentrations in an aerobic digester and anaerobic digesters operated at four temperatures during the 70 days prior to sampling for residual solids. Values are arithmetic means; error terms represent one standard deviation.	330
Table E.2. The number of standards (n), slope, intercept, amplification efficiency determined from a dilution series of standards, r^2 , and quantification limit (QL, copies	

μL^{-1} template) for each real-time PCR assay conducted to generate the data presented in this work. Assays for “Soil Microcosms A1-A3” are also listed in Table D.2..... 333

Table E.3. The quantities of 16S rRNA genes, *intII*, and *sulI* in soil used to initiate microcosms that received aerobically digested, air-dried, anaerobically digested, or untreated residual solids (10/27/11) vs. alkali stabilized or pasteurized residual solids (12/1/11). Values are the arithmetic mean of at least five of nine positive samples (for 10/27/11) or two of three positive samples (for 12/1/11); error terms represent one standard deviation. All other gene targets were below quantification limits in at least six of nine samples (for 10/27/11) or in all three samples (for 12/1/11). 340

Table E.4. First-order kinetic coefficients (k), P , r^2 , and half-lives ($t_{1/2}$) from first-order kinetic models of gene target quantities in residual municipal wastewater solids undergoing pasteurization or alkali stabilization. Error terms for k represent one standard error; all values of k were regressed from eight data points. 341

Table E.5. Evaporation rates and cumulative evaporation in all sets of soil microcosms. Error terms for evaporation rates represent one standard error. Error terms for fraction of initial microcosm mass lost to evaporation and final moisture content represent one standard deviation. 343

Table E.6. First-order kinetic coefficients (k), number of data points (n), r^2 , P , lack-of-fit P (LOF P), and half-lives ($t_{1/2}$) from first-order kinetic models applied to full time series of gene target quantities in triplicate soil microcosms that received different residual municipal wastewater solids. Error terms for k represent the standard error of the mean. 346

Table E.7. First-order kinetic coefficients (k), number of data points (n), r^2 , P , lack-of-fit P (LOF P), and half-lives ($t_{1/2}$) from first-order kinetic models applied to time series of gene target quantities with time zero values removed in triplicate soil microcosms that received different residual municipal wastewater solids. Error terms for k represent the standard error of the mean. 354

List of Figures

Figure 3.1. The quantities of: (A) 16S rRNA genes and (B) fecal indicator bacteria as measured by 16S rRNA genes of all <i>Bacteroides</i> spp. in untreated (closed circles) and treated (open circles) residual solids. Values are the arithmetic mean of triplicate samples; error bars represent one standard deviation. The concentrations of human-specific <i>Bacteroides</i> spp. were approximately 5×10^8 gene copies mL^{-1} in untreated samples, but were below the detection limit (1×10^8 gene copies mL^{-1}) in treated samples.	45
Figure 3.2. The quantities of: (A) <i>erm</i> (B), (B) <i>sulI</i> , (C) <i>tet</i> (A), and (D) <i>tet</i> (W) in untreated (closed circles) and treated (open circles) residual solids. Values are the arithmetic mean of triplicate samples; error bars represent one standard deviation.	47
Figure 3.3. The quantities of: (A) <i>intI1</i> and (B) <i>tet</i> (X) in untreated (closed circles) and treated (open circles) residual solids. Values are the arithmetic mean of triplicate samples; error bars represent one standard deviation.	48
Figure 3.4. The quantities of: (A) 16S rRNA genes, (B) fecal indicator bacteria as measured by 16S rRNA genes of all <i>Bacteroides</i> spp., and (C) fecal indicator bacteria as measured by 16S rRNA genes of human-specific <i>Bacteroides</i> spp. in residual solids undergoing batch treatment. Values are the arithmetic mean of triplicate samples; error bars represent one standard deviation.	50
Figure 3.5. The quantities of: (A) <i>erm</i> (B), (B) <i>intI1</i> , (C) <i>sulI</i> , (D) <i>tet</i> (A), (E) <i>tet</i> (W), and (F) <i>tet</i> (X) in residual solids undergoing batch treatment. Values are the arithmetic mean of triplicate samples; error bars represent one standard deviation.	52
Figure 4.1. The (A) moisture content in three replicate drying beds (closed circles, open circles, and closed triangles represent unique experimental replicates), (B) daily precipitation, and (C) daily maximum (closed circles) and minimum (open circles) temperatures. Values for moisture content are the arithmetic mean of triplicate samples; error bars represent one standard deviation.	67
Figure 4.2. The quantities of (A) 16S rRNA genes, (B) fecal indicator bacteria as measured by 16S rRNA genes of all <i>Bacteroides</i> spp. (AllBac), and (C) fecal indicator bacteria as measured by 16S rRNA genes of human-specific <i>Bacteroides</i> spp. (HF183) in residual solids applied to three replicate drying beds (closed circles, open circles, and closed triangles represent unique experimental replicates). Values are the arithmetic mean of triplicate samples; error bars represent one standard deviation.	69

Figure 4.3. The quantities of <i>intII</i> , <i>sulI</i> , <i>erm(B)</i> , <i>tet(A)</i> , <i>tet(W)</i> , and <i>tet(X)</i> in residual solids applied to three replicate drying beds (closed circles, open circles, and closed triangles represent unique experimental replicates). Values are the arithmetic mean of triplicate samples; error bars represent one standard deviation.	71
Figure 4.4. The ratios of <i>intII</i> , <i>sulI</i> , <i>erm(B)</i> , <i>tet(A)</i> , <i>tet(W)</i> , and <i>tet(X)</i> to the 16S rRNA gene in residual solids applied to three replicate drying beds (closed circles, open circles, and closed triangles represent unique experimental replicates). Values are the arithmetic mean of triplicate samples; error bars represent one standard deviation.	73
Figure 5.1. The temperatures of anaerobic digesters operated at nominal temperatures of 40°C, 56°C, 60°C, and 63°C. Dashed lines represent the mean temperature for each digester. These values were 39.9°C ± 3.4°C, 55.7°C ± 2.2°C, 60.3°C ± 2.3°C, and 63.4°C ± 2.9°C (mean ± standard deviation).	100
Figure 5.2. The mean hydraulic residence time (HRT) for each of four anaerobic digesters operated at nominal temperatures of 40°C, 56°C, 60°C, and 63°C. Dashed lines represent the mean value of HRT at the end of batches. These values were 35.7 ± 1.2, 32.5 ± 0.8, 35.0 ± 0.8, and 33.0 ± 0.7 days (mean ± standard deviation), respectively..	101
Figure 5.3. The volatile solids content of untreated residual municipal wastewater solids and four anaerobic digesters operated at nominal temperatures of 40°C, 56°C, 60°C, and 63°C. Values are the arithmetic mean of triplicate samples; error bars represent one standard deviation.	102
Figure 5.4. The methane content of gas produced by anaerobic digesters operated at nominal temperatures of 40°C, 56°C, 60°C, and 63°C. Values are the arithmetic mean of three or more samples; error bars represent one standard deviation.	103
Figure 5.5. Quantities of 16S rRNA genes, <i>AllBac</i> , and methanogen 16S rRNA genes in untreated residual municipal wastewater solids. Values are the arithmetic mean of triplicate samples; error bars represent one standard deviation.	105
Figure 5.6. Quantities of ARGs, <i>intII</i> , and <i>repA</i> in untreated residual municipal wastewater solids. Values are the arithmetic mean of duplicate or triplicate samples; error bars represent one standard deviation.	106
Figure 5.7. Quantities of 16S rRNA genes during the final three batches (green, orange, and red symbols represent unique batches) in anaerobic digesters operated at nominal temperatures of 40°C, 56°C, 60°C, and 63°C. Values are the arithmetic mean of triplicate samples; error bars represent one standard deviation.	108

Figure 5.8. Quantities of AllBac during the final three batches (green, orange, and red symbols represent unique batches) in anaerobic digesters operated at nominal temperatures of 40°C, 56°C, 60°C, and 63°C. Values are the arithmetic mean of triplicate samples; error bars represent one standard deviation.	110
Figure 5.9. Quantities of methanogen 16S rRNA genes during the final three batches (green, orange, and red symbols represent unique batches) in anaerobic digesters operated at nominal temperatures of 40°C, 56°C, 60°C, and 63°C. Values are the arithmetic mean of triplicate samples; error bars represent one standard deviation.	112
Figure 5.10. Quantities of <i>intII</i> during the final three batches (green, orange, and red symbols represent unique batches) in anaerobic digesters operated at nominal temperatures of 40°C, 56°C, 60°C, and 63°C. Values are the arithmetic mean of triplicate samples; error bars represent one standard deviation.	115
Figure 5.11. Quantities of <i>qnrA</i> during the final three batches (green, orange, and red symbols represent unique batches) in anaerobic digesters operated at nominal temperatures of 40°C, 56°C, 60°C, and 63°C. Values are the arithmetic mean of duplicate or triplicate samples; error bars represent one standard deviation. Dashed lines represent the limit of quantification for data sets that contain one or more experimental observations below that limit.	116
Figure 5.12. Quantities of <i>repA</i> during the final three batches (green, orange, and red symbols represent unique batches) in anaerobic digesters operated at nominal temperatures of 40°C, 56°C, 60°C, and 63°C. Values are the arithmetic mean of duplicate or triplicate samples; error bars represent one standard deviation. Dashed lines represent the limit of quantification for data sets that contain one or more experimental observations below that limit.	117
Figure 5.13. Quantities of <i>tet(W)</i> during the final three batches (green, orange, and red symbols represent unique batches) in anaerobic digesters operated at nominal temperatures of 40°C, 56°C, 60°C, and 63°C. Values are the arithmetic mean of triplicate samples; error bars represent one standard deviation.	118
Figure 5.14. Quantities of <i>tet(X)</i> during the final three batches (green, orange, and red symbols represent unique batches) in anaerobic digesters operated at nominal temperatures of 40°C, 56°C, 60°C, and 63°C. Values are the arithmetic mean of duplicate or triplicate samples; error bars represent one standard deviation. Dashed lines represent the limit of quantification for data sets that contain one or more experimental observations below that limit.	119

Figure 6.1. The quantities of 16S rRNA genes in three replicate soil microcosms (closed circles, open circles, and closed triangles represent unique experimental units) at all loading rates for both experiments. Values are the arithmetic mean of duplicate or triplicate samples; error bars represent one standard deviation. 156

Figure 6.2. The quantities of 16S rRNA genes of all *Bacteroides* spp. in three replicate soil microcosms (closed circles, open circles, and closed triangles represent unique experimental units) at loading rates of 20, 40, and 100 g residual solids kg⁻¹ soil for Experiment 1 and 40 g residual solids kg⁻¹ soil for Experiment 2. Values are the arithmetic mean of duplicate or triplicate samples; error bars represent one standard deviation..... 158

Figure 6.3. The quantities of ARGs and *intI1* in three replicate soil microcosms (closed circles, open circles, and closed triangles represent unique experimental units) at a loading rate of 40 g residual solids kg⁻¹ soil for Experiment 1. Values are the arithmetic mean of duplicate or triplicate samples; error bars represent one standard deviation. ... 160

Figure 6.4. The quantities of ARGs and *intI1* in three replicate soil microcosms (closed circles, open circles, and closed triangles represent unique experimental units) at a loading rate of 40 g residual solids kg⁻¹ soil for Experiment 2. Values are the arithmetic mean of duplicate or triplicate samples; error bars represent one standard deviation. ... 162

Figure 6.5. The kinetic coefficients for (A) quantities of ARGs and *intI1* and (B) ratios of ARGs and *intI1* to the 16S rRNA gene from Experiment 1 as a function of loading rate. Values are from Table 6.4 and Table 6.5; error bars represent the standard error of the mean. Values of “0” have been substituted for kinetic coefficients with *P* > 0.05. Connecting lines are intended as visual aids only. 176

Figure 7.1. The quantities of 16S rRNA genes, AllBac, and HF183 in source residual solids. Values are the arithmetic mean of duplicate or triplicate samples; error bars represent one standard deviation. Quantities of all gene targets were measured prior to centrifugation in alkali stabilized and pasteurized residual solids; they were measured following centrifugation (or centrifugation was not required) in all other residual solids sources. Quantities of HF183 are not shown for residual solids sources where they were below quantification limits (see Table E.2). 191

Figure 7.2. The quantities of ARGs and *intI1* in source residual solids. Values are the arithmetic mean of duplicate or triplicate samples; error bars represent one standard deviation. Quantities of all gene targets were measured prior to centrifugation in alkali stabilized and pasteurized residual solids; they were measured following centrifugation

(or centrifugation was not required) in all other residual solids sources. Quantities of *qnrA* are not shown for residual solids sources where they were below quantification limits (see Table E.2). 192

Figure 7.3. Quantities of 16S rRNA genes and AllBac in soil microcosms that received aerobically digested residual solids. Values are the arithmetic mean of duplicate or triplicate samples; error bars represent one standard deviation. 195

Figure 7.4. Quantities of 16S rRNA genes and AllBac in soil microcosms that received air-dried residual solids. Values are the arithmetic mean of triplicate samples; error bars represent one standard deviation. Dashed lines represent the maximum and minimum limits of quantification for data sets that contain one or more experimental observations below those limits. 196

Figure 7.5. Quantities of 16S rRNA genes and AllBac in soil microcosms that received alkali stabilized residual solids. Values are the arithmetic mean of duplicate or triplicate samples; error bars represent one standard deviation. 197

Figure 7.6. Quantities of 16S rRNA genes and AllBac in soil microcosms that received anaerobically digested (38°C) residual solids. Values are the arithmetic mean of triplicate samples; error bars represent one standard deviation. 198

Figure 7.7. Quantities of 16S rRNA genes and AllBac in soil microcosms that received anaerobically digested (55°C) residual solids. Values are the arithmetic mean of duplicate or triplicate samples; error bars represent one standard deviation. 199

Figure 7.8. Quantities of 16S rRNA genes and AllBac in soil microcosms that received anaerobically digested (62°C) residual solids. Values are the arithmetic mean of duplicate or triplicate samples; error bars represent one standard deviation. Dashed lines represent the maximum and minimum limits of quantification for data sets that contain one or more experimental observations below those limits. 200

Figure 7.9. Quantities of 16S rRNA genes and AllBac in soil microcosms that received anaerobically digested (69°C) residual solids. Values are the arithmetic mean of duplicate or triplicate samples; error bars represent one standard deviation. Dashed lines represent the maximum and minimum limits of quantification for data sets that contain one or more experimental observations below those limits. 201

Figure 7.10. Quantities of 16S rRNA genes and AllBac in soil microcosms that received pasteurized residual solids. Values are the arithmetic mean of triplicate samples; error bars represent one standard deviation. Dashed lines represent the maximum and

minimum limits of quantification for data sets that contain one or more experimental observations below those limits. 202

Figure 7.11. Quantities of 16S rRNA genes, AllBac, and HF183 in soil microcosms that received untreated residual solids. Values are the arithmetic mean of duplicate or triplicate samples; error bars represent one standard deviation. Dashed lines represent the maximum and minimum limits of quantification for data sets that contain one or more experimental observations below those limits. 203

Figure 7.12. Quantities of ARGs and *intI1* in soil microcosms that received air-dried residual solids. Values are the arithmetic mean of duplicate or triplicate samples; error bars represent one standard deviation. Dashed lines represent the maximum and minimum limits of quantification for data sets that contain one or more experimental observations below those limits. 206

Figure 7.13. Quantities of ARGs and *intI1* in soil microcosms that received anaerobically digested (38°C) residual solids. Values are the arithmetic mean of duplicate or triplicate samples; error bars represent one standard deviation. Dashed lines represent the maximum and minimum limits of quantification for data sets that contain one or more experimental observations below those limits. 207

Figure 7.14. Quantities of ARGs and *intI1* in soil microcosms that received aerobically digested residual solids. Values are the arithmetic mean of triplicate samples; error bars represent one standard deviation. 209

Figure 7.15. Quantities of ARGs and *intI1* in soil microcosms that received alkali stabilized residual solids. Values are the arithmetic mean of duplicate or triplicate samples; error bars represent one standard deviation. Dashed lines represent the maximum and minimum limits of quantification for data sets that contain one or more experimental observations below those limits. 210

Figure 7.16. Quantities of ARGs and *intI1* in soil microcosms that received anaerobically digested (55°C) residual solids. Values are the arithmetic mean of duplicate or triplicate samples; error bars represent one standard deviation. Dashed lines represent the maximum and minimum limits of quantification for data sets that contain one or more experimental observations below those limits. 211

Figure 7.17. Quantities of ARGs and *intI1* in soil microcosms that received anaerobically digested (62°C) residual solids. Values are the arithmetic mean of duplicate or triplicate samples; error bars represent one standard deviation. Dashed lines represent the

maximum and minimum limits of quantification for data sets that contain one or more experimental observations below those limits. 212

Figure 7.18. Quantities of ARGs and *intII* in soil microcosms that received anaerobically digested (69°C) residual solids. Values are the arithmetic mean of duplicate or triplicate samples; error bars represent one standard deviation. Dashed lines represent the maximum and minimum limits of quantification for data sets that contain one or more experimental observations below those limits. 213

Figure 7.19. Quantities of ARGs and *intII* in soil microcosms that received pasteurized residual solids. Values are the arithmetic mean of duplicate or triplicate samples; error bars represent one standard deviation. Dashed lines represent the maximum and minimum limits of quantification for data sets that contain one or more experimental observations below those limits. 214

Figure 7.20. Quantities of ARGs and *intII* in soil microcosms that received untreated residual solids. Values are the arithmetic mean of duplicate or triplicate samples; error bars represent one standard deviation. Dashed lines represent the maximum and minimum limits of quantification for data sets that contain one or more experimental observations below those limits. 215

Figure C.1. The pH of anaerobic digesters operated at nominal temperatures of 40°C, 56°C, 60°C, and 63°C. 262

Figure C.2. The total solids content of untreated residual municipal wastewater solids and four anaerobic digesters operated at nominal temperatures of 40°C, 56°C, 60°C, and 63°C. Values are the arithmetic mean of triplicate samples; error bars represent one standard deviation. 263

Figure C.3. The volume of gas produced during eight-day batch cycles by anaerobic digesters operated at nominal temperatures of 40°C, 56°C, 60°C, and 63°C. 264

Figure C.4. The ratios of AllBac and methanogen 16S rRNA genes to 16S rRNA genes in untreated residual municipal wastewater solids. Values are the arithmetic mean of triplicate samples; error bars represent one standard deviation. 265

Figure C.5. The ratios of ARGs, *intII*, and *repA* to 16S rRNA genes in untreated residual municipal wastewater solids. Values are the arithmetic mean of duplicate or triplicate samples; error bars represent one standard deviation. 266

Figure C.6. Quantities of 16S rRNA genes at the end of each of the first seven batches in anaerobic digesters operated at nominal temperatures of 40°C, 56°C, 60°C, and 63°C. Values are the arithmetic mean of triplicate samples; error bars represent one standard deviation.....	267
Figure C.7. Quantities of AllBac at the end of each of the first seven batches in anaerobic digesters operated at nominal temperatures of 40°C, 56°C, 60°C, and 63°C. Values are the arithmetic mean of triplicate samples; error bars represent one standard deviation.	268
Figure C.8. The ratios of AllBac to 16S rRNA genes at the end of each of the first seven batches in anaerobic digesters operated at nominal temperatures of 40°C, 56°C, 60°C, and 63°C. Values are the arithmetic mean of triplicate samples; error bars represent one standard deviation.	269
Figure C.9. The ratios of AllBac to 16S rRNA genes during the final three batches (green, orange, and red symbols represent unique batches) in anaerobic digesters operated at nominal temperatures of 40°C, 56°C, 60°C, and 63°C. Values are the arithmetic mean of triplicate samples; error bars represent one standard deviation.....	270
Figure C.10. Quantities of methanogen 16S rRNA genes at the end of each of the first seven batches in anaerobic digesters operated at nominal temperatures of 40°C, 56°C, 60°C, and 63°C. Values are the arithmetic mean of triplicate samples; error bars represent one standard deviation.....	271
Figure C.11. The ratios of methanogen 16S rRNA genes to 16S rRNA genes at the end of each of the first seven batches in anaerobic digesters operated at nominal temperatures of 40°C, 56°C, 60°C, and 63°C. Values are the arithmetic mean of triplicate samples; error bars represent one standard deviation.	272
Figure C.12. The ratios of methanogen 16S rRNA genes to 16S rRNA genes during the final three batches (green, orange, and red symbols represent unique batches) in anaerobic digesters operated at nominal temperatures of 40°C, 56°C, 60°C, and 63°C. Values are the arithmetic mean of triplicate samples; error bars represent one standard deviation.....	273
Figure C.13. Quantities of <i>intII</i> at the end of each of the first seven batches in anaerobic digesters operated at nominal temperatures of 40°C, 56°C, 60°C, and 63°C. Values are the arithmetic mean of triplicate samples; error bars represent one standard deviation.	274
Figure C.14. The ratios of <i>intII</i> to 16S rRNA genes at the end of each of the first seven batches in anaerobic digesters operated at nominal temperatures of 40°C, 56°C, 60°C,	

and 63°C. Values are the arithmetic mean of triplicate samples; error bars represent one standard deviation. 275

Figure C.15. The ratios of *intI1* to 16S rRNA genes during the final three batches (green, orange, and red symbols represent unique batches) in anaerobic digesters operated at nominal temperatures of 40°C, 56°C, 60°C, and 63°C. Values are the arithmetic mean of triplicate samples; error bars represent one standard deviation. 276

Figure C.16. Quantities of *qnrA* at the end of each of the first seven batches in anaerobic digesters operated at nominal temperatures of 40°C, 56°C, 60°C, and 63°C. Values are the arithmetic mean of duplicate or triplicate samples; error bars represent one standard deviation. Dashed lines represent the limit of quantification for data sets that contain one or more experimental values below that limit..... 277

Figure C.17. The ratios of *qnrA* to 16S rRNA genes at the end of each of the first seven batches in anaerobic digesters operated at nominal temperatures of 40°C, 56°C, 60°C, and 63°C. Values are the arithmetic mean of duplicate or triplicate samples; error bars represent one standard deviation..... 278

Figure C.18. The ratios of *qnrA* to 16S rRNA genes during the final three batches (green, orange, and red symbols represent unique batches) in anaerobic digesters operated at nominal temperatures of 40°C, 56°C, 60°C, and 63°C. Values are the arithmetic mean of duplicate or triplicate samples; error bars represent one standard deviation..... 279

Figure C.19. The ratios of *repA* to 16S rRNA genes during the final three batches (green, orange, and red symbols represent unique batches) in anaerobic digesters operated at nominal temperatures of 40°C, 56°C, 60°C, and 63°C. Values are the arithmetic mean of duplicate or triplicate samples; error bars represent one standard deviation. 280

Figure C.20. Quantities of *tet(W)* at the end of each of the first seven batches in anaerobic digesters operated at nominal temperatures of 40°C, 56°C, 60°C, and 63°C. Values are the arithmetic mean of triplicate samples; error bars represent one standard deviation..... 281

Figure C.21. The ratios of *tet(W)* to 16S rRNA genes at the end of each of the first seven batches in anaerobic digesters operated at nominal temperatures of 40°C, 56°C, 60°C, and 63°C. Values are the arithmetic mean of triplicate samples; error bars represent one standard deviation. 282

Figure C.22. The ratios of *tet(W)* to 16S rRNA genes during the final three batches (green, orange, and red symbols represent unique batches) in anaerobic digesters operated

at nominal temperatures of 40°C, 56°C, 60°C, and 63°C. Values are the arithmetic mean of triplicate samples; error bars represent one standard deviation..... 283

Figure C.23. Quantities of *tet(X)* at the end of each of the first seven batches in anaerobic digesters operated at nominal temperatures of 40°C, 56°C, 60°C, and 63°C. Values are the arithmetic mean of duplicate or triplicate samples; error bars represent one standard deviation. Dashed lines represent the limit of quantification for data sets that contain one or more experimental values below that limit. 284

Figure C.24. The ratios of *tet(X)* to 16S rRNA genes at the end of each of the first seven batches in anaerobic digesters operated at nominal temperatures of 40°C, 56°C, 60°C, and 63°C. Values are the arithmetic mean of duplicate or triplicate samples; error bars represent one standard deviation..... 285

Figure C.25. The ratios of *tet(X)* to 16S rRNA genes during the final three batches (green, orange, and red symbols represent unique batches) in anaerobic digesters operated at nominal temperatures of 40°C, 56°C, 60°C, and 63°C. Values are the arithmetic mean of duplicate or triplicate samples; error bars represent one standard deviation..... 286

Figure D.1. The quantities of ARGs and *intI1* in three replicate soil microcosms (closed circles, open circles, and closed triangles represent unique experimental units) at a loading rate of 20 g residual solids kg⁻¹ soil for Experiment 1. Values are the arithmetic mean of duplicate or triplicate samples; error bars represent one standard deviation. ... 324

Figure D.2. The quantities of ARGs and *intI1* in three replicate soil microcosms (closed circles, open circles, and closed triangles represent unique experimental units) at a loading rate of 100 g residual solids kg⁻¹ soil for Experiment 1. Values are the arithmetic mean of duplicate or triplicate samples; error bars represent one standard deviation. ... 325

Figure D.3. The ratios of ARGs and *intI1* to 16S rRNA genes in three replicate soil microcosms (closed circles, open circles, and closed triangles represent unique experimental units) at a loading rate of 20 g residual solids kg⁻¹ soil for Experiment 1. Values are the arithmetic mean of duplicate or triplicate samples; error bars represent one standard deviation. 326

Figure D.4. The ratios of ARGs and *intI1* to 16S rRNA genes in three replicate soil microcosms (closed circles, open circles, and closed triangles represent unique experimental units) at a loading rate of 40 g residual solids kg⁻¹ soil for Experiment 1. Values are the arithmetic mean of duplicate or triplicate samples; error bars represent one standard deviation. 327

Figure D.5. The ratios of ARGs and <i>intII</i> to 16S rRNA genes in three replicate soil microcosms (closed circles, open circles, and closed triangles represent unique experimental units) at a loading rate of 100 g residual solids kg ⁻¹ soil for Experiment 1. Values are the arithmetic mean of duplicate or triplicate samples; error bars represent one standard deviation.	328
Figure D.6. The ratios of ARGs and <i>intII</i> to 16S rRNA genes in three replicate soil microcosms (closed circles, open circles, and closed triangles represent unique experimental units) at a loading rate of 40 g residual solids kg ⁻¹ soil for Experiment 2. Values are the arithmetic mean of duplicate or triplicate samples; error bars represent one standard deviation.	329
Figure E.1. The temperature of untreated residual solids undergoing pasteurization and the pH of untreated residual solids undergoing alkali stabilization prior to application to soil microcosms.	332
Figure E.2. The quantities of 16S rRNA genes, <i>intII</i> , and <i>tet(X)</i> in residual solids undergoing pasteurization or alkali stabilization. Values are the arithmetic mean of triplicate samples; error bars represent one standard deviation.	345
Figure E.3. Quantities of <i>qnrA</i> in soil microcosms that received untreated residual solids. Values are the arithmetic mean of duplicate or triplicate samples; error bars represent one standard deviation. Dashed lines represent the maximum and minimum limits of quantification for data sets that contain one or more experimental observations below those limits.	362

Chapter 1: Introduction

Antibiotics are a critical tool for modern medicine. The beginning of the antibiotic age in the mid-20th century marked the beginning of a vast improvement in the medical community's ability to protect human health (1). Diseases once known to be virulent and deadly were rendered common and harmless. However, the development of resistance to antibiotics among pathogens is a serious threat to their sustainable use.

The medical community has undertaken several strategies to circumvent and manage the development of antibiotic resistance, including developing new antibiotics, limiting frivolous antibiotic use, and prescribing cocktails of multiple antibiotics to individual patients. However, resistance is now becoming more difficult to manage with these strategies alone. The rate at which new antibiotics are deployed for public use has slowed considerably since the mid-20th century (2). Furthermore, the rise of multiply resistant pathogens and pathogens resistant to even the most state-of-the-art antibiotics is beginning to stretch the limits of the existing antibiotic arsenal (3,4). It is becoming clear that complimentary strategies for managing the proliferation of antibiotic resistance will be required in the near future.

One such new strategy relies on identifying bacterial antibiotic resistance genes (ARGs) as environmental contaminants (5). ARGs are a convenient focus in this context for two reasons. They can be readily detected and quantified using analytical biochemistry, and they are also the fundamental mechanism by which resistance is conveyed from one microorganism to another and through the natural environment. The ultimate goal of this strategy is to identify environmental reservoirs of ARGs in order to

reduce the quantity of ARGs that they contain. This perspective has, in fact, led to the identification of numerous environmental reservoirs of ARGs, including surface waters, aquaculture facilities, and agricultural waste (5–20). The municipal wastewater treatment process is one of the most significant reservoirs of ARGs (5,10,21–32), and within this process, the residual municipal wastewater solids contain the vast majority of ARGs that are discharged to the environment (27).

While residual municipal wastewater solids have been identified as an important environmental reservoir of ARGs, significant additional work is needed to investigate potential strategies for mitigating the size of this reservoir. That is, further work is needed to assess potential *treatment* and *management* strategies for ARGs in residual municipal wastewater solids. The global hypothesis underlying this work is that *the residual municipal wastewater solids treatment process can be designed to intentionally reduce the quantity of ARGs it discharges to the natural environment*. Designing this process to destroy ARGs would provide an antibiotic resistance management strategy that is complimentary to existing strategies.

Residual municipal wastewater solids are currently treated using an infrastructure that could be optimized and upgraded to reduce the number of ARGs it discharges to the environment. There is currently a critical lack of knowledge related to achieving this goal, however, despite the obvious significance of residual municipal wastewater solids as an environmental reservoir of ARGs. For instance, the degree to which some existing residual solids treatment technologies (e.g. air drying) can remove ARGs from residual municipal wastewater solids has not been assessed. Furthermore, while other

technologies have been investigated (e.g. anaerobic digestion), the degree to which they can continue to be optimized for ARG removal from residual solids is not well understood, and few design criteria related to ARG removal (e.g. kinetic decay coefficients) are available. We also currently lack a rational basis upon which to compare and select among alternative treatment technologies. Finally, the fate of ARGs in treated residual solids following disposal (i.e. land-application) is unknown.

The objective of this work was to address some of these gaps in the existing body of knowledge related to designing the residual municipal wastewater solids treatment and disposal process for ARG removal. The following chapters investigate several technologies that have not previously been considered for their ability to remove ARGs from residual municipal wastewater solids. Two of these technologies, air drying and alkali (i.e. lime) stabilization, are either used at a large number of municipal wastewater treatment plants or are applied to a large fraction of the treated residual solids produced in the United States each year (Chapter 4 and Chapter 7). A third technology (anaerobic digestion at temperatures greater than or equal to 60°C) holds promise based on the observation that increasing temperatures in anaerobic digesters may increase the rate and extent of ARG removal in residual municipal wastewater solids (Chapter 5). This work also presents detailed kinetic analyses of several technologies and residual solids disposal practices that contribute to our ability to select among alternative treatment technologies for removing ARGs from residual solids (Chapter 3, Chapter 4, Chapter 5, Chapter 6, and Chapter 7). Two chapters provide evidence that operating treatment units in batch configurations, rather than as continuous-flow reactors, may improve the removal of

ARGs from residual solids (Chapter 3 and Chapter 5). Two chapters also illustrate selection for ARGs in some treatment technologies based on how their presumed ecological niches relate to the treatment environments (Chapter 3 and Chapter 4). Furthermore, class 1 integrons are identified throughout this work as an early, promising candidate for consideration as a design gene (Chapter 3, Chapter 4, Chapter 5, Chapter 6, and Chapter 7). Finally, this work illustrates the general fate of ARGs in treated residual solids applied to soil (Chapter 6) and presents an initial investigation into how the selection of residual solids treatment technologies in the treatment plant can affect the fate of ARGs following application to soil (Chapter 7).

Chapter 2: The Role of Municipal Wastewater Treatment in Mitigating the Spread of Antibiotic Resistance

2.1 Antibiotics

Antibiotics are widely used and critical tools for protecting human health. First discovered and developed for widespread use between 1929 and 1940 (33,34), our original arsenal of sulphanilamide and penicillin has now grown to include over 90 individual drugs in more than a dozen major classes (35). Between 1940 and 1950, the crude death rate due to infectious disease dropped from approximately 200 deaths per 100,000 persons to about 100 deaths per 100,000 persons (1). A large portion of this decline was due to widespread use of antibiotics, along with improved hygiene and sanitation and the development of vaccines to prevent viral diseases (36).

Definitions for the term “antibiotic” are often nebulous at best. A frequently cited definition is “a chemical substance produced by a microorganism that kills or inhibits the growth of another microorganism” (37). Under this definition, antibiotics are often considered to be a subset of antimicrobials, which are generally regarded as any chemicals that kill microorganisms (including bacteria, fungi, and protozoa) or inhibit their growth (37,38). However, this definition excludes the large number of widely used synthetic and semi-synthetic drugs that are also, paradoxically, referred to as “antibiotics” in common practice. This exclusion is due to the somewhat arbitrary specification that antibiotics must be “produced by a microorganism”. Synthetic and semi-synthetic antibiotics are not direct products of natural microbial biosynthetic pathways and therefore more closely fit the definition of antimicrobial, though they behave and are

commonly referred to as antibiotics. However, if the “produced by a microorganism” specification is dropped from the definition of “antibiotic”, a new specification must be added. Antibiotics must work at relatively low concentrations, so as to exclude substances like organic acids, hydrogen peroxide, and ethanol (all of which are antimicrobial) that are not practical for internal application to higher organisms, particularly humans and animals (34). Thus, from a strictly anthropocentric point of view, antibiotics – both “natural” and “synthetic” – may be most thoroughly defined as low molecular weight (< 1000 Daltons) organic compounds that inhibit or kill prokaryotes *specifically* and at dilute concentrations (38–40).

Traditionally, natural antibiotics are viewed as an evolutionary adaptation conferring a competitive advantage to their producers in diverse ecosystems (41). While an antibiotic-producing microorganism will generally not be sensitive to the compound or compounds that it produces, its neighbors in a mixed microbial community may be. As a result, the antibiotic producer can inhibit or eliminate other microorganisms with which it is competing (e.g. for carbon, nitrogen, etc.) by releasing antibiotic compounds into its local environment (42). This concept originated with initial discoveries of antibiotic compounds, including Alexander Fleming’s seminal (and accidental) discovery of penicillin. Fleming observed that a compound released by a colony of *Penicillium* contaminating petri dishes in his lab caused nearby *Staphylococcus* cells to lyse (33). Other early researchers found that microbial communities in soil environments contained a large variety of microorganisms capable of producing substances that inhibited the growth of other microorganisms (43). Thus it was concluded that antibiotic compounds

served as agents of intercellular chemical warfare in natural environments, and the properties that made them useful in that regard were subsequently exploited with great success for application to human needs (39,43).

Today, antibiotics are used for treating microbial infections and prophylaxis in human and veterinary medicine, as well as for growth promotion in agriculture. Direct treatment of bacterial infections in human hosts was the first and is still the most critical task to which antibiotics may be applied, and their use for this purpose provides obvious human health benefits (34,39,44). Antibiotics are useful for the same purpose in agricultural animals, which can increase overall productivity in agricultural operations (45). Antibiotics can also be used for prophylaxis (i.e. disease prevention), often at lower concentrations than what would be used for treatment of an actual infection (45,46). Though prophylaxis can be (and frequently is) practiced in human medicine (e.g. antibiotics administered to prevent infection during surgery or in patients with immune deficiencies), antibiotics employed for this purpose are also quite common in agriculture and aquaculture (46,47). Antibiotics used in agriculture for prophylaxis often serve a second purpose of growth promotion. Agricultural use of antibiotics for prophylaxis and growth promotion is highly controversial – and has even been banned in the European Union – due to evidence that it contributes to the development of antibiotic resistance in human pathogens (45,48). Thus, while application in agriculture makes up a very large ($\geq 70\%$) portion of their overall use by mass (35,49), antibiotics are still most critical for treating microbial infections in humans.

Antibiotics inhibit microbial growth via one of three primary mechanisms, and each major class of antibiotics exhibits one of these mechanisms exclusively. Antibiotics may block cell wall biosynthesis, protein synthesis (i.e. inhibit translation), or nucleic acid synthesis (i.e. DNA replication and repair or transcription). Major classes of antibiotics that block cell wall biosynthesis include β -lactams and glycopeptides, while antibiotics inhibiting protein synthesis include the macrolides, tetracyclines, and aminoglycosides (50,51). Common molecular targets associated with the inhibition of cell wall biosynthesis include transpeptidases and the D-Ala-D-Ala termini of peptidoglycan, while peptidyltransferase is a common target associated with the inhibition of protein synthesis (51). Sulfonamides block nucleic acid synthesis by targeting nucleic acid precursors (folic acids), while quinolones are known to uniquely halt nucleic acid synthesis by targeting enzymes associated with those functions (e.g. ciprofloxacin and nalidixic acid both target the α subunit of DNA gyrase) (3,50,51).

The development of modern, clinically useful antibiotics – both natural and synthetic – began in the first half of the 20th century with sulfonamides and penicillin. Sulfonamides, synthetic drugs that were developed in the 1930s, were the first compounds widely used as antibiotics (34). These drugs were successfully applied to the treatment of some previously common and deadly infectious diseases just before the start of World War II. For instance, use of sulphanilamide and sulphapyridine to treat puerperal pyrexia, an extremely high fever associated with childbirth and caused by hemolytic streptococci, led to a decrease in the disease's mortality rate by a factor of more than 3 between 1935 and 1940 (34). However, the sulfa drugs could not control all

infectious diseases, resulting in a need for more effective and broad-spectrum antibiotic agents (37). Penicillin would prove to be a first step in meeting this need. Though it was discovered somewhat earlier than the first sulfonamides (1928-1929), penicillin was not successfully extracted from culture media and developed for clinical use until 1940 (33,34). During World War II, penicillin was found to be highly effective for treating staphylococcal and pneumococcal infections among members of the military. It was also superior to the sulfa drugs for treating streptococcal infections, and at the conclusion of the war, penicillin was made available to the general public (37).

The success of penicillin led to substantial concerted research efforts aimed at discovering new compounds with similar useful properties. Thus, the 1940s and 1950s saw a number of new natural antibiotics made available, including the first aminoglycoside (streptomycin), the first tetracyclines (chlortetracycline and oxytetracycline), the first macrolide (erythromycin), and the first glycopeptide (vancomycin) (Table 2.1). It was also found that the chemical structure of these natural compounds could be manipulated to adjust their effectiveness, specificity towards target organisms, or to reduce unwanted side-effects (34). As a result, numerous analogs of many of the original natural antibiotic compounds were developed, such that many antibiotics now in common use are often semi-synthetic derivatives of some natural antibiotic discovered in the mid-20th century (51).

Table 2.1. A timeline detailing the development and/or discovery of important antibiotic compounds. Data are compiled from Reference 34 and references noted in right-most column.

Drug	Class	Type	Year	Reference
Penicillin	β -lactam: Penicillins	Natural	1929/1940	(52)
Sulphanilamide	Sulfonamide	Synthetic	1932	(53)
Sulphapyridine	Sulfonamide	Synthetic	1938	(53)
Streptomycin	Aminoglycoside	Natural	1944	(54)
Chloramphenicol	Chloramphenicol	Natural	1947	(55)
Cephalosporin	β -lactam: Cephalosporins	Natural	1948	(56)
Chlortetracycline	Tetracycline	Natural	1948	(57)

Oxytetracycline	Tetracycline	Natural	1950	(57)
Erythromycin	Macrolide	Natural	1952	(58)
Vancomycin	Glycopeptide	Natural	1956	(59)
Kanamycin	Aminoglycoside	Natural	1957	(54)
Rifamycin	Ansamycin	Natural	1957	(60)
Methicillin	β -lactam: Penicillins	Semi-synthetic	1960	(52,61)
Ampicillin	β -lactam: Penicillins	Semi-synthetic	1961	(52,61)
Spectinomycin	Aminoglycoside	Natural	1961	(54)
Lincomycin	Lincosamide	Natural	1962	(62)
Naladixic acid	Quinolone	Synthetic	1962	(63)

Gentamicin	Aminoglycoside	Natural	1963	(54)
Tobramycin	Aminoglycoside	Natural	1964	(54)
Norfloxacin	Quinolone: Fluoroquinolones	Synthetic	1980-1984	(63)
Ciprofloxacin	Quinolone: Fluoroquinolones	Synthetic	1987-1989	(63)
Clarithromycin	Macrolide	Semi-synthetic	1991	(58)
Linezolid	Oxazolidinones	Synthetic	2000	(64)

Exceptions to this trend obviously include synthetic antibiotics. While the original antibiotic drugs (i.e. the sulfonamide drugs) were in fact synthetic, advances in producing new synthetic antibiotics have been sparse compared to those associated with natural and semi-synthetic compounds (see Table 2.1). After a dry spell in the development of synthetic antibiotics following the sulfa drugs, the first quinolone, nalidixic acid, was made available in 1962. Further refinements of this class of compounds, specifically the addition of fluorine groups at various positions on their dual-ring structure, have led to the development of important drugs like ciprofloxacin and norfloxacin (63). So-called fluoroquinolone antibiotics are now among the most widely used in clinical practice (51).

Antibiotics are now used on a scale that would have likely been difficult to foresee for those involved in their early development and application. In the United States, more than 90 antibiotic compounds, including natural, semi-synthetic, and synthetic species, are sold for use in human and/or veterinary medicine (35,49). Of the many compounds used in both fields of medicine, antibiotics in the tetracycline class make up the largest fraction of U.S. sales by mass (5.8×10^6 kg in 2011, 98% for food-producing animals), followed by penicillins (2.3×10^6 kg in 2011, 38% for food-producing animals) (35,49). Other important antibiotic classes used in both human and veterinary medicine include sulfonamides (850,000 kg in 2011, 44% for food-producing animals), macrolides (750,000 kg in 2011, 78% for food-producing animals), and cephalosporins (520,000 kg in 2011, 5% for food-producing animals) (35,49). In total, the United States uses approximately 15×10^6 kg of antibiotics every year, although this value includes

approximately 4×10^6 kg yr⁻¹ of ionophores, which are used exclusively for food-producing animals (35,49). Total global antibiotic use has been estimated to be on the order of 90 to 180 million kg yr⁻¹ (Kümmerer 2009). This widespread use results in many tangible benefits that increase the overall quality of human life, but it has also led to a new problem: bacterial resistance to antibiotics.

2.2 Antibiotic Resistance

Resistance to antibiotics, which develops as an inevitable consequence of antibiotic use, is widespread and has significant consequences. In the United States, antibiotic resistant infections now account for at least two million illnesses and 23,000 deaths each year (65). This number of deaths is on par with those due to Parkinson's disease in 2010 (approximately 22,000) and represents a conservative estimate, as it does not include the many additional deaths from other conditions complicated by antibiotic-resistant infections (65,66). Antibiotic-resistant infections have been shown to be associated with attributable costs of between \$19,000 and \$29,000 per patient and to increase death rates 2-fold relative to antibiotic-sensitive infections (67). The frequency with which resistance to individual antibiotics is encountered also often increases with time (68), which renders older antibiotics less effective and creates an “arms race” between rates of antibiotic development and rates of bacterial adaptation to new antibiotics.

A straightforward definition for “resistance” to an antibiotic is “continued growth of microorganisms in the presence of [what should be] cytotoxic concentrations of antibiotics” (69). The distinction between antibiotic-susceptible and antibiotic-resistant

microorganisms, however, is not as clear as it may initially seem based on this definition. Resistance is quantified for individual combinations of antibiotic and microorganism using disc diffusion assays, and the results are expressed as minimum inhibitory concentrations (MICs). MICs vary, sometimes widely, based on both the microorganism and the antibiotic (Table 2.2). Furthermore, MICs do not represent neat dividing lines between susceptible and resistant microorganisms, but rather, the centers of occasionally wide distributions of inhibitory antibiotic concentrations (70). MICs have been defined for numerous combinations of different antibiotics and specific pathogens, but are usually undefined for environmental microorganisms, so the concept of “resistance” in a strict sense is vaguer with respect to these microorganisms.

Table 2.2. Median minimum inhibitory concentrations (MIC) of major antibiotic classes for a model gram-negative microorganism (*Escherichia coli*) and a model gram-positive microorganism (*Staphylococcus aureus*).

Class	Drug	Median MIC (mg/L)		Reference
		<i>E. coli</i>	<i>S. aureus</i>	
Aminoglycosides	Gentamicin	0.5	0.25	(54)
	Streptomycin	8	4	
	Spectinomycin	8	64	
β-lactams: cephalosporins	Cefalotin	4 - 8	0.25 - 0.5	(56)
β-lactams: penicillins	Amoxicillin	4	0.1	(52)
	Ampicillin	4	0.06 - 1	

	Benzylpenicillin	64	0.03	
	Methicillin	≥ 128	1	
Chloramphenicols	Chloramphenicol	2 - 8	2 - 8	(55)
Diaminopyrimidines	Trimethoprim	0.05 - > 64	0.2 - 2	(71)
Glycopeptides	Vancomycin	> 32	1 - 2	(59)
Lincosamides	Lincomycin	> 64	0.5 - 2	(62)
Macrolides	Erythromycin	8 - 32	0.1 - 1	(58)
Oxazolidinones	Linezolid	> 32	0.06 - 4	(64)
Quinolones	Nalidixic acid	4 - 8	≥ 64	(63)
Quinolones: Fluoroquinolones	Ciprofloxacin	≥ 0.06	0.25 - 1	(63)

	Norfloxacin	0.25	1	
Rifamycins	Rifampicin	8 - 16	0.008 - 0.06	(60)
Sulfonamides	Sulfamethoxazole	4 - 8	4 - 32	(53)
Tetracyclines	Chlortetracycline	8 - 16	0.5 - > 32	(57)
	Oxytetracycline	2 - 16	2 - > 32	

The mechanisms of antibiotic resistance are fairly well understood, and generally fall into one of three broad categories. These include efflux pumps, enzymatic modification, and ribosomal protection proteins (68,69). Efflux pumps are proteins embedded in the bacterial cell membrane that actively transport antibiotics and other compounds from the cytoplasm to the cell's surrounding environment (69). Enzymatic modification includes modification of either the molecular target of an antibiotic or the modification of the antibiotic itself, while ribosomal protection proteins bind to bacterial ribosomes to block the active sites some antibiotics are designed to take advantage of (69,72).

Despite this small number of general antibiotic resistance mechanisms, the biochemical diversity of the specific cellular processes and structures that fall into these categories is significant (69), and the antibiotic resistance genes (ARGs) that form the genetic basis for antibiotic resistance are correspondingly numerous. Some individual ARGs are specific to particular antibiotics, while others provide resistance to multiple antibiotics. Efflux pumps in particular are frequently found to be relatively non-specific with regard to what compounds they are able to interact with (69). ARGs have been discovered for nearly every antibiotic in existence, and some antibiotics are associated with relatively large numbers of different ARGs (73,74). For some antibiotics, ARGs have been found corresponding to every resistance mechanism (73,74). For example, at least 45 ARGs are known to encode resistance to the group of macrolide, lincosamides, and streptogramin B antibiotics (74). This group of 45 ARGs includes 10 putative efflux pumps (ATP-binding transporters and major facilitators), 14 putative enzymatic

modification mechanisms (esterases, hydrolases, phosphorylases, and transferases), and 21 putative ribosomal protection proteins (rRNA methyltransferases). Similarly, there are at least 32 known tetracycline resistance genes, with 20 encoding putative efflux pumps, one encoding a putative enzymatic modification mechanism, and nine encoding putative ribosomal protection proteins (two of the 32 genes code for unknown products) (73).

The incidence of ARGs in pathogens was once assumed to be the result of random point mutations in homologous genes. However, we now know that ARGs are ancient relative to human time scales, and many probably originate from environmental – not pathogenic – microorganisms (75–78). Thus, a substantial amount of modern resistance is likely to be due to the horizontal exchange of existing ARGs themselves (79). There are three mechanisms by which horizontal gene transfer occurs: conjugation, transduction, and transformation (79). Conjugation is the direct sharing of genetic material between two prokaryotic microorganisms, via the extension of a pilus from one microorganism to the other (80). Transduction occurs when bacteriophages randomly pack host genetic material into new phages, and those phages infect a new host, thereby transferring genetic material from one prokaryotic microorganism to another (80,81). Finally, transformation is the uptake of exogenous genetic material into the cell cytoplasm (80).

The mechanisms of horizontal gene transfer are at least partially facilitated by mobile genetic elements. In addition to bacteriophages, important examples of mobile genetic elements include plasmids, transposons, and integrons (79). Plasmids are

circular, double-stranded and closed segments of DNA that carry non-essential genes (80). They can be transformed, although conjugal transfer is frequently thought of as the most significant horizontal gene transfer mechanism for plasmids (79). Transposons are recombinant DNA sequences that can transfer among different sites on chromosomes and/or plasmids using non-homologous recombination (80). Transposons can be transduced and transformed, although conjugal transfer is frequently thought of as the most significant horizontal gene transfer mechanism for them as well (79). The critical components of an integron include an integrase gene from the tyrosine-recombinase family, a primary recombination site, and an outward-oriented promoter (82). Integrons are of particular interest because they convert exogenous open reading frames (ORFs, i.e. potential “new” genes) to functional genes. The integrase gene recombines circularized ORFs (a.k.a. “gene cassettes”) at the primary recombination site downstream from the promoter in order to integrate them into a cell’s genetic regulatory system (82). Integrons are frequently found on plasmids and transposons, and transposons themselves can be found on plasmids (3,79). Whether combined or not, integrons, plasmids, and transposons also enable the accumulation of multiple ARGs by an individual bacterium, thereby contributing to the incidence of multiple antibiotic resistance (69). Thus, mobile genetic elements enable ARGs to spread relatively quickly through mixed microbial communities via horizontal gene transfer and also potentially facilitate the development and maintenance of multiply-resistant genotypes.

The historical development of resistance to antibiotics has closely paralleled the development of antibiotics themselves (Table 2.3). Resistance has developed to virtually

all classes of antibiotics, and it tends to develop rapidly. For antibiotics listed in both Table 2.1 and Table 2.3, the time span between the development of an antibiotic and the first report of resistance to that antibiotic is frequently on the order of 10 years. The antibiotic resistance threats currently identified as the most “urgent” by the Centers for Disease Control and Prevention include carbapenem-resistant Enterobacteriaceae and *Neisseria gonorrhoeae* resistant to any of cefixime, ceftriaxone, azithromycin, or tetracycline (65). These two threats are followed closely by a group of 12 “serious” threats that includes methicillin-resistant *Staphylococcus aureus* (MRSA), *Mycobacterium tuberculosis* resistant to individual or multiple antibiotics, and two multi-drug resistant microorganisms (*Acinetobacter* and *Pseudomonas aeruginosa*) (65). MRSA is an opportunistic pathogen that is frequently community acquired (i.e. acquired outside the hospital), resistant to multiple antibiotics in addition to methicillin, and has probably acquired resistance through horizontal gene transfer (83,84). *M. tuberculosis* was in decline as a cause of morbidity and mortality in the U.S. until the late 20th century, but it has once again become a serious public health challenge since acquiring resistance to antibiotics (85). Multi-drug resistant microorganisms, which have developed with increasing frequency in the last 15 years, are particularly expensive and difficult to treat in practice because many alternative antibiotics are often ineffective against them (3).

Table 2.3. A timeline outlining the development of antibiotic resistance. Data are adapted and compiled from References 61 and 65. Microorganisms were not identified for Reference 61.

Antibiotic	Microorganism	Year	Reference
Sulfonamides		1940s	(61)
Penicillin	<i>Staphylococcus</i>	1940	(65)
Tetracycline		1953	(61)
Chloramphenicol		1959	(61)
Streptomycin		1959	(61)
Tetracycline	<i>Shigella</i>	1959	(65)
Methicillin	<i>Staphylococcus</i>	1962	(65)
Penicillin	Pneumococcus	1965	(65)
Erythromycin	<i>Streptococcus</i>	1968	(65)
Cephalosporins		late 1960s	(61)
Ampicillin		1973	(61)
Gentamicin	<i>Enterococcus</i>	1979	(65)

Ceftazidime	Enterobacteriaceae	1987	(65)
Erythromycin		1988	(61)
Vancomycin	<i>Enterococcus</i>	1988	(65)
Levofloxacin	Pneumococcus	1996	(65)
Imipenem	Enterobacteriaceae	1998	(65)
MDR ^a	Tuberculosis	2000	(65)
Linezolid	<i>Staphylococcus</i>	2001	(65)
Vancomycin	<i>Staphylococcus</i>	2002	(65)
MDR ^a	<i>Acinetobacter</i>	2004	(65)
MDR ^a	<i>Pseudomonas</i>	2005	(65)
Ceftriaxone	<i>Neisseria gonorrhoeae</i>	2009	(65)
MDR ^a	Enterobacteriaceae	2009	(65)
Ceftaroline	<i>Staphylococcus</i>	2011	(65)

^aMDR indicates “multi-drug resistant” microorganisms.

The current strategy for dealing with antibiotic resistance consists of multiple complementary components. These components include developing new antibiotics, developing alternatives to antibiotics (e.g. bacteriophage therapy), prescribing multiple

antibiotic cocktails for individual infections, cycling antibiotics over time scales of decades, and reducing or eliminating the use of antibiotics for purposes other than human medicine (e.g. as growth promoters in agriculture) (2,3,69,86–90). Many of these components, however, are currently working minimally or not at all. For instance, the rate at which new antibiotics are developed and deployed has slowed considerably in recent years, largely due to economic pressures in the pharmaceutical industry (2,91). Furthermore, the research underlying our understanding of potential alternatives to antibiotics is still at such a fundamental level that results along these lines seem unlikely to appear in the immediate future. The use of multiple antibiotics to treat individual infections can work well, although it still relies, in part, on the efficacy of individual antibiotics and is also hampered by the development of multi-drug resistant pathogens. Antibiotic cycling holds promise, but its benefits can be undone by compensatory mutations, co-selection of ARGs that are not under selective pressure with ARGs or other traits that are under selective pressure, and ARGs that carry either minimal fitness costs or that provide a fitness advantage even in the absence of antibiotic selective pressure (69). Finally, the reduction or elimination of antibiotic use for purposes other than human medicine seems prudent (92) and there is evidence for the effectiveness of policies intended to achieve reduced frequency of antibiotic resistance among bacteria isolated from humans (93). However, such measures have so far proven to be politically difficult to enact in the U.S. Antibiotic resistance will continue to require a prolonged, multi-component strategy to overcome it, but the complications and shortcomings of the existing strategies are such that new additions complementing them are needed.

Members of the environmental science and engineering community have offered one such promising new addition, which is based on the consideration of ARGs as environmental contaminants.

2.3 Antibiotic Resistance Genes as Environmental Contaminants

The consideration of ARGs as environmental contaminants (5) is based on two attributes of ARGs. First, as outlined in the previous section, ARGs are responsible for adverse human health outcomes. Second, the distribution of ARGs in the environment provides the opportunity for human exposure to them. The ultimate source of ARGs circulating in the environment is likely to be the gastrointestinal tract of humans and food-producing animals undergoing antibiotic treatment. These ARGs then enter the environment in feces. (A substantial body of literature is concerned with transmission of antibiotic resistance from food-producing animals via meat; while this route of exposure is likely important, it is beyond the scope of this work). In the United States and many other countries, fecal wastes are disposed of via direct land-disposal (in the case of food-producing animals) or are treated in a municipal wastewater treatment plants (in the case of humans) prior to land-disposal of the treated solids and discharge of the treated liquid fraction to surface waters. Thus, ARGs have been reported in agricultural waste and aquaculture facilities (5,6,11,12,16,19,20,94–116), as well as in sewage and all stages of the municipal wastewater treatment process, even in treated wastewater after undergoing “best available” treatment practices (5,10,15,21–32,99,103,112,117–147). Furthermore, as a result of current disposal practices for agricultural waste and human sewage, ARGs have been found in soil (including on vegetables at harvest) (11,78,99,104,124,135,148–

158), surface water environments (including beaches, sediments, biofilms, and “pristine” environments presumably unaffected by anthropogenic activities) (5,7–10,13–15,17,18,21,99,103,108,112,117,119,124,136,159–165) groundwater (including in aquifers recharged with treated wastewater) (6,94,101,102,152,166), aerosols (167), and even the drinking water treatment process (including finished plant water and tap water) (5,15,168). The ARGs catalogued in these reports encode resistance to virtually all antibiotic classes, are distributed in numerous locations across the globe, and have been found in a large variety of bacterial genera.

The wide distribution of ARGs in the environment is the result of traditional fate and transport processes for both organic chemicals (as would be the case for extracellular DNA) and microorganisms. Organic chemical fate and transport mechanisms relevant to extracellular ARGs would seem to include biodegradation, hydrolysis, oxidation, photolysis, and sorption, along with physical transport of dissolved ARGs in water or sorbed ARGs with airborne or waterborne particulate matter (169). Potential fate and transport mechanisms for ARGs contained within bacterial cells would seem to include cell division, endogenous decay, and sorption, along with physical transport of bacterial cells in water and air and physical transport of sorbed bacterial cells with airborne or waterborne particulate matter. These fate and transport mechanisms, whether for extracellular or intracellular ARGs, seem reasonable, and important evidence linking human activities to the occurrence of ARGs in natural environments provides indirect support for their significance (14,18,112). However, explicit investigation of their effects has occurred in only a handful of studies (100,115,170).

The fate and transport mechanisms for extracellular and intracellular ARGs are complicated by the additional fate and transport mechanisms presented by the mechanisms of horizontal gene transfer. For instance, because transformation enables the uptake of extracellular DNA by microorganisms, it enables a “state change” that determines whether an ARG is subject to fate and transport mechanisms for organic chemicals or fate and transport mechanisms for microorganisms. Similarly, because conjugation and transduction both enable the transfer of ARGs between microorganisms with, potentially, different abilities to survive in specific environments, ARGs could conceivably be transferred from pathogens lacking the ability to survive in, for example, surface water, to environmental microorganisms that can easily survive in surface water. In such a case, the environmental microorganisms may serve as a temporary reservoir of ARGs that carries them through the environment until coming in contact with pathogens and transferring the ARGs back. Bacteriophages themselves may also act as temporary carriers of ARGs through environments that are hostile to other hosts.

Like ARGs themselves, the mobile genetic elements that enable horizontal gene transfer are distributed widely in the environment. They have been identified in agricultural waste and aquaculture facilities (including bacteriophages carrying ARGs) (20,96,97,99,104,106,108–110,171), as well as in sewage and all stages of the municipal wastewater treatment process (including multi-resistance plasmids, multi-resistance integrons, and integron-borne plasmids) (10,24,32,99,120,121,123,124,126,130–134,136–139,141–147,171–178). Mobile genetic elements enabling horizontal gene transfer have also been described in soil (including plasmids and transposons associated

with multiple ARGs) (99,104,124,151–153,155–158,171,179), surface water environments (including sediments and biofilms and including multi-resistance plasmids) (7,10,99,108,136,141,159,160,164,172,173,177,178,180–183), groundwater (152), and aerosols (167). As with ARGs, the mobile genetic elements catalogued in these reports carry resistance genes for virtually all antibiotic classes, are distributed in numerous locations across the globe, and have been found in a large variety of bacterial genera.

The ultimate goal of identifying the distribution of ARGs and ARG-associated mobile genetic elements in the environment is to inform management strategies to reduce human exposure to ARGs. This assumes, of course, that reduced exposure to ARGs will result in reduced antibiotic resistant infections and thereby preserve the efficacy of our existing antibiotic arsenal. We currently lack strong evidence that reducing environmental exposure to ARGs results in a reduction in the frequency with which antibiotic resistant infections occur. However, the strategy of reducing the number of ARGs circulating in the environment (and potentially exposed to humans) could be pursued as a method of disease prevention based on the precautionary principle. This requires the identification of the largest reservoirs of ARGs and subsequent reduction of their size. The municipal wastewater treatment process is undoubtedly among the largest reservoirs of ARGs. Furthermore, the bulk of the biomass, and as a result, the bulk of the ARGs that exit the municipal wastewater treatment process do so in the residual municipal wastewater solids (27). Thus, residual municipal wastewater solids treatment may be a highly effective point at which to control the number of anthropogenic ARGs circulating in the environment.

2.4 Treatment of Residual Municipal Wastewater Solids as an Opportunity to Mitigate the Spread of Antibiotic Resistance

Treatment of residual municipal wastewater solids takes place within an existing infrastructure that holds promise for being upgraded and optimized to reduce the number of ARGs discharged to the environment. The primary goals of residual solids treatment are to reduce the water, organic carbon, and pathogen content of untreated residual municipal wastewater solids (184). Achieving these goals makes treated residual solids easier to dispose of, less offensive, less attractive to disease vectors, and safer for humans that happen to come in direct contact with them. Residual solids treatment technologies, termed Processes to Significantly Reduce Pathogens (PSRPs), include aerobic digestion between 15°C and 20°C, air drying at ambient temperatures above 0°C, anaerobic digestion between 20°C and 55°C, composting at temperatures above 40°C, and lime stabilization (185). Following treatment in a PSRP, treated residual solids are typically disposed of in landfills or are land-applied to agricultural fields (186). In the United States, approximately 50% of treated residual solids are land-applied to agricultural fields (186). Additionally, treatment technologies termed Processes to Further Reduce Pathogens (PFRPs) can be used as alternatives to PSRPs when treated residual solids are more likely to come in direct contact with humans (e.g. when treated residual solids are sold as garden fertilizers) and must be treated to a higher standard (184). PFRPs include aerobic digestion at temperatures between 55°C and 60°C, beta ray irradiation, composting at temperatures above 55°C, gamma ray irradiation, heat drying at

temperatures above 80°C, heat treatment at temperatures above 180°C, and pasteurization at temperatures above 70°C (185).

Because PSRPs and PFRPs are largely intended to “stabilize” (i.e. kill) microorganisms in residual municipal wastewater solids, they should also reduce ARG quantities in residual solids. Previous work has shown laboratory-scale aerobic digestion (between 22°C and 55°C) to be largely ineffective at removing ARGs from residual solids (121). However, full-scale anaerobic digestion (between 50°C and 60°C) has been demonstrated to reduce ARG quantities in residual solids by at least 75% (24), while laboratory-scale anaerobic digestion (between 35°C and 59°C) has achieved reductions of up to 80% to 90% (121,131). Furthermore, one study (121) demonstrated that increasing the digestion temperature may increase the rate and extent of ARG removal from residual municipal wastewater solids in anaerobic digestion, although this effect has not been fully reproducible (131) and appears to depend, in part, on both the specific ARG and the flow configuration of the digester. Despite these important advances, however, a number of critical knowledge gaps remain with regard to removing ARGs from residual municipal wastewater solids during residual solids treatment.

For instance, the full array of PSRPs and PFRPs has yet to be evaluated for its potential to destroy ARGs. This is a problem, because approximately 80% of treatment plants in the United States use a technology other than anaerobic digestion (currently the most frequently investigated technology with regard to ARGs) for residual solids treatment (186). Important examples of treatment technologies that should probably be investigated due to either the number of treatment plants that employ the technology or

the amount of residual solids produced with the technology include air-drying beds, composting, and lime stabilization. Air-drying beds are used at approximately 30% of all municipal wastewater treatment plants in the United States for dewatering treated residual solids, while composting is used to treat approximately 21% of all residual solids produced in the United States (186). Lime stabilization is used at approximately 18% of U.S. municipal wastewater treatment plants to treat approximately 13% of all residual solids produced nationally (186). Because of their widespread use, there is a need to investigate the performance of these types of treatment technology for their ability to remove ARGs from residual municipal wastewater solids.

Furthermore, even for the treatment technologies that *have* been investigated, we have little rational basis for selecting among alternative technologies. For any given treatment objective, selection of alternative treatment technologies is typically governed by operating costs (e.g. energy and chemical inputs and outputs) and capital costs (e.g. tank size). Understanding these costs requires detailed process design, which itself frequently relies on understanding the kinetics of the underlying biological, chemical, or physical processes. However, only one study to date (121) has considered the kinetics of ARG removal during treatment of residual solids. Thus, we must develop a more thorough understanding of the kinetics of ARG removal from residual solids in many different alternative technologies in order to select the most appropriate technology rationally. Furthermore, because we cannot possibly design our residual solids treatment infrastructure to consider all ARGs (see Section 2.2), the identification of a “design gene” or a subset of design genes seems warranted. In this context, a design gene would be a

genetic element related to antibiotic resistance in humans that possesses some combination of 1) serious human health consequences and 2) relatively slow rates of removal from residual solids. Thus, understanding the kinetic behavior of a design gene would appropriately constrain the design of individual treatment units and the selection of alternative treatment technologies.

Finally, almost no attention has been paid to the fate of ARGs following the treatment and ultimate disposal (i.e. land-application) of residual municipal wastewater solids. This is a critical gap in our current body of knowledge, because approximately 50% of all treated residual municipal wastewater solids in the United States are ultimately disposed of via land-application (186). The potential exists for these ARGs to accumulate in soil (150), and whether they accumulate or not, several plausible transport mechanisms have been outlined (see Section 2.3) that could result in human exposure to ARGs originating from land-applied treated residual solids. We must improve our understanding of how long, and in what quantities, ARGs from treated residual solids persist in soil following land-application of treated residual solids in order to guide decisions related to the frequency and mass loading rate of treated residual solids at individual field sites.

Chapter 3: Aerobic Digestion Reduces the Quantity of Antibiotic Resistance Genes in Residual Municipal Wastewater Solids

This chapter has been published in the journal *Frontiers in Microbiology* and is cited as:

Burch TR, Sadowsky MJ, LaPara TM. Aerobic digestion reduces the quantity of antibiotic resistance genes in residual municipal wastewater solids. *Front. Microbiol.* **2013**, 4:Article 17.

Frontiers in Microbiology is an online, open access journal. The copyright on this article has been retained by the authors according to the “Frontiers Conditions for Website Use” and “Frontiers General Conditions for Authors”.

Numerous initiatives have been undertaken to circumvent the problem of antibiotic resistance, including the development of new antibiotics, the use of narrow spectrum antibiotics, and the reduction of inappropriate antibiotic use. We propose an alternative but complimentary approach to reduce antibiotic resistant bacteria by implementing more stringent technologies for treating municipal wastewater, which is known to contain large quantities of antibiotic resistant bacteria and antibiotic resistance genes (ARGs). In this study, we investigated the ability of conventional aerobic digestion to reduce the quantity of ARGs in untreated wastewater solids. A bench-scale aerobic digester was fed untreated wastewater solids collected from a full-scale municipal wastewater treatment facility. The reactor was operated under semi-continuous-flow conditions for more than 200 days at a residence time of approximately 40 days. During this time, the quantities of *tet(A)*, *tet(W)*, and *erm(B)* decreased by more than 90%. In contrast, *intII* did not decrease, and *tet(X)* increased in quantity by a factor of five. Following operation in semi-continuous-flow mode, the aerobic digester was converted to batch mode to determine the first-order decay coefficients, with half-lives ranging from as short as 2.8 days for *tet(W)* to as long as 6.3 days for *intII*. These results demonstrated that aerobic digestion can be used to reduce the quantity of ARGs in untreated wastewater solids, but that rates can vary substantially depending on the reactor design and the specific ARG.

3.1 Introduction

The resistance of pathogenic bacteria to antibiotic chemotherapy is a growing problem with significant consequences for public health. In the United States, methicillin-resistant *Staphylococcus aureus* (MRSA) infections lead to more fatalities than the combination of HIV/AIDs, Parkinson's disease, and homicides, and the estimated economic cost of antibiotic resistance ranges from \$21 to 34 billion dollars per year (187). In response, medical practitioners have attempted to reduce the number of inappropriate and unnecessary antibiotic prescriptions. The biomedical research community is also focusing its research efforts to develop new antibiotics as well as alternatives to antibiotic chemotherapy (2,88,89). Finally, in Sweden and Switzerland, the use of antibiotics in agriculture for growth promotion and prophylaxis has been banned (87,188).

Despite these initiatives, a significant body of research suggests that antibiotic resistant bacteria (ARB) are becoming increasingly more prevalent (3,4,61). An alternative, but complementary, approach to reducing the prevalence of ARB would be to identify pertinent reservoirs of resistance and then to implement appropriate technologies to ameliorate these reservoirs. Consistent with this approach, numerous studies have identified untreated municipal wastewater (raw sewage) as a significant reservoir of ARB and antibiotic resistance genes (ARGs) (21,28,30,31,144,189–192). Municipal wastewater treatment processes, therefore, should represent an important opportunity to mitigate the quantity of this reservoir of antibiotic resistance.

Although prior research has demonstrated that the treated municipal wastewater also contains substantial concentrations of ARB and ARGs (5,9,10,192), a mass balance on wastewater treatment operations suggests that > 99% of the ARB and ARGs in untreated municipal wastewater accumulate in the residual wastewater solids. These are subsequently treated by numerous technologies to reduce their nutrient and pathogen content (to varying degrees) prior to their disposal on agricultural land (184). There have been relatively few investigations on the different technologies used for treating residual wastewater solids and their associated effectiveness at mitigating ARB and ARGs. Diehl and LaPara (2010) observed relatively little removal of ARGs in aerobic digestion processes operated at 22-55°C, but observed increasingly effective removal of ARGs in anaerobic digestion processes at temperature > 37°C. In contrast, Ma *et al.* (2011) observed little benefit of increasing the temperature of anaerobic digestion beyond 37°C.

In the present research, we undertook a detailed investigation of the effectiveness of a bench-scale conventional aerobic digestion process at mitigating the quantity of ARGs in untreated residual wastewater solids. Although our prior research had observed no effect of aerobic digestion on the quantity of ARGs in wastewater solids (121), these previous experiments were performed in relatively small bioreactors with a mean hydraulic residence time of 4 days. Assuming that ARGs decay at a relatively slow rate (i.e., half-lives > 4 days), this experimental design would have been insufficient to observe significant reductions in ARGs. This short time period used in our prior experimental design is also pertinent because the United States Environmental Protection Agency requires that aerobic digestion processes have a mean hydraulic residence time of

40 days (when operated at 20°C) to qualify as a “process to significantly reduce pathogens” (PSRP), which must be achieved before these treated wastewater solids can be applied to agricultural land for their disposal (albeit with some restrictions) (184). This research is of considerable practical importance because numerous full-scale municipal wastewater treatment facilities currently utilize aerobic digestion processes to treat their wastewater solids, particularly those that treat less than 10 million gallons of wastewater each day (at higher flow rates, other technologies are considered more practical and economical).

3.2 Materials and Methods

Experimental Design. A 10-liter aerobic digester was operated at room temperature with a mean residence time of 40 days and a minimum dissolved oxygen (DO) concentration of 2 mg/L. The digester was inoculated with 10 liters of untreated residual municipal wastewater solids from a full-scale municipal wastewater treatment plant. Mixing and aeration were provided by pumping atmospheric air through a stone diffuser located at the bottom of the reactor vessel at a rate sufficient to prevent settling of solids and to maintain the minimum DO concentration. Typical operating variables, including temperature, DO, pH, total solids (TS), volatile solids (VS), and inert solids (IS) were monitored throughout the entire time period the digester was in operation (193). Water loss due to evaporation was monitored and replaced by adding appropriate volumes of deionized water to the digester.

The digester was operated for more than 175 days while being fed on a weekly basis untreated residual municipal wastewater solids. The digester was considered to

have reached steady-state conditions once the residence time for inert solids had been maintained at 41.1 ± 0.5 days (mean \pm standard deviation) for a time period of 35 days. Once steady-state conditions had been established, the operating mode of the digester was shifted to better reflect continuous-flow operating conditions by feeding untreated residual municipal wastewater solids on a daily basis from Day 180 to Day 191. Following this semi-continuous flow phase, the aerobic digester was operated for an additional 27 days while being fed on a weekly basis untreated residual municipal wastewater solids. On Day 218, half of the digester contents (i.e. 5 liters) were replaced with untreated residual municipal wastewater solids to allow the determination of decay coefficients in a batch-like reactor.

Sample Collection and Genomic DNA Extraction and Purification. Triplicate samples (100 μ L) were collected from larger aliquots (50 to 300 mL) of digester contents to ensure accurate sample collection volumes. Samples were then diluted with 500 μ L of lysis buffer (120 mM sodium phosphate buffer, 5% dodecyl sulfate, pH 8.0 ± 0.1) and subjected to three consecutive freeze-thaw cycles followed by incubation at 70°C for 90 minutes. Genomic DNA was then extracted using a FastDNA Spin Kit (MP Biomedicals LLC, Solon, OH) according to the manufacturer's instructions.

Real-Time PCR. Real-time PCR was used to quantify the concentrations of three different genes that encode resistance to tetracycline (*tet(A)*, *tet(W)*, and *tet(X)*), one gene that encodes resistance to erythromycin (*erm(B)*), one gene that encodes resistance to sulfonamides (*sulI*), and the integrase gene of class 1 integrons (*intI1*). The three tetracycline resistance genes were selected because they represent each of the three

known mechanisms of tetracycline resistance (efflux pumps, ribosomal protection proteins, and enzymatic modification) (73). The erythromycin gene, *erm*(B), was chosen because it encodes an rRNA methyltransferase that confers resistance to macrolides, lincosamides, and streptogramin B (74). Prior work has demonstrated that all five of these ARGs are present at substantial concentrations in wastewater and/or wastewater solids (10,27,121). Class 1 integrons were quantified because of their association with multiple antibiotic resistance. These integrons enable bacteria to collect multiple, exogenous ARGs and modulate their expression (82). qPCR was also used to determine the concentrations of 16S rRNA genes (a measure of total bacterial biomass), all *Bacteroides* spp. (a measure of total fecal bacteria), and human-specific *Bacteroides* spp. (a measure of human fecal bacteria) (194–196). Additional information regarding the use of qPCR to quantify these genes can be found in Table A.1.

Real-time PCR was carried out on an Eppendorf Mastercycler EP Realplex thermal cycler (Eppendorf, Westbury, NY). PCR assays were optimized to reduce or eliminate the formation of primer-dimers and non-specific products. Typical PCR assays began with a 1 minute initial denaturation at 95°C. This step was followed by 40 cycles of denaturation at 95°C for 15 seconds and combined annealing and extension at the primer-specific annealing temperature for 1 minute. Typical reaction volumes were 25 µL and consisted of 12.5 µL of BioRad iTaq SYBR Green Supermix with ROX (Life Science Research, Hercules, CA), 25 µg of bovine serum albumin, optimized quantities of forward and reverse primers, and approximately 1 ng of template genomic DNA. Each analysis consisted of three replicates. Standards were made from positive controls

selected from municipal wastewater solids using our qPCR primers. These positive controls were then ligated into a pGEM-T Easy cloning vector, transformed into JM109 competent cells, and extracted from cell cultures using an alkaline lysis procedure (197). The DNA concentration of cell extracts was quantified using a TD-700 fluorometer and Hoechst 33258 dye. Each standard curve consisted of a 10-fold dilution series containing at least 5 standards ($r^2 \geq 0.99$). Amplification efficiencies were typically $100\% \pm 10\%$.

Data Analysis. All data obtained from groups of triplicate samples were treated as if they had been obtained from a normal distribution (i.e. means and standard deviations were used to describe the data). This assumption of normal distributions was based on results from Shapiro-Wilk normality tests performed in SigmaPlot 12.0 that indicated the complete semi-continuous flow data series for most gene targets could not be distinguished from a normal distribution ($P > 0.05$). Analysis of variance (ANOVA; Microsoft Excel 2010) was used with data from the semi-continuous flow experiment to determine the statistical significance of differences in gene target concentrations between untreated and treated residual solids samples.

Simple linear regression (Arc 1.06) was used with log-transformed data from the batch experiment to determine the goodness of fit of the data to a first-order kinetic model. The first-order kinetic model was chosen based on previous empirical observations that it tends to fit this type of data well. Values of P used to compare the relative statistical significance of different kinetic coefficients (Table A.2) were determined using Welch's t-test for unequal n and unequal sample variance. The sample

variance for each estimated first-order kinetic coefficient was obtained from the estimated standard error for that coefficient as provided by Arc 1.06.

3.3 Results

Semi-Continuous-Flow Operating Mode. With respect to typically monitored operating variables, the lab-scale aerobic digester performed as an appropriate experimental model simulation during the semi-continuous flow experimental period (Table 3.1). The pH was circumneutral, digester temperature was the same as the ambient air temperature, and dissolved oxygen concentrations were well above the target dissolved oxygen concentration of 2 mg/L. The total and volatile solids concentrations for the untreated and treated solids were well within ranges typically encountered in practice (2%-5% TS, 0.6%-3% VS) (184). The fractions of total and volatile solids destroyed were 26% and 41%, respectively, which is also typical for a full-scale aerobic digestion process (184).

Table 3.1. Operating variables during operation in semi-continuous-flow mode.

Variable	Mean	±	Standard Deviation
pH	7.5	± 0.2	<i>n</i> = 12
Temperature (°C)	17.0	± 0.3	<i>n</i> = 12
Dissolved Oxygen (mg/L)	5.8	± 1.5	<i>n</i> = 12
Hydraulic Residence Time (days)	13.5	± 0.7	<i>n</i> = 12
Untreated Total Solids	4.6%	± 0.04%	<i>n</i> = 4
Treated Total Solids	3.4%	± 0.3%	<i>n</i> = 4
Total Solids Destruction	26.3%	± 6.0%	<i>n</i> = 4
Total Solids Residence Time (days)	33.1	± 0.4	<i>n</i> = 12
Untreated Volatile Solids	3.2%	± 0.05%	<i>n</i> = 4
Treated Volatile Solids	1.9%	± 0.1%	<i>n</i> = 4
Volatile Solids Destruction	41.1%	± 4.8%	<i>n</i> = 4
Volatile Solids Residence Time (days)	27.7	± 0.6	<i>n</i> = 12
Untreated Inert Solids	1.5%	± 0.02%	<i>n</i> = 4

Treated Inert Solids	1.5% \pm 0.1%	$n = 4$
Inert Solids Destruction	-5.7% \pm 8.4%	$n = 4$
Inert Solids Residence Time (days)	41.7 \pm 0.1	$n = 12$

The aerobic digester eliminated a substantial fraction of bacterial biomass and fecal indicator bacteria (FIB) as measured by qPCR targeting the 16S rRNA gene and 16S rRNA genes specific for all *Bacteroides* spp. and for human-specific *Bacteroides* spp. (Figure 3.1). The concentrations of 16S rRNA genes were 77% lower in treated samples compared to the untreated samples. This indicates net destruction of total bacterial biomass in the digester, consistent with the total and volatile solids removal. Significant removal was observed for both types of FIB. The concentrations of all *Bacteroides* spp. were 99.9% lower in treated samples compared to untreated samples. Similarly, the concentrations of human-specific *Bacteroides* spp. were approximately 5×10^8 gene copies mL^{-1} in untreated samples, but were below the detection limit (1×10^8 gene copies mL^{-1}) in treated samples.

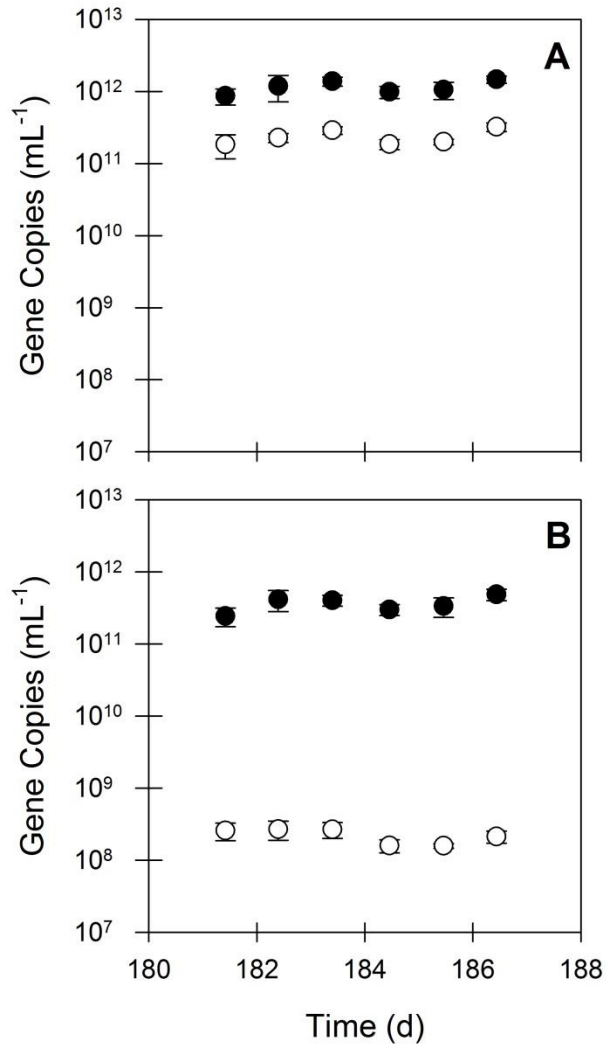


Figure 3.1. The quantities of: (A) 16S rRNA genes and (B) fecal indicator bacteria as measured by 16S rRNA genes of all *Bacteroides* spp. in untreated (closed circles) and treated (open circles) residual solids. Values are the arithmetic mean of triplicate samples; error bars represent one standard deviation. The concentrations of human-specific *Bacteroides* spp. were approximately 5×10^8 gene copies mL⁻¹ in untreated samples, but were below the detection limit (1×10^8 gene copies mL⁻¹) in treated samples.

The untreated wastewater solids contained substantial quantities of each of the ARGs investigated in this study. The quantities of *intI1*, *sul1*, and *tet(W)* were similar, present at a concentration of approximately 10^{10} gene copies mL^{-1} . In contrast, the concentration of *erm(B)* was approximately 10^{11} gene copies mL^{-1} , and the concentrations of *tet(A)* and *tet(X)* were approximately 10^9 gene copies mL^{-1} . Given that the concentrations of 16S rRNA genes were approximately 10^{12} gene copies mL^{-1} in the untreated solids, the ratio of the various antibiotic resistance determinants examined in this study to bacterial cells ranged from approximately 0.1% for *tet(A)* and *tet(X)* to 1% for *intI1*, *sul1*, and *tet(W)*, and to 10% for *erm(B)*.

The bench-scale aerobic digester removed between 85% and 98% of *erm(B)*, *sul1*, *tet(A)*, and *tet(W)* during the semi-continuous flow experimental period (Figure 3.2), which was substantially greater than that for bacterial biomass (i.e. 16S rRNA genes). In contrast, the quantity of *intI1* was not statistically different ($P = 0.17$) in the untreated and treated solids, suggesting that aerobic digestion operated in semi-continuous flow mode does not eliminate *intI1* (Figure 3.3). Furthermore, the ratio of *intI1* to 16S rRNA genes increased in the treatment process from 0.8% to 3%, indicating that aerobic digestion likely selects for bacterial cells possessing a class 1 integron. Interestingly, the aerobic digestion process also appeared to select for bacterial cells containing *tet(X)*, as the quantity of this gene was 5-fold greater in the treated solids than in the untreated solids.

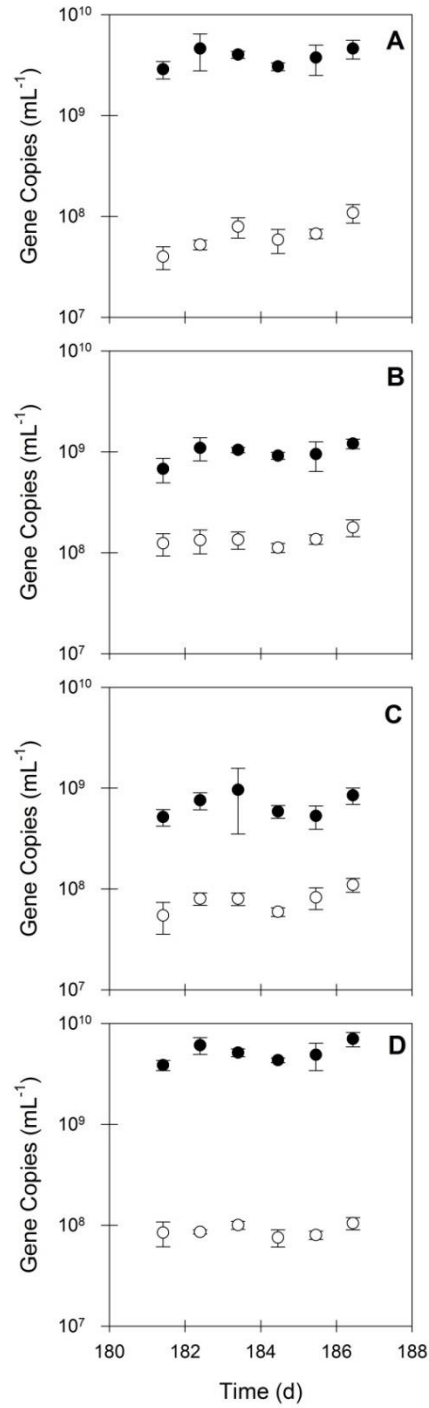


Figure 3.2. The quantities of: (A) *erm(B)*, (B) *sull*, (C) *tet(A)*, and (D) *tet(W)* in untreated (closed circles) and treated (open circles) residual solids. Values are the arithmetic mean of triplicate samples; error bars represent one standard deviation.

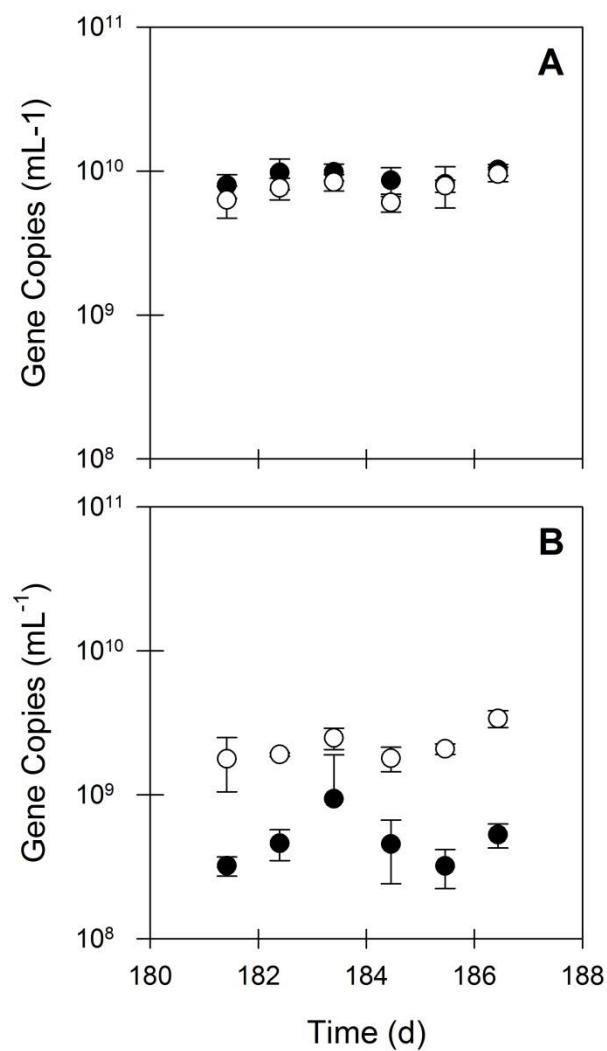


Figure 3.3. The quantities of: (A) *intII* and (B) *tet(X)* in untreated (closed circles) and treated (open circles) residual solids. Values are the arithmetic mean of triplicate samples; error bars represent one standard deviation.

Batch Operating Mode. Following the semi-continuous flow experimental phase, the aerobic digester was shifted to batch mode to determine decay rates for each target gene. As with the previous experimental phase, typically monitored operating variables indicated that the digester operated as an appropriate simulation of a full-scale aerobic digester. The pH rose from a semi-continuous phase value between 7 and 7.5 to just above 8 following the addition of untreated residual solids, but then gradually decreased to between 7 and 7.5. A substantial decrease in dissolved oxygen concentration to less than 1 mg/L was initially observed, but increased to > 4 mg/L within 24 hours and remained so for the duration of the batch experiment.

A significant decay rate was observed for 16S rRNA genes and FIB during operation in batch mode (Figure 3.4). The quantities of 16S rRNA genes decayed by 90% during the 20-day batch experiment ($t_{1/2} = 5.5$ d; Table 3.2). In contrast, all *Bacteroides* spp. decayed by nearly four orders of magnitude over 20 days ($t_{1/2} = 1.4$ d; Table 3.2), whereas human-specific *Bacteroides* spp. decayed to below the detection limit within one week of beginning the batch experimental phase ($t_{1/2} = 4.6$ d; Table 3.2).

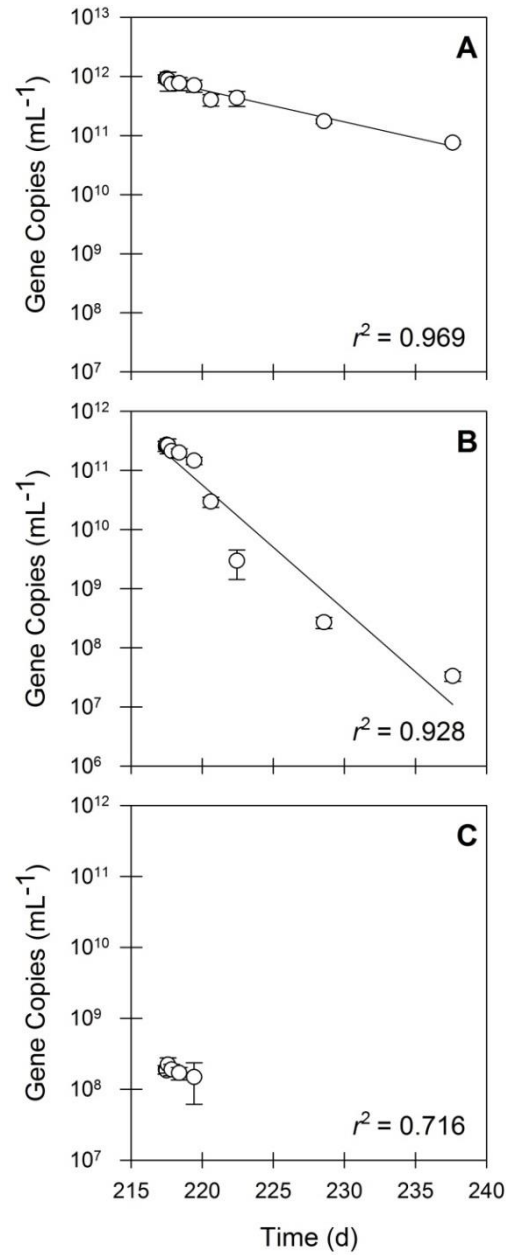


Figure 3.4. The quantities of: (A) 16S rRNA genes, (B) fecal indicator bacteria as measured by 16S rRNA genes of all *Bacteroides* spp., and (C) fecal indicator bacteria as measured by 16S rRNA genes of human-specific *Bacteroides* spp. in residual solids undergoing batch treatment. Values are the arithmetic mean of triplicate samples; error bars represent one standard deviation.

In contrast to operation in semi-continuous flow mode, the quantities of all of the antibiotic resistance determinants, including *intI1* and *tet(X)*, declined in the batch experimental phase (Figure 3.5). The quantities of *erm(B)* and *tet(W)* declined by approximately two orders of magnitude during the 20-day experiment, whereas the quantities of *intI1*, *sulI*, *tet(A)*, and *tet(X)* each declined by one order of magnitude during the same time period. Correspondingly, the first-order decay rates varied considerably among individual gene targets. The *intI1* and *tet(X)* genes decayed the most slowly, each with a half-life of approximately 6 days (Table 3.2). These rates of decay were statistically similar to each other as well as to the rate of decay for the 16S rRNA gene (Table A.2). In contrast, the first-order decay rates were significantly ($P < 0.05$) more rapid for the remaining gene targets, with half-lives ranging from 2.8 days to 4.6 days (Table 3.2). These rates of decay were significantly faster than the decay rate for 16S rRNA genes (Table A.2).

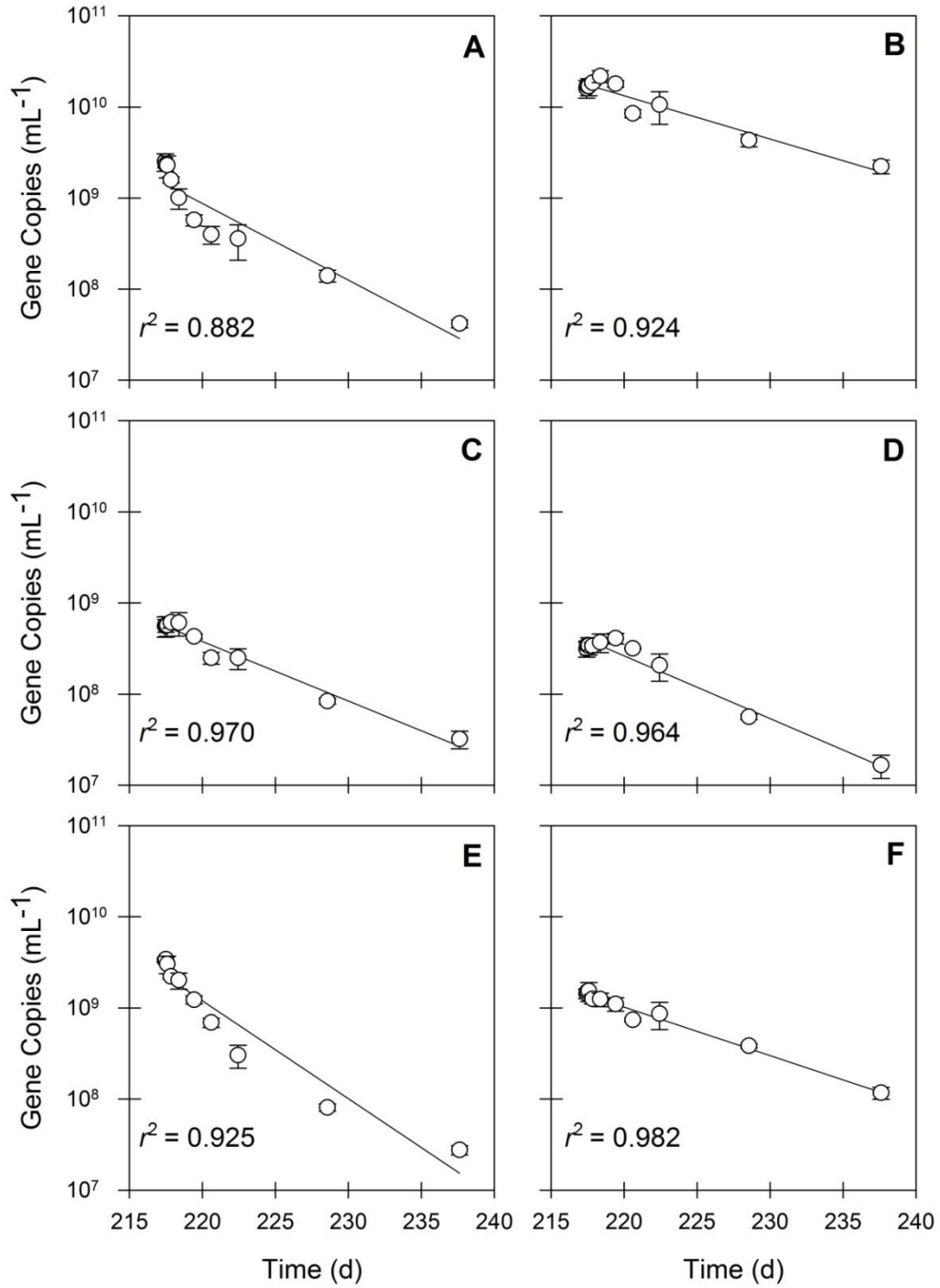


Figure 3.5. The quantities of: (A) *erm(B)*, (B) *intI1*, (C) *sulI*, (D) *tet(A)*, (E) *tet(W)*, and (F) *tet(X)* in residual solids undergoing batch treatment. Values are the arithmetic mean of triplicate samples; error bars represent one standard deviation.

Table 3.2. Summary of first-order degradation kinetic model parameter estimates for the 16S rRNA gene, fecal indicator bacteria as measured by 16S rRNA genes of all *Bacteroides* spp., fecal indicator bacteria as measured by 16S rRNA genes of human-specific *Bacteroides* spp., *erm*(B), *intI1*, *sulI*, *tet*(A), *tet*(W), and *tet*(X) during batch mode operation. All rates were regressed from 10 data points (except human-specific *Bacteroides* spp., $n = 6$) and are statistically significant ($P < 0.05$).

Gene Target	Standard		$t_{1/2}$ (days)
	k (day ⁻¹)	± Error (day ⁻¹)	
16S rRNA gene	0.13	± 0.008	5.5
All <i>Bacteroides</i> spp.	0.49	± 0.048	1.4
Human-specific <i>Bacteroides</i> spp.	0.15	± 0.047	4.6
<i>erm</i> (B)	0.19	± 0.025	3.6
<i>intI1</i>	0.11	± 0.011	6.3
<i>sulI</i>	0.15	± 0.009	4.6
<i>tet</i> (A)	0.16	± 0.011	4.4
<i>tet</i> (W)	0.25	± 0.025	2.8
<i>tet</i> (X)	0.12	± 0.006	5.7

3.4 Discussion

The long-term goal of our research is to determine how the numerous technologies used to treat municipal wastewater can simultaneously be used to eliminate the substantial quantities of ARB and ARGs that are known to exist in untreated sewage. The present study makes an important advance in our knowledge by elucidating the extent and rate by which aerobic digestion can be used to eliminate ARGs. This research is practically important because the overwhelming majority of ARB and ARGs in raw sewage ultimately end up in the residual wastewater solids, and a recent study suggested that more than 2,200 municipal wastewater treatment facilities use this technology to produce more than 85,000 dry tons of treated wastewater solids in the United States each year (186).

In most cases, the rate of disappearance of different ARGs exceeded that of the total number of bacteria (as measured by 16S rRNA gene copies), suggesting that these ARGs were actively eliminated during the aerobic digestion process. Although there is only very limited data presently available in the published literature, these disappearance rates are generally similar to the rates that were previously observed during anaerobic digestion at 37°C (121). In contrast, the quantities of *tet(X)* and *intII* decayed at a rate similar to that of all bacteria, suggesting that these genes were passively eliminated, paralleling the decline in the total number of bacteria. This observation is substantially different than our previous study, in which both *tet(X)* and *intII* rapidly declined in bench-scale anaerobic digestion processes operated at temperatures of 37°C or higher (121). Therefore, the rates by which different ARGs decay in a conventional aerobic

digestion process are either similar to or slower than the decay rates observed in anaerobic digestion processes. This apparent inferiority of aerobic digestion is pertinent because anaerobic digestion is also a commonly used technology to treat residual wastewater solids (184).

This research also demonstrated that reactor design has a major effect on the fate of ARGs during the treatment of residual municipal wastewater solids. The most obvious difference occurred with *tet(X)*, which declined under batch experimental conditions but increased substantially in semi-continuous flow conditions. Similarly, the quantity of *intII* declined under batch conditions but remained static during semi-continuous-flow operation. In contrast, model results suggest that the quantities of *erm(B)* and *tet(W)* declined more rapidly in semi-continuous flow operation than would be suggested by the first-order decay coefficient elucidated under batch conditions (analyses not shown). Previous researchers have suggested that reactor design affects the removal of ARGs during wastewater solids digestion (131); our results support this hypothesis. Additional research is needed to clarify the importance of reactor design and the disappearance of ARGs during the digestion of wastewater solids.

A growing body of evidence suggests that class 1 integrons, which are linked to multiple antibiotic resistance, are particularly prominent in wastewater (24,32,131,137,198). Our research has shown significant variation in removal efficiencies of *intII* depending on the specific technology (i.e., anaerobic digestion achieves better and more efficient removal than aerobic digestion) and the specific operating conditions (temperature, flow regime, etc.). Additional research is needed to

better understand the fate and gene cassette content of class 1 integrons in residual solids treatment systems.

Prior research has suggested that *sulI* flanks all class 1 integrons (82). When the aerobic digester was operated in semi-continuous flow mode, however, the quantities of *sulI* genes declined by almost an order of magnitude, whereas the quantities of *intI1* were similar in the treated and in the untreated residual solids. Similarly, the rate by which *sulI* declined in batch operating mode was significantly faster than the rate by which *intI1* declined ($P = 0.01$; Table A.2). This suggests that the coupling of the *sulI* gene to class 1 integrons is not universal; additional research is needed to better understand the relationship between class 1 integrons and *sulI* genes in the unit operations used to treat wastewater solids.

The most significant limitation of our research is the use of real-time quantitative PCR targeting various ARGs as a surrogate for ARB. The genes quantified here could be present in dead but intact bacteria or in bacteria in which the gene is non-functional. Similarly, the identity of the ARB harboring the ARGs detected in this study, and their clinical significance, remain unknown. Finally, only a select group of ARGs were targeted; even though these genes represent several important classes of antibiotics and all three known molecular mechanisms of resistance to tetracycline, they cover a relatively small cross-section of possible resistance gene targets.

In conclusion, aerobic digestion can be used to eliminate antibiotic resistance genes in untreated wastewater solids, but rates can vary substantially depending on the reactor design and the specific ARG examined. This information represents a critical

step towards our long-term goal of applying wastewater treatment technologies to mitigate the spread of antibiotic resistance. This knowledge is particularly useful to wastewater treatment engineers as they compare the relative merits of alternative residual solids treatment technologies and for designing specific unit operations to eliminate ARGs. Specifically, aerobic digestion technology, which is used by numerous full-scale municipal wastewater treatment facilities, appears less effective at eliminating ARGs than both conventional and high temperature anaerobic digestion.

Chapter 4: Air-Drying Beds Reduce the Quantities of Antibiotic Resistance Genes and Class 1 Integrons in Residual Municipal Wastewater Solids

This chapter has been published in the journal *Environmental Science & Technology* and is cited as:

Burch TR, Sadowsky MJ, LaPara TM. Air-drying beds reduce the quantities of antibiotic resistance genes and class 1 integrons in residual municipal wastewater solids. *Environ. Sci. Technol.* **2013**, 47(17):9965–9971.

It is republished here with permission from the American Chemical Society.

© 2013 American Chemical Society

This study investigated whether air-drying beds reduce antibiotic resistance gene (ARG) concentrations in residual municipal wastewater solids. Three laboratory-scale drying beds were operated for a period of nearly 100 days. Real-time PCR was used to quantify 16S rRNA genes, 16S rRNA genes specific to fecal bacteria (AllBac) and human fecal bacteria (HF183), the integrase gene of class 1 integrons (*intI1*), and five ARGs representing a cross-section of antibiotic classes and resistance mechanisms (*erm(B)*, *sulI*, *tet(A)*, *tet(W)*, and *tet(X)*). Air-drying beds were capable of reducing all gene target concentrations by 1 to 5 orders of magnitude, and the nature of this reduction was consistent with both a net decrease in the number of bacterial cells and lack of selection within the microbial community. Half-lives varied between 1.5 d (HF183) and 5.4 d (*tet(X)*) during the first 20 d of treatment. After the first 20 d of treatment, however, half-lives varied between 8.6 d (*tet(X)*) and 19.3 d (AllBac), and 16S rRNA gene, *intI1*, and *sulI* concentrations did not change ($P > 0.05$). These results demonstrate that air-drying beds can reduce ARG and *intI1* concentrations in residual municipal wastewater solids within timeframes typical of operating practices.

4.1 Introduction

Antibiotics are important to the success of modern medicine. Bacterial resistance to antibiotics, however, is believed to be an inevitable consequence of their use and eventually negates their benefits (199). Two solutions to the resistance problem are typically employed by medical practitioners. The first is to prescribe newer antibiotics for which there has not been sufficient time for resistance to develop (3). The second is to prescribe a combination of antibiotics to be taken simultaneously; this combination is typically lethal to the infectious microorganisms because multiple resistance is not as frequent as resistance to a single antibiotic (3). Unfortunately, both approaches are becoming less effective, which has led to a search for new solutions for managing antibiotic resistance.

As part of these efforts, antibiotic resistance genes (ARGs) have been identified as an emerging pollutant of concern (5). As with all pollutants, a critical component of elucidating and managing the fate of ARGs is identifying the environmental reservoirs from which they are currently discharged. One of the most important environmental reservoirs of ARGs appears to be municipal wastewater. ARGs have been found in relatively high concentrations at almost every point in the municipal wastewater treatment process, including the raw influent, primary effluent, aeration tanks, secondary effluent, and residual solids (5,10,21–32). The residual solids are of particular interest because they contain the vast majority of prokaryotic biomass in the treatment process, and, as a result, the vast majority of ARGs discharged from the treatment process (27). Thus, residual municipal wastewater solids treatment could be targeted as a key point in

the treatment process to implement strategies to reduce the quantity of ARGs discharged from municipal wastewater treatment plants.

Previous work has demonstrated the potential for some existing treatment technologies to reduce concentrations of ARGs in residual municipal wastewater solids. For instance, full-scale thermophilic anaerobic digestion has been demonstrated to remove substantial fractions ($\geq 75\%$) of *intI1*, *tet(A)*, *tet(O)*, and *tet(X)* relative to 16S rRNA genes (24). Furthermore, removal of 80% to 90% of *intI1*, *sul1*, *sul2*, *tet(G)*, and *tet(X)* genes has been demonstrated in laboratory-scale mesophilic anaerobic digestors, while similar removal efficiencies have been demonstrated for *intI1*, *sul1*, *sul2*, *erm(B)*, *erm(F)*, and *tet(W)* in laboratory-scale thermophilic anaerobic digestors (131). Half-lives for *intI1*, *tet(A)*, *tet(L)*, *tet(O)*, *tet(W)*, and *tet(X)* in anaerobic digestors appear to be on the order of days and may decrease with increasing temperature (121). However, the effect that other existing residual solids treatment technologies may have on ARG removal is poorly understood. These alternative technologies (e.g. aerobic digestion, air-drying, composting, lime stabilization, etc.) might also offer opportunities for reducing ARG concentrations in residual solids. Furthermore, approximately 80% of all treatment plants in the country employ technologies other than anaerobic digestion for treatment of residual solids (186). Many of these treatment plants serve small municipalities with limited financial and technical resources and, as a result, use less sophisticated types of residual solids treatment technology. Because of this, there is a need to assess the treatment potential of these technologies for their ability to remove ARGs.

Our overall hypothesis is that existing technologies for treating residual municipal wastewater solids can be used to reduce ARG concentrations during solids treatment. The goal of the work presented here was to assess the potential of air-drying beds to remove ARGs from municipal wastewater solids. Air drying is designated in the U.S. as a “Process to Significantly Reduce Pathogens” (PSRP). It is used to produce Class B treated residual solids at more than 400 U.S. wastewater treatment plants and is also used to dewater treated solids at approximately 30% of treatment plants in the United States (185,186). Air drying is accomplished by loading wastewater solids to a relatively shallow depth onto an outdoor drying bed, typically constructed of gravel, sand, and concrete or wood (184). The solids are left to dry for a minimum of three months, with an average ambient daily temperature above 0°C for at least two of those three months (185). Air-drying beds cause strong odors and tend to require a large physical footprint relative to alternative technologies. However, they are also simple to operate and are characterized by relatively low capital costs. As a result, they may represent a tractable strategy for removing ARGs from municipal wastewater solids in smaller treatment plants and sparsely populated municipalities if they are found to reduce ARG concentrations effectively.

4.2 Materials and Methods

Experimental Design. Three drying beds were constructed outdoors at the University of Minnesota. Each drying bed was approximately 0.6 m wide, 0.6 m long, and 0.6 m deep with two 8 cm (diameter) holes drilled in the bottom to allow for water drainage. A 15 cm layer of gravel, covered by a 15 cm layer of sand, was placed into

each drying bed to support the residual solids and allow for drainage. Residual solids, which consisted of a mixture of primary and secondary solids, were collected from a full-scale treatment plant in southern Minnesota.

Precipitation and temperature data were obtained from the Minnesota Climatology Working Group website for National Weather Service Station 214884 (44° 55' N, 93° 11' W) located near St. Anthony Falls, which is approximately 2 km west of where the drying beds were located. Moisture content was quantified periodically by collecting and weighing approximately 15 g triplicate samples from each drying bed. Solids were dried overnight at 103°C, allowed to cool in a desiccator, and weighed again. Moisture content was calculated as the fraction of the total mass lost during the drying process.

Sample Collection and Genomic DNA Extraction. Three 200 µL replicates (for “liquid” samples) or 500 mg replicates (for “dry” samples) were collected directly from the surface of each drying bed following thorough horizontal and vertical mixing of the drying bed contents. Each liquid sample was diluted with 500 µL of lysis buffer (120 mM sodium phosphate buffer, 5% dodecyl sulfate, pH 8.0 ± 0.1) and subjected to three consecutive freeze-thaw cycles followed by incubation at 70°C for 90 minutes. Genomic DNA was then extracted using a FastDNA Spin Kit (MP Biomedicals LLC, Solon, OH). Each dry sample was stored at -20°C until being mixed with 500 µL of lysis buffer (CLS-TC, MP Biomedicals LLC, Solon, OH) in bead-beating tubes (Lysis Matrix E, MP Biomedicals LLC, Solon, OH). Each tube was then subjected to bead-beating for 30 s in

a Bio101 Savant FastPrep instrument followed by genomic DNA extraction using a FastDNA Spin Kit for Soil (MP Biomedicals LLC, Solon, OH).

Quantitative PCR. Real-time quantitative PCR (qPCR) was used to quantify the concentrations of three tetracycline resistance genes (*tet(A)*, *tet(W)*, and *tet(X)*), an erythromycin resistance gene (*erm(B)*), a sulfonamide resistance gene (*sulI*), and the integrase gene of class 1 integrons (*intI1*) (24,95,151,200–202). The tetracycline resistance genes represent each of the three known tetracycline resistance mechanisms: efflux pumps, ribosomal protection proteins, and enzymatic modification systems, respectively (73). The erythromycin resistance gene encodes an rRNA methyltransferase that confers resistance to macrolides, lincosamides, and streptogramin B (74). These drugs are among the most frequently prescribed antibiotics in human medicine. Class 1 integrons were quantified due to their association with multiple antibiotic resistance; they enable bacteria to collect multiple, exogenous ARGs and modulate their expression (82). Real-time PCR was also used to determine the concentrations of 16S rRNA genes (a measure of total bacterial biomass), all *Bacteroides* spp. 16S rRNA genes (AllBac, a measure of total fecal material), and human-specific *Bacteroides* spp. 16S rRNA genes (HF183, a measure of human fecal material) (194–196,203). The primer sequences, expected amplicon size, and annealing temperature of each gene target can be found in Table B.1.

Real-time PCR was carried out using an Eppendorf Mastercycler EP Realplex thermal cycler (Eppendorf, Westbury, NY). PCR assays were optimized to reduce or eliminate the formation of primer-dimers and other non-specific products. Typical qPCR

assays began with a 1 min initial denaturation at 95°C, followed by 40 cycles of denaturation at 95°C for 15 s and combined annealing and extension at the primer-specific annealing temperature for 1 min. Reaction volumes of 25 µL consisted of 12.5 µL of BioRad iTaq SYBR Green Supermix with ROX (Life Science Research, Hercules, CA), 25 µg of bovine serum albumin, optimized quantities of forward and reverse primers, and approximately 1 ng of template genomic DNA. Standards were made from PCR products selected from municipal wastewater solids or well-described bacterial isolates. PCR products were ligated into a pGEM-T Easy cloning vector, transformed into JM109 competent cells, and extracted from cell cultures using an alkaline lysis procedure (197). The DNA concentrations of qPCR standards were quantified using a TD-700 fluorometer and Hoechst 33258 dye. The standard curve for each real-time PCR assay consisted of a 10-fold dilution series of the qPCR standard containing at least 7 points ($r^2 \geq 0.99$). Amplification efficiencies were $100\% \pm 12\%$ (maximum deviation from 100%).

Data Analysis. Simple linear regression (obtained using Arc 1.06) was used to determine the goodness of fit of the data to both a monophasic first-order kinetic model and a biphasic first-order kinetic model. The monophasic first-order kinetic model was initially hypothesized based on previous empirical observations that it tends to fit this type of data well for a variety of gene targets in several different environmental conditions (115,121,170,204). It also provides a useful interpretive tool and basis of comparison to other studies that may consider different gene targets and environmental conditions. However, a formal lack-of-fit test provided evidence that several time series

of gene target concentrations varied significantly ($P \leq 0.05$) from the fitted monophasic first-order kinetic models (205). A biphasic first-order model was subsequently hypothesized based on the observation that the time series trends of drying bed moisture content and several gene targets appeared to be biphasic, with the major switch in rates occurring at approximately 20 d. A biphasic pattern is also consistent with empirical observations of the behavior of gene targets representing ARGs in surface waters and fecal indicators in manure-amended soils (115,206,207). The biphasic first-order model was constructed by splitting each time series of gene target concentrations into two phases and determining independent first-order kinetic fits for each phase using simple linear regression (obtained using Arc 1.06). The first phase of each biphasic model contains gene target concentrations for times less than 20 d, while the second phase contains gene target concentrations for times greater than 20 d.

4.3 Results

Residual municipal wastewater solids in each bed dried substantially over the course of the experiment despite several relatively large precipitation events (> 2 cm) during the first 50 d (Figure 4.1). Drying took place over the course of more than 3 months, during which the ambient air temperature remained above 0°C. The moisture content of the drying solids was approximately 70% after 10 d, which is consistent with expectations for full-scale drying beds operated under favorable conditions (184).

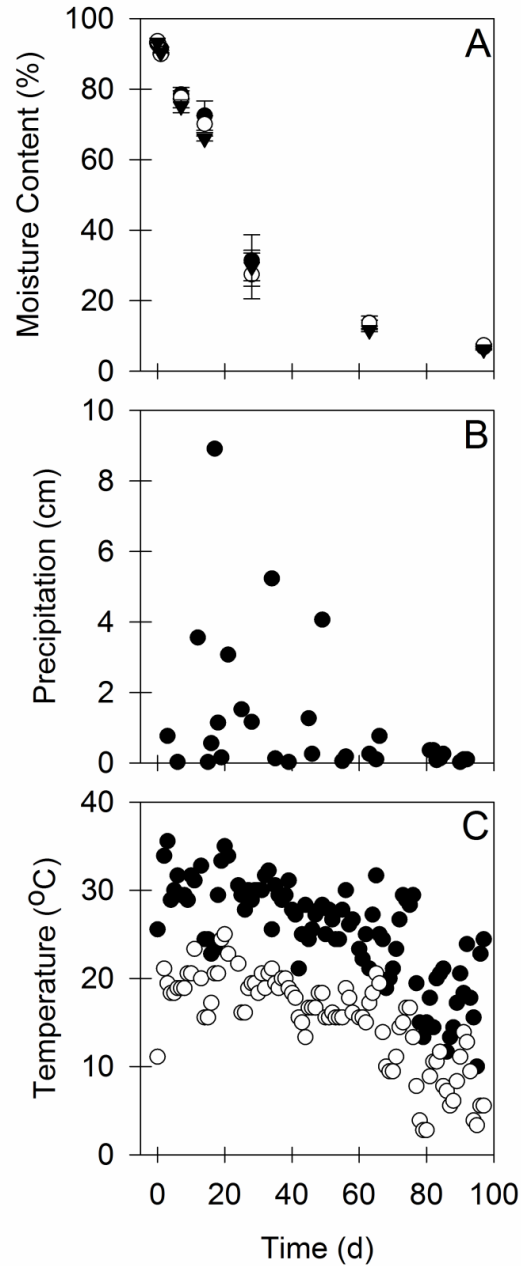


Figure 4.1. The (A) moisture content in three replicate drying beds (closed circles, open circles, and closed triangles represent unique experimental replicates), (B) daily precipitation, and (C) daily maximum (closed circles) and minimum (open circles) temperatures. Values for moisture content are the arithmetic mean of triplicate samples; error bars represent one standard deviation.

Total bacterial biomass and the concentrations of fecal bacteria decreased over time, although they followed separate patterns (Figure 4.2). The concentration of 16S rRNA genes decreased by an order of magnitude during the first 10 d and then remained constant for the duration of the experiment. In contrast, the concentration of all *Bacteroides* spp. 16S rRNA genes decreased rapidly by 4 orders of magnitude during the first 30 d and continued to decrease for the remainder of the experiment. Similarly, the concentration of human-specific *Bacteroides* spp. 16S rRNA genes decreased rapidly during the first 10 d of the experiment, after which they were below the detection limit (5.7×10^7 copies g⁻¹ dry weight).

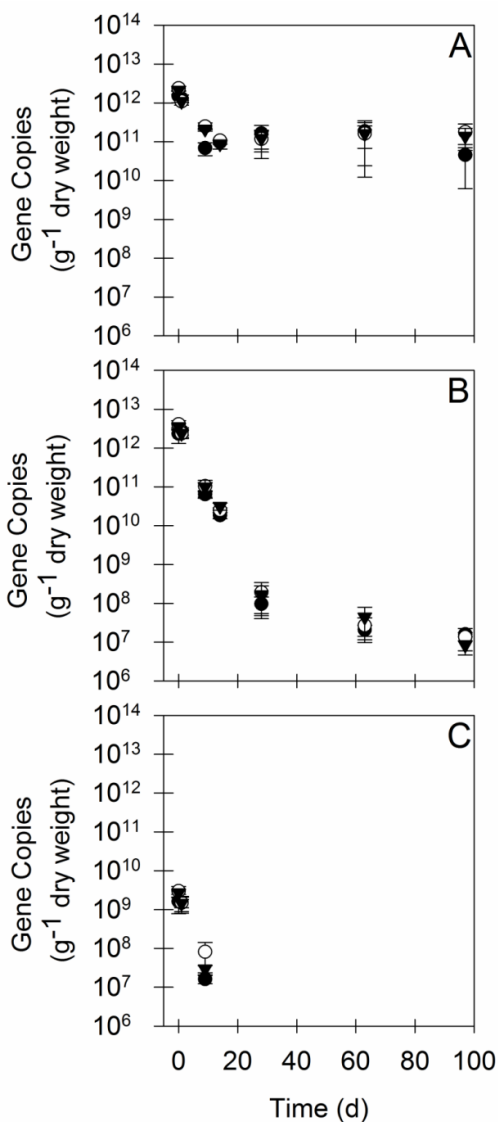


Figure 4.2. The quantities of (A) 16S rRNA genes, (B) fecal indicator bacteria as measured by 16S rRNA genes of all *Bacteroides* spp. (AllBac), and (C) fecal indicator bacteria as measured by 16S rRNA genes of human-specific *Bacteroides* spp. (HF183) in residual solids applied to three replicate drying beds (closed circles, open circles, and closed triangles represent unique experimental replicates). Values are the arithmetic mean of triplicate samples; error bars represent one standard deviation.

Concentrations of all ARGs and *intI1* decreased, although the rate and extent depended on the specific gene target (Figure 4.3). Two targets, *intI1* and *sulI*, exhibited patterns similar to that of the 16S rRNA gene; they decreased by an order of magnitude within the first 10 d and then remained constant for the remainder of the experiment. In contrast, concentrations of *erm(B)*, *tet(A)*, and *tet(W)* all decreased by 4 to 5 orders of magnitude during the course of the experiment. The concentration of *tet(X)*, however, exhibited a unique pattern among the gene targets examined in this study. The *tet(X)* concentration initially decreased by an order of magnitude within the first 10 d, but then increased by nearly 2 orders of magnitude by 27 d, after which it again decreased for the remainder of the experiment.

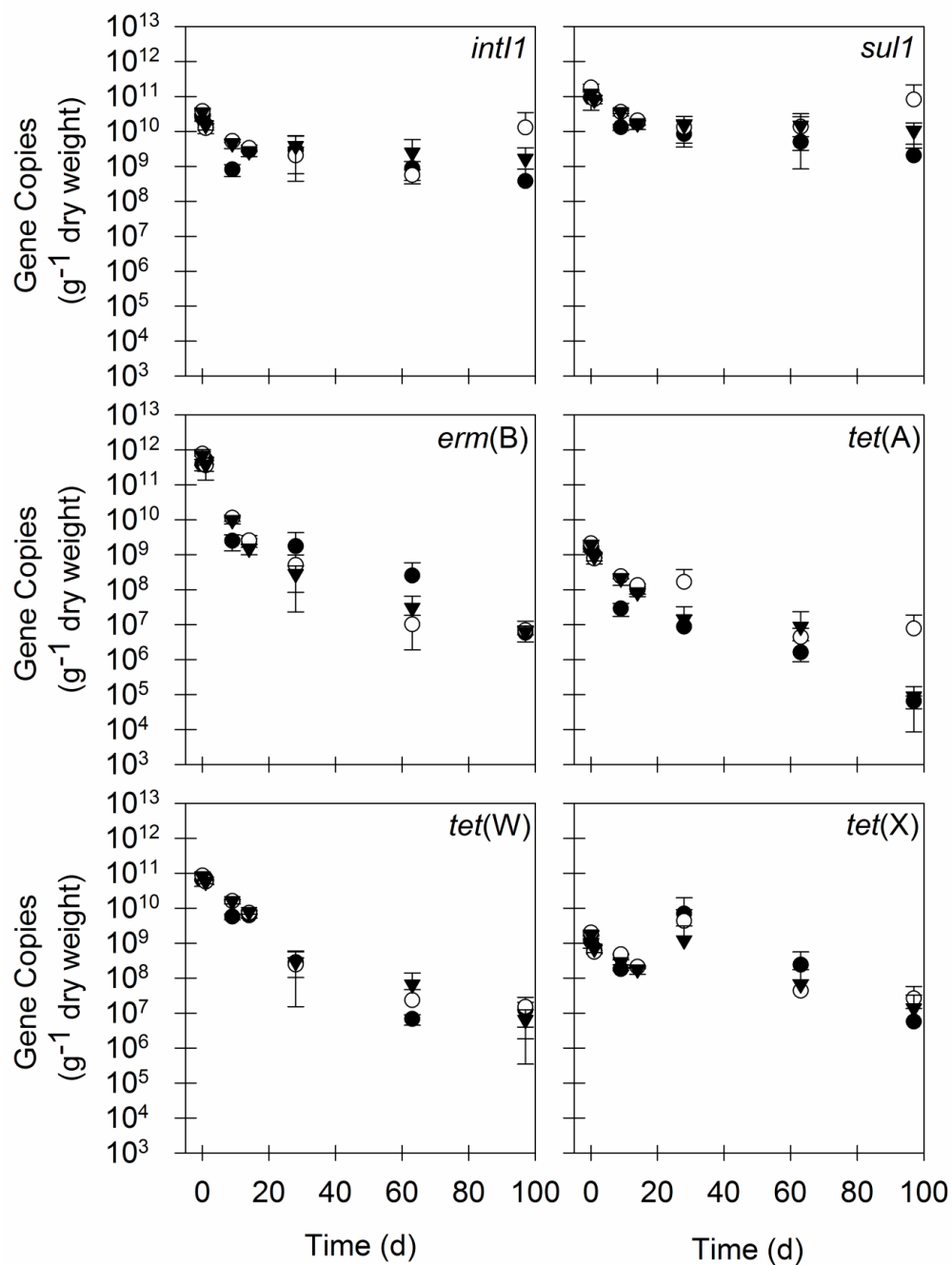


Figure 4.3. The quantities of *int11*, *sul1*, *erm(B)*, *tet(A)*, *tet(W)*, and *tet(X)* in residual solids applied to three replicate drying beds (closed circles, open circles, and closed triangles represent unique experimental replicates). Values are the arithmetic mean of triplicate samples; error bars represent one standard deviation.

The ratios of ARGs and *intI1* to the 16S rRNA gene concentration exhibited distinct patterns compared to absolute concentrations (Figure 4.4). The ratios of *intI1* and *sulI* to the 16S rRNA gene remained constant throughout the experiment, while the ratios of *tet(A)* and *tet(W)* to the 16S rRNA gene remained constant for time less than 20 d, after which they decreased. Only the ratio of *erm(B)* decreased throughout the course of the experiment relative to 16S rRNA genes, and the ratio of *tet(X)* to 16S rRNA genes initially increased for the first 20 d, after which it decreased.

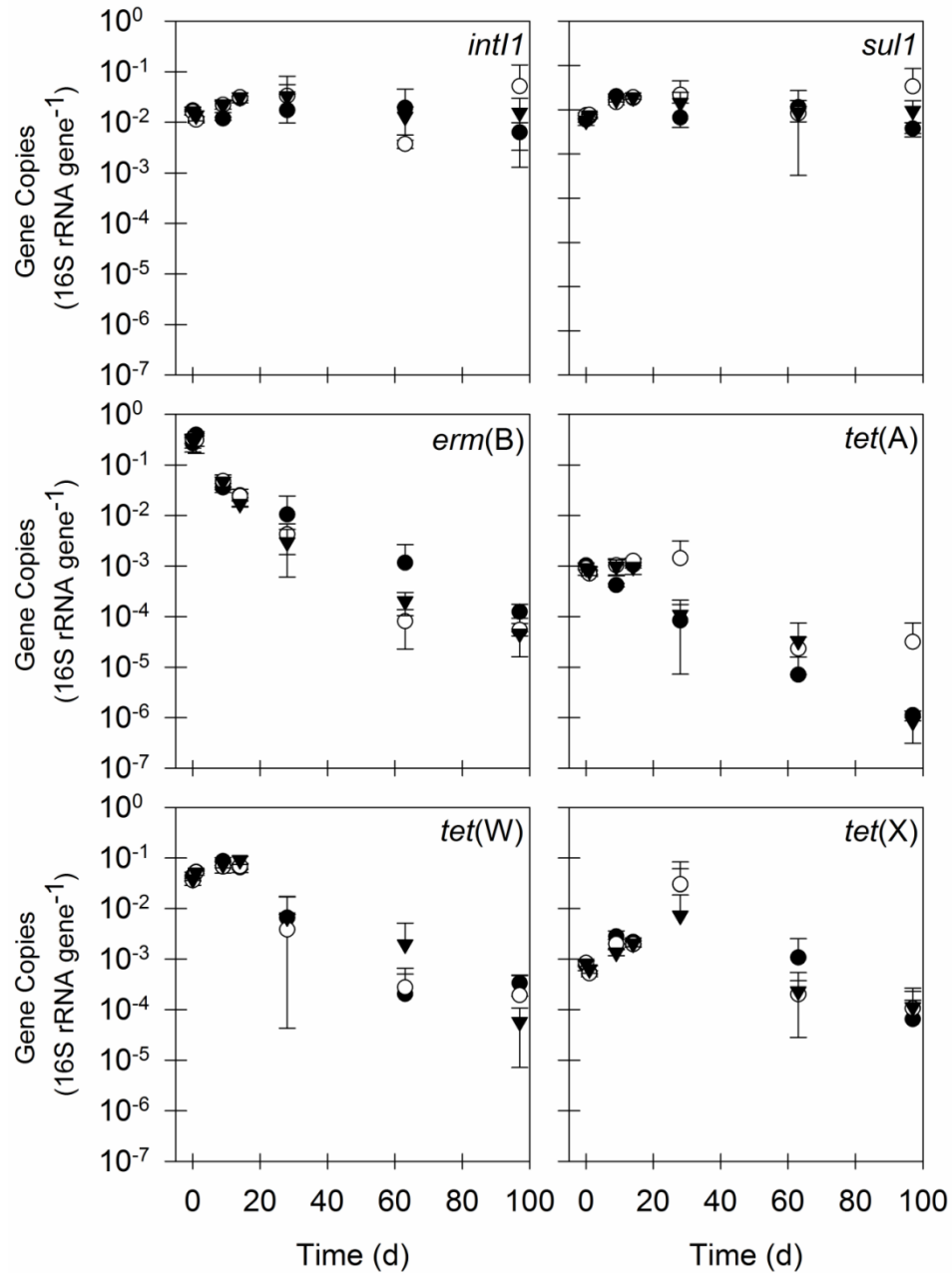


Figure 4.4. The ratios of *intI1*, *sul1*, *erm(B)*, *tet(A)*, *tet(W)*, and *tet(X)* to the 16S rRNA gene in residual solids applied to three replicate drying beds (closed circles, open circles, and closed triangles represent unique experimental replicates). Values are the arithmetic mean of triplicate samples; error bars represent one standard deviation.

A biphasic first-order kinetic model fit the data better than a monophasic first-order kinetic model for concentrations of ARGs and *intII* (Table 4.1 and Table 4.2). When the concentrations of each gene target were modeled as monophasic first-order kinetic processes, half-lives varied between 1.5 d (16S rRNA gene of human-specific *Bacteroides* spp.) and 36.7 d (16S rRNA gene). However, according to lack-of-fit P values, only the concentrations of *tet(A)* and the 16S rRNA gene from human-specific *Bacteroides* spp. fit a monophasic first-order model well ($P > 0.05$). In contrast, 15 of 17 time series for the biphasic models are characterized by favorable ($P > 0.05$) lack-of-fit P values. Half-lives for concentrations of gene targets in the first 20 d of the experiment varied between 1.5 d for the human-specific *Bacteroides* spp. 16S rRNA gene and 5.4 d for *tet(X)*. Half-lives for concentrations of gene targets after the first 20 d varied between 8.6 d for *tet(X)* and 19.3 d for all *Bacteroides* spp. 16S rRNA genes, while concentrations of the 16S rRNA gene, *intII*, and *sulI* did not change ($P > 0.05$).

Table 4.1. First-order kinetic coefficients (k)^a, half-lives ($t_{1/2}$), r^2 , and lack-of-fit P from monophasic first-order kinetic models of gene target concentrations in 3 replicate drying beds.

Gene Target	k (d ⁻¹) ± Std. Error (d ⁻¹)	$t_{1/2}$ (d)	r^2	Lack-of-fit P
16S rRNA gene	-1.9×10 ⁻² ± 6.8×10 ⁻³	36.7	0.29	< 1×10 ⁻⁴
all <i>Bacteroides</i> spp.	-1.3×10 ⁻¹ ± 1.5×10 ⁻²	5.4	0.79	< 1×10 ⁻⁴
human-specific <i>Bacteroides</i> spp.	-4.7×10 ⁻¹ ± 3.9×10 ⁻²	1.5	0.95	0.99
<i>erm</i> (B)	-1.1×10 ⁻¹ ± 1.2×10 ⁻²	6.4	0.81	< 1×10 ⁻⁴
<i>intI1</i>	-2.2×10 ⁻² ± 7.2×10 ⁻³	31.7	0.32	2×10 ⁻⁵
<i>sulI</i>	-2.0×10 ⁻² ± 6.2×10 ⁻³	35.3	0.34	0.05

<i>tet</i> (A)	$-7.9 \times 10^{-2} \pm 8.7 \times 10^{-3}$	8.8	0.81	0.34
<i>tet</i> (W)	$-9.5 \times 10^{-2} \pm 8.2 \times 10^{-3}$	7.3	0.88	$< 1 \times 10^{-4}$
<i>tet</i> (X)	$-4.0 \times 10^{-2} \pm 7.9 \times 10^{-3}$	17.2	0.58	1×10^{-4}

^aAll kinetic coefficients were regressed from 21 data points (7 time points \times 3 replicate drying beds), except for the human-specific *Bacteroides* spp. coefficient, which was regressed from 9 data points (3 time points \times 3 replicate drying beds). All kinetic coefficients are statistically significant ($P < 0.05$).

Table 4.2. First-order kinetic coefficients (k)^a, half-lives ($t_{1/2}$), r^2 , P , and lack-of-fit P from biphasic first-order kinetic models of gene target concentrations in 3 replicate drying beds.

Gene Target	Phase	k (d ⁻¹)	±	Std. Error (d ⁻¹)	$t_{1/2}$ (d)	r^2	P	Lack-of-fit P
16S rRNA gene	< 20 days	-2.2×10 ⁻¹	±	2.2×10 ⁻²	3.2	0.91	< 1×10 ⁻⁴	0.12
16S rRNA gene	> 20 days	-3.5×10 ⁻³	±	5.3×10 ⁻³	200.8	0.06	0.54	0.28
all <i>Bacteroides</i> spp.	< 20 days	-3.6×10 ⁻¹	±	1.6×10 ⁻²	1.9	0.98	< 1×10 ⁻⁴	0.05
all <i>Bacteroides</i> spp.	> 20 days	-3.6×10 ⁻²	±	4.5×10 ⁻³	19.3	0.90	1×10 ⁻⁴	0.22
human-specific <i>Bacteroides</i> spp.	< 20 days	-4.7×10 ⁻¹	±	3.9×10 ⁻²	1.5	0.95	< 1×10 ⁻⁴	0.99
human-specific <i>Bacteroides</i> spp.	> 20 days	ND ^b			ND	ND	ND	ND

<i>erm</i> (B)	< 20 days	-4.2×10^{-1}	\pm	3.0×10^{-2}	1.6	0.95	$< 1 \times 10^{-4}$	0.09
<i>erm</i> (B)	> 20 days	-6.7×10^{-2}	\pm	1.2×10^{-2}	10.4	0.81	9×10^{-4}	0.66
<i>intI1</i>	< 20 days	-1.7×10^{-1}	\pm	3.3×10^{-2}	4.1	0.72	5×10^{-4}	0.08
<i>intI1</i>	> 20 days	-5.1×10^{-3}	\pm	1.3×10^{-2}	136.0	0.02	0.71	0.35
<i>sulI</i>	< 20 days	-1.4×10^{-1}	\pm	1.7×10^{-2}	5.1	0.86	$< 1 \times 10^{-4}$	0.32
<i>sulI</i>	> 20 days	2×10^{-4}	\pm	1.3×10^{-2}	-3,191.3	0.00	0.99	0.83
<i>tet</i> (A)	< 20 days	-2.1×10^{-1}	\pm	3.5×10^{-2}	3.4	0.78	1×10^{-4}	0.14
<i>tet</i> (A)	> 20 days	-6.3×10^{-2}	\pm	2.0×10^{-2}	11.0	0.58	2×10^{-2}	0.84
<i>tet</i> (W)	< 20 days	-1.8×10^{-1}	\pm	1.6×10^{-2}	3.9	0.92	$< 1 \times 10^{-4}$	0.29

<i>tet</i> (W)	> 20 days	-4.7×10^{-2}	$\pm 9.5 \times 10^{-3}$	14.7	0.78	2×10^{-3}	0.13
<i>tet</i> (X)	< 20 days	-1.3×10^{-1}	$\pm 2.0 \times 10^{-2}$	5.4	0.80	1×10^{-4}	0.03
<i>tet</i> (X)	> 20 days	-8.1×10^{-2}	$\pm 1.1 \times 10^{-2}$	8.6	0.89	1×10^{-4}	0.24

^aAll kinetic coefficients for time less than 20 d were regressed from 12 data points (4 time points \times 3 replicate drying beds), except for the human-specific *Bacteroides* spp. coefficient, which was regressed from 9 data points (3 time points \times 3 replicate drying beds). All kinetic coefficients for time greater than 20 d were regressed from 9 data points (3 time points \times 3 replicate drying beds).

^bHuman-specific *Bacteroides* spp. were below the detection limit (5.7×10^7 copies g⁻¹ dry weight) for time greater than 20 d, so *k* was not determined (ND).

A biphasic first-order kinetic model also fit well for the ratios of ARGs and *intI1* to the 16S rRNA gene (Table 4.3). During the first 20 d of the experiment, the half-life for the ratio of *erm(B)* to 16S rRNA genes was 3.3 d, and the ratio of *tet(A)* to 16S rRNA genes did not change ($P > 0.05$). Ratios of the remaining ARGs and *intI1* to 16S rRNA genes actually increased ($P \leq 0.05$) during the first 20 d, with doubling times varying between 7.9 d for *tet(X)* and 16.9 d for *tet(W)*. After the first 20 d, the ratios of *intI1* and *sulI* to 16S rRNA genes did not change ($P > 0.05$), while half-lives for ratios of the remaining ARGs to 16S rRNA genes varied between 9.0 d for *tet(X)* and 15.9 d for *tet(W)*.

Table 4.3. First-order kinetic coefficients (k)^a, half-lives ($t_{1/2}$), r^2 , P , and lack-of-fit P from biphasic first-order kinetic models of gene target to 16S rRNA gene ratios in 3 replicate drying beds.

Gene Target	Phase	k (d ⁻¹)	±	Std. Error (d ⁻¹)	$t_{1/2}$ (d)	r^2	P	Lack-of-fit P
<i>erm</i> (B)	< 20 days	-2.1×10 ⁻¹	±	1.2×10 ⁻²	3.4	0.97	< 1×10 ⁻⁴	0.01
<i>erm</i> (B)	> 20 days	-6.3×10 ⁻²	±	1.1×10 ⁻²	11.1	0.82	8×10 ⁻⁴	0.29
<i>intI1</i>	< 20 days	5.0×10 ⁻²	±	1.2×10 ⁻²	-13.8	0.63	2×10 ⁻³	0.04
<i>intI1</i>	> 20 days	-1.6×10 ⁻³	±	1.2×10 ⁻²	421.3	0.00	0.89	0.09
<i>sul1</i>	< 20 days	8.2×10 ⁻²	±	8.1×10 ⁻³	-8.5	0.91	< 1×10 ⁻⁴	0.02
<i>sul1</i>	> 20 days	-2.7×10 ⁻³	±	8.1×10 ⁻³	259.5	0.02	0.75	0.69

<i>tet</i> (A)	< 20 days	1.1×10^{-2}	$\pm 1.4 \times 10^{-2}$	-63.5	0.06	0.45	0.24
<i>tet</i> (A)	> 20 days	-6.0×10^{-2}	$\pm 1.9 \times 10^{-2}$	11.7	0.59	2×10^{-2}	0.94
<i>tet</i> (W)	< 20 days	4.1×10^{-2}	$\pm 8.2 \times 10^{-3}$	-16.9	0.71	6×10^{-4}	0.02
<i>tet</i> (W)	> 20 days	-4.4×10^{-2}	$\pm 1.2 \times 10^{-2}$	15.9	0.64	1×10^{-2}	0.09
<i>tet</i> (X)	< 20 days	8.8×10^{-2}	$\pm 1.4 \times 10^{-2}$	-7.9	0.79	1×10^{-4}	9×10^{-3}
<i>tet</i> (X)	> 20 days	-7.7×10^{-2}	$\pm 1.0 \times 10^{-2}$	9.0	0.89	1×10^{-4}	0.05

^aAll kinetic coefficients for time less than 20 d were regressed from 12 data points (4 time points \times 3 replicate drying beds). All kinetic coefficients for time greater than 20 d were regressed from 9 data points (3 time points \times 3 replicate drying beds).

4.4 Discussion

Air-drying beds can be used to reduce ARG concentrations in residual municipal wastewater solids. In this study, the concentrations of gene targets for *erm*(B), *tet*(A), *tet*(W), and *tet*(X) were reduced by 2 to 5 orders of magnitude over the course of 100 d, while concentrations of the most persistent gene targets in the group, *intI1* and *sul1*, were reduced by approximately an order of magnitude. The extents of gene loss found here are comparable to those found for the same genes in other treatment technologies, including mesophilic anaerobic digestion, thermophilic anaerobic digestion, and aerobic digestion (24,121,131,204). Thus, small municipalities with limited resources, which are likely to find drying beds appealing for residual solids treatment due to their low capital and operating costs, may be able to achieve significant reduction of ARG concentrations with air-drying beds. Furthermore, municipalities that use drying beds for dewatering treated residual solids (approximately 30% in the U.S.) may be able to use air-drying beds to provide further ARG removal in addition to that achieved by upstream treatment units (186).

Drying beds, however, do not reduce ARG concentrations in residual municipal wastewater solids as quickly as other treatment technologies. The half-lives determined here for *erm*(B), *intI1*, *sul1*, *tet*(A), *tet*(W), and *tet*(X) within the first 20 d of treatment in drying beds are similar to those in aerobic digestion at approximately 20°C, where they vary between approximately 3 and 6 d (204). However, half-lives for *intI1*, *tet*(A), *tet*(W), and *tet*(X) vary between 0.7 and 5 d in mesophilic anaerobic digestion and between 0.2 and 2 d in thermophilic anaerobic digestion (121). As a result, air-drying

beds may not be as practical an option for removing ARGs at wastewater treatment plants with large flow volumes, because the relatively slow kinetics will require treatment units with extremely large physical footprints.

The persistence of *intI1*, which represents class 1 integrons, may be of particular concern. Integrons enable bacteria to collect and manage multiple exogenous genes with little or no genetic cost (82). When integrons contain multiple ARGs, they may result in microorganisms resistant to multiple antibiotics, which are the most difficult to treat in patients with antibiotic resistant infections. Thus, the most persistent gene target considered in this work may also represent the genetic element with the most serious consequences for human health. However, the relationship between class 1 integrons and the ARGs considered in this work is not clear, because ARG concentrations decrease substantially while concentrations of *intI1* are relatively persistent. Future work should be directed at determining the genetic content of integrons that persist during residual solids treatment (198). If these integrons are found to harbor multiple ARGs, then *intI1* may qualify for consideration as a “design gene”. Under the “ARGs are pollutants” paradigm, the design gene would be the gene that limits the design (e.g. tank size) of individual treatment units because its concentration is reduced most slowly among all the potential genes that might be of interest due to their consequences for human health.

We hypothesize that reduction of ARG and *intI1* concentrations in residual municipal wastewater solids during this study was due to both a net decrease in the number of bacterial cells (i.e. 16S rRNA genes) and lack of selection for ARGs within the bacterial community. The biphasic first-order kinetic model shows that

concentrations of all ARGs and *intI1* are reduced relatively quickly within the first 20 d, after which degradation appears to slow down significantly or stop (Table 4.2). The rates at which *intI1* and *sulI* concentrations are reduced relative to 16S rRNA genes, however, are not statistically significant throughout the course of the experiment (Table 4.3). Furthermore, the first-order rate coefficients for *tet(A)* and *tet(W)* normalized to 16S rRNA genes are also not statistically significant for time less than 20 d, while concentrations of *tet(X)* normalized to 16S rRNA genes increase for time < 20 d. Thus, all reduction of these gene concentrations during the first 20 d appears to be due to a net decrease in the number of bacterial cells (i.e. reduction of 16S rRNA gene concentrations), while any reduction that takes place after 20 d for *tet(A)*, *tet(W)*, and *tet(X)* appears to be due to lack of selection for ARGs within the microbial community. As a result, the overall first-order rate coefficients for concentrations of all ARGs and *intI1* (Table 4.2) in each phase are equal to the sum of the 16S rRNA gene first-order rate coefficient for that phase and the first-order rate coefficient for the ARG (or *intI1*) relative to 16S rRNA genes for that same phase (Table 4.3). This suggests that ARGs can be removed from residual municipal wastewater solids both by enhancing net cell death and by optimizing conditions in treatment units to avoid selection for known ecological characteristics (e.g. redox regime) of particular ARGs.

Although the approach used here provides the advantages of being quantitative and culture-independent, it has several significant limitations. First, our real-time qPCR protocol does not provide the capability to distinguish between genes that are in live or dead bacterial cells. Similarly, our qPCR protocol does not indicate whether genes can

be expressed in their current bacterial hosts. Finally, this study investigates only a small fraction of the known ARGs. For example, at least 30 ARGs are known to encode tetracycline resistance, yet we have considered only 3 (73). We have attempted to include a cross-section of resistance mechanisms, antibiotic classes, and genes of clinical relevance, but the fate of the ARGs considered here does not necessarily reflect that of all ARGs.

**Chapter 5: The Kinetics of Declining Antibiotic Resistance Gene and
Class 1 Integron Quantities During Hyperthermophilic Anaerobic
Digestion of Residual Municipal Wastewater Solids**

A number of treatment technologies have been investigated for their potential to remove antibiotic resistance genes (ARGs), which are increasingly regarded as environmental pollutants, from residual municipal wastewater solids. The work presented here investigates hyperthermophilic ($\geq 60^{\circ}\text{C}$) anaerobic digestion for this purpose. Four laboratory-scale anaerobic digesters were operated in eight-day batch cycles at temperatures of 40°C , 56°C , 60°C , and 63°C . Two tetracycline resistance genes (*tet(W)* and *tet(X)*), a fluoroquinolone resistance gene (*qnrA*), the integrase gene of class 1 integrons (*intI1*), the origin of replication of incompatibility group A/C plasmids (*repA*), 16S rRNA genes, 16S rRNA genes of all *Bacteroides* spp. (AllBac), and 16S rRNA genes of methanogens were quantified using real-time PCR. ARG and *intI1* quantities decreased at all temperatures, and the form of most of these decreases was found to best fit a modified form of the Collins-Selleck disinfection kinetic model. The magnitude of Collins-Selleck kinetic parameters tended to increase with temperature, although these increases were often not statistically significant ($P \geq 0.05$). This work demonstrates the potential for hyperthermophilic anaerobic digestion to be an effective technology for removing ARGs and *intI1* from residual municipal wastewater solids. It also demonstrates the benefits of a modified form of the Collins-Selleck kinetic model for describing trends of ARG and *intI1* quantities with time during semi-batch anaerobic digestion of residual municipal wastewater solids.

5.1 Introduction

Pathogenic resistance to antibiotic chemotherapy is a significant public health dilemma. Antibiotic resistant infections account for at least two million illnesses and 23,000 deaths per year in the United States (65). Meanwhile, the rate of antibiotic development has slowed considerably in recent years, from more than 15 new approved drugs between 1980 and 1984 to just one between 2010 and 2012 (65). Potential solutions to antibiotic resistance include redoubling efforts to develop new antibiotics, developing alternatives to antibiotics, and making major policy decisions to use antibiotics more frugally (e.g. in agriculture) (2,87–89,188). This multi-component approach is likely to continue well into the future, and researchers from the environmental science and engineering community have recently proposed an additional component to complement existing strategies. This new approach relies on identifying antibiotic resistance genes (ARGs) as environmental contaminants (5), identifying their environmental reservoirs, and developing technology and management strategies to minimize their discharge from these reservoirs.

One of the largest identified reservoirs appears to be residual municipal wastewater solids (27). Prior research has demonstrated that existing treatment technologies can reduce the quantities of ARGs and *intI1* discharged from the municipal wastewater treatment process in treated residual wastewater solids. These technologies include air-drying beds, mesophilic and thermophilic aerobic digestion, and mesophilic and thermophilic anaerobic digestion (121,131,204,208). Among these, variants of anaerobic digestion seem critically important because mesophilic anaerobic digestion is

currently used to treat approximately 50% of all residual municipal wastewater solids produced in the United States (186), and thermophilic anaerobic digestion represents an infrastructural and operational upgrade to mesophilic anaerobic digestion that could be pursued as an alternative treatment strategy if found to be more effective at removing ARGs from residual wastewater solids.

Thermophilic anaerobic digestion has been demonstrated to substantially outperform mesophilic anaerobic digestion at times, although the benefits of increasingly higher temperatures are not clear, and the relative performance of the two technologies appears to vary a great deal based on flow regime in addition to temperature. For instance, semi-continuous-flow thermophilic (47°C, 52°C, and 59°C) digestion has been demonstrated to achieve up to one to three orders of magnitude greater removal of *erm*(B), *erm*(F), *tet*(O), and *tet*(W) compared to mesophilic (37°C) anaerobic digestion, although differences in extent of ARG removal among the three thermophilic digestion temperatures were frequently not obvious (131). In the same work, semi-continuous-flow thermophilic digestion at all three temperatures also performed the same or worse for removing *intI1*, *sul1*, *sul2*, *tet*(C), *tet*(G), and *tet*(X) relative to mesophilic anaerobic digestion (131). In contrast, semi-batch thermophilic (55°C) anaerobic digesters operated in five-day batch cycles were shown to reduce quantities of *intI1*, *tet*(A), *tet*(O), *tet*(W), and *tet*(X) by an additional order of magnitude relative to mesophilic (37°C) anaerobic digesters operated under otherwise similar conditions (121). A similar dependence of the extents of removal for ARGs and *intI1* on flow regime has also been demonstrated for aerobic digestion at 15°C (204).

The objective of this work was to assess the potential for semi-batch hyperthermophilic ($\geq 60^{\circ}\text{C}$) anaerobic digestion to remove ARGs and *intI1* from residual municipal wastewater solids. It was hypothesized that, just as thermophilic anaerobic digestion increased rates of removal relative to mesophilic anaerobic digestion during semi-batch treatment, increasing digestion temperatures into the hyperthermophilic range would provide even faster rates of removal. The experiment described here was designed to produce relatively long batch periods of anaerobic digestion to facilitate kinetic modeling and to maximize differences in the degree of ARG and *intI1* removal among different temperatures. Two hyperthermophilic digesters were operated at 60°C and 63°C . Two additional digesters were operated at 40°C and 56°C in order to act as experimental controls. All four digesters were operated for ten eight-day batches at relatively steady end-of-batch residence times. The influent (untreated residual municipal wastewater solids) and effluent of each digester were sampled for all ten batches, and within-batch time series of samples were collected for each of the final three batches. Real-time PCR was used to quantify bacterial 16S rRNA genes, 16S rRNA genes of all *Bacteroides* spp. (AllBac), 16S rRNA genes of methanogens, *intI1*, *qnrA*, *repA*, *tet(W)*, and *tet(X)* in all samples. Data from the first seven batches for each digester were used to assess the degree to which digesters achieved consistent removal of each gene target, and data from the final three batches for each digester were fit against first-order, second-order, and a modified form of the Collins-Selleck kinetic expressions in order to determine their goodness of fit to those models.

5.2 Materials and Methods

Experimental Design. Four six-L anaerobic digesters were inoculated with a mixture of untreated residual municipal wastewater solids and mesophilic anaerobic digester solids from a full-scale municipal wastewater treatment plant in southern Minnesota. The digesters were operated at temperatures of 40°C, 56°C, 60°C, and 63°C with residence times between 32 and 36 days. Mixing was provided by magnetic stir plates and heating was provided by heat tape controlled by Johnson Controls A419ABG-3C Electronic Temperature Controls equipped with Johnson Controls A99B Series Temperature Sensors (Johnson Controls, Milwaukee, WI). After each digester achieved consistent methane production, the four digesters were operated for 80 days while being fed untreated residual municipal wastewater solids every eight days. Samples were collected for genomic DNA extraction from each digester at the end of each of the first seven eight-day batches and at six time points within each of the final three eight-day batches. Samples were collected for genomic DNA extraction from the untreated residual municipal wastewater solids at the beginning of each eight-day batch.

Typical operating variables, including temperature, pH, total solids (TS), volatile solids (VS), inert solids (IS), gas production, and gas methane content were monitored throughout the entire time period the digesters were in operation. Temperature was read directly from the A419ABG-3C Electronic Temperature Control units, while pH was measured using a Corning 430 (Corning, Tewksbury, MA) pH meter and a Pinnacle Model 476466 3-in-1 Electrode (Nova Analytics Corporation, Woburn, MA). TS was measured by collecting approximately 50-mL triplicate samples from each digester and

recording the fraction of mass remaining for each sample following overnight oven-drying at 103°C to 105°C. VS was measured by combusting the remaining oven-dried fraction of each sample at 550°C for at least two hours and recording the fraction of mass lost during combustion. Gas production was measured by collecting the gas produced during each feeding cycle in a 16-L Tedlar bag and then forcing the contents of the bag through a gas meter and recording the total volume of gas that had been contained in the bag. Finally, methane content was measured using a Hewlett Packard HP 6890 Series gas chromatographer (GC) with a thermal conductivity detector (TCD).

Sample Collection and Genomic DNA Extraction. Triplicate samples (100 µL) were collected from larger aliquots (50 to 300 mL) of digester contents to ensure accurate sample collection volumes. Samples were then diluted with 500 µL of lysis buffer (120 mM sodium phosphate buffer, 5% dodecyl sulfate, pH 8.0 ± 0.1) and subjected to three consecutive freeze-thaw cycles followed by incubation at 70°C for 90 minutes. Genomic DNA was extracted using a FastDNA SPIN Kit (MP Biomedicals LLC, Solon, OH) according to the manufacturer's instructions.

Quantitative PCR. Real-time PCR was conducted to quantify 16S rRNA genes, AllBac, 16S rRNA genes of methanogens, the integrase gene of class 1 integrons (*intI1*), a fluoroquinolone resistance gene (*qnrA*), and two tetracycline resistance genes (*tet(X)* and *tet(W)*) as described previously (8,24,95,195,196,201,209). The 16S rRNA gene was quantified as a measure of total bacterial biomass, AllBac was used as a representative fecal indicator, and 16S rRNA genes of methanogens were quantified as an additional line of evidence for methanogenesis in the anaerobic digesters. The integrase of class 1

integrations was quantified due to its association with multiple antibiotic resistance and horizontal gene transfer (82). The fluoroquinolone resistance gene was quantified because it confers resistance to one of the most recently developed and widely used human antibiotics. Finally, the tetracycline resistance genes represent two of the three known tetracycline resistance mechanisms: enzymatic modification systems (*tet(X)*) and ribosomal protection proteins (*tet(W)*) (73). Furthermore, *tet(X)* requires the presence of oxygen to be expressed (210,211), while *tet(W)* tends to be found in anaerobic microorganisms (212). As a result, these genes may be expected to exhibit divergent fates during anaerobic digestion of residual municipal wastewater solids as has been demonstrated for aerobic digestion of residual municipal wastewater solids (204). Real-time PCR was also used to quantify the origin of replication (replication initiation protein A) for incompatibility group A/C plasmids (*repA*). The *repA* method was developed in collaboration with Timothy Johnson and Kevin Lang of the University of Minnesota Department of Veterinary and Biomedical Sciences (St. Paul, Minnesota, United States). Table C.1 contains the forward and reverse primer sequences, expected amplicon sizes, and primer annealing temperatures for all gene targets considered in this work (8,24,95,195,196,201,213).

Real-time PCR assays were carried out on an Eppendorf Mastercycler EP Realplex thermal cycler (Eppendorf, Westbury, NY). Thermal cycles began with 1 min of initial denaturation at 95°C, followed by 40 cycles of denaturation at 95°C for 15 s and combined annealing and extension for 1 min at the primer-specific annealing temperature. PCR assays were optimized to reduce or eliminate the formation of primer

dimers, and melting curves were conducted for all assays following amplification to screen for non-specific products. Melting curves began with 15 s at the primer-specific annealing temperature followed by a 20 min ramp up to 95°C and a final hold at 95°C for 15 s. Reaction volumes were 25 µL and consisted of 12.5 µL of BioRad iTaq SYBR Green Supermix with ROX (Life Science Research, Hercules, CA) or iTaq Universal SYBR Green Supermix (Life Science Research, Hercules, CA), 25 µg of bovine serum albumin, 12.5 pmol of forward primer, 6.25 pmol of reverse primer, and approximately 1 ng of template genomic DNA. Standards were prepared by initially amplifying gene targets from well-described bacterial isolates or municipal wastewater solids using PCR. PCR products were then ligated into the pGEM-T Easy cloning vector and transformed into either JM109 or DH5α competent cells. Cloned plasmids were extracted from cell cultures using either an alkaline lysis procedure (197) or a QIAprep Spin Miniprep Kit (Qiagen, Valencia, CA). Plasmid DNA concentrations in these extracts were determined using a TD-700 fluorometer and Hoechst 33258 dye. Separate standard curves were constructed for each individual assay (i.e. each 96-well plate contained a standard curve), and each standard curve consisted of a 10-fold serial dilution of an aliquot of plasmid DNA extract. The number of standards, slope, intercept, amplification efficiency, r^2 , and quantification limit for each standard curve are provided in Appendix C (Table C.2). Of the 32 assays performed, 19 (59%) had amplification efficiencies of 100% ± 10% (maximum deviation from 100%) with $r^2 \geq 0.99$ for a minimum of six points on each standard curve. The absolute values by which amplification efficiencies for the

remaining 13 assays deviated from 100% were between 11% and 19% with $r^2 \geq 0.99$ for a minimum of seven points on each standard curve.

Each triplicate sample was analyzed once to produce triplicate analytical measurements for each soil microcosm on each sample date. Thus, these triplicate measurements reflect the combined variability of DNA extraction and real-time PCR. Values represented in figures and tables are typically the arithmetic mean of triplicate measurements. If, however, only one sample in a triplicate set amplified for any given gene target, then that value was discarded and the set of triplicates that it belonged to were collectively reported as less than the quantification limit. If two samples in a triplicate set amplified, then the arithmetic mean of those two values was reported as representing the set of triplicates that they belonged to. These cases are referred to as being duplicate samples in figure captions.

Data Analysis. Linear regression (R 2.15.0) was used to estimate the goodness of fit of the data from the final three eight-day batches for each digester to several kinetic models including a first-order kinetic model (Equation 5.1), a second-order kinetic model (Equation 5.2), and a modified form of the Collins-Selleck disinfection model (Equation 5.3) (214,215). A first-order kinetic model was initially hypothesized because previous work has shown the decline of ARG and *intI1* quantities in several different types of natural and engineered systems to follow first-order trends (115,121,170,204,206,208). First-order kinetic models also provide a valuable descriptive and interpretive tool that is useful for comparing results across different gene targets and environments. However, a formal lack-of-fit test (205) provided strong evidence against the null hypothesis that the

natural logarithm of gene target quantities (or ARG and *intI1* ratios to 16S rRNA gene quantities) varied linearly with respect to time for a large fraction of the time series in this data set. As a result, the other two kinetic models were investigated to determine if either provided a more suitable fit to the data. A formal non-constant variance test (205) was also used to test the null hypothesis that any given transformation of the data, corresponding to a particular kinetic model, produced a distribution of errors with constant variance as a function of the fitted model values.

Equation 5.1:

$$\frac{dC}{dt} = kC$$

Equation 5.2:

$$\frac{dC}{dt} = kC^2$$

Equation 5.3:

$$C = C_0 \left(\frac{t}{b} \right)^k$$

The first-order and second-order models were fit to the data by integrating the differential kinetic expressions and solving for a linear relationship between gene target concentration (C) and time (t) to fit to the general form of the linear regression expression. The modified Collins-Selleck expression replaces the unitless Collins-Selleck coefficient of specific lethality ($-\Lambda_{CS}$) from the traditional Collins-Selleck model (214) with a unitless generic kinetic parameter (k) and models analyte concentration (C) as a function of time (t) rather than chlorine dose (Ct). In this context, time can be thought of as representing a “dose” of anaerobic digestion at a given temperature. The

modified Collins-Selleck model was fit to the data by taking its logarithm and solving for a linear relationship between the logarithm of C and the logarithm of t .

5.3 Results

Operating Conditions. The digesters operated as adequate experimental simulations of full-scale anaerobic digesters while achieving the intended experimental temperature and flow-regime characteristics (Figure 5.1, Figure 5.2, Figure 5.3, Figure 5.4, Figure C.1, Figure C.2, and Figure C.3). Although the temperature of each digester varied substantially on a day-to-day basis, the differences in mean temperature among all the digesters over the entire 80-day experiment were statistically significant ($P \leq 1 \times 10^{-6}$, Welch's t-tests). The mean hydraulic residence times at the end of batches varied between averages of approximately 33 (56°C) and 37 (40°C) days and pH was circumneutral in each digester over the entire course of the experiment. Total solids in the untreated residual municipal wastewater solids declined from approximately 5% to just over 4%, while total solids in the anaerobic digesters remained relatively constant between 3.5% and 4%. Similarly, volatile solids in the untreated residual municipal wastewater solids declined steadily from approximately 3.5% to 3%, while volatile solids in the anaerobic digesters remained relatively constant between approximately 2% and 2.5%. Total solids removal efficiencies in the digesters varied between 12% (at 60°C) and 24% (at 40°C), while volatile solids removal efficiencies in the digesters varied between 25% (at 60°C) and 37% (at 40°C). The gas production and gas methane content for the mesophilic (40°C) digester differed from that of the thermophilic and hyperthermophilic digesters. Both gas production and methane content varied

considerably over time at 40°C, with a major peak in both quantities at 40 d. In contrast, gas production and methane content varied less for the thermophilic and hyperthermophilic digesters and was substantially lower than peak methane content at 40°C (approximately 20% versus more than 60%). The methane production normalized to volatile solids destruction at 40°C, 56°C, 60°C, and 63°C was 169 ± 137 , 73 ± 62 , 39 ± 32 , and 90 ± 49 (mean \pm standard deviation) L CH₄ kg⁻¹ VS destroyed, respectively.

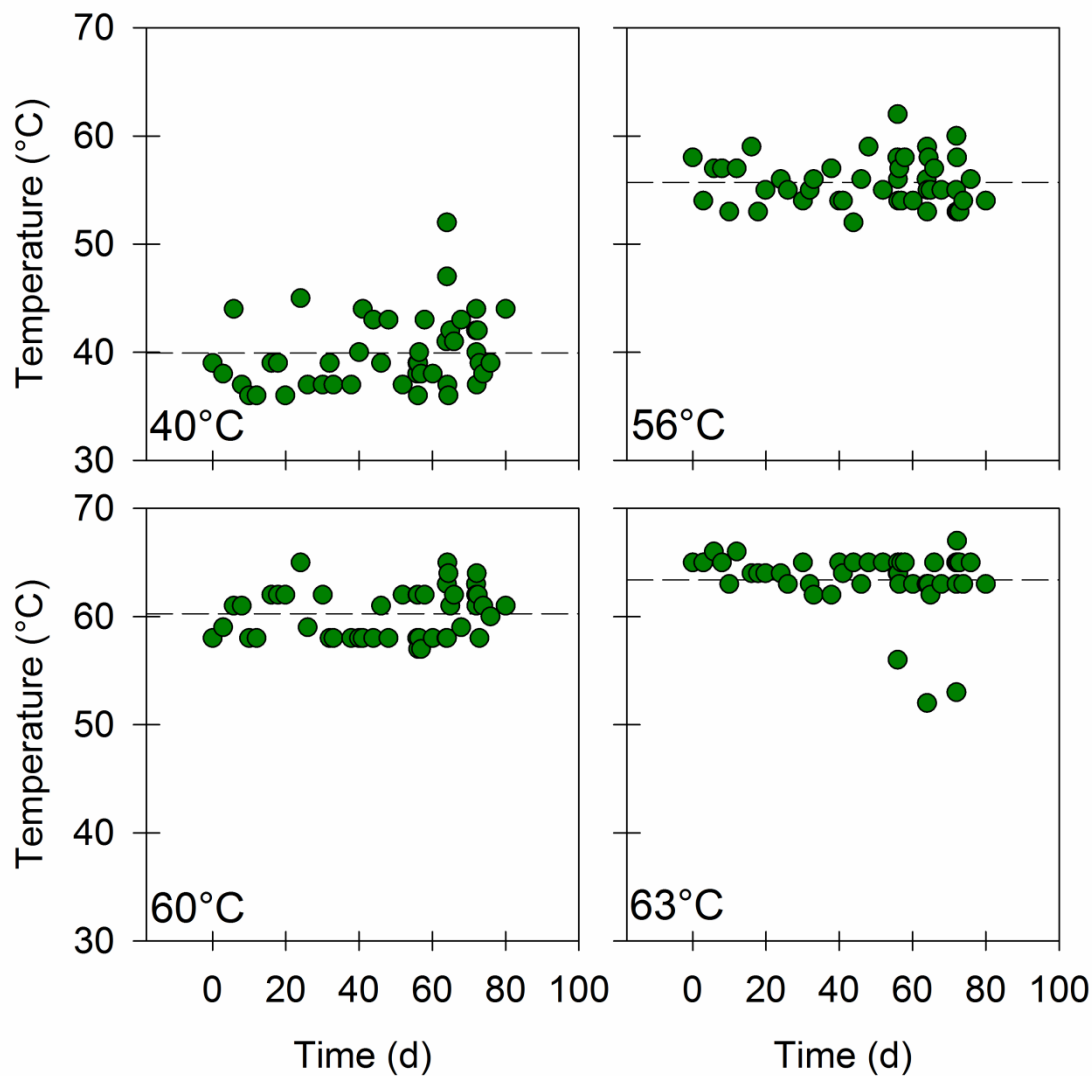


Figure 5.1. The temperatures of anaerobic digesters operated at nominal temperatures of 40°C, 56°C, 60°C, and 63°C. Dashed lines represent the mean temperature for each digester. These values were $39.9^{\circ}\text{C} \pm 3.4^{\circ}\text{C}$, $55.7^{\circ}\text{C} \pm 2.2^{\circ}\text{C}$, $60.3^{\circ}\text{C} \pm 2.3^{\circ}\text{C}$, and $63.4^{\circ}\text{C} \pm 2.9^{\circ}\text{C}$ (mean \pm standard deviation).

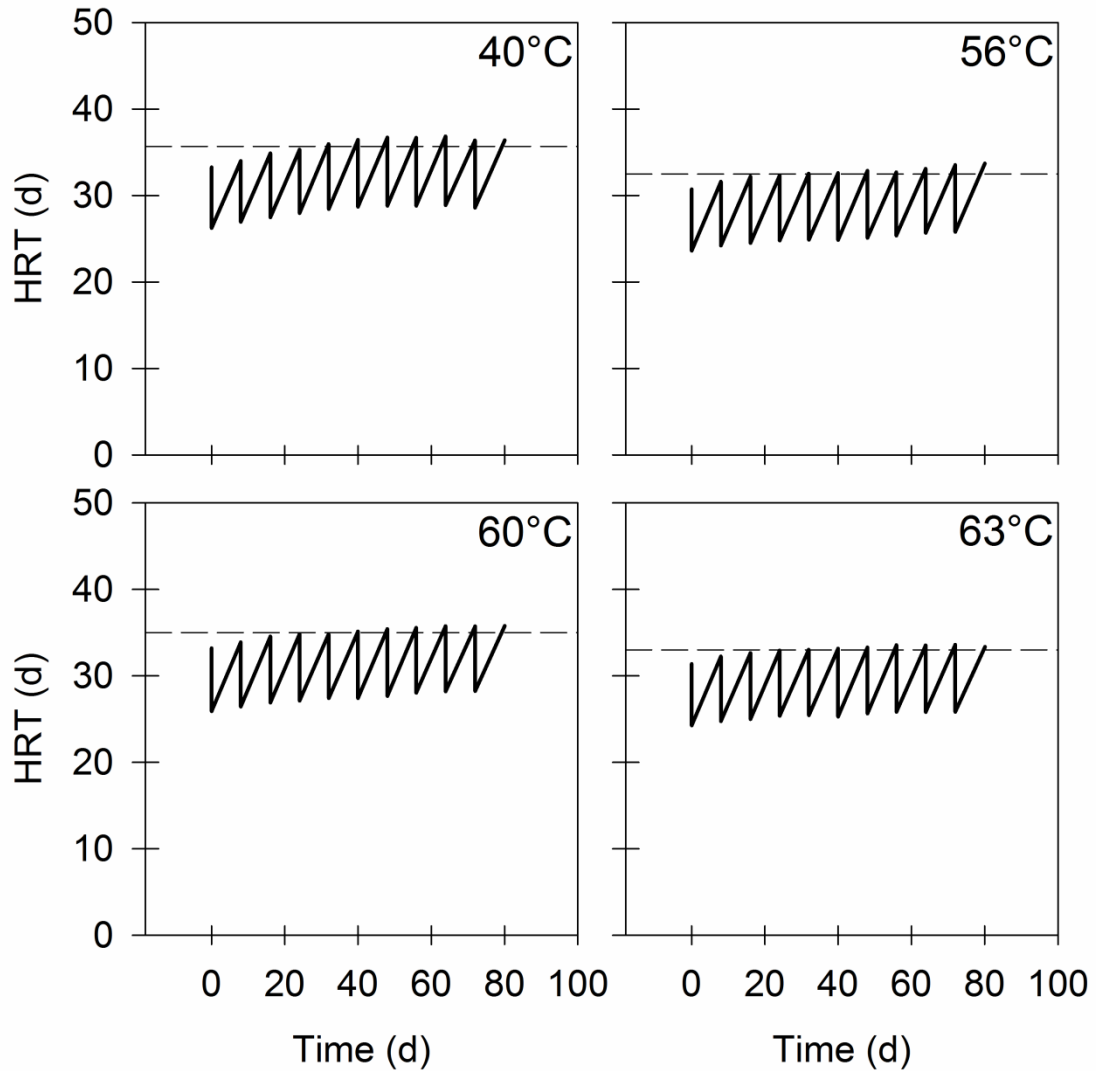


Figure 5.2. The mean hydraulic residence time (HRT) for each of four anaerobic digesters operated at nominal temperatures of 40°C, 56°C, 60°C, and 63°C. Dashed lines represent the mean value of HRT at the end of batches. These values were 35.7 ± 1.2 , 32.5 ± 0.8 , 35.0 ± 0.8 , and 33.0 ± 0.7 days (mean \pm standard deviation), respectively.

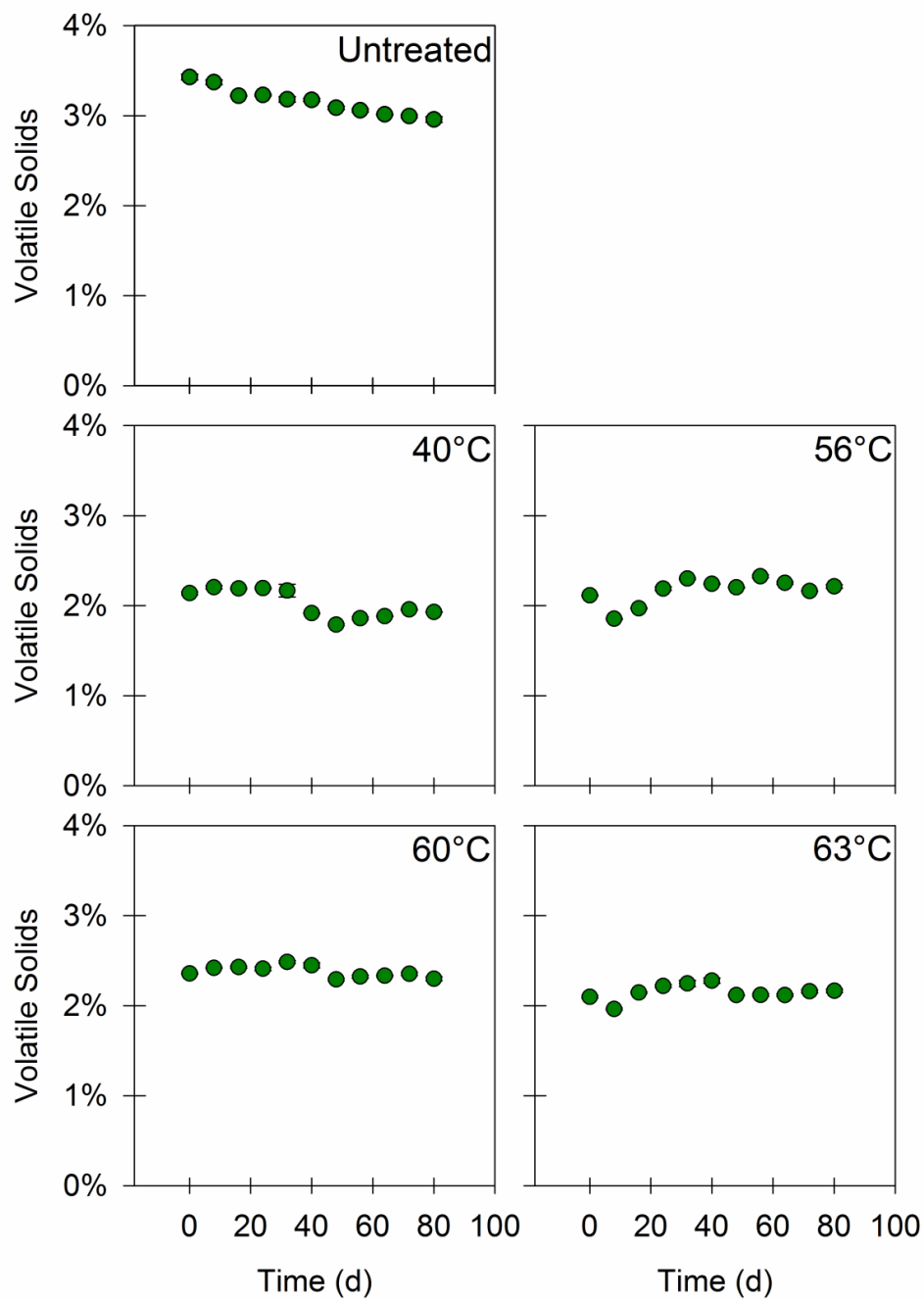


Figure 5.3. The volatile solids content of untreated residual municipal wastewater solids and four anaerobic digesters operated at nominal temperatures of 40°C, 56°C, 60°C, and 63°C. Values are the arithmetic mean of triplicate samples; error bars represent one standard deviation.

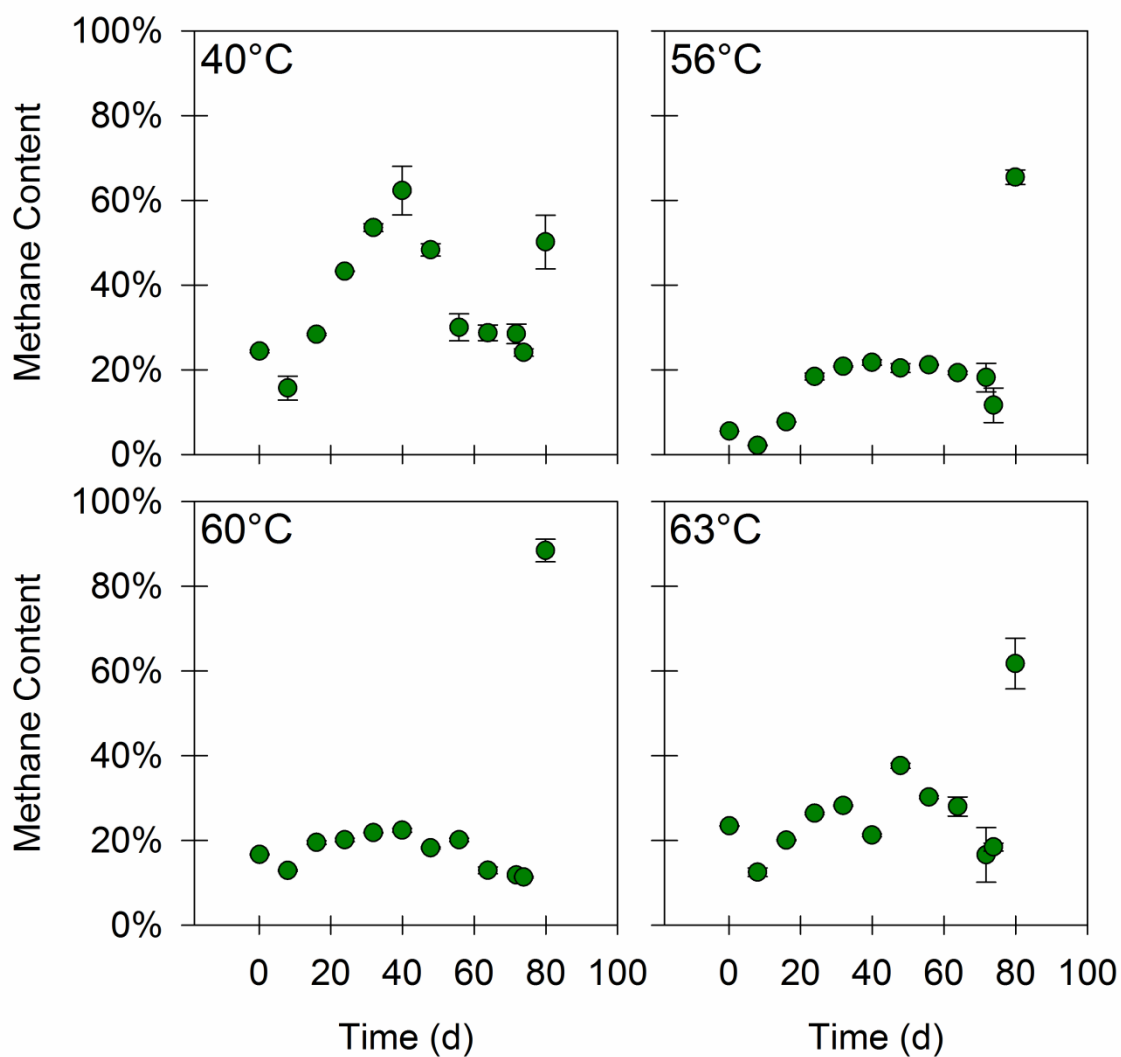


Figure 5.4. The methane content of gas produced by anaerobic digesters operated at nominal temperatures of 40°C, 56°C, 60°C, and 63°C. Values are the arithmetic mean of three or more samples; error bars represent one standard deviation.

Gene Target Quantities in Untreated Residual Solids. Quantities of all gene targets were relatively consistent with time in untreated residual municipal wastewater solids, although they varied considerably across gene targets (Figure 5.5, Figure 5.6, Figure C.4, and Figure C.5). Quantities of 16S rRNA genes were approximately 1×10^{12} copies mL^{-1} and were considerably less variable than quantities of AllBac or methanogen 16S rRNA genes. Methanogen 16S rRNA genes made up approximately 0.2% of the community's 16S rRNA genes, while AllBac quantities were approximately twice as high as 16S rRNA genes. This discrepancy appears to be the result of an inaccurately quantified AllBac standard, and as a result, AllBac quantities in this work are less accurate than those of other gene targets. Relative changes of AllBac quantities remain valid, however, because the same AllBac standard was used for all AllBac assays. Quantities of ARGs, *intII*, and *repA* were all lower than those of 16S rRNA genes and varied considerably from gene to gene. Quantities of *intII* and *tet(W)* were the highest among this group, on the order of 10^{10} copies mL^{-1} , and were more numerous than methanogen 16S rRNA genes. Quantities of *qnrA* and *repA* were considerably lower, on the order of 10^7 copies mL^{-1} . The ratios of ARGs, *intII*, and *repA* to 16S rRNA genes exhibited the same relative relationships as the volume-normalized quantities.

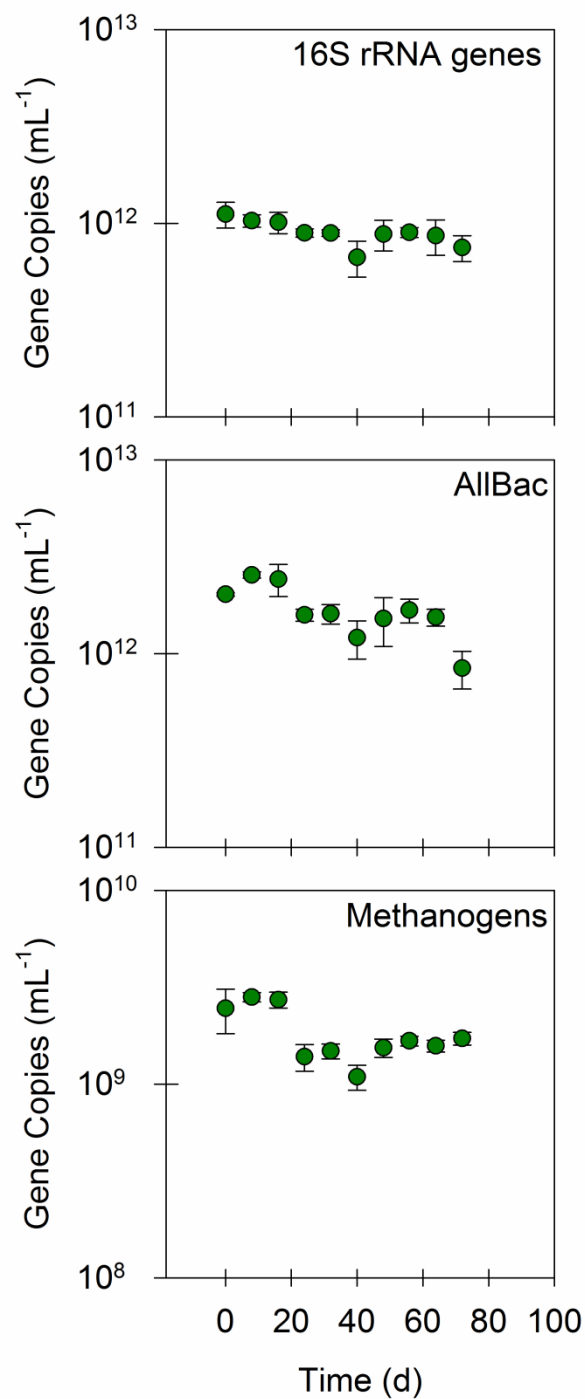


Figure 5.5. Quantities of 16S rRNA genes, AllBac, and methanogen 16S rRNA genes in untreated residual municipal wastewater solids. Values are the arithmetic mean of triplicate samples; error bars represent one standard deviation.

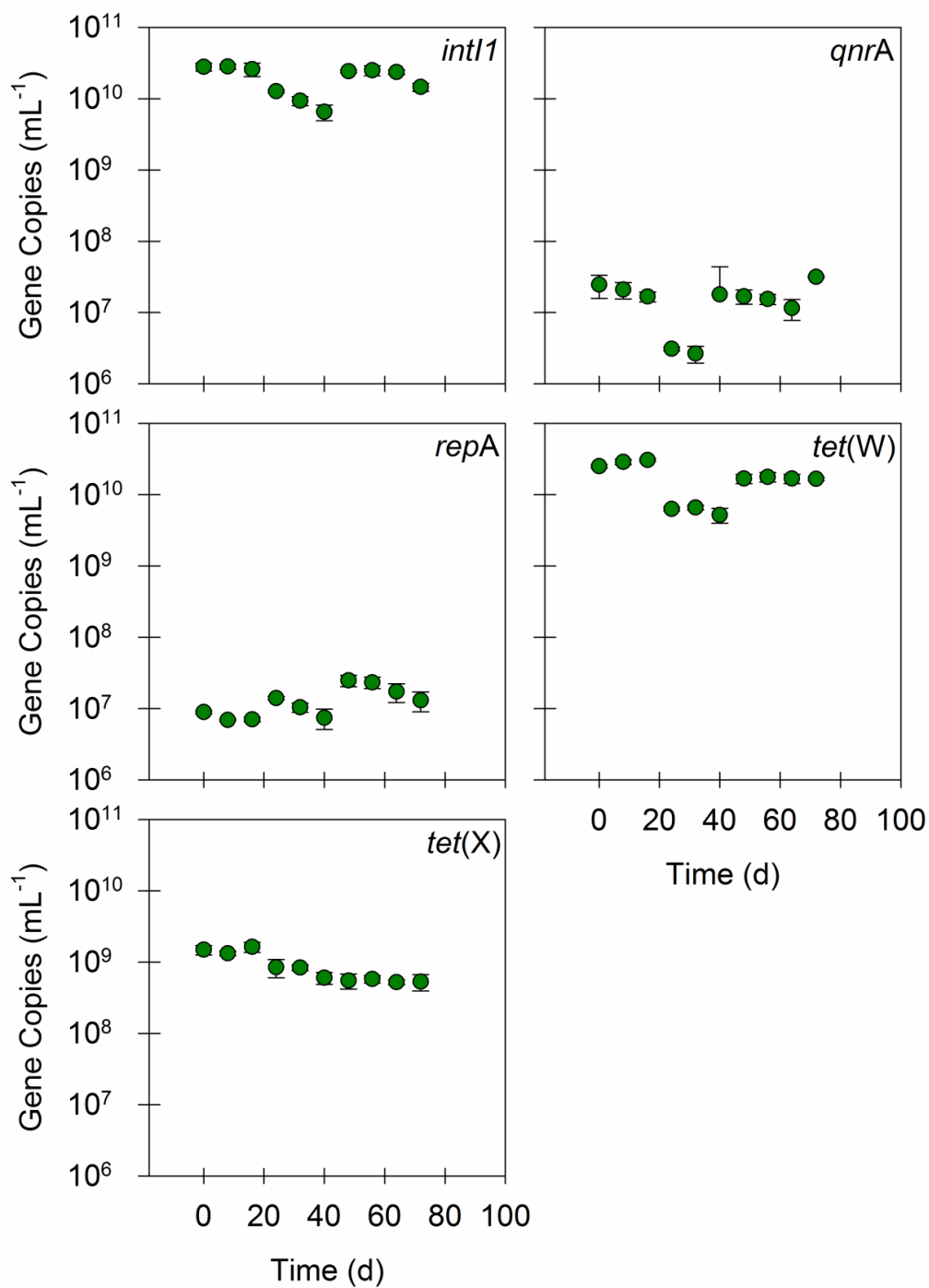


Figure 5.6. Quantities of ARGs, *intI1*, and *repA* in untreated residual municipal wastewater solids. Values are the arithmetic mean of duplicate or triplicate samples; error bars represent one standard deviation.

Total Bacterial Biomass. The extent to which 16S rRNA genes were removed from untreated residual municipal wastewater solids by anaerobic digestion varied by temperature (Figure 5.7 and Figure C.6). An approximately 7-fold reduction in 16S rRNA gene quantities was achieved in the first seven eight-day batches at 40°C, while the thermophilic and hyperthermophilic digesters achieved between 11-fold (at 56°C) and 25-fold (at 60°C) reductions in 16S rRNA gene quantities over the same time period. A significant portion of the overall 16S rRNA gene removal for the thermophilic digesters occurred during the first two days of each eight-day batch, after which 16S rRNA gene quantities leveled off at relatively constant values that were consistent with those from the end points of the first seven eight-day batches.

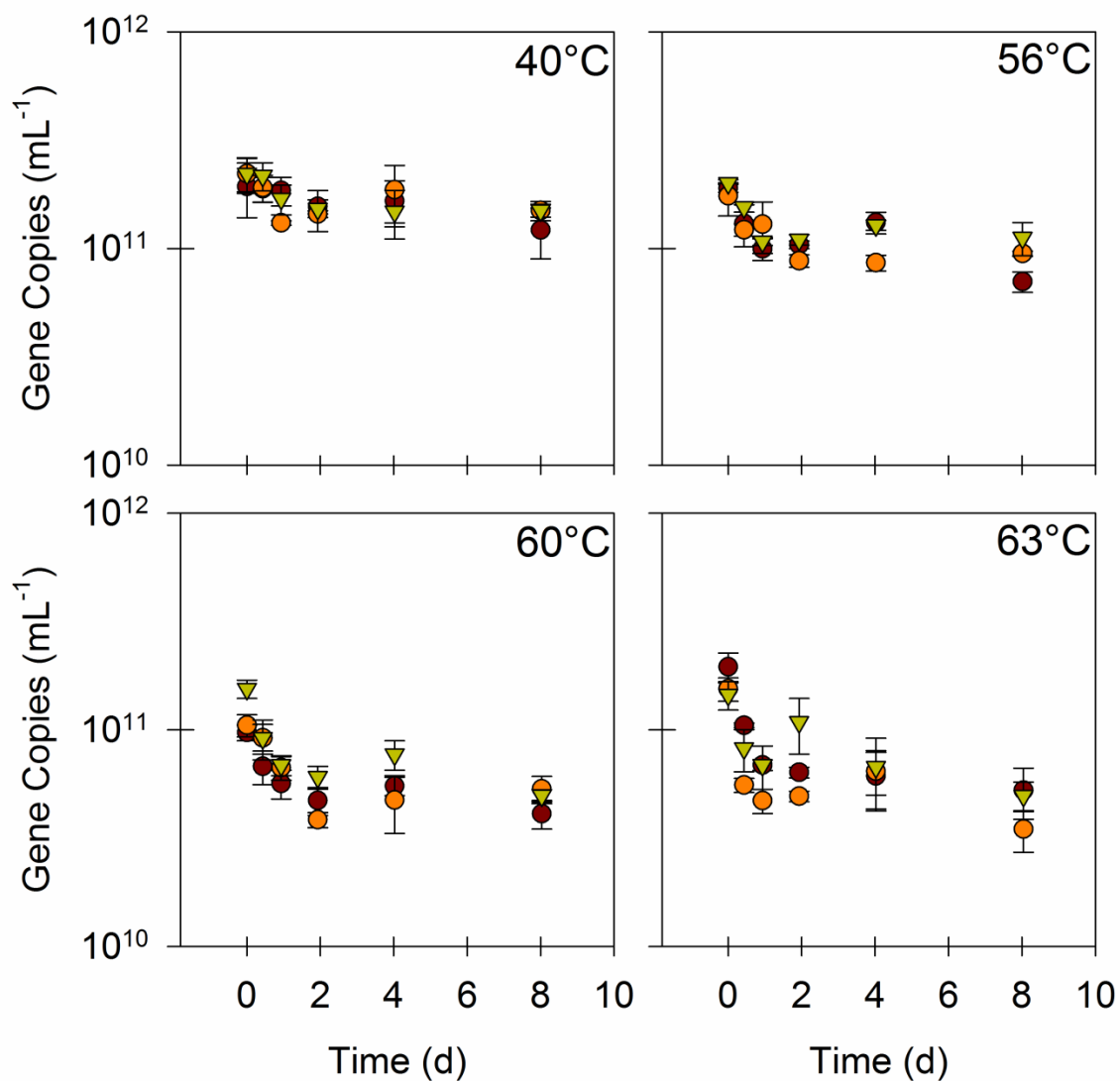


Figure 5.7. Quantities of 16S rRNA genes during the final three batches (green, orange, and red symbols represent unique batches) in anaerobic digesters operated at nominal temperatures of 40°C, 56°C, 60°C, and 63°C. Values are the arithmetic mean of triplicate samples; error bars represent one standard deviation.

Fecal Bacterial Biomass. Quantities of AllBac were significantly more reduced by anaerobic digestion than 16S rRNA gene quantities, although the relationship between the extent of removal and temperature was less clear (Figure 5.8, Figure C.7, Figure C.8, and Figure C.9). A 160-fold reduction in AllBac quantities was achieved in the first seven eight-day batches at 40°C. At thermophilic and hyperthermophilic temperatures, however, reductions of AllBac quantities varied between 66-fold (at 60°C) and 140-fold (at 63°C) over the same time period. Ratios of AllBac to 16S rRNA genes were reduced 24-fold at 40°C during the first seven eight-day batches and between approximately 3-fold (at 60°C) and 9-fold (at 56°C) at thermophilic and hyperthermophilic temperatures. Like 16S rRNA gene quantities, AllBac quantities during the final three eight-day batches decline most rapidly in the first two days of each batch at thermophilic and hyperthermophilic temperatures, after which they approach quantities that are consistent with those from the end points of the first seven eight-day batches. The difference between initial rates of decline and rates of decline at the end of batches, however, is less pronounced compared to 16S rRNA genes. Furthermore, the ratios of AllBac to 16S rRNA genes during the final three eight-day batches appear to decline at steady rates regardless of temperature.

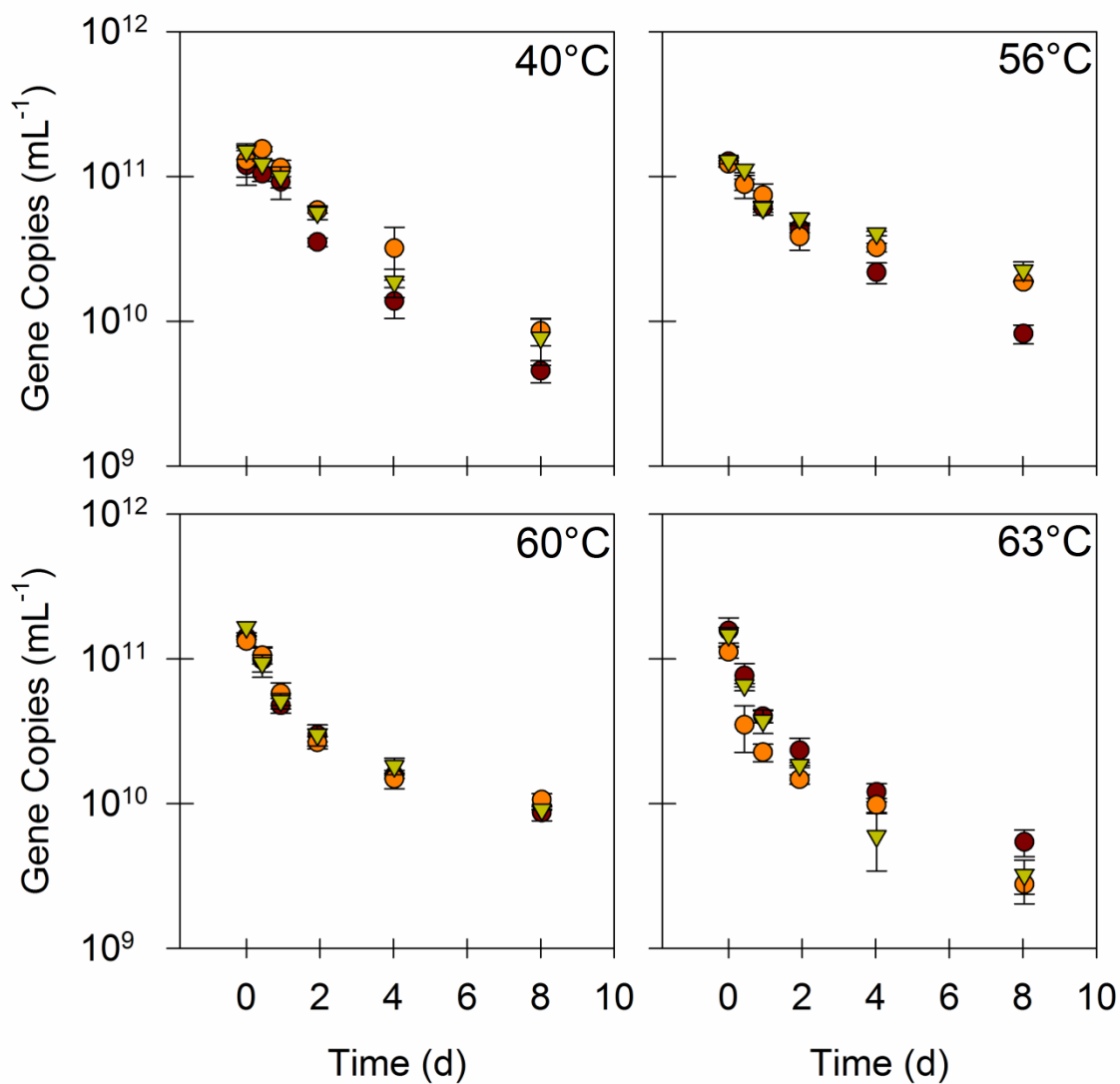


Figure 5.8. Quantities of AllBac during the final three batches (green, orange, and red symbols represent unique batches) in anaerobic digesters operated at nominal temperatures of 40°C, 56°C, 60°C, and 63°C. Values are the arithmetic mean of triplicate samples; error bars represent one standard deviation.

Methanogens. The extent to which methanogen 16S rRNA gene quantities decreased during anaerobic digestion was much less than that of AllBac or 16S rRNA genes in general and varied with temperature (Figure 5.9, Figure C.10, Figure C.11, and Figure C.12). Methanogen 16S rRNA gene quantities were enriched at 40°C during the first seven eight-day batches, with a major peak in methanogen quantities coinciding with major peaks in gas production and methane content at approximately 40 d. Methanogen 16S rRNA genes accounted for between approximately 1% and 10% of the total 16S rRNA genes in the 40°C digester during this time period. In contrast, methanogen 16S rRNA gene quantities were reduced between 5-fold (at 56°C) and 13-fold (at 60°C) at thermophilic and hyperthermophilic temperatures during the first seven eight-day batches and remained relatively constant. The ratios of methanogen 16S rRNA genes to 16S rRNA genes, however, increased approximately 2-fold in all thermophilic and hyperthermophilic digesters over this same time period. Thus, methanogen 16S rRNA genes were enriched to account for between approximately 0.2% and 0.8% of the total 16S rRNA genes in thermophilic and hyperthermophilic digesters despite undergoing a net decrease in their absolute numbers. The majority of this enrichment occurred during the first two days of each eight-day batch, with ratios of methanogen 16S rRNA genes to 16S rRNA genes remaining constant thereafter at 40°C and decreasing steadily at thermophilic temperatures.

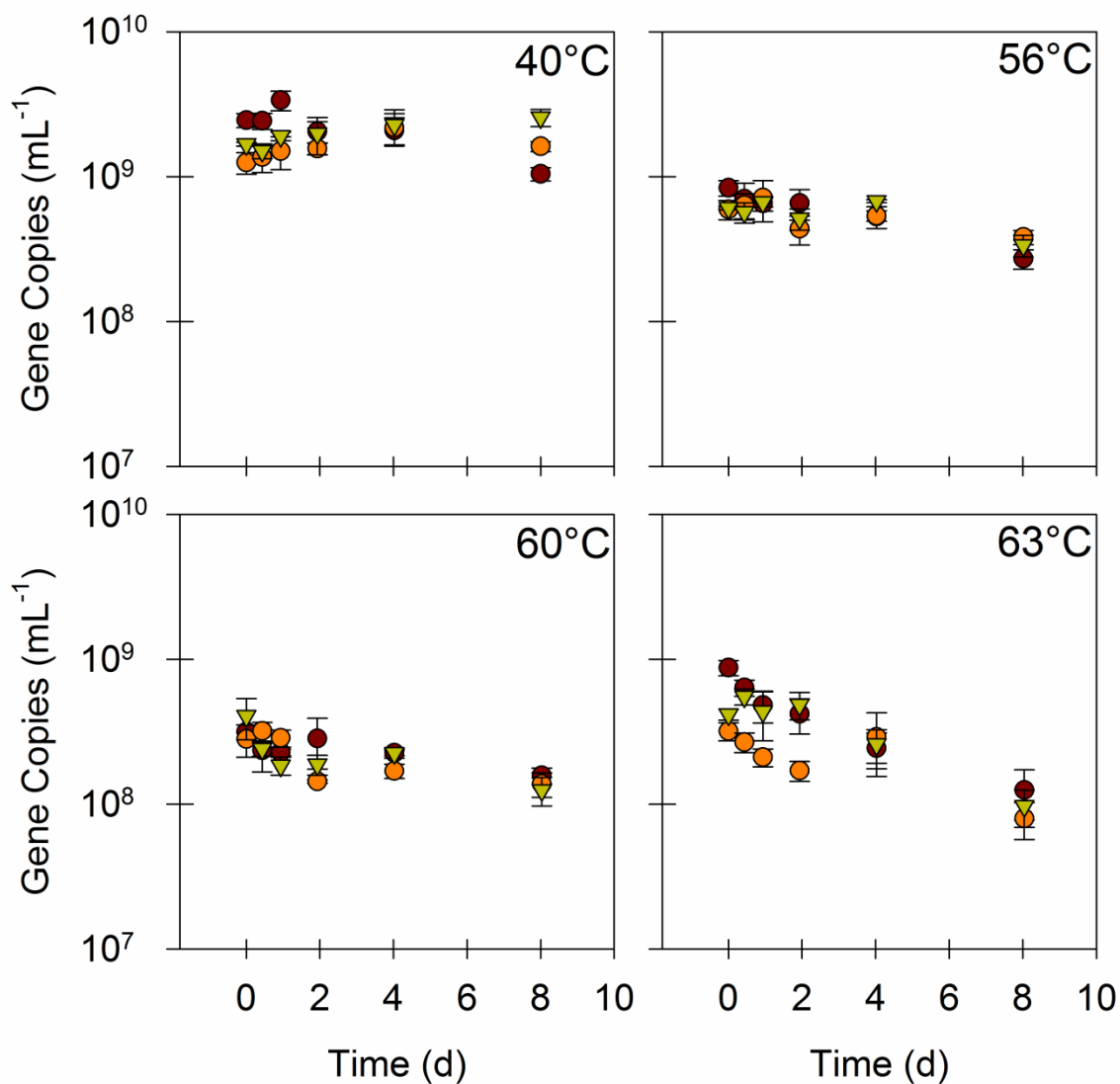


Figure 5.9. Quantities of methanogen 16S rRNA genes during the final three batches (green, orange, and red symbols represent unique batches) in anaerobic digesters operated at nominal temperatures of 40°C, 56°C, 60°C, and 63°C. Values are the arithmetic mean of triplicate samples; error bars represent one standard deviation.

ARGs, *repA*, and *intII*. The extents of removal for ARGs, *intII*, and *repA* during anaerobic digestion were higher at thermophilic and hyperthermophilic temperatures than at 40°C (Figure 5.10, Figure 5.11, Figure 5.12, Figure 5.13, Figure 5.14, Figure C.13, Figure C.14, Figure C.15, Figure C.16, Figure C.17, Figure C.18, Figure C.19, Figure C.20, Figure C.21, Figure C.22, Figure C.23, Figure C.24, and Figure C.25). Quantities of *intII*, *tet(W)*, and *tet(X)* were reduced on average by approximately 11-fold (*tet(W)*) to 23-fold (*tet(X)*) at 40°C during the first seven eight-day batches. Quantities of the same gene targets were reduced by between approximately 53-fold (*tet(W)*, 63°C) and 1,300-fold (*tet(X)*, 63°C) at thermophilic and hyperthermophilic temperatures, with a median reduction in gene target quantity of 110-fold (*intII*, 60°C). Quantities of *qnrA* at 40°C and quantities of *repA* at all temperatures were below quantification limits at the end of each of the first seven eight-day batches. It is apparent that some reduction in these gene targets' quantities occurred, with at least 2-fold (*repA*) to 17-fold (*qnrA*) removal at 40°C and at least 2-fold (*repA*, 63°C) to 130-fold (*qnrA*, 60°C) removal at thermophilic and hyperthermophilic temperatures. These trends with temperature were approximately the same for ratios of *intII*, *tet(W)*, and *tet(X)* to 16S rRNA genes. These ratios were reduced approximately 2-fold (*tet(W)*) to 3-fold (*tet(X)*) at 40°C and approximately 3-fold (*tet(X)*, 60°C) to 71-fold (*tet(X)*, 63°C) at thermophilic and hyperthermophilic temperatures. The natures of the decline in ARG, *intII*, and *repA* quantities during each batch were similar to those observed for 16S rRNA genes and AllBac, particularly at higher temperatures. A significant portion of the reduction in gene quantities occurred within the first two days of each batch, after which the rate of decline

either slowed considerably (for *intII*, *tet(W)*, and *tet(X)*) or gene target quantities were below quantification limits (for *qnrA* and *repA*).

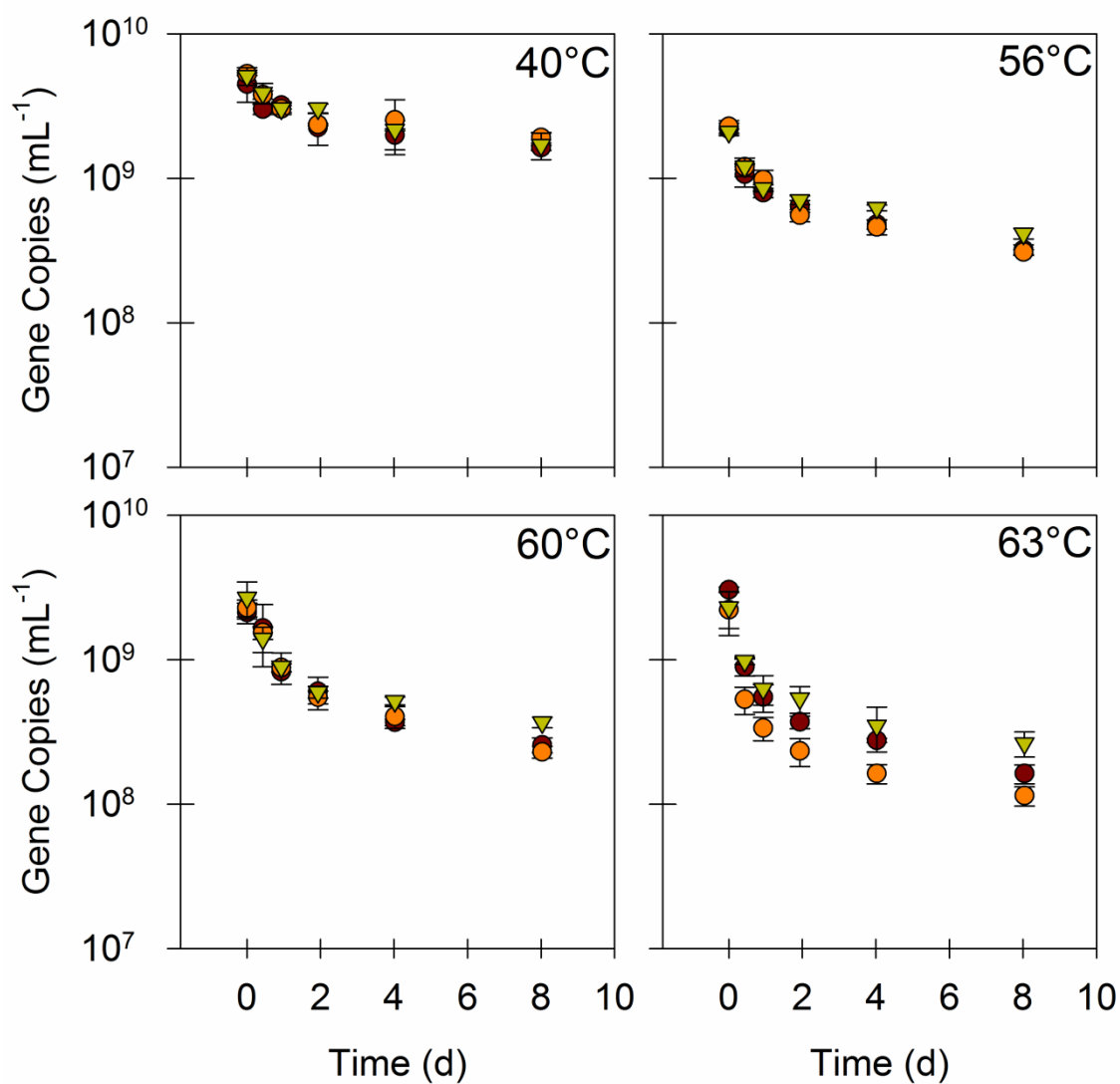


Figure 5.10. Quantities of *intII* during the final three batches (green, orange, and red symbols represent unique batches) in anaerobic digesters operated at nominal temperatures of 40°C, 56°C, 60°C, and 63°C. Values are the arithmetic mean of triplicate samples; error bars represent one standard deviation.

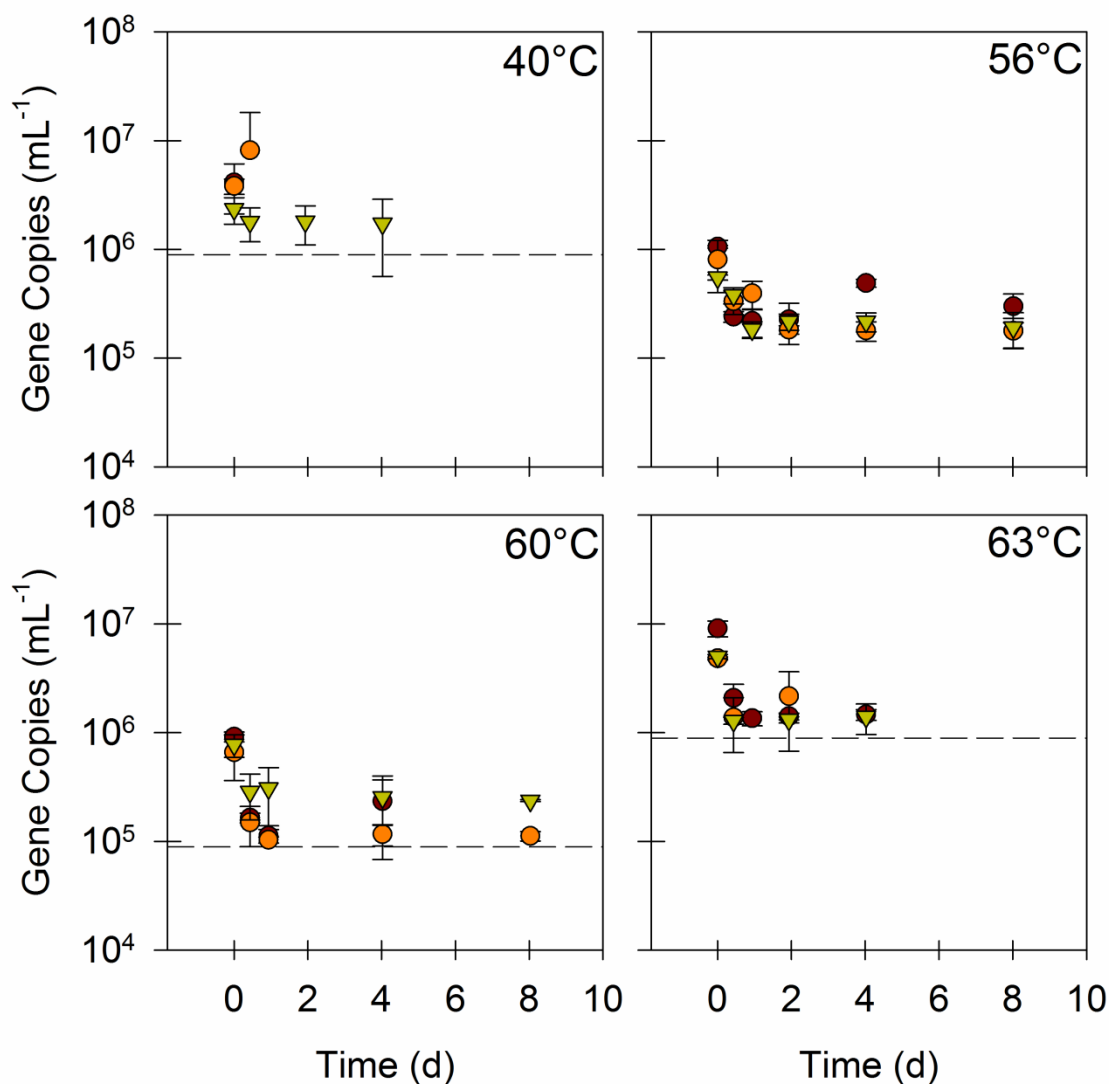


Figure 5.11. Quantities of *qnrA* during the final three batches (green, orange, and red symbols represent unique batches) in anaerobic digesters operated at nominal temperatures of 40°C, 56°C, 60°C, and 63°C. Values are the arithmetic mean of duplicate or triplicate samples; error bars represent one standard deviation. Dashed lines represent the limit of quantification for data sets that contain one or more experimental observations below that limit.

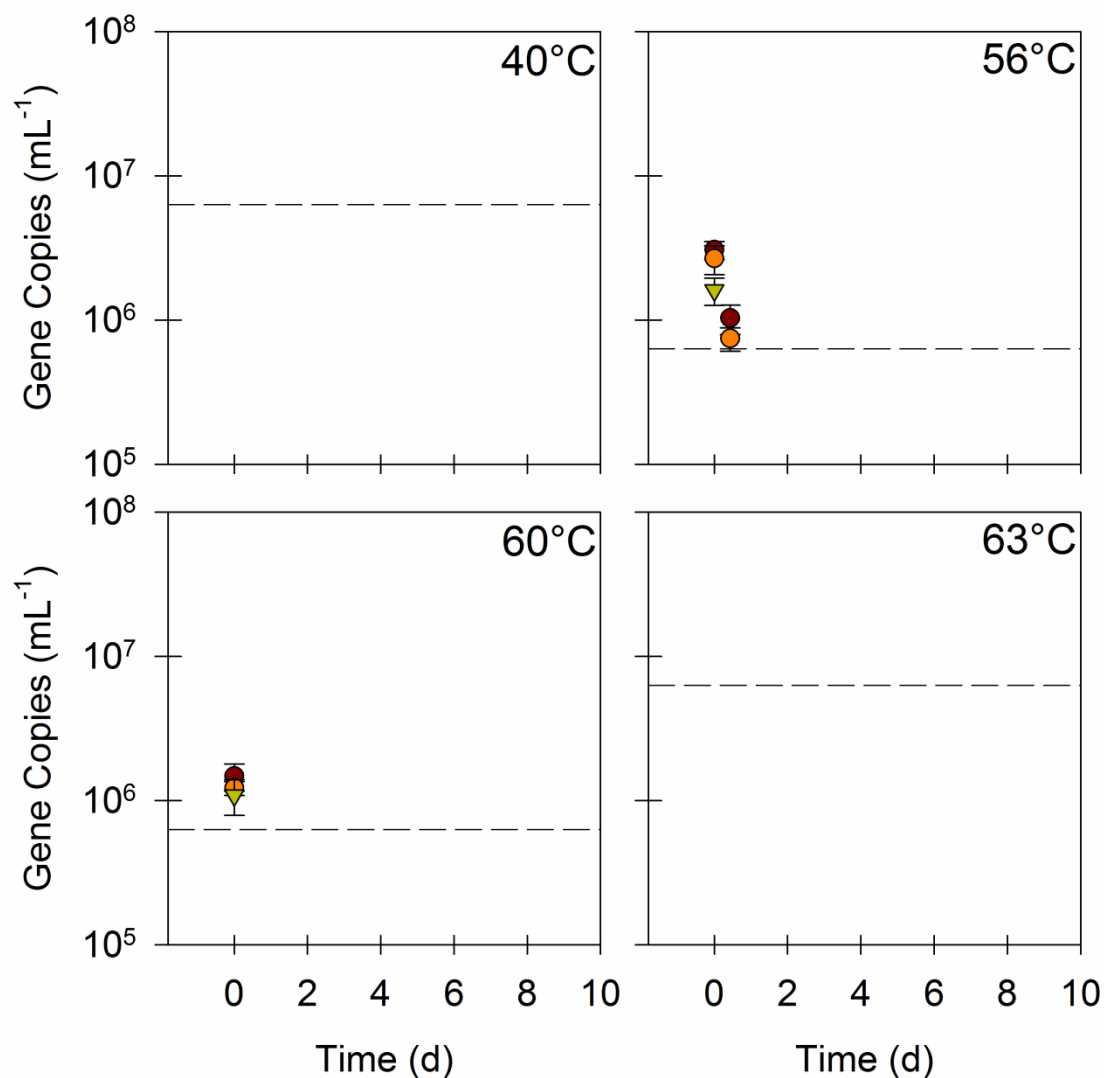


Figure 5.12. Quantities of *repA* during the final three batches (green, orange, and red symbols represent unique batches) in anaerobic digesters operated at nominal temperatures of 40°C, 56°C, 60°C, and 63°C. Values are the arithmetic mean of duplicate or triplicate samples; error bars represent one standard deviation. Dashed lines represent the limit of quantification for data sets that contain one or more experimental observations below that limit.

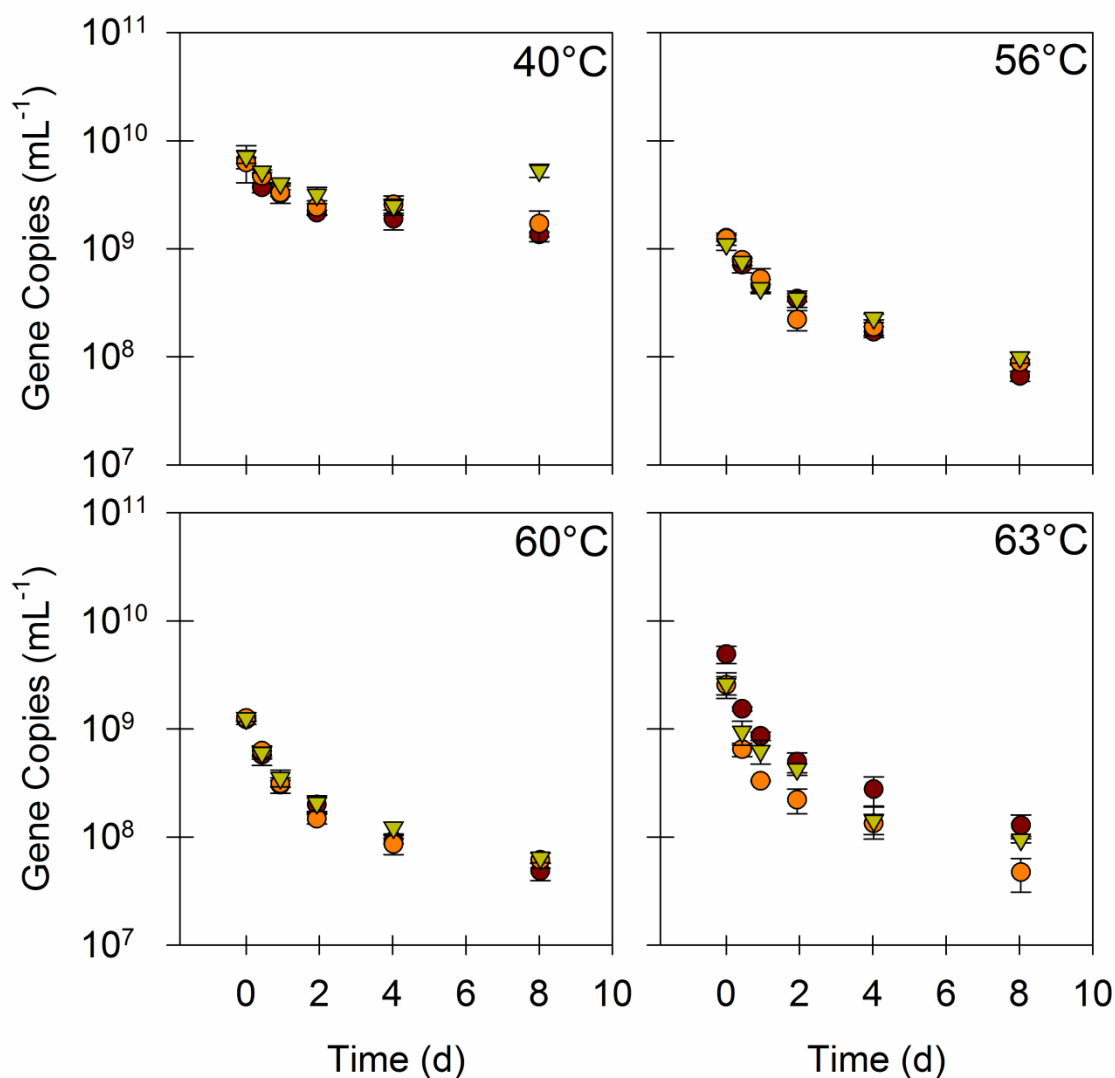


Figure 5.13. Quantities of *tet(W)* during the final three batches (green, orange, and red symbols represent unique batches) in anaerobic digesters operated at nominal temperatures of 40°C, 56°C, 60°C, and 63°C. Values are the arithmetic mean of triplicate samples; error bars represent one standard deviation.

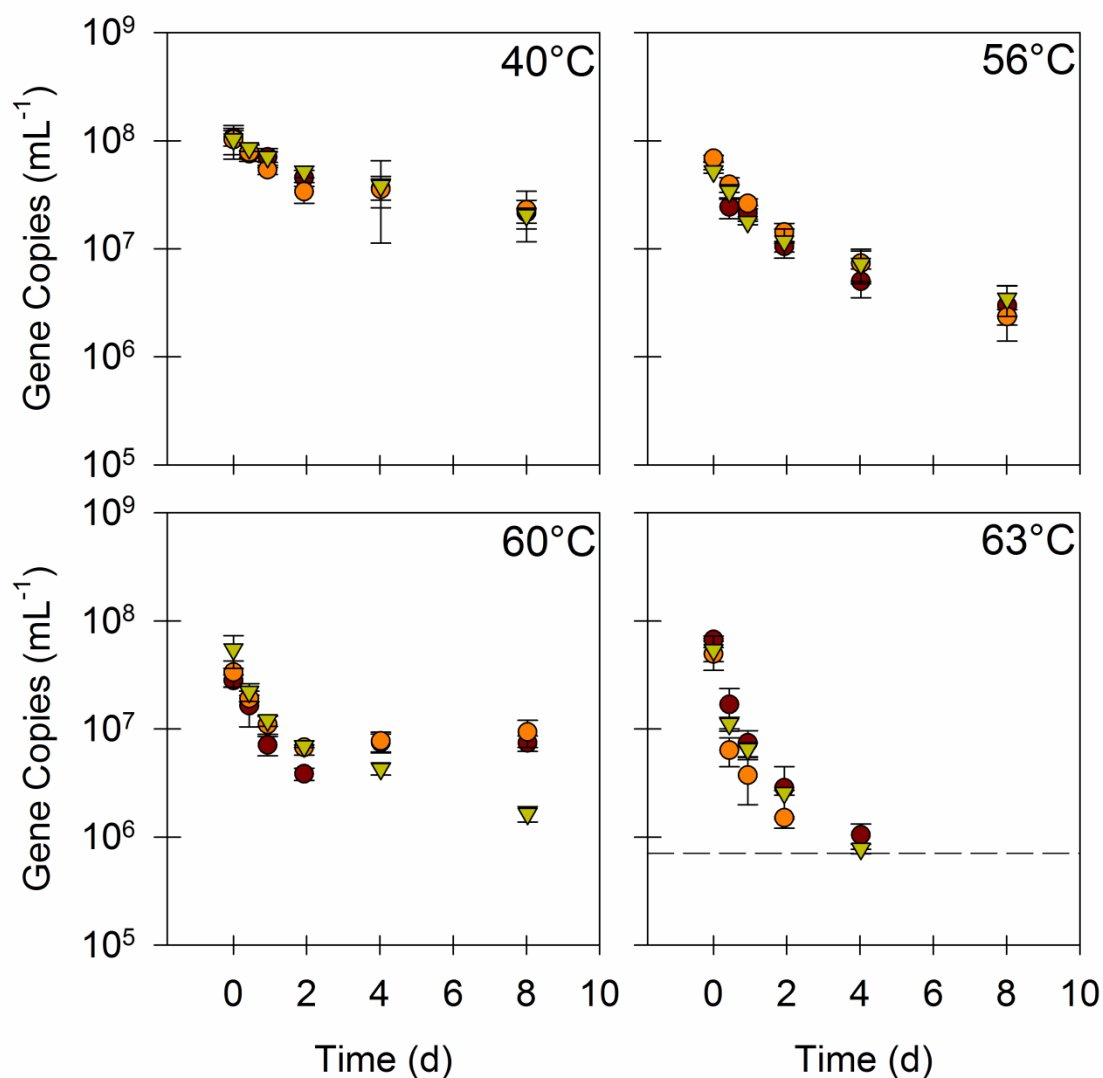


Figure 5.14. Quantities of *tet(X)* during the final three batches (green, orange, and red symbols represent unique batches) in anaerobic digesters operated at nominal temperatures of 40°C, 56°C, 60°C, and 63°C. Values are the arithmetic mean of duplicate or triplicate samples; error bars represent one standard deviation. Dashed lines represent the limit of quantification for data sets that contain one or more experimental observations below that limit.

Kinetic Modeling. Out of the three models considered here, the Collins-Selleck kinetic model tended to produce the best fit to the majority of the time series (Table C.3, Table C.4, and Table C.5). The Collins-Selleck model produced 37 out of 50 non-trivial (degrees of freedom ≥ 3) linear regression fits with ANOVA P values < 0.05 , 46 out of 50 fits with LOF P values ≥ 0.05 , and 44 out of 50 fits with NCV P values ≥ 0.05 . Furthermore, visual inspection of residuals plots and the fit of the kinetic models to both transformed and untransformed data (figures not shown) confirmed that the Collins-Selleck model tended to fit time series exhibiting retarded kinetics particularly well. In contrast, the first-order kinetic model produced only 19 of 50 fits with LOF P values ≥ 0.05 , although it produced a slightly higher number (40 out of 50) of fits with ANOVA P values < 0.05 and 50 out of 50 fits with NCV P values ≥ 0.05 . The first-order kinetic model was also clearly the best fit model for a handful of time series that, based on visual inspection, clearly displayed linear relationships between the logarithm of gene target quantities (or ratios to 16S rRNA genes) and time. The second-order kinetic model produced only 30 out of 50 fits with NCV P values ≥ 0.05 and 18 valid (corresponding to NCV P values ≥ 0.05) LOF P values ≥ 0.05 .

The magnitudes of fitted kinetic coefficients of all models tended to vary with temperature, although differences between mesophilic and thermophilic temperatures were more obvious than differences between thermophilic and hyperthermophilic temperatures (Table 5.1, Table 5.2, and Table C.6). The absolute values of the Collins-Selleck k parameters for *intII*, *tet(W)*, and *tet(X)* quantities normalized to sample volume increased by factors of 1.7 (*intII*) to 2.9 (*tet(W)*) from 40°C to 56°C, while the absolute

values of the Collins-Selleck k parameters for the same gene target quantities normalized to 16S rRNA genes increased by factors of 2.0 (*tet(X)*) to 4.0 (*tet(W)*). Between 56°C and 60°C, only the increase of the Collins-Selleck k parameter for *intII* mL⁻¹, which increased by a factor of 1.4, was statistically significant ($P = 3 \times 10^{-3}$, Welch's t-test). The Collins-Selleck k parameters for all remaining gene quantities, whether normalized to sample volume or 16S rRNA gene quantities, either did not change ($P \geq 0.05$, Welch's t-test) or decreased. Similarly, none of the differences in Collins-Selleck k values between 56°C and 63°C were statistically significant ($P \geq 0.05$, Welch's t-test), and only the increases in the Collins-Selleck k values for *tet(X)* (normalized to both sample volume and 16S rRNA genes) were statistically significant ($P < 0.01$, Welch's t-test) between 60°C and 63°C. The values of Collins-Selleck b parameters showed no clear relationship with temperature. The general trends in values of k , however, were the same for first-order and second-order models, with all coefficients tending to increase with temperature.

Table 5.1. Fitted values of k and calculated half-lives ($t_{1/2}$) from an ordinary least squares fit of the first-order kinetic model to each time series of gene target quantities or ratios of gene target quantities to 16S rRNA genes. Error terms represent the standard error of the mean.

Target	Units (copies)	Temperature	k^a (day ⁻¹)	$t_{1/2}$ (days)
16S rRNA gene	mL ⁻¹	40°C	$-3.9 \times 10^{-2} \pm 1.2 \times 10^{-2}$	17.6
16S rRNA gene	mL ⁻¹	56°C	$-6.0 \times 10^{-2} \pm 1.9 \times 10^{-2}$	11.5
16S rRNA gene	mL ⁻¹	60°C	$-7.8 \times 10^{-2} \pm 2.5 \times 10^{-2}$	8.8
16S rRNA gene	mL ⁻¹	63°C	$-1.0 \times 10^{-1} \pm 3.1 \times 10^{-2}$	6.8
AllBac	mL ⁻¹	40°C	$-3.9 \times 10^{-1} \pm 2.6 \times 10^{-2}$	1.8
AllBac	mL ⁻¹	56°C	$-2.5 \times 10^{-1} \pm 2.7 \times 10^{-2}$	2.8
AllBac	mL ⁻¹	60°C	$-3.2 \times 10^{-1} \pm 3.6 \times 10^{-2}$	2.2

AllBac	mL^{-1}	63°C	-4.0×10^{-1}	\pm	4.6×10^{-2}	1.7
AllBac	$(16\text{S rRNA gene})^{-1}$	40°C	-3.5×10^{-1}	\pm	2.5×10^{-2}	2.0
AllBac	$(16\text{S rRNA gene})^{-1}$	56°C	-1.9×10^{-1}	\pm	1.9×10^{-2}	3.7
AllBac	$(16\text{S rRNA gene})^{-1}$	60°C	-2.4×10^{-1}	\pm	2.2×10^{-2}	2.9
AllBac	$(16\text{S rRNA gene})^{-1}$	63°C	-3.0×10^{-1}	\pm	3.1×10^{-2}	2.3
Methanogen 16S rRNA genes	mL^{-1}	40°C	-7.3×10^{-3}	\pm	2.5×10^{-2}	94.8
Methanogen 16S rRNA genes	mL^{-1}	56°C	-8.5×10^{-2}	\pm	1.4×10^{-2}	8.2
Methanogen 16S rRNA genes	mL^{-1}	60°C	-8.7×10^{-2}	\pm	1.9×10^{-2}	8.0
Methanogen 16S rRNA genes	mL^{-1}	63°C	-1.9×10^{-1}	\pm	3.2×10^{-2}	3.7
Methanogen 16S rRNA genes	$(16\text{S rRNA gene})^{-1}$	40°C	3.4×10^{-2}	\pm	2.7×10^{-2}	-20.5

Methanogen 16S rRNA genes	(16S rRNA gene) ⁻¹	56°C	-2.4×10 ⁻²	±	2.1×10 ⁻²	29.0
Methanogen 16S rRNA genes	(16S rRNA gene) ⁻¹	60°C	-8.8×10 ⁻³	±	2.0×10 ⁻²	78.8
Methanogen 16S rRNA genes	(16S rRNA gene) ⁻¹	63°C	-8.7×10 ⁻²	±	3.0×10 ⁻²	8.0
<i>intII</i>	mL ⁻¹	40°C	-1.1×10 ⁻¹	±	1.6×10 ⁻²	6.4
<i>intII</i>	mL ⁻¹	56°C	-1.9×10 ⁻¹	±	2.8×10 ⁻²	3.7
<i>intII</i>	mL ⁻¹	60°C	-2.3×10 ⁻¹	±	3.2×10 ⁻²	3.0
<i>intII</i>	mL ⁻¹	63°C	-2.5×10 ⁻¹	±	5.3×10 ⁻²	2.7
<i>intII</i>	(16S rRNA gene) ⁻¹	40°C	-6.7×10 ⁻²	±	1.3×10 ⁻²	10.3
<i>intII</i>	(16S rRNA gene) ⁻¹	56°C	-1.3×10 ⁻¹	±	1.6×10 ⁻²	5.5
<i>intII</i>	(16S rRNA gene) ⁻¹	60°C	-1.5×10 ⁻¹	±	1.9×10 ⁻²	4.5

<i>intII</i>	(16S rRNA gene) ⁻¹	63°C	-1.5×10 ⁻¹	±	3.0×10 ⁻²	4.6
<i>qnrA</i>	mL ⁻¹	40°C	-1.6×10 ⁰	±	8.8×10 ⁻¹	0.4
<i>qnrA</i>	mL ⁻¹	56°C	-8.5×10 ⁻²	±	4.2×10 ⁻²	8.2
<i>qnrA</i>	mL ⁻¹	60°C	-1.9×10 ⁻¹	±	1.3×10 ⁻¹	3.7
<i>qnrA</i>	mL ⁻¹	63°C	-3.3×10 ⁻¹	±	1.7×10 ⁻¹	2.1
<i>qnrA</i>	(16S rRNA gene) ⁻¹	40°C	-1.7×10 ⁰	±	1.0×10 ⁰	0.4
<i>qnrA</i>	(16S rRNA gene) ⁻¹	56°C	-2.5×10 ⁻²	±	3.2×10 ⁻²	28.2
<i>qnrA</i>	(16S rRNA gene) ⁻¹	60°C	-5.3×10 ⁻²	±	1.2×10 ⁻¹	13.1
<i>qnrA</i>	(16S rRNA gene) ⁻¹	63°C	-1.2×10 ⁻¹	±	9.5×10 ⁻²	5.9
<i>repA</i>	mL ⁻¹	40°C	ND ^b			

<i>repA</i>	mL ⁻¹	56°C	-2.1×10 ⁰ ± 9.8×10 ⁻¹	0.3
<i>repA</i>	mL ⁻¹	60°C	ND ^b	
<i>repA</i>	mL ⁻¹	63°C	ND ^b	
<i>repA</i>	(16S rRNA gene) ⁻¹	40°C	ND ^b	
<i>repA</i>	(16S rRNA gene) ⁻¹	56°C	-1.2×10 ⁰ ± 1.2×10 ⁰	0.6
<i>repA</i>	(16S rRNA gene) ⁻¹	60°C	ND ^b	
<i>repA</i>	(16S rRNA gene) ⁻¹	63°C	ND ^b	
<i>tet(W)</i>	mL ⁻¹	40°C	-1.1×10 ⁻¹ ± 3.4×10 ⁻²	6.6
<i>tet(W)</i>	mL ⁻¹	56°C	-3.0×10 ⁻¹ ± 2.8×10 ⁻²	2.3
<i>tet(W)</i>	mL ⁻¹	60°C	-3.4×10 ⁻¹ ± 4.3×10 ⁻²	2.1

<i>tet</i> (W)	mL ⁻¹	63°C	-3.8×10 ⁻¹	±	5.8×10 ⁻²	1.8
<i>tet</i> (W)	(16S rRNA gene) ⁻¹	40°C	-6.5×10 ⁻²	±	2.9×10 ⁻²	10.6
<i>tet</i> (W)	(16S rRNA gene) ⁻¹	56°C	-2.4×10 ⁻¹	±	1.7×10 ⁻²	2.9
<i>tet</i> (W)	(16S rRNA gene) ⁻¹	60°C	-2.6×10 ⁻¹	±	2.6×10 ⁻²	2.7
<i>tet</i> (W)	(16S rRNA gene) ⁻¹	63°C	-2.8×10 ⁻¹	±	3.7×10 ⁻²	2.5
<i>tet</i> (X)	mL ⁻¹	40°C	-1.8×10 ⁻¹	±	1.8×10 ⁻²	3.9
<i>tet</i> (X)	mL ⁻¹	56°C	-3.5×10 ⁻¹	±	3.4×10 ⁻²	2.0
<i>tet</i> (X)	mL ⁻¹	60°C	-1.9×10 ⁻¹	±	5.7×10 ⁻²	3.6
<i>tet</i> (X)	mL ⁻¹	63°C	-1.0×10 ⁰	±	2.0×10 ⁻¹	0.7
<i>tet</i> (X)	(16S rRNA gene) ⁻¹	40°C	-1.4×10 ⁻¹	±	1.4×10 ⁻²	5.0

<i>tet</i> (X)	(16S rRNA gene) ⁻¹	56°C	-2.8×10 ⁻¹ ± 2.9×10 ⁻²	2.4
<i>tet</i> (X)	(16S rRNA gene) ⁻¹	60°C	-1.2×10 ⁻¹ ± 4.4×10 ⁻²	5.9
<i>tet</i> (X)	(16S rRNA gene) ⁻¹	63°C	-8.0×10 ⁻¹ ± 8.6×10 ⁻²	0.9

^aSee Table C.3 for ANOVA *P* values, which are equal to values of *P* for *k*, as well as other summary metrics that describe the quality of fit of the model to the data.

^bQuantities of some gene targets were above quantification limits for only $n \leq 2$ time points, so *k* was not determined (ND).

Table 5.2. Fitted values of k and b from an ordinary least squares fit of the modified Collins-Selleck kinetic model to each time series of gene target quantities or ratios of gene target quantities to 16S rRNA genes. Error terms represent the standard error of the mean.

Target	Units (copies)	Temperature	k^a (unitless)	b (days)
16S rRNA gene	mL^{-1}	40°C	$-8.9 \times 10^{-2} \pm 3.5 \times 10^{-2}$	9.3×10^{-2}
16S rRNA gene	mL^{-1}	56°C	$-1.0 \times 10^{-1} \pm 3.9 \times 10^{-2}$	1.0×10^{-2}
16S rRNA gene	mL^{-1}	60°C	$-1.6 \times 10^{-1} \pm 4.9 \times 10^{-2}$	2.7×10^{-2}
16S rRNA gene	mL^{-1}	63°C	$-1.4 \times 10^{-1} \pm 7.0 \times 10^{-2}$	1.8×10^{-3}
AllBac	mL^{-1}	40°C	$-9.9 \times 10^{-1} \pm 9.0 \times 10^{-2}$	5.4×10^{-1}
AllBac	mL^{-1}	56°C	$-5.9 \times 10^{-1} \pm 6.9 \times 10^{-2}$	2.9×10^{-1}
AllBac	mL^{-1}	60°C	$-7.9 \times 10^{-1} \pm 3.1 \times 10^{-2}$	2.4×10^{-1}

AllBac	mL^{-1}	63°C	-9.0×10^{-1}	\pm	6.3×10^{-2}	1.7×10^{-1}
AllBac	$(16\text{S rRNA gene})^{-1}$	40°C	-9.0×10^{-1}	\pm	1.0×10^{-1}	6.4×10^{-1}
AllBac	$(16\text{S rRNA gene})^{-1}$	56°C	-4.9×10^{-1}	\pm	6.0×10^{-2}	5.8×10^{-1}
AllBac	$(16\text{S rRNA gene})^{-1}$	60°C	-6.2×10^{-1}	\pm	3.5×10^{-2}	4.3×10^{-1}
AllBac	$(16\text{S rRNA gene})^{-1}$	63°C	-7.6×10^{-1}	\pm	8.9×10^{-2}	4.0×10^{-1}
Methanogen 16S rRNA genes	mL^{-1}	40°C	-7.0×10^{-3}	\pm	8.5×10^{-2}	6.7×10^5
Methanogen 16S rRNA genes	mL^{-1}	56°C	-2.0×10^{-1}	\pm	6.5×10^{-2}	5.7×10^{-1}
Methanogen 16S rRNA genes	mL^{-1}	60°C	-1.8×10^{-1}	\pm	7.1×10^{-2}	1.3×10^{-1}
Methanogen 16S rRNA genes	mL^{-1}	63°C	-4.4×10^{-1}	\pm	1.1×10^{-1}	4.8×10^{-1}
Methanogen 16S rRNA genes	$(16\text{S rRNA gene})^{-1}$	40°C	8.8×10^{-2}	\pm	9.1×10^{-2}	3.2×10^{-2}

Methanogen 16S rRNA genes	(16S rRNA gene) ⁻¹	56°C	-8.9×10 ⁻²	±	5.8×10 ⁻²	6.0×10 ¹
Methanogen 16S rRNA genes	(16S rRNA gene) ⁻¹	60°C	-2.2×10 ⁻²	±	4.7×10 ⁻²	9.1×10 ³
Methanogen 16S rRNA genes	(16S rRNA gene) ⁻¹	63°C	-3.0×10 ⁻¹	±	7.9×10 ⁻²	6.1×10 ⁰
<i>intII</i>	mL ⁻¹	40°C	-2.3×10 ⁻¹	±	2.2×10 ⁻²	1.1×10 ⁻¹
<i>intII</i>	mL ⁻¹	56°C	-3.9×10 ⁻¹	±	3.6×10 ⁻²	8.3×10 ⁻²
<i>intII</i>	mL ⁻¹	60°C	-5.5×10 ⁻¹	±	3.2×10 ⁻²	1.6×10 ⁻¹
<i>intII</i>	mL ⁻¹	63°C	-4.9×10 ⁻¹	±	8.0×10 ⁻²	3.6×10 ⁻²
<i>intII</i>	(16S rRNA gene) ⁻¹	40°C	-1.4×10 ⁻¹	±	3.3×10 ⁻²	1.1×10 ⁻¹
<i>intII</i>	(16S rRNA gene) ⁻¹	56°C	-2.9×10 ⁻¹	±	3.9×10 ⁻²	1.8×10 ⁻¹
<i>intII</i>	(16S rRNA gene) ⁻¹	60°C	-3.9×10 ⁻¹	±	4.9×10 ⁻²	3.4×10 ⁻¹

<i>intI1</i>	(16S rRNA gene) ⁻¹	63°C	-3.5×10 ⁻¹	±	5.0×10 ⁻²	1.2×10 ⁻¹
<i>qnrA</i>	mL ⁻¹	40°C			ND ^b	
<i>qnrA</i>	mL ⁻¹	56°C	-9.0×10 ⁻²	±	9.1×10 ⁻²	5.6×10 ⁻⁶
<i>qnrA</i>	mL ⁻¹	60°C	-1.6×10 ⁻²	±	1.2×10 ⁻¹	1.6×10 ⁻³³
<i>qnrA</i>	mL ⁻¹	63°C	-1.6×10 ⁻¹	±	1.3×10 ⁻¹	6.1×10 ⁻⁵
<i>qnrA</i>	(16S rRNA gene) ⁻¹	40°C			ND ^b	
<i>qnrA</i>	(16S rRNA gene) ⁻¹	56°C	1.4×10 ⁻²	±	7.3×10 ⁻²	1.8×10 ¹⁸
<i>qnrA</i>	(16S rRNA gene) ⁻¹	60°C	1.0×10 ⁻¹	±	2.3×10 ⁻¹	4.0×10 ²
<i>qnrA</i>	(16S rRNA gene) ⁻¹	63°C	-7.8×10 ⁻²	±	1.3×10 ⁻¹	1.2×10 ⁻⁴
<i>repA</i>	mL ⁻¹	40°C			ND ^b	

<i>repA</i>	mL ⁻¹	56°C			ND ^b	
<i>repA</i>	mL ⁻¹	60°C			ND ^b	
<i>repA</i>	mL ⁻¹	63°C			ND ^b	
<i>repA</i>	(16S rRNA gene) ⁻¹	40°C			ND ^b	
<i>repA</i>	(16S rRNA gene) ⁻¹	56°C			ND ^b	
<i>repA</i>	(16S rRNA gene) ⁻¹	60°C			ND ^b	
<i>repA</i>	(16S rRNA gene) ⁻¹	63°C			ND ^b	
<i>tet</i> (W)	mL ⁻¹	40°C	-2.4×10 ⁻¹	± 7.3×10 ⁻²		5.7×10 ⁻²
<i>tet</i> (W)	mL ⁻¹	56°C	-7.0×10 ⁻¹	± 5.6×10 ⁻²		2.3×10 ⁻¹
<i>tet</i> (W)	mL ⁻¹	60°C	-7.8×10 ⁻¹	± 3.0×10 ⁻²		1.6×10 ⁻¹

<i>tet</i> (W)	mL ⁻¹	63°C	-8.1×10 ⁻¹	±	6.3×10 ⁻²	1.1×10 ⁻¹
<i>tet</i> (W)	(16S rRNA gene) ⁻¹	40°C	-1.5×10 ⁻¹	±	7.8×10 ⁻²	4.5×10 ⁻²
<i>tet</i> (W)	(16S rRNA gene) ⁻¹	56°C	-6.0×10 ⁻¹	±	5.1×10 ⁻²	4.0×10 ⁻¹
<i>tet</i> (W)	(16S rRNA gene) ⁻¹	60°C	-6.3×10 ⁻¹	±	5.7×10 ⁻²	2.6×10 ⁻¹
<i>tet</i> (W)	(16S rRNA gene) ⁻¹	63°C	-6.7×10 ⁻¹	±	4.1×10 ⁻²	2.4×10 ⁻¹
<i>tet</i> (X)	mL ⁻¹	40°C	-4.2×10 ⁻¹	±	3.5×10 ⁻²	2.5×10 ⁻¹
<i>tet</i> (X)	mL ⁻¹	56°C	-8.0×10 ⁻¹	±	6.7×10 ⁻²	2.1×10 ⁻¹
<i>tet</i> (X)	mL ⁻¹	60°C	-4.3×10 ⁻¹	±	1.5×10 ⁻¹	5.1×10 ⁻²
<i>tet</i> (X)	mL ⁻¹	63°C	-1.1×10 ⁰	±	1.3×10 ⁻¹	9.2×10 ⁻²
<i>tet</i> (X)	(16S rRNA gene) ⁻¹	40°C	-3.4×10 ⁻¹	±	4.2×10 ⁻²	3.4×10 ⁻¹

<i>tet</i> (X)	(16S rRNA gene) ⁻¹	56°C	-6.9×10 ⁻¹	± 7.7×10 ⁻²	3.3×10 ⁻¹
<i>tet</i> (X)	(16S rRNA gene) ⁻¹	60°C	-2.7×10 ⁻¹	± 1.3×10 ⁻¹	7.4×10 ⁻²
<i>tet</i> (X)	(16S rRNA gene) ⁻¹	63°C	-9.7×10 ⁻¹	± 1.3×10 ⁻¹	1.8×10 ⁻¹

^aSee Table C.5 for ANOVA *P* values, which are equal to values of *P* for *k*, as well as other summary metrics that describe the quality of fit of the model to the data.

^bQuantities of some gene targets were above quantification limits for only $n \leq 2$ time points, so *k* was not determined (ND).

5.4 Discussion

Hyperthermophilic anaerobic digestion holds promise as a treatment technology that can remove ARGs and *intI1* from residual municipal wastewater solids. Hyperthermophilic digestion outperformed both mesophilic anaerobic digestion and thermophilic anaerobic digestion by tending to increase the magnitude of kinetic parameters with temperature. The difference in performance between hyperthermophilic and thermophilic anaerobic digestion was not as clear as the difference between thermophilic and mesophilic digestion, however. As a result, future work should focus on varying other operational conditions within the hyperthermophilic temperature range, like hydraulic residence time and flow regime, to determine if hyperthermophilic anaerobic digestion can be optimized to further enhance the removal of ARGs and *intI1* from residual municipal wastewater solids relative to thermophilic anaerobic digestion. These future efforts would be aided by continued consideration of the kinetics of ARG and *intI1* removal, because they provide an excellent means for comparing performance among various treatment conditions. An important caveat to this approach is that the kinetic model must be appropriate for the data. For the results presented here, a modified form of the Collins-Selleck kinetic model was found to be the most appropriate of the models considered, because it could describe retarded rate kinetics well. Visual inspection of some previous results (121) indicates that the same model could be appropriate for those previous data as well.

The fact that the modified form of the Collins-Selleck model tended to be the best fit model for most of the time series in this work is likely a reflection of cell death being

the primary driver, particularly in the early stages of each batch, of ARG removal in these treatment units. The Collins-Selleck model was originally developed to describe the kinetics of bacterial inactivation with chlorine (215). This process is often characterized by values of the logarithm of concentration that decline at a retarded rate with time (184,214), which was the same trend observed for many gene targets in this work. The typical explanation for retarded rate kinetics during chlorine disinfection is that the distribution of bacterial community members' resistance to chlorine is initially relatively wide, and that as the less resistant microorganisms in the community are eliminated, the observed rate of decline in bacterial concentrations slows because the distribution of resistance to chlorine narrows to include only those microorganisms that are most resistant to the disinfectant (184,214). It seems likely that a similar process occurs during anaerobic digestion. The initial distribution of bacterial community members' ability to survive in an anaerobic environment at a particular temperature is probably quite wide, but as members of the original community die off, this distribution narrows to include only those microorganisms most able to cope with the conditions presented by the anaerobic digestion environment. As a result, observed quantities of 16S rRNA genes, 16S rRNA genes of microorganisms unable to survive under the given conditions (e.g. AllBac), and other gene targets associated with microorganisms unable to survive under the given conditions (i.e. ARGs, *int11*, and *repA*) all decrease with time in a trend consistent with disinfection (i.e. mixed-community cell death) kinetics. This may also offer a potential explanation for why semi-batch thermophilic and hyperthermophilic anaerobic digestion appear to be superior to semi-batch mesophilic anaerobic digestion

for removing ARGs and *intI1* from residual solids. Due to the unique environments they impose, thermophilic and hyperthermophilic anaerobic digesters significantly narrow the subset of the initial distribution of microorganisms (and the ARGs and integrons that they carry) that will survive to the end of treatment.

This work suggests that batch or semi-batch treatment of residual municipal wastewater solids at relatively long target solids residence times may hold promise as an effective means of reducing the quantities of ARGs and *intI1* discharged from the municipal wastewater treatment process. Quantities of all gene targets in this work decreased during eight-day semi-batches at target residence times of 30 to 35 d. A similar result has been demonstrated during batch aerobic digestion at a target residence time of approximately 40 d, even when semi-continuous-flow aerobic digestion at the same target residence time failed to remove *intI1* and enriched *tet(X)* (204). At shorter target residence times (15 d) and with five-day batches, however, some gene targets tended to decrease in quantity during mesophilic and thermophilic anaerobic digestion while *tet(L)* tended to remain unchanged and *tet(W)* decreased only at thermophilic temperatures (121). Similarly, semi-continuous-flow mesophilic anaerobic digestion at relatively short residence times (10 d and 20 d) causes some ARGs to decrease in quantity during treatment and others to increase (131). This may be due to continuous-flow or semi-continuous-flow environments inducing feast-famine cycles of cell growth, while batch or semi-batch treatment environments ultimately induce only famine (i.e. cell death).

The distribution of gene cassettes on class 1 integrons in residual municipal wastewater solids needs to be examined more thoroughly in order to critically assess the factors governing the fate of class 1 integrons during treatment of residual municipal wastewater solids. Class 1 integrons are a potentially important gene target on which to focus treatment and management strategies intended to reduce the number of ARGs discharged from the municipal wastewater treatment process because they enable both horizontal gene transfer of ARGs and the accumulation of multiple resistance genotypes (82). However, their fate during treatment of residual municipal wastewater solids has been demonstrated to vary widely depending on operating conditions. Semi-batch thermophilic anaerobic digestion was demonstrated to remove *intI1* to a greater extent than semi-batch mesophilic anaerobic digestion in both this work and a previous study (121). However, other studies have demonstrated semi-continuous-flow mesophilic anaerobic digestion at solids residence times of both 10 d and 20 d to outperform semi-continuous-flow thermophilic anaerobic digestion (131). Quantities of *intI1* have also been demonstrated to remain unchanged during semi-continuous-flow aerobic digestion at 15°C (204) and to increase by approximately two orders of magnitude during semi-continuous-flow aerobic digestion following semi-continuous-flow anaerobic digestion (131). These disparate results could be plausibly explained by the hypothesis that the relationship between the distribution of gene cassettes on class 1 integrons and the treatment environment determines a selective advantage (or lack thereof) for the integron's host. However, the majority of the current body of knowledge regarding the distribution of gene cassettes on integrons in the municipal wastewater treatment process

is focused on treatment stages other than residual solids treatment (198). Understanding the distribution of gene cassettes, ARGs or otherwise, on integrons in residual solids undergoing treatment in various technologies will be critical to determining how their fate can be controlled during residual solids treatment.

This work adds support to previous results suggesting that the relationship between the ecological conditions of the treatment unit and the presumed ecological niche of specific ARGs (or *intI1*) can have a significant impact on the effectiveness of the treatment technology (204,208). This can be illustrated by comparing the differing fates of *tet(W)*, which is associated with anaerobic microorganisms (212), and *tet(X)*, which requires oxygen to be functional (210,211), during anaerobic and aerobic digestion. During aerobic digestion of residual municipal wastewater solids under semi-continuous-flow conditions, *tet(W)* quantities are reduced by more than an order of magnitude, while *tet(X)* quantities are enriched approximately 5-fold (204). Similarly, although quantities of both gene targets are reduced during aerobic digestion under batch conditions, *tet(W)* quantities are reduced at a significantly faster rate ($P = 6 \times 10^{-4}$) than *tet(X)* (204). In contrast, quantities of *tet(W)* were reduced 11-fold at 40°C in the current study, while quantities of *tet(X)* were reduced 23-fold at 40°C. This suggests that the ecological conditions of individual treatment units might be optimized relative to the ecological niches of particular ARGs to provide additional controls over the fate of ARGs in those systems. Furthermore, depending on the ARG or ARGs that limit the design of a particular residual solids treatment system, ideal treatment processes may consist of

multiple treatment units that alternate between extremes in terms of ecological conditions (e.g. redox conditions).

The major limitations of this work are related to the semi-batch design of the anaerobic digesters and to the well-known limitations of culture-independent analytical approaches. While the potential benefits of semi-batch treatment of residual municipal wastewater solids have been discussed above, the semi-batch design of the digesters examined here does not reflect the design of existing full-scale (i.e. continuous-flow or semi-continuous-flow) anaerobic digesters. Thus, these results, and in particular the specific kinetic parameters presented here, may not be readily transferable to the existing infrastructure. Furthermore, the real-time PCR protocol used in this work cannot distinguish gene targets in pathogens from those in non-pathogens or gene targets in living bacteria from those in dead bacteria or present as extracellular DNA in the sample matrix. This work also investigates a very small handful (three) of ARGs along with *intI1* and *repA*. There are numerous known ARGs, plasmids, and other genetic elements related to antibiotic resistance, and the fate of those considered here does not necessarily represent that of all the others.

**Chapter 6: The Fate of Antibiotic Resistance Genes and Class 1
Integrans in Soil Microcosms Following the Application of Treated
Residual Municipal Wastewater Solids from Full-Scale Treatment
Facilities**

Substantial quantities of antibiotic resistance genes (ARGs) are discharged in treated residual municipal wastewater solids. While the fate of ARGs in residual solids treatment units is under scrutiny, their fate following treatment has received minimal attention. The objective of this work was to determine kinetic coefficients for ARG and class 1 integron quantities in soil following simulated land-application of treated residual solids. Treated residual solids from two full-scale treatment plants were applied to sets of triplicate soil microcosms in two experiments. Experiment 1 investigated loading rates of 20, 40, and 100 g residual solids kg⁻¹ soil in a sand mixture, while Experiment 2 investigated a loading rate of 40 g kg⁻¹ in a silt loam. Six ARGs (*erm*(B), *qnrA*, *sulI*, *tet*(A), *tet*(W), and *tet*(X)), the integrase of class 1 integrons (*intI1*), the origin of replication of incompatibility group A/C plasmids (*repA*), 16S rRNA genes, 16S rRNA genes of all *Bacteroides* spp. (AllBac), and 16S rRNA genes of human-specific *Bacteroides* spp. (HF183) were quantified using real-time PCR. ARG and *intI1* quantities declined in most microcosms, with statistically significant ($P < 0.05$) half-lives varying between 13 d (*erm*(B), Experiment 1, 100 g kg⁻¹) and 81 d (*intI1*, Experiment 1, 40 g kg⁻¹). First-order kinetic coefficients for ARGs and *intI1* varied more substantially with gene target than with loading rate in Experiment 1, and ARGs and *intI1* were as persistent ($P \geq 0.05$, Welch's t-test) or more persistent ($P < 0.05$, Welch's t-test) in Experiment 2 compared to Experiment 1. These kinetic coefficients can be used to optimize the residual solids disposal process to reduce the quantities of ARGs and *intI1* discharged from municipal wastewater treatment plants.

6.1 Introduction

Resistance of pathogenic bacteria to antibiotic chemotherapy is a major global public health predicament (3,199). As a result, the bacterial antibiotic resistance genes (ARGs) that confer resistance are increasingly regarded as environmental pollutants (5). ARGs have been found in a number of environmental reservoirs, including surface waters, aquaculture facilities, and agricultural waste (5–20). The municipal wastewater treatment process, however, is one of the most significant reservoirs of ARGs. Numerous studies have reported the detection of ARGs at all stages of the treatment process (5,10,21–32). The vast majority of these ARGs, along with the vast majority of prokaryotic biomass, are discharged from the municipal wastewater treatment process in the treated residual solids (27). As a result, the residual solids treatment step could be an excellent target for the application of strategies intended to eliminate ARGs from the municipal wastewater treatment process.

Existing technologies can remove ARGs from residual municipal wastewater solids. Aerobic digestion, air-drying beds, mesophilic anaerobic digestion, and thermophilic anaerobic digestion have all been demonstrated to reduce ARG quantities in residual municipal wastewater solids in laboratory-scale treatment units (121,131,132,204,208). Mesophilic and thermophilic anaerobic digestion have also been demonstrated to reduce ARG quantities at a full-scale treatment facility (24). Efforts have been undertaken to optimize these treatment technologies for reducing ARG quantities, as some work has investigated varying temperatures, residence times, and pretreatment options (121,131).

In contrast, the fate of the ARGs in treated residual solids following their application to agricultural soils remains poorly understood. Understanding the fate of ARGs in such soils is important because approximately 50% of all treated residual municipal wastewater solids in the United States are ultimately disposed of via land-application (186). Furthermore, this scenario potentially leads to several plausible transport pathways that could result in human exposure to ARGs. These pathways include transport in microorganisms in stormwater runoff to surface waters used for recreation and drinking water sources (216) as well as aerosolization of microorganisms over local and even global scales (217–221).

The objective of this research was to determine the rate at which ARG quantities decline in soils following the application of treated residual municipal wastewater solids. An initial experiment (Experiment 1) was performed to test the hypothesis that ARG quantities would decline more slowly at higher mass loading rates of residual solids to soil. Soil microcosms were constructed using a sand mixture, and dewatered treated residual solids from a full-scale treatment facility were mixed with the soil at loading rates of 20, 40, and 100 g residual solids kg⁻¹ soil. These loading rates are within the range of those commonly used in practice (184). This procedure was then repeated in a second experiment (Experiment 2) using a similar source of residual municipal wastewater solids and a different soil type (silt loam). Experiment 2 used a loading rate of 40 g residual solids kg⁻¹ soil. A set of representative ARGs and the integrase of class 1 integrons (*intI1*) were quantified over time in all soil microcosms using real-time PCR.

The quantities of ARGs and *intI1* declined over time under most experimental conditions, with half-lives on the order of months.

6.2 Materials and Methods

Experimental Design. Two experiments were conducted using two different soils and residual wastewater solids from two different treatment facilities. Triplicate microcosms were constructed for each experimental condition by adding 200 g of soil to a 710-mL sealable plastic container (Rubbermaid Consumer Products, Fairlawn, OH). Soil 1 was a 1:1 mixture of sand with homogenized and sieved (2 mm) soil cuttings from the vadose and saturated zones of an aquifer in southwestern Minnesota. The composition of Soil 1 was 90% sand, 1.8% silt, and 8.3% clay, with an average organic matter fraction of 0.006 by mass. Soil 2 was a Waukegan silt loam (fine-silty, mixed, mesic Typic Hapludoll) with an initial moisture content of $12.1\% \pm 0.3\%$ (mean \pm standard deviation). Residual Solids 1 and 2 were dewatered treated residual municipal wastewater solids collected from similar full-scale treatment plants. Residual Solids 1 were collected from a 24 MGD plant in eastern Minnesota that uses mesophilic anaerobic digestion for residual solids treatment. Residual Solids 2 were collected from an 11 MGD plant in southern Minnesota that uses mesophilic anaerobic digestion for solids treatment and a belt filter press for dewatering. Residual Solids 2 had an initial moisture content of $82.8\% \pm 0.5\%$ (mean \pm standard deviation). All microcosms were stored at room temperature (approximately 20°C). Evaporative water losses for all microcosms were estimated by weighing the microcosms at approximately monthly intervals and assuming that all mass loss was due to evaporation of water.

Sample Collection and Genomic DNA Extraction. Triplicate samples of approximately 0.5 g were collected from each soil microcosm at each time point. Samples were then stored at -20 °C until genomic DNA was extracted and purified using the FastDNA Spin Kit for Soil (MP Biomedicals, Solon, OH) and a BIO 101 Thermo Savant FastPrep FP120 Cell Disruptor (Qbiogene, Inc., Carlsbad, CA).

Real-time PCR. Real-time PCR was used to quantify 11 different gene targets. Three of these gene targets represent different fractions of prokaryotic biomass. The 16S rRNA gene was quantified as a measure of total bacterial biomass, while AllBac was used as a representative fecal indicator (195), and HF183 was used as an indicator of human feces (194,203). Six gene targets correspond to ARGs that collectively represent a cross-section of antibiotic classes (macrolides, tetracyclines, sulfonamides, and fluoroquinolones) and resistance mechanisms. The final two gene targets were the integrase gene of class 1 integrons (*intII*) and the origin of replication (replication initiation protein A) for incompatibility group A/C plasmids (*repA*), each of which represents the potential for both horizontal gene transfer and the accumulation of multiple ARGs (82,222). The *repA* method was developed in collaboration with Timothy Johnson and Kevin Lang of the University of Minnesota Department of Veterinary and Biomedical Sciences (St. Paul, Minnesota, United States). The forward and reverse primer sequences, expected amplicon sizes, and primer annealing temperatures for all gene targets are listed in Appendix D (Table D.1) (8,24,95,151,195,196,200–202).

Real-time PCR assays were carried out on an Eppendorf Mastercycler EP Realplex thermal cycler (Eppendorf, Westbury, NY). Thermal cycles typically began

with 1 min of initial denaturation at 95°C, followed by 40 cycles of denaturation at 95°C for 15 s and combined annealing and extension for 1 min at the primer-specific annealing temperature. PCR assays were optimized to reduce or eliminate the formation of primer dimers, and melting curves were typically conducted for all assays following amplification to screen for non-specific products. Melting curves began with 15 s at the primer-specific annealing temperature followed by a 20 min ramp up to 95°C and a final hold at 95°C for 15 s. Reaction volumes were 25 µL and consisted of 12.5 µL of BioRad iTaq SYBR Green Supermix with ROX (Life Science Research, Hercules, CA), 25 µg of bovine serum albumin, 12.5 pmol of forward primer, 6.25 pmol of reverse primer, and approximately 1 ng of template genomic DNA. Standards were prepared by initially amplifying gene targets from well-described bacterial isolates or municipal wastewater solids using PCR. PCR products were then ligated into the pGEM-T Easy cloning vector and transformed into either JM109 or DH5α competent cells. Cloned plasmids were extracted from cell cultures using either an alkaline lysis procedure (197) or a QIAprep Spin Miniprep Kit (Qiagen, Valencia, CA). Plasmid DNA concentrations in these extracts were determined using a TD-700 fluorometer and Hoechst 33258 dye. Separate standard curves were constructed for each individual assay (i.e. each 96-well plate contained a standard curve), and each standard curve consisted of a 10-fold serial dilution of an aliquot of plasmid DNA extract. The number of standards, slope, intercept, amplification efficiency, r^2 , and quantification limit for each standard curve are provided in Appendix D (Table D.2). Of the 51 assays performed, 38 (74%) had amplification efficiencies of $100\% \pm 10\%$ (maximum deviation from 100%) with $r^2 \geq 0.98$ for a

minimum of five points on each standard curve. The absolute values by which amplification efficiencies for the remaining 13 assays deviated from 100% were between 11% and 21% with $r^2 \geq 0.99$ for a minimum of seven points on each standard curve.

Each triplicate sample was analyzed once to produce triplicate analytical measurements for each soil microcosm on each sample date. Thus, these triplicate measurements reflect the combined variability of DNA extraction and real-time PCR. Values represented in figures and tables are typically the arithmetic mean of triplicate measurements. If, however, only one sample in a triplicate set amplified for any given gene target, then that value was discarded and the set of triplicates that it belonged to were collectively reported as less than the quantification limit. If two samples in a triplicate set amplified, then the arithmetic mean of those two values was reported as representing the set of triplicates that they belonged to. These cases are referred to as being duplicate samples in figure captions.

Data Analysis. Simple linear regression (Arc 1.06) was used to determine first-order kinetic coefficients for all time series of gene target quantities and all time series of ARG and *intI1* ratios to the 16S rRNA gene. A first-order kinetic model was hypothesized because previous work has shown the decline of ARG and *intI1* quantities in several different types of natural and engineered systems to follow first-order trends (115,121,170,204,206,208). First-order kinetic models also provide a valuable descriptive and interpretive tool that is useful for comparing results across different gene targets and environments. A formal lack-of-fit test was applied to test the null hypothesis

that the natural logarithm of gene target quantities (or ARG and *intI1* ratios to 16S rRNA gene quantities) varied linearly with respect to time (205).

6.3 Results

Initial and Operating Conditions. Two experiments were performed using different soil types (a sand mixture in Experiment 1 and silt loam soil in Experiment 2) and residual solids from two different wastewater treatment facilities. Experiments 1 and 2 were similar with respect to evaporation and initial ARG and *intI1* quantities in the residual solids (Table 6.1 and Table 6.2). The rates and extents of water loss during the experiments were low and similar across groups of microcosms despite differences in soil type, residual solids loading rates, and residual solids source. Similarly, the quantities of 16S rRNA genes, AllBac, and *tet(A)* in Residual Solids 1 and 2 were not significantly different ($P \geq 0.05$). Quantities of *erm(B)*, *intI1*, and *sulI* differed significantly ($P < 0.05$), but minimally, by factors of two to four. Only quantities of HF183, *tet(W)*, and *tet(X)* differed ($P < 0.05$) substantially between the two residual solids sources. Quantities of *tet(W)* and *tet(X)* differed by factors of 12 and nearly 60, respectively, while HF183 was on the order of 10^3 copies mg^{-1} wet mass in Residual Solids 1 but was below the quantification limit (2.3×10^3 copies mg^{-1} wet mass) for Residual Solids 2. Finally, quantities of *qnrA* were extremely low, and quantities of *repA* were below the quantification limit (2.0×10^3 copies mg^{-1} wet mass) in Residual Solids 2, so they were not quantified in Residual Solids 1.

Table 6.1. Net evaporation rates and the total mass of water lost to evaporation (expressed as the fraction of the initial mass of soil and residual solids present in each microcosm) for sets of three replicate microcosms at all loading rates for each experiment. Error terms represent the standard error of the mean.

Loading Rate (g kg⁻¹)	Experiment	Net Evaporation Rate^a (mm H₂O day⁻¹)	Fraction of Initial Microcosm Mass Lost to Evaporation
0	1	2×10 ⁻³ ± 3×10 ⁻⁴	3.5% ± 1.1%
20	1	2×10 ⁻³ ± 4×10 ⁻⁴	3.6% ± 1.2%
40	1	1×10 ⁻³ ± 1×10 ⁻⁴	2.0% ± 0.4%
100	1	2×10 ⁻³ ± 2×10 ⁻⁴	2.0% ± 0.6%
0	2	2×10 ⁻³ ± 9×10 ⁻⁵	3.3% ± 0.6%
40	2	2×10 ⁻³ ± 6×10 ⁻⁵	3.4% ± 0.3%

^aNet evaporation rates were determined using linear regression (Arc 1.06). The predictor was time, and the cumulative mass of water lost from each group of replicate soil microcosms (i.e. three values at each time point) was used as the response variable. All evaporation rates are statistically significant ($P < 0.05$).

Table 6.2. The quantities of all gene targets in both residual solids sources. Values are the arithmetic mean of triplicate samples; error terms represent one standard deviation.

Gene Target	Gene Copies (mg ⁻¹ wet mass)					
	Residual Solids 1			Residual Solids 2		
16S rRNA genes	4.5×10 ⁸	±	2×10 ⁷	9.2×10 ⁸	±	4×10 ⁸
AllBac	1.6×10 ⁷	±	1×10 ⁶	1.2×10 ⁷	±	5×10 ⁶
HF183 ^a	4.2×10 ³	±	8×10 ²	< 2.3×10 ³		
<i>erm</i> (B)	3.1×10 ⁶	±	4×10 ⁵	1.9×10 ⁶	±	4×10 ⁵
<i>intI1</i>	2.1×10 ⁵	±	2×10 ⁴	6.7×10 ⁵	±	2×10 ⁵
<i>qnrA</i>	ND ^b			2.7×10 ¹	±	2×10 ¹
<i>repA</i>	ND ^b			< 2.0×10 ³		
<i>sulI</i>	6.0×10 ⁵	±	1×10 ⁵	2.1×10 ⁶	±	5×10 ⁵
<i>tet</i> (A)	3.7×10 ⁴	±	4×10 ³	4.4×10 ⁴	±	1×10 ⁴
<i>tet</i> (W)	6.4×10 ⁵	±	3×10 ⁴	7.8×10 ⁶	±	3×10 ⁶
<i>tet</i> (X)	3.4×10 ⁵	±	5×10 ⁴	5.8×10 ³	±	3×10 ³

^aHF183 quantities were below the quantification limit in Residual Solids 2.

^bQuantities of *qnrA* and *repA* were extremely low or below the quantification limit, respectively, in Residual Solids 2, so they were not determined (ND) in Residual Solids 1.

Negative Control Microcosms. Experiments 1 and 2 differed with respect to ARG and *intI1* quantities in experimental negative control microcosms (Table 6.3). All ARGs and *intI1* were below quantification limits in Soil 1 throughout the experiment, except for *sul1*, which appeared in low quantities at three time points. In contrast, *sul1* and *intI1* were detected at 15 of 24 and 24 of 24 time points, respectively, in Soil 2 during the experiment, although these background quantities were low relative to those found in both residual solids. The *erm(B)* and *tet(X)* gene targets also appeared in relatively low quantities at a handful of time points, while quantities of *tet(A)* and *tet(W)* were below quantification limits throughout Experiment 2.

Table 6.3. The number of data points with quantifiable values (*n*) and quantities for AllBac, HF183, ARGs, and *intI1* in triplicate experimental negative control microcosms for both experiments. Values are the arithmetic mean of *n* data points; error terms represent one standard deviation.

Gene Target	Experiment 1		Experiment 2	
	<i>n</i> ^a	Gene Copies (mg ⁻¹ wet mass)	<i>n</i> ^b	Gene Copies (mg ⁻¹ wet mass)
AllBac	0	NA	4	420 ± 300
HF183	0	NA		ND ^c
<i>erm</i> (B)	0	NA	5	1,100 ± 200
<i>intI1</i>	0	NA	15	970 ± 400
<i>sul1</i>	3	92 ± 40	24	520 ± 200
<i>tet</i> (A)	0	NA	0	NA
<i>tet</i> (W)	0	NA	0	NA
<i>tet</i> (X)	0	NA	1	140

^aOut of 18 total data points for Experiment 1 (3 microcosms × 6 time points per microcosm).

^bOut of 24 total data points for Experiment 2 (3 microcosms × 8 time points per microcosm).

^cQuantities of HF183 were below the quantification limit (2.4×10^3 copies mg^{-1} wet mass) in soil microcosms that received residual solids in Experiment 2, so they were not determined (ND) for the negative control microcosms.

Total Bacterial Biomass. Experiments 1 and 2 also differed with respect to total bacterial biomass (Figure 6.1). Soil 2 contained a larger (one to two orders of magnitude) quantity of 16S rRNA genes than Soil 1. However, 16S rRNA gene quantities in both soils were within the range of previously reported values for direct cell counts in soil (223). Quantities of 16S rRNA genes in both sets of experimental negative controls were low relative to those found in both residual solids and either increased (Soil 1, $P < 0.05$) by less than an order of magnitude or remained constant (Soil 2, $P \geq 0.05$). The initial quantities of 16S rRNA genes in microcosms that received residual solids were higher than in experimental negative controls for both experiments, and remained constant ($P \geq 0.05$) or decreased ($P < 0.05$) by less than an order of magnitude.

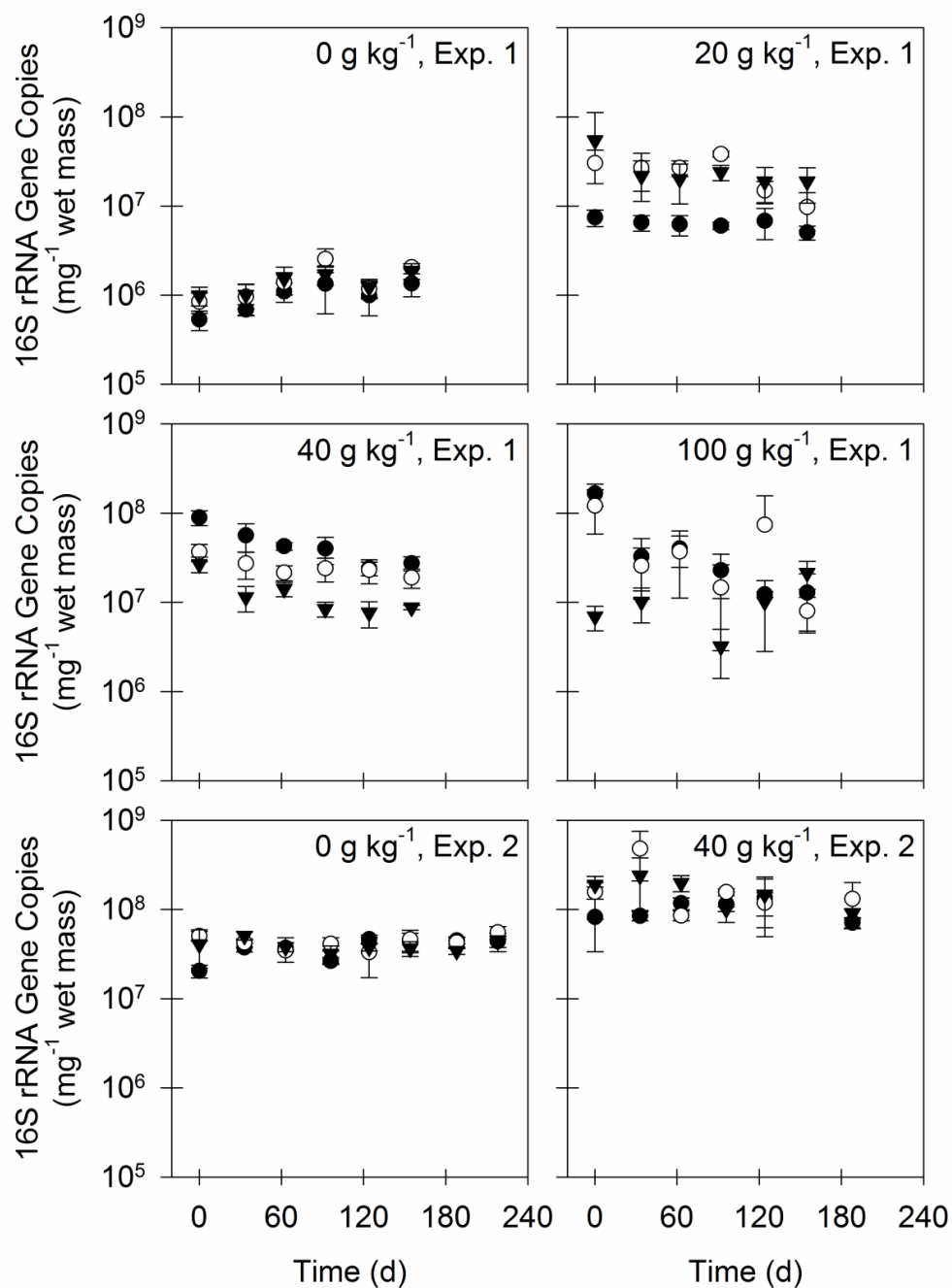


Figure 6.1. The quantities of 16S rRNA genes in three replicate soil microcosms (closed circles, open circles, and closed triangles represent unique experimental units) at all loading rates for both experiments. Values are the arithmetic mean of duplicate or triplicate samples; error bars represent one standard deviation.

Fecal Bacterial Biomass. Experiments 1 and 2 were similar with respect to indicators for fecal bacterial biomass, and fecal biomass followed a different trend with time compared to total bacterial biomass (Figure 6.2). Quantities of AllBac were generally below quantification limits in negative control microcosms for both experiments, except for several sporadic appearances at low quantities in Experiment 2 (Table 6.3). Quantities of AllBac were relatively high in microcosms that received residual solids for both experiments, and initial quantities in microcosms that received 40 g residual solids kg⁻¹ soil were similar for the two experiments. These initially high quantities decreased by approximately three orders of magnitude or more for both experiments, which was consistent with the behavior of genetic markers for other fecal indicators in soil (207). Quantities of HF183 were below quantification limits (5.9×10^2 to 1.5×10^3 copies mg⁻¹ wet mass) in all microcosms throughout Experiment 1, except for the initial time points in the microcosms containing the most residual solids, where it occurred at $1.2 \times 10^3 \pm 3 \times 10^2$ copies mg⁻¹ wet mass. Quantities of HF183 were also below the quantification limit (2.4×10^3 copies mg⁻¹ wet mass) throughout Experiment 2 in the microcosms that received residual solids.

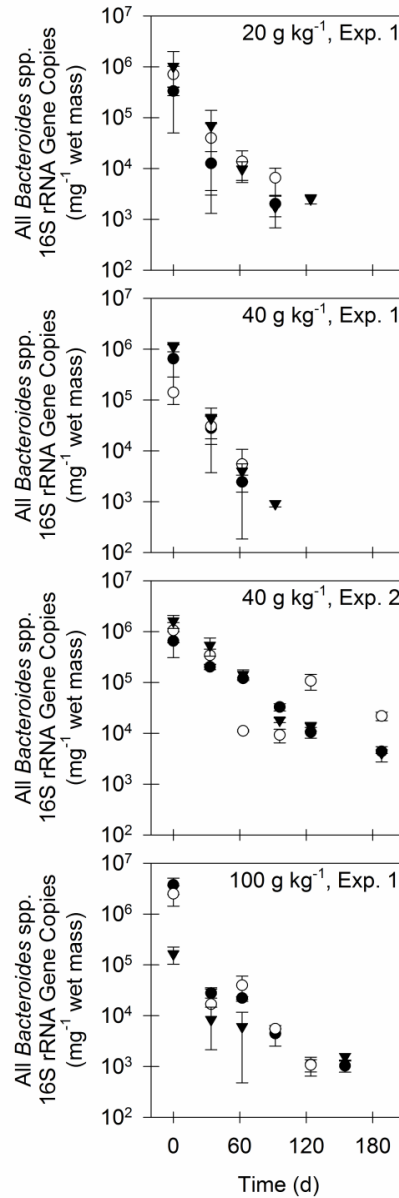


Figure 6.2. The quantities of 16S rRNA genes of all *Bacteroides* spp. in three replicate soil microcosms (closed circles, open circles, and closed triangles represent unique experimental units) at loading rates of 20, 40, and 100 g residual solids kg⁻¹ soil for Experiment 1 and 40 g residual solids kg⁻¹ soil for Experiment 2. Values are the arithmetic mean of duplicate or triplicate samples; error bars represent one standard deviation.

ARGs and *intI1*. ARG and *intI1* quantities in microcosms that received residual solids decreased with time for nearly all cases in Experiment 1 (Figure 6.3, Figure D.1, Figure D.2, Figure D.3, Figure D.4, and Figure D.5). The extents of these decreases varied between approximately one order of magnitude (e.g. *sulI* for 40 g kg⁻¹) and four orders of magnitude (e.g. *erm(B)* for 100 g kg⁻¹). The only quantities that remained constant ($P \geq 0.05$) were those of *sulI* in microcosms receiving 100 g kg⁻¹ of treated residual solids. Similar trends were also observed for the ratios of ARGs and *intI1* to the 16S rRNA gene. All ratios decreased ($P < 0.05$) by one to four orders of magnitude over the course of approximately six months. The only ratios that remained constant ($P \geq 0.05$) were those of *intI1* and *sulI* in microcosms receiving 40 g kg⁻¹ of residual solids and *intI1* in microcosms receiving 100 g kg⁻¹ of residual solids.

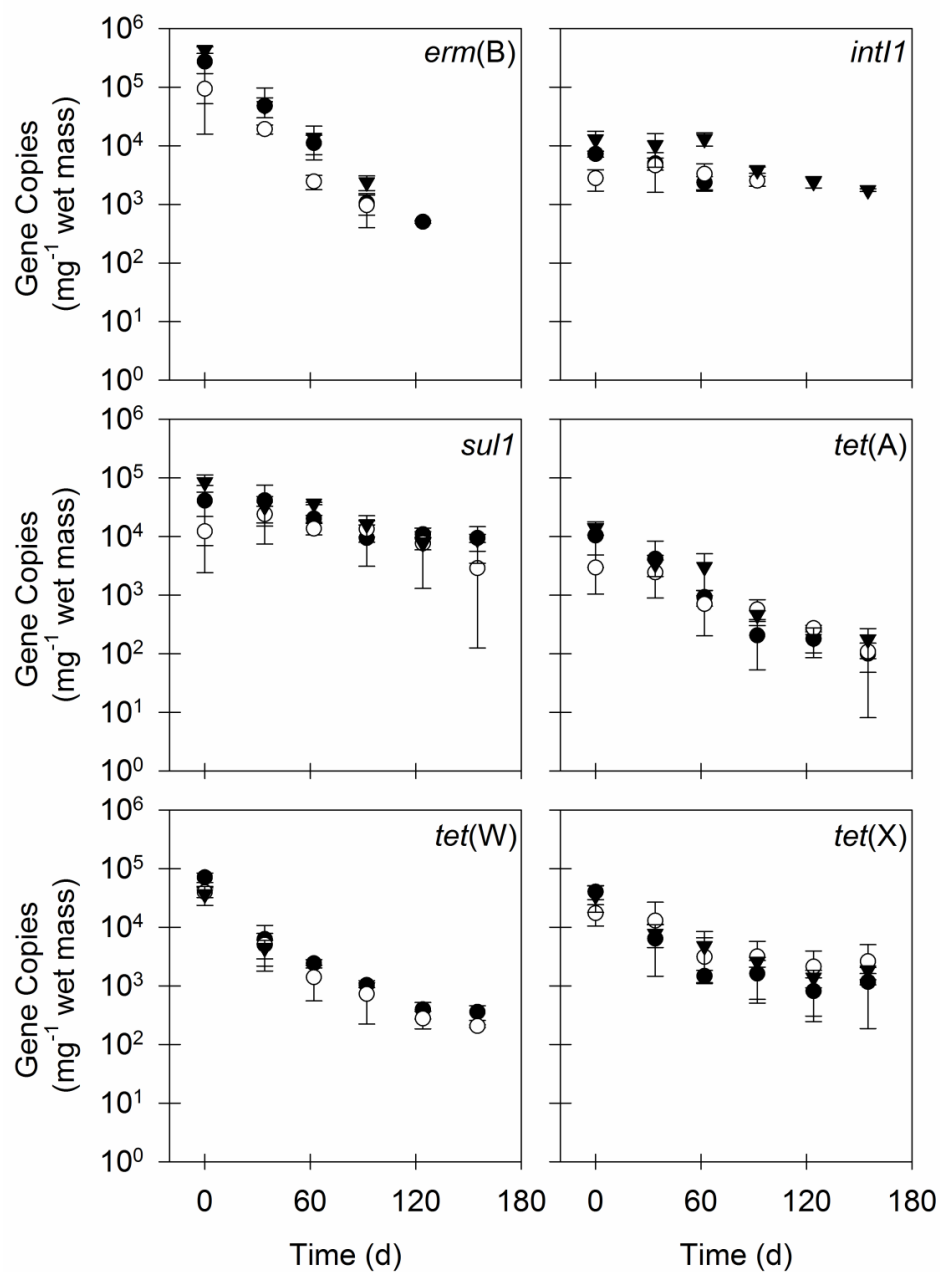


Figure 6.3. The quantities of ARGs and *intI1* in three replicate soil microcosms (closed circles, open circles, and closed triangles represent unique experimental units) at a loading rate of 40 g residual solids kg⁻¹ soil for Experiment 1. Values are the arithmetic mean of duplicate or triplicate samples; error bars represent one standard deviation.

In contrast, the quantities of ARGs and *intI1* in microcosms that received residual solids only decreased for half of the gene targets considered in Experiment 2 (Figure 6.4 and Figure D.6). Initial quantities were within one order of magnitude of those for the 40 g kg⁻¹ microcosms from Experiment 1, except for quantities of *tet(X)*, which were 18-fold higher in the Experiment 1 microcosms. The initially large quantities of *erm(B)*, *sulI*, and *tet(W)* all decreased ($P < 0.05$) to similar extents as they did in Experiment 1. Quantities of *intI1*, *tet(A)*, and *tet(X)*, however, all remained constant ($P \geq 0.05$) throughout Experiment 2. Quantities of *qnrA* and *repA* were below quantification limits throughout Experiment 2 (4.9×10^2 and 2.1×10^2 copies mg⁻¹ wet mass, respectively) in microcosms that received residual solids, so they were not quantified in any other microcosms from Experiment 1 or 2. The trends for ratios of ARGs and *intI1* to 16S rRNA genes were similar. Ratios of *erm(B)*, *sulI*, and *tet(W)* all decreased ($P < 0.05$), while ratios of *intI1* and *tet(X)* did not change ($P \geq 0.05$), and the ratio of *tet(A)* to 16S rRNA genes actually increased ($P < 0.05$) during Experiment 2.

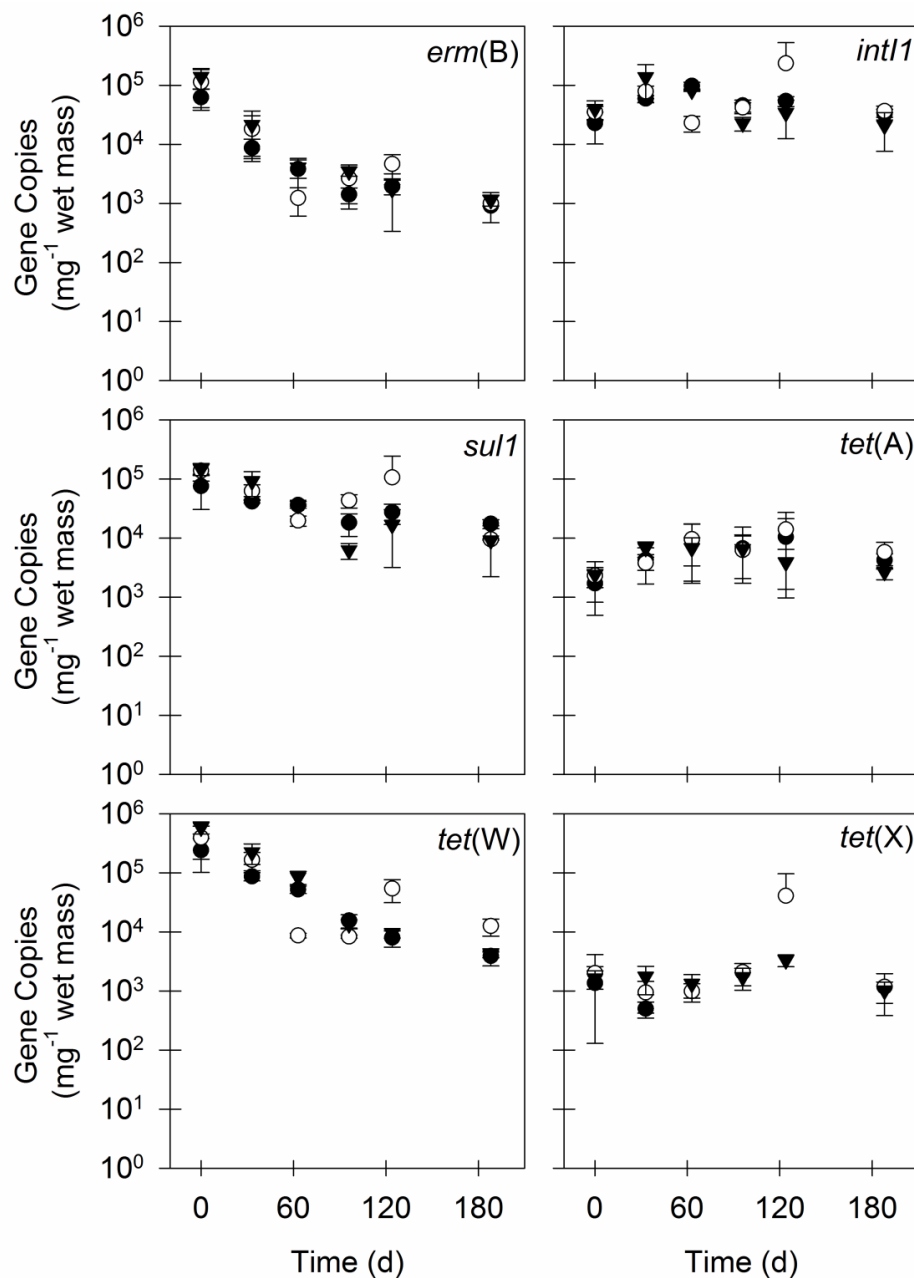


Figure 6.4. The quantities of ARGs and *intI1* in three replicate soil microcosms (closed circles, open circles, and closed triangles represent unique experimental units) at a loading rate of 40 g residual solids kg⁻¹ soil for Experiment 2. Values are the arithmetic mean of duplicate or triplicate samples; error bars represent one standard deviation.

Kinetic Modeling. A first-order kinetic model described the trends in gene target quantities as a function of time reasonably well for soil microcosms in both Experiment 1 and 2 (Table 6.4 and Table 6.5). The lack-of-fit test provided significant ($P < 0.05$) evidence against the null hypothesis for only 14 of the 65 (i.e. 22%) time series to which it could be applied ($n \geq 3$, values for experimental replicates at a minimum of one time point). The 16S rRNA gene was relatively persistent in both experiments. It varied from having a half-life of 110 d (Experiment 1, 40 g kg⁻¹) to a doubling time of 150 d (Experiment 1, negative control microcosms), and most (four of six) of its first-order kinetic coefficients were not statistically significant ($P < 0.05$). In contrast, most (20 of 24) first-order kinetic coefficients for ARGs and *intI1* in microcosms that received residual solids were statistically significant ($P < 0.05$). Statistically significant half-lives for ARGs and *intI1* varied between 13 d (*erm(B)*, Experiment 1, 100 g kg⁻¹) and 81 d (*intI1*, Experiment 1, 40 g kg⁻¹), and the half-lives of AllBac bracketed the low end of this range at values between 10 d (Experiment 1, 40 g kg⁻¹) and 26 d (Experiment 2, 40 g kg⁻¹). Similar trends were observed for the ratios of ARGs and *intI1* to 16S rRNA genes in microcosms that received residual solids. Most (19 of 24) first-order kinetic coefficients for these ratios were statistically significant ($P < 0.05$), and their associated half-lives varied between 15 d (*erm(B)*, Experiment 1, 40 and 100 g kg⁻¹) and 200 d (*tet(X)*, Experiment 1, 100 g kg⁻¹), except for *sulI* at 100 g kg⁻¹ in Experiment 1, which had a doubling time of 150 d.

Table 6.4. First-order kinetic coefficients (k), P , number of data points (n), lack-of-fit P (LOF P), r^2 , and half-lives ($t_{1/2}$) from first-order kinetic models of gene target quantities in three replicate soil microcosms at all loading rates (LR, g treated residual municipal wastewater solids kg⁻¹ soil) for both experiments.

Gene Target	Experiment	LR	$k \pm \text{Standard Error}$ (day ⁻¹)	P	n	LOF P	r^2	$t_{1/2}$ (days)
16S rRNA gene	1	0	$4.8 \times 10^{-3} \pm 1 \times 10^{-3}$	3×10^{-3}	18	0.05	0.44	-150
16S rRNA gene	1	20	$-4.5 \times 10^{-3} \pm 3 \times 10^{-3}$	0.17	18	0.98	0.11	150
16S rRNA gene	1	40	$-6.1 \times 10^{-3} \pm 3 \times 10^{-3}$	0.04	18	0.96	0.24	110
16S rRNA gene	1	100	$-7.5 \times 10^{-3} \pm 4 \times 10^{-3}$	0.11	17	0.66	0.16	93
16S rRNA gene	2	0	$9.4 \times 10^{-4} \pm 6 \times 10^{-4}$	0.13	24	0.63	0.10	-740
16S rRNA gene	2	40	$-2.7 \times 10^{-3} \pm 2 \times 10^{-3}$	0.14	18	0.63	0.13	260

AllBac	1	0			ND ^a				
AllBac	1	20	$-5.0 \times 10^{-2} \pm 6 \times 10^{-3}$		$< 1 \times 10^{-4}$	12	0.10	0.86	14
AllBac	1	40	$-7.2 \times 10^{-2} \pm 7 \times 10^{-3}$		$< 1 \times 10^{-4}$	10	0.61	0.94	10
AllBac	1	100	$-4.2 \times 10^{-2} \pm 7 \times 10^{-3}$		$< 1 \times 10^{-4}$	15	0.04	0.74	17
AllBac	2	0	$3.5 \times 10^{-3} \pm 5 \times 10^{-3}$		0.54	4	0.64	0.21	-200
AllBac	2	40	$-2.6 \times 10^{-2} \pm 4 \times 10^{-3}$		$< 1 \times 10^{-4}$	18	0.20	0.73	26
<i>erm</i> (B)	1	0			ND ^a				
<i>erm</i> (B)	1	20	$-3.9 \times 10^{-2} \pm 4 \times 10^{-3}$		$< 1 \times 10^{-4}$	18	0.64	0.87	18
<i>erm</i> (B)	1	40	$-5.3 \times 10^{-2} \pm 5 \times 10^{-3}$		$< 1 \times 10^{-4}$	13	0.84	0.92	13

<i>erm(B)</i>	1	100	$-5.3 \times 10^{-2} \pm 8 \times 10^{-3}$	$< 1 \times 10^{-4}$	15	0.01	0.77	13
<i>erm(B)</i>	2	0	$-3.8 \times 10^{-4} \pm 1 \times 10^{-3}$	0.78	5	0.19	0.03	1,800
<i>erm(B)</i>	2	40	$-2.2 \times 10^{-2} \pm 3 \times 10^{-3}$	$< 1 \times 10^{-4}$	18	7×10^{-4}	0.72	32
<i>intI1</i>	1	0		ND ^a				
<i>intI1</i>	1	20	$-2.3 \times 10^{-2} \pm 7 \times 10^{-3}$	0.01	10	0.96	0.56	30
<i>intI1</i>	1	40	$-8.6 \times 10^{-3} \pm 3 \times 10^{-3}$	0.03	13	0.99	0.37	81
<i>intI1</i>	1	100	$-9.3 \times 10^{-3} \pm 4 \times 10^{-3}$	0.03	17	0.75	0.29	75
<i>intI1</i>	2	0	$-6.2 \times 10^{-5} \pm 2 \times 10^{-3}$	0.97	15	0.99	0.00	11,000
<i>intI1</i>	2	40	$-1.6 \times 10^{-3} \pm 3 \times 10^{-3}$	0.55	18	0.13	0.02	440

<i>sul1</i>	1	0	$-4.7 \times 10^{-3} \pm 1 \times 10^{-2}$	0.76	3	ND ^b	0.13	150
<i>sul1</i>	1	20	$-1.3 \times 10^{-2} \pm 3 \times 10^{-3}$	2×10^{-4}	18	0.71	0.59	53
<i>sul1</i>	1	40	$-1.2 \times 10^{-2} \pm 2 \times 10^{-3}$	1×10^{-4}	18	0.95	0.65	57
<i>sul1</i>	1	100	$-2.7 \times 10^{-3} \pm 3 \times 10^{-3}$	0.41	18	0.75	0.04	250
<i>sul1</i>	2	0	$-4.7 \times 10^{-4} \pm 1 \times 10^{-3}$	0.73	24	0.58	0.01	1,500
<i>sul1</i>	2	40	$-1.1 \times 10^{-2} \pm 3 \times 10^{-3}$	6×10^{-4}	18	0.26	0.53	63
<i>tet(A)</i>	1	0	ND ^a					
<i>tet(A)</i>	1	20	$-2.5 \times 10^{-2} \pm 5 \times 10^{-3}$	1×10^{-3}	11	0.44	0.72	28
<i>tet(A)</i>	1	40	$-2.8 \times 10^{-2} \pm 2 \times 10^{-3}$	$< 1 \times 10^{-4}$	18	0.65	0.90	25

<i>tet</i> (A)	1	100	$-1.9 \times 10^{-2} \pm 4 \times 10^{-3}$	1×10^{-4}	18	0.29	0.63	37
<i>tet</i> (A)	2	0		ND ^a				
<i>tet</i> (A)	2	40	$2.8 \times 10^{-3} \pm 2 \times 10^{-3}$	0.21	18	4×10^{-3}	0.10	-240
<i>tet</i> (W)	1	0		ND ^a				
<i>tet</i> (W)	1	20	$-3.3 \times 10^{-2} \pm 3 \times 10^{-3}$	$< 1 \times 10^{-4}$	17	1×10^{-3}	0.91	21
<i>tet</i> (W)	1	40	$-3.3 \times 10^{-2} \pm 3 \times 10^{-3}$	$< 1 \times 10^{-4}$	14	4×10^{-3}	0.91	21
<i>tet</i> (W)	1	100	$-4.3 \times 10^{-2} \pm 2 \times 10^{-2}$	0.03	9	0.19	0.52	16
<i>tet</i> (W)	2	0		ND ^a				
<i>tet</i> (W)	2	40	$-2.2 \times 10^{-2} \pm 3 \times 10^{-3}$	$< 1 \times 10^{-4}$	18	0.16	0.74	31

<i>tet</i> (X)	1	0			ND ^a				
<i>tet</i> (X)	1	20	$-2.3 \times 10^{-2} \pm 6 \times 10^{-3}$		2×10^{-3}	17	0.89	0.48	30
<i>tet</i> (X)	1	40	$-1.8 \times 10^{-2} \pm 3 \times 10^{-3}$		$< 1 \times 10^{-4}$	18	0.02	0.73	38
<i>tet</i> (X)	1	100	$-1.2 \times 10^{-2} \pm 4 \times 10^{-3}$		0.01	17	0.67	0.34	59
<i>tet</i> (X)	2	0			ND ^a				
<i>tet</i> (X)	2	40	$3.5 \times 10^{-3} \pm 4 \times 10^{-3}$		0.45	14	0.04	0.05	-200

^aQuantities of some gene targets were above quantification limits for only $n \leq 2$ time points, so k was not determined (ND).

^bQuantities of *sulI* were above quantification limits in only one soil microcosm at a loading rate of 0 g residual solids kg⁻¹ soil for Experiment 1, so the lack-of-fit test could not be conducted, and LOF P was not determined (ND).

Table 6.5. First-order kinetic coefficients (k), P , number of data points (n), lack-of-fit P (LOF P), r^2 , and half-lives ($t_{1/2}$) from first-order kinetic models of ratios of ARGs and *intI1* to 16S rRNA genes in three replicate soil microcosms at all loading rates (LR, g treated residual municipal wastewater solids kg⁻¹ soil) for both experiments.

Gene Target	Experiment	LR	$k \pm$ Standard Error (day ⁻¹)			P	n	LOF P	r^2	$t_{1/2}$ (days)
<i>erm</i> (B)	1	0	ND ^a							
<i>erm</i> (B)	1	20	-3.4×10 ⁻²	±	3×10 ⁻³	< 1×10 ⁻⁴	18	0.41	0.89	20
<i>erm</i> (B)	1	40	-4.6×10 ⁻²	±	7×10 ⁻³	< 1×10 ⁻⁴	13	0.98	0.81	15
<i>erm</i> (B)	1	100	-4.7×10 ⁻²	±	7×10 ⁻³	< 1×10 ⁻⁴	15	< 1×10 ⁻⁴	0.79	15
<i>erm</i> (B)	2	0	-1.0×10 ⁻³	±	8×10 ⁻⁴	0.28	5	0.04	0.36	680
<i>erm</i> (B)	2	40	-1.9×10 ⁻²	±	3×10 ⁻³	< 1×10 ⁻⁴	18	1×10 ⁻⁴	0.66	36

<i>intI1</i>	1	0	ND ^a							
<i>intI1</i>	1	20	-1.3×10^{-2}	\pm	3×10^{-3}	3×10^{-3}	9	0.70	0.75	52
<i>intI1</i>	1	40	3.1×10^{-3}	\pm	6×10^{-3}	0.61	13	0.99	0.02	-220
<i>intI1</i>	1	100	-8.8×10^{-4}	\pm	1×10^{-3}	0.51	17	0.13	0.03	780
<i>intI1</i>	2	0	-1.6×10^{-3}	\pm	2×10^{-3}	0.39	15	1.00	0.06	440
<i>intI1</i>	2	40	1.2×10^{-3}	\pm	2×10^{-3}	0.59	18	0.28	0.02	-560
<i>sulI</i>	1	0	-1.7×10^{-2}	\pm	1×10^{-2}	0.36	3	ND ^b	0.71	40
<i>sulI</i>	1	20	-7.6×10^{-3}	\pm	2×10^{-3}	1×10^{-3}	18	0.74	0.48	91
<i>sulI</i>	1	40	-6.1×10^{-3}	\pm	4×10^{-3}	0.11	18	0.90	0.15	110

<i>sull</i>	1	100	4.7×10^{-3}	\pm	2×10^{-3}	0.02	17	0.67	0.30	-150
<i>sull</i>	2	0	-1.6×10^{-3}	\pm	1×10^{-3}	0.27	24	0.82	0.06	450
<i>sull</i>	2	40	-8.1×10^{-3}	\pm	3×10^{-3}	6×10^{-3}	18	0.16	0.39	86
<i>tet</i> (A)	1	0	ND ^a							
<i>tet</i> (A)	1	20	-2.6×10^{-2}	\pm	4×10^{-3}	1×10^{-4}	11	0.54	0.84	27
<i>tet</i> (A)	1	40	-2.2×10^{-2}	\pm	4×10^{-3}	$< 1 \times 10^{-4}$	18	0.94	0.69	32
<i>tet</i> (A)	1	100	-1.2×10^{-2}	\pm	2×10^{-3}	$< 1 \times 10^{-4}$	17	0.32	0.79	58
<i>tet</i> (A)	2	0	ND ^a							
<i>tet</i> (A)	2	40	6.0×10^{-3}	\pm	2×10^{-3}	0.02	18	0.08	0.28	-120

<i>tet</i> (W)	1	0	ND ^a							
<i>tet</i> (W)	1	20	-2.8×10^{-2}	\pm	4×10^{-3}	$< 1 \times 10^{-4}$	17	0.26	0.75	24
<i>tet</i> (W)	1	40	-2.9×10^{-2}	\pm	3×10^{-3}	$< 1 \times 10^{-4}$	14	0.01	0.90	24
<i>tet</i> (W)	1	100	-3.5×10^{-2}	\pm	8×10^{-3}	3×10^{-3}	9	5×10^{-3}	0.74	20
<i>tet</i> (W)	2	0	ND ^a							
<i>tet</i> (W)	2	40	-1.9×10^{-2}	\pm	3×10^{-3}	$< 1 \times 10^{-4}$	18	0.07	0.72	36
<i>tet</i> (X)	1	0	ND ^a							
<i>tet</i> (X)	1	20	-1.9×10^{-2}	\pm	4×10^{-3}	2×10^{-4}	17	0.32	0.62	37
<i>tet</i> (X)	1	40	-1.2×10^{-2}	\pm	4×10^{-3}	7×10^{-3}	18	0.59	0.37	57

<i>tet</i> (X)	1	100	$-3.4 \times 10^{-3} \pm 1 \times 10^{-3}$	0.02	17	0.47	0.33	200
<i>tet</i> (X)	2	0		ND ^a				
<i>tet</i> (X)	2	40	$5.9 \times 10^{-3} \pm 5 \times 10^{-3}$	0.22	14	0.03	0.12	-120

^aQuantities of some gene targets were above quantification limits for only $n \leq 2$ time points, so k was not determined (ND).

^bQuantities of *sulI* were above quantification limits in only one soil microcosm at a loading rate of 0 g residual solids kg⁻¹ soil for Experiment 1, so the lack-of-fit test could not be conducted, and LOF P was not determined (ND).

The first-order kinetic coefficients determined for Experiment 1 tended to vary more by gene target than by loading rate (Figure 6.5). The largest kinetic coefficients (i.e. slowest decline in gene quantities) tended to be those of *intII* and *sulI*, while *erm(B)* tended to have the smallest (i.e. fastest decline in gene quantities). There was no clear relationship between the collective values of kinetic coefficients and the solids-to-soil mass loading rate, as kinetic coefficients for quantities of some gene targets appeared to increase with loading rate while others appeared to decrease. Furthermore, few of the apparent increases or decreases with loading rate were significant. Only 4 of 18 possible comparisons (i.e. comparing kinetic coefficients for 40 g kg⁻¹ to 20 g kg⁻¹, 100 g kg⁻¹ to 40 g kg⁻¹, and 100 g kg⁻¹ to 20 g kg⁻¹) for kinetic coefficients describing the changes in quantities of ARGs and *intII* were significant ($P < 0.05$, Welch's t-test), and 8 of 18 possible comparisons for kinetic coefficients describing changes in ratios of ARGs and *intII* to the 16S rRNA gene were significant ($P < 0.05$, Welch's t-test). Also, the largest changes in kinetic coefficients with loading rate for individual gene targets were smaller than the largest differences in kinetic coefficients between different gene targets at the same loading rates.

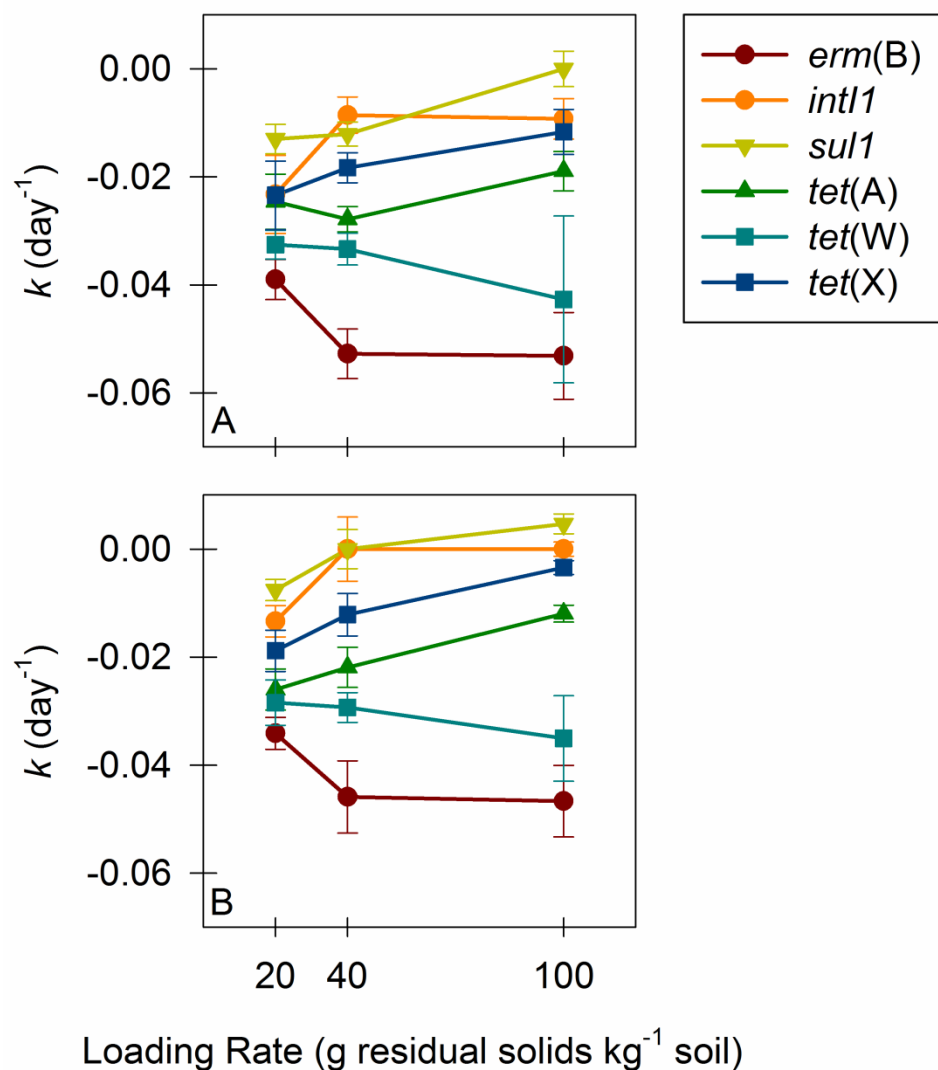


Figure 6.5. The kinetic coefficients for (A) quantities of ARGs and *intI1* and (B) ratios of ARGs and *intI1* to the 16S rRNA gene from Experiment 1 as a function of loading rate. Values are from Table 6.4 and Table 6.5; error bars represent the standard error of the mean. Values of “0” have been substituted for kinetic coefficients with $P > 0.05$. Connecting lines are intended as visual aids only.

Quantities of several gene targets declined at a slower rate in Experiment 2 than in the equivalent (i.e. 40 g kg⁻¹) microcosms from Experiment 1. The differences in kinetic coefficients for the 16S rRNA gene, *intI1*, and *sulI* between Experiments 1 and 2 were not statistically significant ($P \geq 0.05$, Welch's t-test). The same differences for AllBac, *erm(B)*, *tet(A)*, *tet(W)*, and *tet(X)*, however, were statistically significant ($P < 0.05$, Welch's t-test). The quantities of these gene targets declined between 30% and 100% more slowly in Experiment 2 compared to Experiment 1. Similar results were found for the ratios of ARGs and *intI1* to 16S rRNA genes. The difference in rates at which ratios of *intI1* and *sulI* declined were not significant ($P \geq 0.05$, Welch's t-test) between the two experiments. The ratios of *erm(B)*, *tet(W)*, and *tet(X)*, however, all declined more slowly ($P < 0.05$, Welch's t-test) in Experiment 2 than in Experiment 1, and the ratios of *tet(A)* actually increased in Experiment 2 while they decreased in Experiment 1.

6.4 Discussion

Quantities of ARGs and *intI1* start high and decline at relatively slow rates in soil to which treated residual municipal wastewater solids have been applied. While previous work has indicated that the vast majority of ARGs in the municipal wastewater treatment process are ultimately discharged to the environment in the residual solids (27), the relative persistence of ARGs in soil following land-application of treated residual solids has not been investigated. This is important because approximately 50% of all residual solids produced in the United States are land-applied (186), and, as shown here, treated residual solids contain large quantities of ARGs that are relatively persistent in the soil environment. Initial ARG and *intI1* quantities were often several orders of magnitude

higher than the quantification limit for HF183, a human-specific fecal indicator, in microcosms that received residual solids, and half-lives for *intII*, *sulI*, *tet(A)*, and *tet(X)* were longer than those of AllBac, a fecal indicator. Furthermore, half-lives of *erm(B)*, *intII*, *sulI*, *tet(A)*, *tet(W)*, and *tet(X)* in this work varied from weeks to months, whereas the half-lives of the same genes in a laboratory-scale aerobic digester and in laboratory-scale mesophilic and laboratory-scale thermophilic anaerobic digestors have been demonstrated to vary from hours to days (121,204). Thus, ARGs and *intII* can persist for longer periods of time and at comparable or substantially larger quantities than at least some fecal indicators. Also, the removal of ARGs and *intII* from residual municipal wastewater solids can probably be carried out most effectively within the treatment plant (i.e. during solids treatment) prior to land-application.

The relative persistence of ARGs and *intII* from treated residual municipal wastewater solids in soil provides adequate time for off-site transport, and ultimately, human exposure to ARGs. For example, the most significant risk of exposure to residual wastewater solids, other than direct ingestion, is inhalation of residual solids aerosols during land-application by populations living near land-application sites (224). The estimated inhalable dose of treated residual solids at 165 m from an emission source during disc-incorporation (i.e. land-application) of 40 to 110 g of Class B residual solids kg^{-1} soil has been estimated to be between 2 and 8 μg (218). Based on the quantities of ARGs and *intII* reported here, this would correspond to an inhalable ARG (or *intII*) dose of 10 (*tet(X)*, Residual Solids 2) to 60,000 (*tet(W)*, Residual Solids 2) copies. This likely represents a worst-case scenario that would occur immediately upon land-application of

treated residual solids. However, the persistence of ARGs and *intII* in soil at relatively high concentrations for time periods on the order of months provides the opportunity for other transport and exposure events during mechanical disturbances of the soil (e.g. tilling, planting, or high-wind events) or in runoff during storm events. The human health risks posed by these potential events are not currently well understood and need to be critically evaluated.

Contrary to expectations, the mass loading rate of treated residual solids to soil did not affect the persistence of ARGs and *intII* in soil significantly. This indicates that the mass loading rate of residual solids to soil is unlikely to be a useful variable for controlling the fate of ARGs and *intII* in land-applied treated residual solids. The potential exists, however, for ARGs and *intII* to accumulate in soil to which treated residual solids are applied repeatedly. For example, *sulI* and *sul2* have been demonstrated to accumulate in agricultural soil to which animal manure containing sulfadiazine has been applied repeatedly at a loading rate of 40 g manure kg⁻¹ soil (150). This loading rate is within the range of those typically used for treated municipal wastewater solids on agricultural fields, which vary between 12 and 2,250 Mg ha⁻¹ (184) (1.5 to 290 g residual solids kg⁻¹ dry soil for solids that are mechanically incorporated into the soil to a depth of 0.6 m). Furthermore, dewatered residual solids are generally applied at loading rates on the higher end of this range (184). The first-order kinetic coefficients determined in this work, which investigated loading rates of 20 to 100 g residual solids kg⁻¹ soil, should therefore be useful for managing the frequency with which treated residual solids are land-applied to individual fields.

One of the most persistent gene targets in all soil microcosms that received treated residual solids was *intI1*, which is similar to our previous results in aerobic digestion and air-drying beds (204,208). Integrons enable both horizontal gene transfer and the collection of multiple ARGs (82). This characteristic makes them particularly significant from a public health standpoint, and when considered in context of how frequently they are found in the environment, suggests that more research ought to be directed at understanding their distribution and genetic contents in the environment (198). It may be that these integrons are found to be empty or contain genes that are more-or-less innocuous from a public health perspective. If, however, integrons are found to frequently contain multiple ARGs, then they may be appropriate specific targets for treatment systems and management strategies intended to remove ARGs from residual municipal wastewater solids.

The advantages of the approach used in this work are that it is quantitative, culture-independent, and isolates the mixture of soil and residual solids in a closed and reasonably homogenous system. However, there are a number of limitations related to the use of both real-time PCR and soil microcosms that may influence our results. Most importantly, the real-time PCR protocol used in this work cannot distinguish gene targets in pathogens from those in non-pathogens. Similarly, it cannot distinguish gene targets in living bacteria from those in dead bacteria or present as extracellular DNA in the soil matrix. The real-time PCR protocol also provides no information regarding the expression of gene targets in living hosts and cannot distinguish full-length genes from partial gene fragments that coincidentally contain the primer annealing sites. Also,

because the soil microcosms were closed and stored indoors, they did not simulate the effects of direct sunlight, natural fluctuations in moisture content and temperature, or the presence of a full soil ecosystem on the rates at which ARG and *intI1* quantities decline in soil. Finally, the work presented in this manuscript investigates only a small fraction of known ARGs.

**Chapter 7: Effects of Several Processes to Significantly Reduce
Pathogens and Processes to Further Reduce Pathogens on the Fate of
Antibiotic Resistance Genes and Class 1 Integrins in Soil
Microcosms Following the Application of Treated Residual
Municipal Wastewater Solids**

Antibiotic resistance genes (ARGs) can persist for months at high concentrations in soil microcosms following application of treated residual municipal wastewater solids from full-scale treatment facilities. The objective of this research was to assess the effects of alternative treatment technologies on this persistence. Treated residual solids from laboratory-scale treatment units were applied to sets of triplicate soil microcosms. The treatment technologies included aerobic digestion, air drying, alkali stabilization, anaerobic digestion at 38°C, anaerobic digestion at 55°C, anaerobic digestion at 62°C, anaerobic digestion at 69°C, and pasteurization. Soil microcosms containing untreated residual solids from a full-scale treatment facility were also included. Six ARGs (*erm*(B), *qnrA*, *sulI*, *tet*(A), *tet*(W), and *tet*(X)), the integrase gene of class 1 integrons (*intI1*), 16S rRNA genes, 16S rRNA genes of all *Bacteroides* spp. (AllBac), and 16S rRNA genes of human-specific *Bacteroides* spp. (HF183) were quantified using real-time PCR. ARG and *intI1* quantities decreased in most microcosms, but the nature of the decrease varied depending on treatment technology. ARG and *intI1* quantities decreased slowly, with half-lives of 19 (*erm*(B), untreated) to 76 (*tet*(A), aerobically digested) d, in microcosms that received aerobically digested or untreated residual solids. However, ARG and *intI1* quantities in microcosms that received alkali stabilized, pasteurized, or anaerobically digested (at 55°C, 62°C, or 69°C) residual solids decreased by a median of 95.0% (*tet*(W), anaerobically digested at 55°C) within one month and then persisted at relatively low concentrations thereafter. These results demonstrate that the selection of residual solids treatment technology can be used to decrease the persistence of ARGs and *intI1* in soil following land-application of treated residual municipal wastewater solids.

7.1 Introduction

The development of resistance to antibiotics among pathogens is a major public health dilemma with serious health and financial consequences (65,67). A number of strategies are being pursued to mitigate the effects of antibiotic resistance, including the development of new antibiotics, the development of alternatives to antibiotics, and the reduction of antibiotic use for purposes other than treating disease in humans (2,86–90). An alternative, and complementary, strategy consists of identifying and managing antibiotic resistance genes (ARGs) as environmental contaminants (5). This has led to the identification of numerous environmental reservoirs of ARGs, including surface waters, aquaculture facilities, and agricultural waste (5–20). One of the largest reservoirs, however, appears to be the municipal wastewater treatment process (5,10,21–32) and, in particular, the residual municipal wastewater solids, which contain the vast majority of ARGs that exit the municipal wastewater treatment process (27). As a result, residual solids treatment may present an excellent opportunity to control the quantity of ARGs circulating in the environment.

Previous results have demonstrated the potential for existing treatment technologies to remove ARGs from residual solids. These technologies, referred to as Processes to Significantly Reduce Pathogens (PSRPs) and Processes to Further Reduce Pathogens (PFRPs) (185), are currently designed to reduce the water, organic carbon, and pathogen content of untreated residual municipal wastewater solids (184). However, PSRPs and PFRPs have also been demonstrated to remove ARGs from untreated residual municipal wastewater solids (121,131,204,208), both by reducing the overall number of

microorganisms in the residual solids and by creating environmental conditions that fail to select for particular ARGs based on their ecological niches (208) (Chapter 5). Aerobic digestion, air-drying beds, and anaerobic digestion have all been demonstrated to remove ARGs from residual municipal wastewater solids to varying degrees, and it also appears that their capacities in this regard can be optimized by adding pretreatment steps, increasing treatment temperatures, and inducing feast-famine (i.e. batch) cycles (121,131,204,208) (Chapter 5).

The degree to which all of these technologies affect the fate of ARGs in soil following land-application of treated residual solids, however, is unknown. This is a significant gap in the body of knowledge, because approximately 50% of all treated residual municipal wastewater solids in the United States are land-applied (186). Furthermore, previous work has indicated that ARGs originating in treated residual solids can persist for months at relatively high concentrations in soil following land-application (Chapter 6), thereby creating the opportunity for off-site transport of, and ultimately human exposure to, ARGs with stormwater or airborne particulate matter (100,167). Many PSRPs and PFRPs are already widespread in the U.S. (186) or could be added to existing infrastructure with relative ease. Thus, their implementation for controlling the quantities of ARGs circulating in the environment could represent a tractable management strategy for preventing antibiotic resistant infections.

The objective of this work was to determine how a variety of PSRPs and PFRPs affected the persistence of ARGs and class 1 integrons in soil following land-application of treated residual solids. A group of five PSRPs and one PFRP was considered. The

PSRPs included aerobic digestion at 15°C, air drying, alkali (i.e. lime) stabilization, anaerobic digestion at 38°C, and anaerobic digestion at 55°C. The PFRP was pasteurization. In addition to these six technologies, anaerobic digestion at 62°C and 69°C, technologies not classified under the PSRP/PFRP scheme, were also considered, along with untreated residual municipal wastewater solids. The untreated residual solids represent a “worst-case scenario” positive control for the application of ARGs to soil. Residual solids from each of the nine sources were added to soil microcosms, and the quantities of several ARGs and the integrase gene of class 1 integrons were determined in each microcosm using real-time PCR over an approximately six-month time series.

7.2 Materials and Methods

Experimental Design. Soil microcosms were constructed as described in Section 6.2 using the Waukegan silt loam soil (fine-silty, mixed, mesic Typic Hapludoll) from that experiment. Soil microcosms from the current experiment were constructed and sampled concurrently with soil microcosms containing Soil 2 from the previously described experiment, and the negative control (i.e. soil only) microcosms from the previously described experiment also served as negative controls for the current experiment. Triplicate microcosms were constructed for each of nine residual solids sources. Residual solids from eight different treatment technologies were considered, including aerobic digestion, air drying, alkali stabilization, anaerobic digestion at 38°C, anaerobic digestion at 55°C, anaerobic digestion at 62°C, anaerobic digestion at 69°C, and pasteurization. Aerobically and anaerobically digested residual solids were collected from the laboratory-scale treatment units described in Table E.1. Air-dried residual

solids were collected from composite samples of the laboratory-scale air-drying beds described in (208). Alkali stabilized and pasteurized residual solids were produced in the lab on December 1, 2011, from untreated residual solids collected on November 30, 2011, from a full-scale (11 MGD) municipal wastewater treatment plant in southern Minnesota. To produce alkali stabilized residual solids, the pH (Fisher Scientific Accumet Model 15 pH meter with automatic temperature correction and an Accumet 13-620-221 probe) of untreated residual solids was increased to above 12 for a period of two hours using sodium hydroxide (Figure E.1). The pH was then neutralized using hydrochloric acid. To produce pasteurized residual solids, the temperature of untreated residual solids was increased to above 70°C (temperature measured with Fisher Scientific Accumet Model 15 pH meter) for a period of 30 minutes (Figure E.1). A ninth residual solids source was untreated residual municipal wastewater solids from the same 11 MGD plant in southern Minnesota, but collected at an earlier date (October 26, 2011). Soil microcosms that received no residual solids (i.e. negative controls), aerobically digested residual solids, air-dried residual solids, or untreated residual solids were initiated on October 27, 2011. Soil microcosms that received anaerobically digested residual solids were initiated on October 28, 2011, and soil microcosms that received alkali stabilized or pasteurized residual solids were initiated on December 1, 2011. Residual solids treated in air-drying beds were added directly to their respective soil microcosms, but all other residual solids were centrifuged (30 min at 5,000 rpm and 10°C in a Beckman J2-HS centrifuge) to dewater them prior to addition to the soil microcosms. Residual solids were added to the soil microcosms at a mass loading rate of approximately 40 g

dewatered residual solids kg^{-1} soil (wet mass), which is typical of mass loading rates used in practice (184). All microcosms were stored at room temperature (approximately 20°C). Evaporative water losses for all microcosms were estimated by weighing the microcosms at approximately monthly intervals and assuming that all mass loss was due to evaporation of water.

Sample Collection, Genomic DNA Extraction, and Real-time PCR. Sample collection, genomic DNA extraction, and real-time PCR were conducted as described in Section 6.2, except that *repA* could not be quantified reliably in samples from the current work and was discarded from the data set as a result. The forward and reverse primer sequences, expected amplicon sizes, and primer annealing temperatures for all gene targets are listed in Appendix D (Table D.1) (8,24,95,151,195,196,200–202). The number of standards, slope, intercept, amplification efficiency, r^2 , and quantification limit for each standard curve are provided in Appendix E (Table E.2). Of the 58 assays performed, 26 (45%) had amplification efficiencies of $100\% \pm 10\%$ (maximum deviation from 100%) with $r^2 \geq 0.99$ for a minimum of five points on each standard curve. The absolute values by which amplification efficiencies for the remaining 32 assays deviated from 100% were between 11% and 27% (median of 15%) with $r^2 \geq 0.98$ for a minimum of five points on each standard curve.

Data Analysis. Simple linear regression (Arc 1.06) was used to determine first-order kinetic coefficients for time series of gene target quantities. A first-order kinetic model was hypothesized because previous work has shown the decline of ARG and *intII* quantities in several different types of natural and engineered systems to follow first-

order trends (115,121,170,204,206,208). First-order kinetic models also provide a valuable descriptive and interpretive tool that is useful for comparing results across different gene targets and environments. A formal lack-of-fit test was applied to test the null hypothesis that the natural logarithm of gene target quantities varied linearly with respect to time (205).

7.3 Results

Initial and Operating Conditions. Gene target quantities in soil were similar among all sets of microcosms, although initial gene target quantities in source residual solids varied based on the experimental treatment (Table 6.3, Table E.3, Table E.4, Table E.5, Figure 7.1, Figure 7.2, and Figure E.2). Initial gene target quantities in soil used to initiate sets of microcosms on separate dates were reasonably similar, with measurable quantities varying by a factor of five or less. As described in Chapter 6, quantities of all *Bacteroides* spp. 16S rRNA genes (AllBac), human-specific *Bacteroides* spp. 16S rRNA genes (HF183), ARGs, and *intI1* were generally very low or below quantification limits and changed little from their initial values in negative control microcosms. Quantities of 16S rRNA genes, ARGs, and *intI1* tended to be highest in alkali stabilized and pasteurized residual solids, followed by aerobically digested and untreated residual solids. Quantities of 16S rRNA genes, *intI1*, and *tet(X)* all decreased ($P < 0.05$) or remained constant ($P \geq 0.05$) during alkali stabilization and pasteurization. The higher gene target quantities in alkali stabilized and pasteurized residual solids compared to untreated residual solids may be due to differences in how initial gene target quantities were measured in these different residual solids sources (see Figure 7.1, Figure 7.2, and

following paragraph). They may also reflect true differences in gene target quantities between residual solids sampled on October 26, 2011 and residual solids sampled on November 30, 2011. Evaporation rates were similar among all sets of soil microcosms, and microcosms lost between approximately 29% (aerobically digested) and 61% (air-dried and anaerobically digested at 38°C) of their initial moisture content during the experiment.

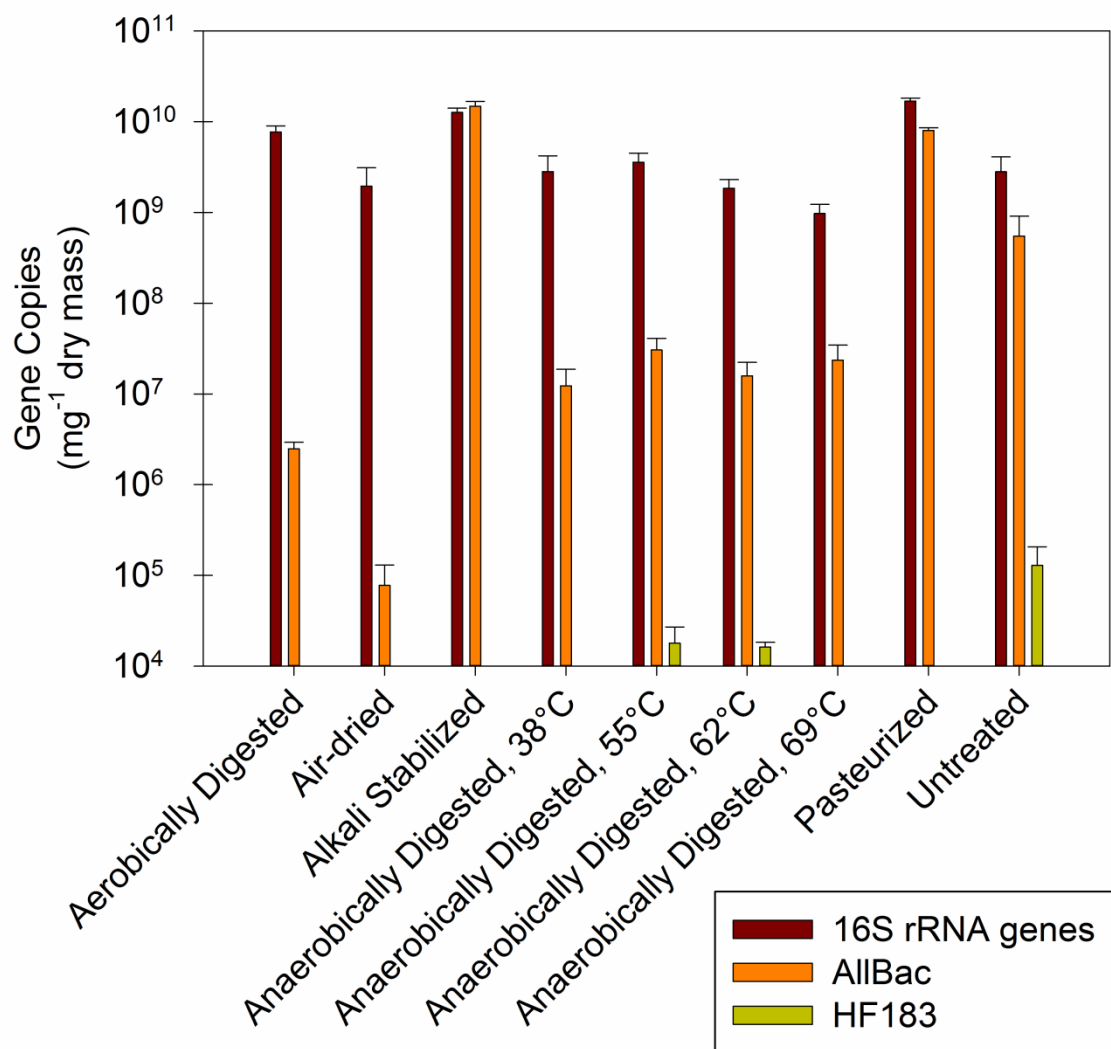


Figure 7.1. The quantities of 16S rRNA genes, AllBac, and HF183 in source residual solids. Values are the arithmetic mean of duplicate or triplicate samples; error bars represent one standard deviation. Quantities of all gene targets were measured prior to centrifugation in alkali stabilized and pasteurized residual solids; they were measured following centrifugation (or centrifugation was not required) in all other residual solids sources. Quantities of HF183 are not shown for residual solids sources where they were below quantification limits (see Table E.2).

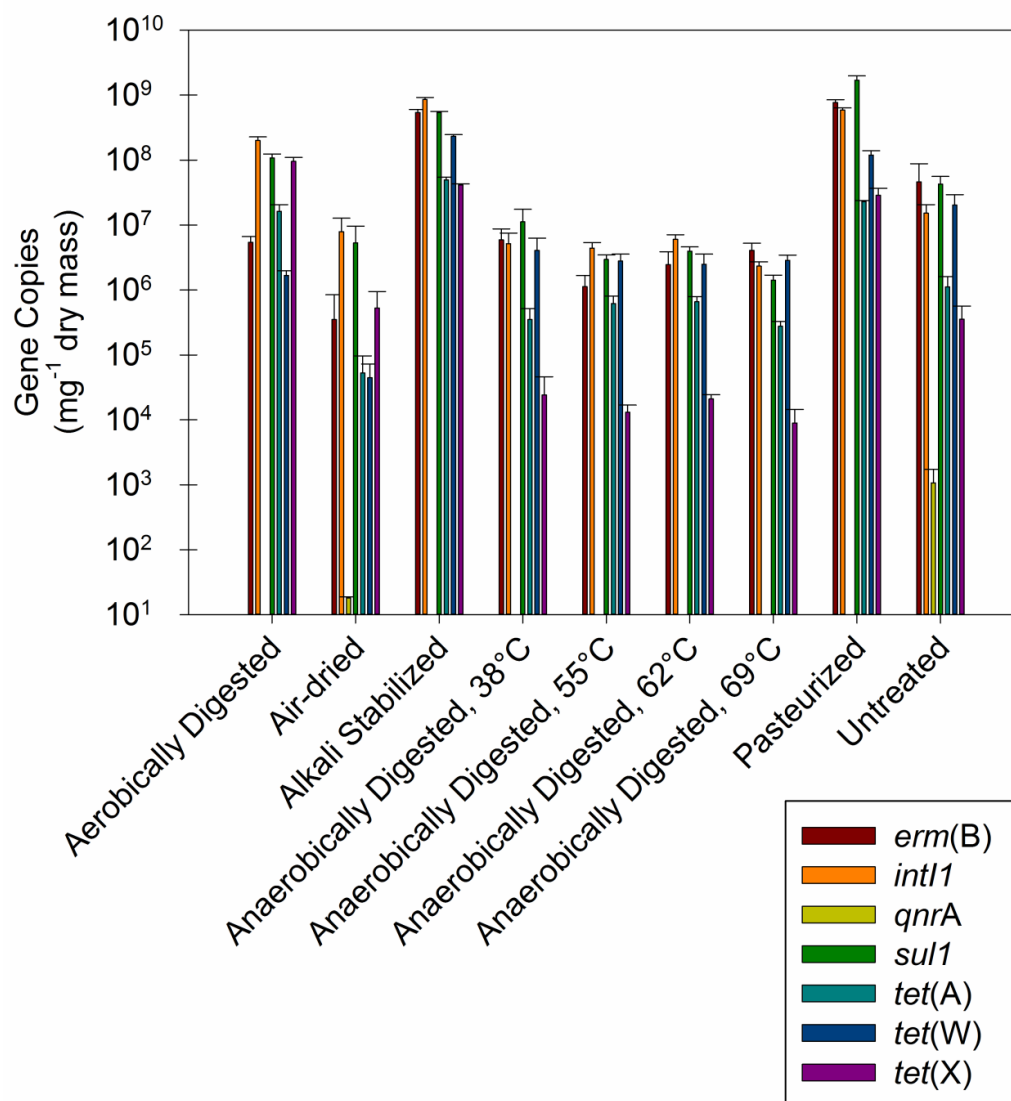


Figure 7.2. The quantities of ARGs and *intI1* in source residual solids. Values are the arithmetic mean of duplicate or triplicate samples; error bars represent one standard deviation. Quantities of all gene targets were measured prior to centrifugation in alkali stabilized and pasteurized residual solids; they were measured following centrifugation (or centrifugation was not required) in all other residual solids sources. Quantities of *qnrA* are not shown for residual solids sources where they were below quantification limits (see Table E.2).

Mass balances based on gene target quantities in soil and source residual solids were able to account for initial gene target quantities within a factor of six for 48 of 68 (71%) cases. A notable exception to this was for all gene targets in soil microcosms that received alkali stabilized residual solids. Measurements of initial gene target quantities in these microcosms were all well below values predicted by mass balances by factors of one (*erm*(B)) to 52 (*intI1*). Furthermore, the initial quantities of five of eight gene targets (*AllBac*, *intI1*, *sul1*, *tet*(A), and *tet*(X)) were below values predicted by mass balances by factors of more than 20. All gene targets were quantified prior to centrifugation in alkali stabilized and pasteurized residual solids, while all gene targets were quantified following centrifugation in other residual solids sources (or centrifugation was not required). Thus, the most likely explanation for this discrepancy in gene target recovery is that a large fraction of DNA was extracellular in alkali stabilized residual solids, and that the extracellular DNA was inadvertently separated from the residual solids during centrifugation. In support of this hypothesis, measured initial gene target quantities in soil microcosms that received pasteurized residual solids were also relatively low compared to expectations, varying by factors of four (*tet*(A)) to 12 (*AllBac*) from estimates based on mass balances.

First-order Kinetic Modeling. Two first-order kinetic models were developed to describe the data (Table E.6 and Table E.7). The first consisted of a single first-order kinetic model applied to the entire time series of data for each gene target in each set of soil microcosms. Only 17 of a possible 64 (27%) fits using this approach were characterized by acceptable ($P > 0.05$) lack-of-fit P values, however. Visual inspection

of the data indicated that this was likely due to drastic changes in gene target quantities between time zero and the second sampling time for many soil microcosms. Thus, the second model that was developed consisted of a single first-order kinetic model applied to all time series of gene target quantities with the time zero values removed. Using this approach, 51 of a possible 59 (86%) fits were characterized by acceptable ($P > 0.05$) lack-of-fit P values. Time series for which the second model was considered the better fit are described in terms of an initial percentage decrease between time zero and the second sampling time.

Measures of Bacterial Biomass. Trends in the quantities of 16S rRNA genes were largely similar for all experimental treatments (Figure 7.3, Figure 7.4, Figure 7.5, Figure 7.6, Figure 7.7, Figure 7.8, Figure 7.9, Figure 7.10, and Figure 7.11). Quantities of 16S rRNA were constant ($P > 0.05$) throughout the experiment for all experimental treatments other than aerobically digested, pasteurized, and untreated residual solids. These constant 16S rRNA gene quantities varied between $1.5 \times 10^7 \pm 3 \times 10^6$ (alkali stabilized) and $9.3 \times 10^7 \pm 7 \times 10^7$ (anaerobically digested at 38°C) copies mg^{-1} dry mass (mean \pm standard deviation). Quantities of 16S rRNA genes in microcosms that received aerobically digested, pasteurized, or untreated residual solids declined ($P \leq 0.05$) at relatively slow rates, with half-lives varying between 120 (aerobically digested) and 230 (untreated) d.

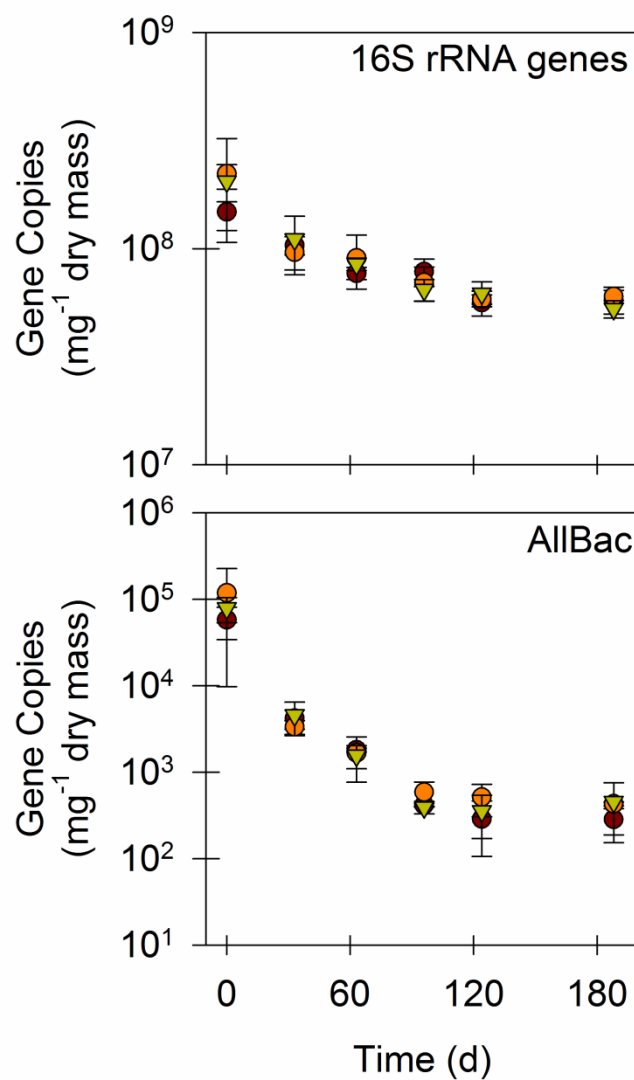


Figure 7.3. Quantities of 16S rRNA genes and AllBac in soil microcosms that received aerobically digested residual solids. Values are the arithmetic mean of duplicate or triplicate samples; error bars represent one standard deviation.

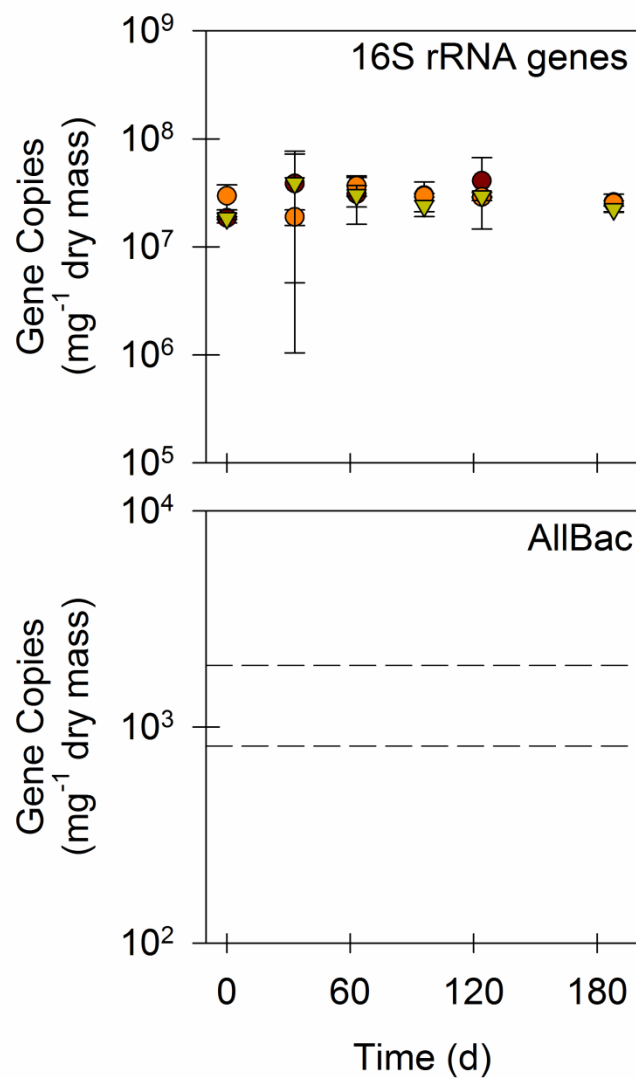


Figure 7.4. Quantities of 16S rRNA genes and AllBac in soil microcosms that received air-dried residual solids. Values are the arithmetic mean of triplicate samples; error bars represent one standard deviation. Dashed lines represent the maximum and minimum limits of quantification for data sets that contain one or more experimental observations below those limits.

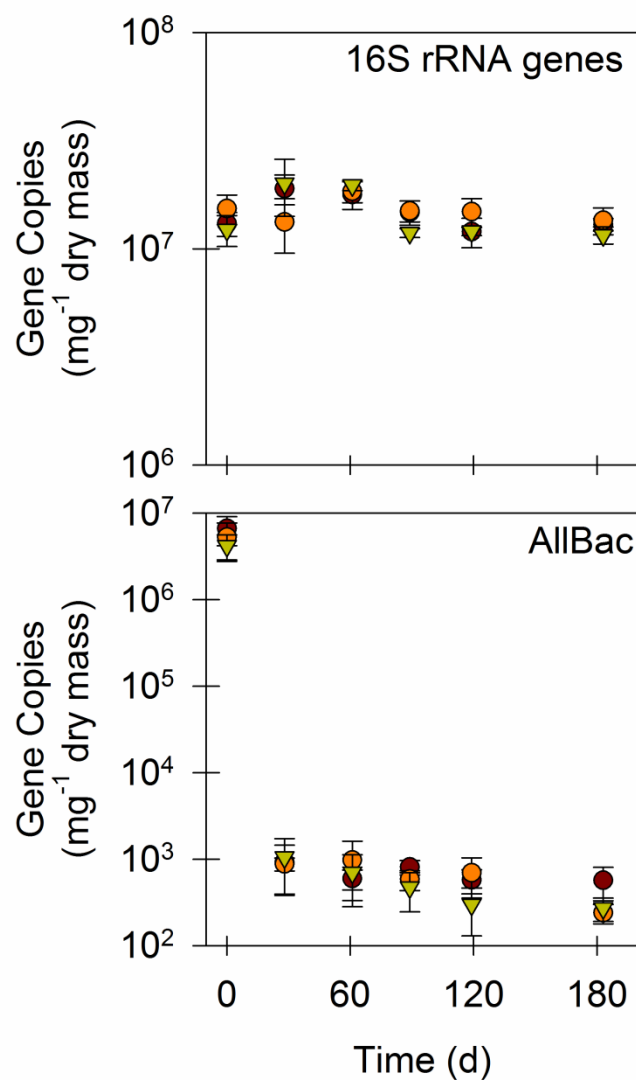


Figure 7.5. Quantities of 16S rRNA genes and AllBac in soil microcosms that received alkali stabilized residual solids. Values are the arithmetic mean of duplicate or triplicate samples; error bars represent one standard deviation.

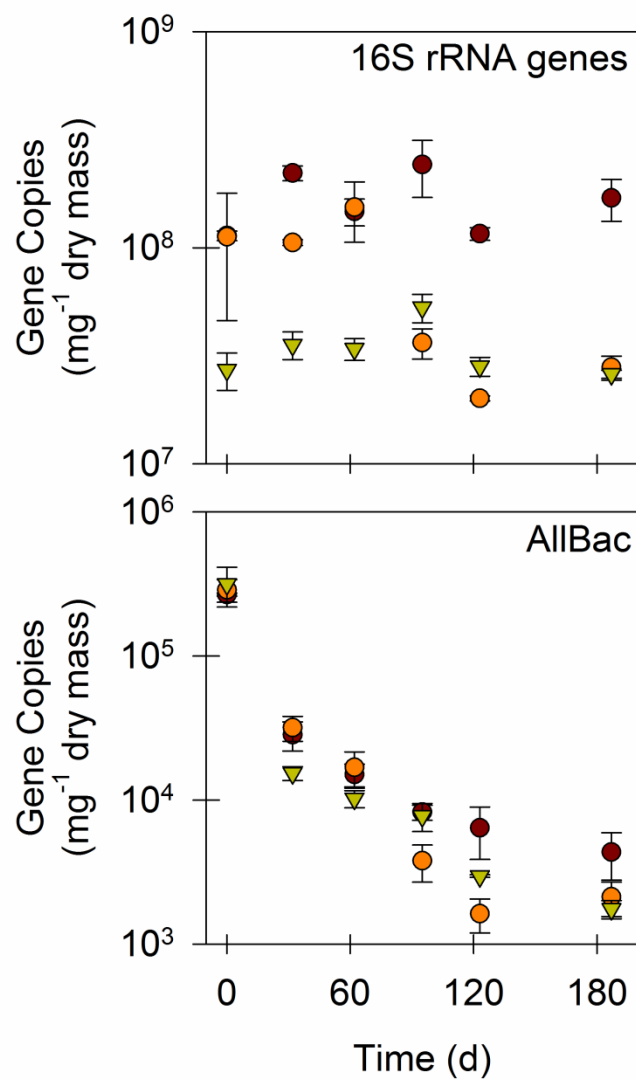


Figure 7.6. Quantities of 16S rRNA genes and AllBac in soil microcosms that received anaerobically digested (38°C) residual solids. Values are the arithmetic mean of triplicate samples; error bars represent one standard deviation.

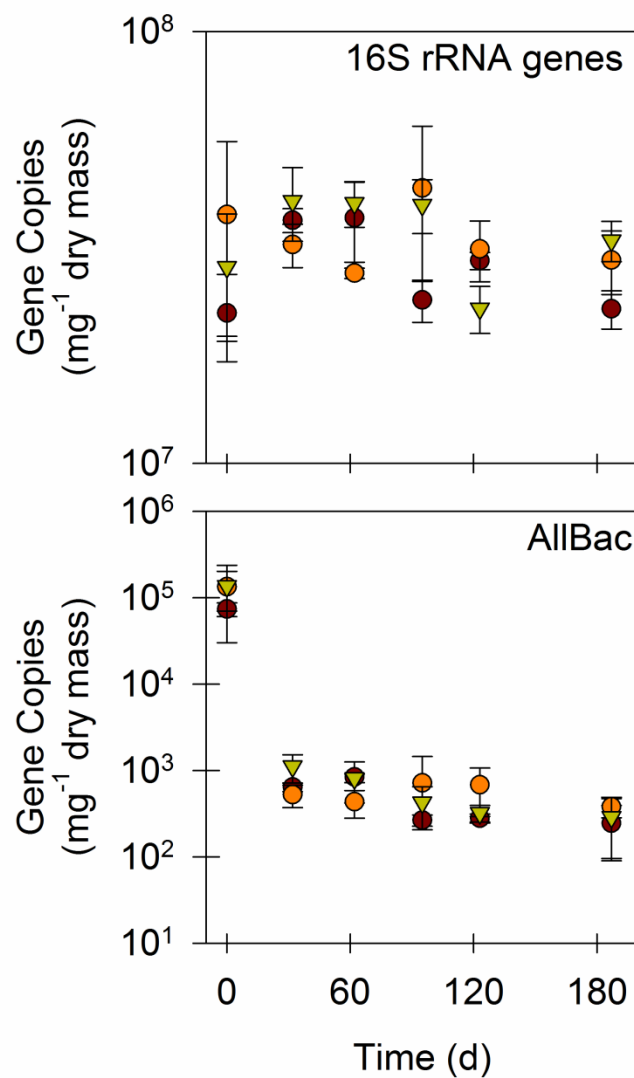


Figure 7.7. Quantities of 16S rRNA genes and AllBac in soil microcosms that received anaerobically digested (55°C) residual solids. Values are the arithmetic mean of duplicate or triplicate samples; error bars represent one standard deviation.

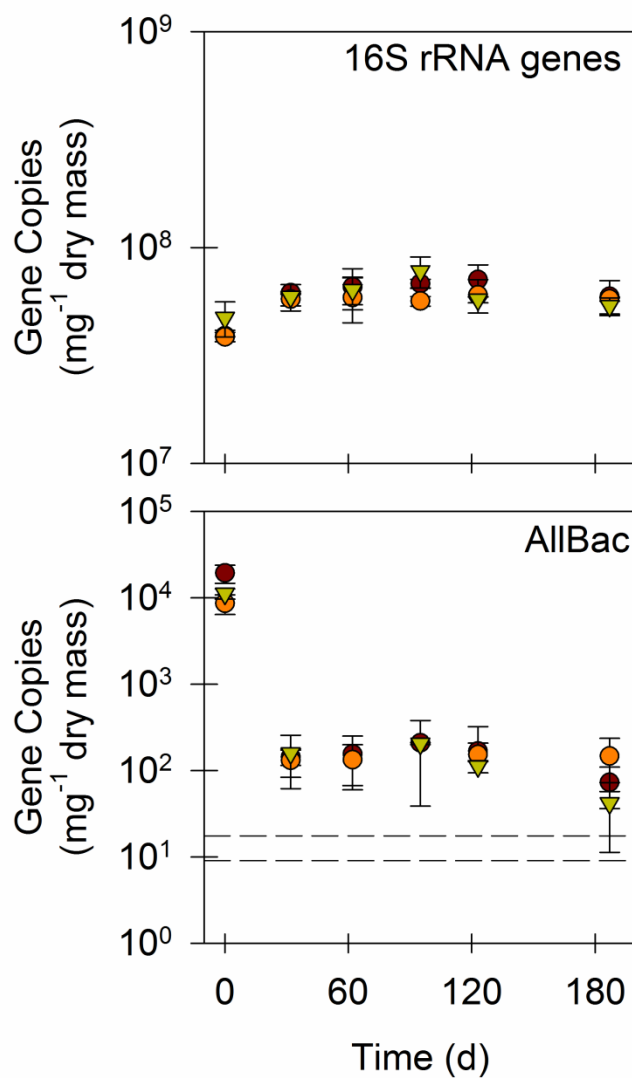


Figure 7.8. Quantities of 16S rRNA genes and AllBac in soil microcosms that received anaerobically digested (62°C) residual solids. Values are the arithmetic mean of duplicate or triplicate samples; error bars represent one standard deviation. Dashed lines represent the maximum and minimum limits of quantification for data sets that contain one or more experimental observations below those limits.

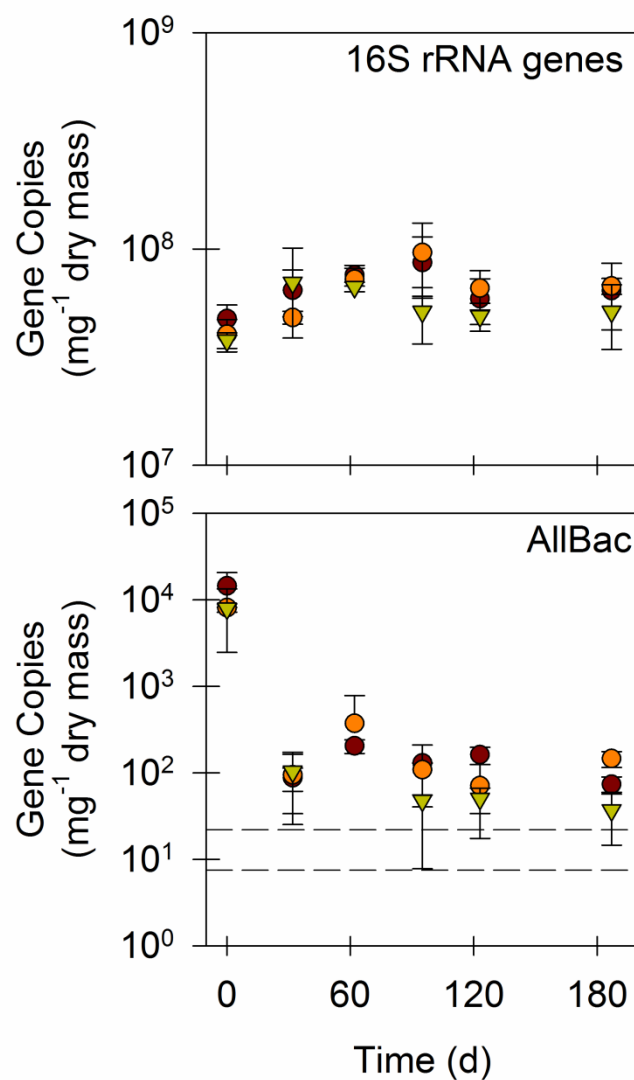


Figure 7.9. Quantities of 16S rRNA genes and AllBac in soil microcosms that received anaerobically digested (69°C) residual solids. Values are the arithmetic mean of duplicate or triplicate samples; error bars represent one standard deviation. Dashed lines represent the maximum and minimum limits of quantification for data sets that contain one or more experimental observations below those limits.

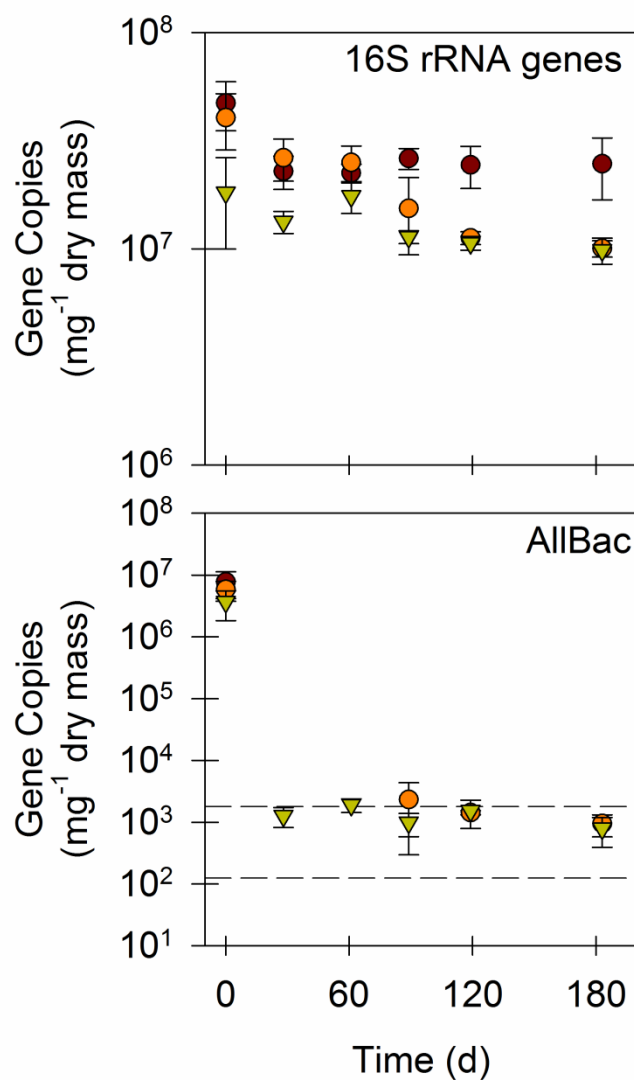


Figure 7.10. Quantities of 16S rRNA genes and AllBac in soil microcosms that received pasteurized residual solids. Values are the arithmetic mean of triplicate samples; error bars represent one standard deviation. Dashed lines represent the maximum and minimum limits of quantification for data sets that contain one or more experimental observations below those limits.

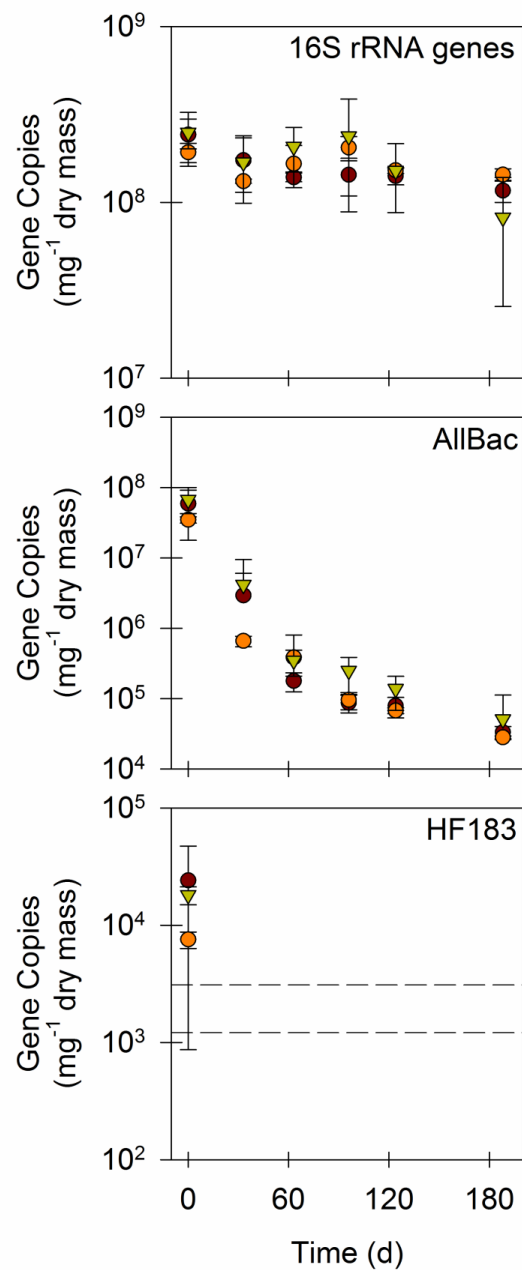


Figure 7.11. Quantities of 16S rRNA genes, AllBac, and HF183 in soil microcosms that received untreated residual solids. Values are the arithmetic mean of duplicate or triplicate samples; error bars represent one standard deviation. Dashed lines represent the maximum and minimum limits of quantification for data sets that contain one or more experimental observations below those limits.

In contrast to 16S rRNA genes, AllBac quantities declined ($P \leq 0.05$) in all microcosms regardless of the experimental treatment (Figure 7.3, Figure 7.4, Figure 7.5, Figure 7.6, Figure 7.7, Figure 7.8, Figure 7.9, Figure 7.10, and Figure 7.11). The nature of the decline, however, varied somewhat based on the experimental treatment. AllBac quantities in microcosms that received alkali stabilized residual solids, pasteurized residual solids, and residual solids digested anaerobically at temperatures of 55°C, 62°C, and 69°C decreased sharply within the first 32 d by between $98.77\% \pm 0.42\%$ (anaerobically digested at 62°C) and $99.98\% \pm 0.01\%$ (alkali stabilized) (mean \pm standard deviation). Following this initially sharp drop, AllBac quantities in these microcosms either remained constant ($P > 0.05$, anaerobically digested at 69°C and pasteurized) or decreased ($P \leq 0.05$) slowly for the remainder of the experiment, with half-lives varying between 100 (alkali stabilized) and 170 (anaerobically digested at 60°C) d. In contrast, AllBac quantities in microcosms that received aerobically digested, anaerobically digested at 38°C, and untreated residual solids tended to decrease throughout the experiment. Initial decreases in these microcosms were between $91.1\% \pm 3.5\%$ (anaerobically digested at 38°C) and $95.7\% \pm 2.2\%$ (untreated) (mean \pm standard deviation), and half-lives following this initial decrease varied between 29 (untreated) and 46 (anaerobically digested at 38°C) d. Finally, AllBac was completely below quantification limits (8.2×10^2 to 1.9×10^3 copies mg^{-1} dry mass) in soil microcosms that received air-dried residual solids, and HF183 dropped below quantification limits (1.2×10^3 to 3.1×10^3 copies mg^{-1} dry mass) within the first 33 d in soil microcosms that received untreated residual solids, so it was not quantified in the remaining microcosms.

ARGs and *intI1*. ARG and *intI1* quantities in soil microcosms that received air-dried residual solids or residual solids that were anaerobically digested at 38°C varied more with the specific gene target than with the experimental treatment (Figure 7.12 and Figure 7.13). In the soil microcosms that received air-dried residual solids, *erm*(B) and *tet*(W) were mostly or completely below quantification limits (3.5×10^3 to 8.2×10^3 copies mg^{-1} dry mass for *erm*(B) and 2.7×10^2 to 6.4×10^2 copies mg^{-1} dry mass for *tet*(W)), while quantities of the remaining ARGs and *intI1* either did not change ($P > 0.05$) or decreased ($P \leq 0.05$) slowly, with half-lives on the order of 100 d. For soil microcosms that received residual solids anaerobically digested at 38°C, *tet*(X) quantities are below quantification limits (range) by 33 d, while *erm*(B) and *tet*(W) quantities decreased by $98.4\% \pm 0.4\%$ and $97.4\% \pm 1.1\%$ (mean \pm standard deviation), respectively, within the first 33 d. Quantities of *erm*(B) and *tet*(W) remain constant ($P > 0.05$) following this initial decrease. In contrast, *sulI* quantities decrease ($P \leq 0.05$) throughout the experiment, with a half-life of on the order of 70 d. Furthermore, *intI1* and *tet*(A) quantities actually increase by factors of 2.2 ± 0.2 and 11.9 ± 3.0 , respectively, within the first 33 d. Following these initial increases, *intI1* and *tet*(A) quantities decrease for the remainder of the experiment, with half-lives of 75 and 45 d, respectively.

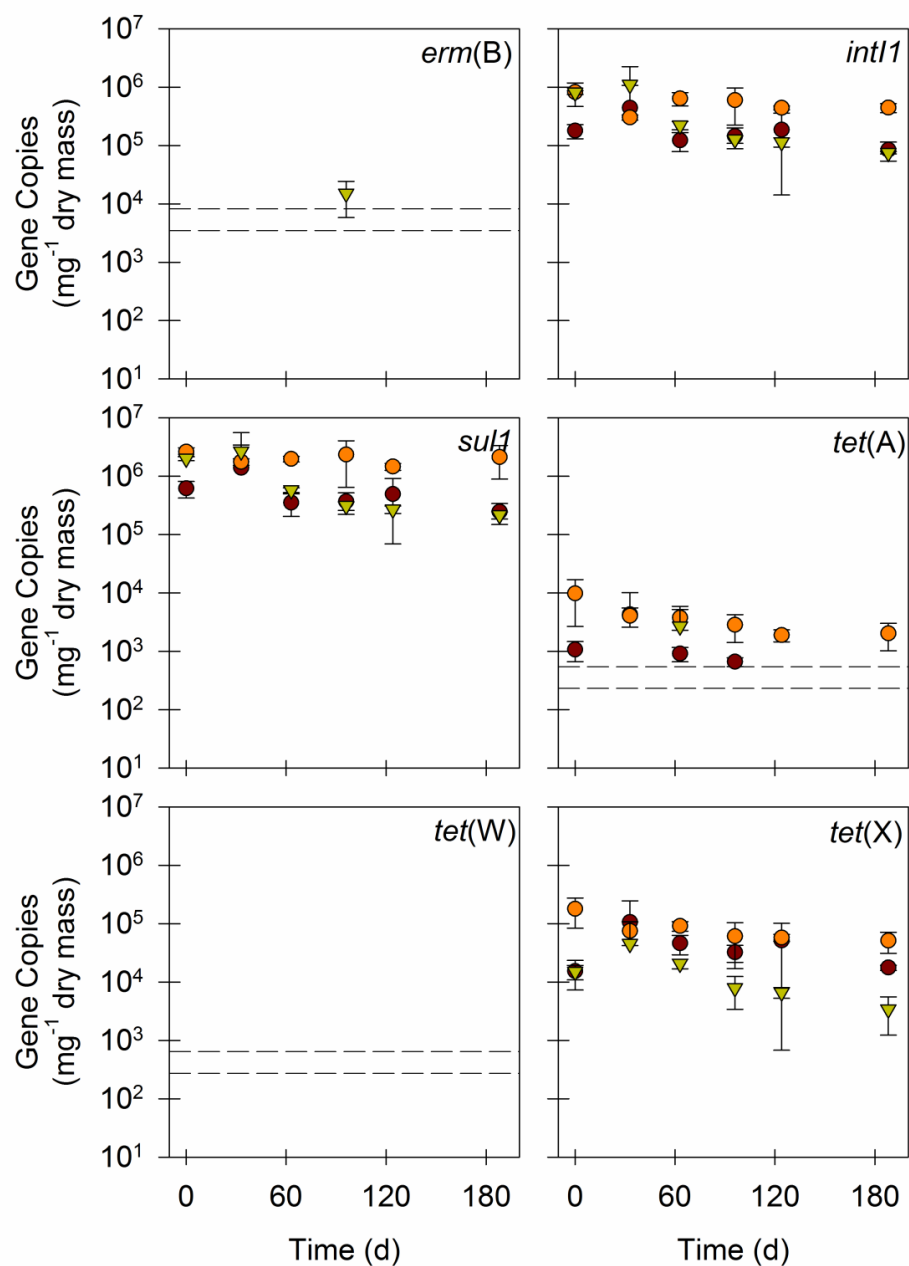


Figure 7.12. Quantities of ARGs and *int11* in soil microcosms that received air-dried residual solids. Values are the arithmetic mean of duplicate or triplicate samples; error bars represent one standard deviation. Dashed lines represent the maximum and minimum limits of quantification for data sets that contain one or more experimental observations below those limits.

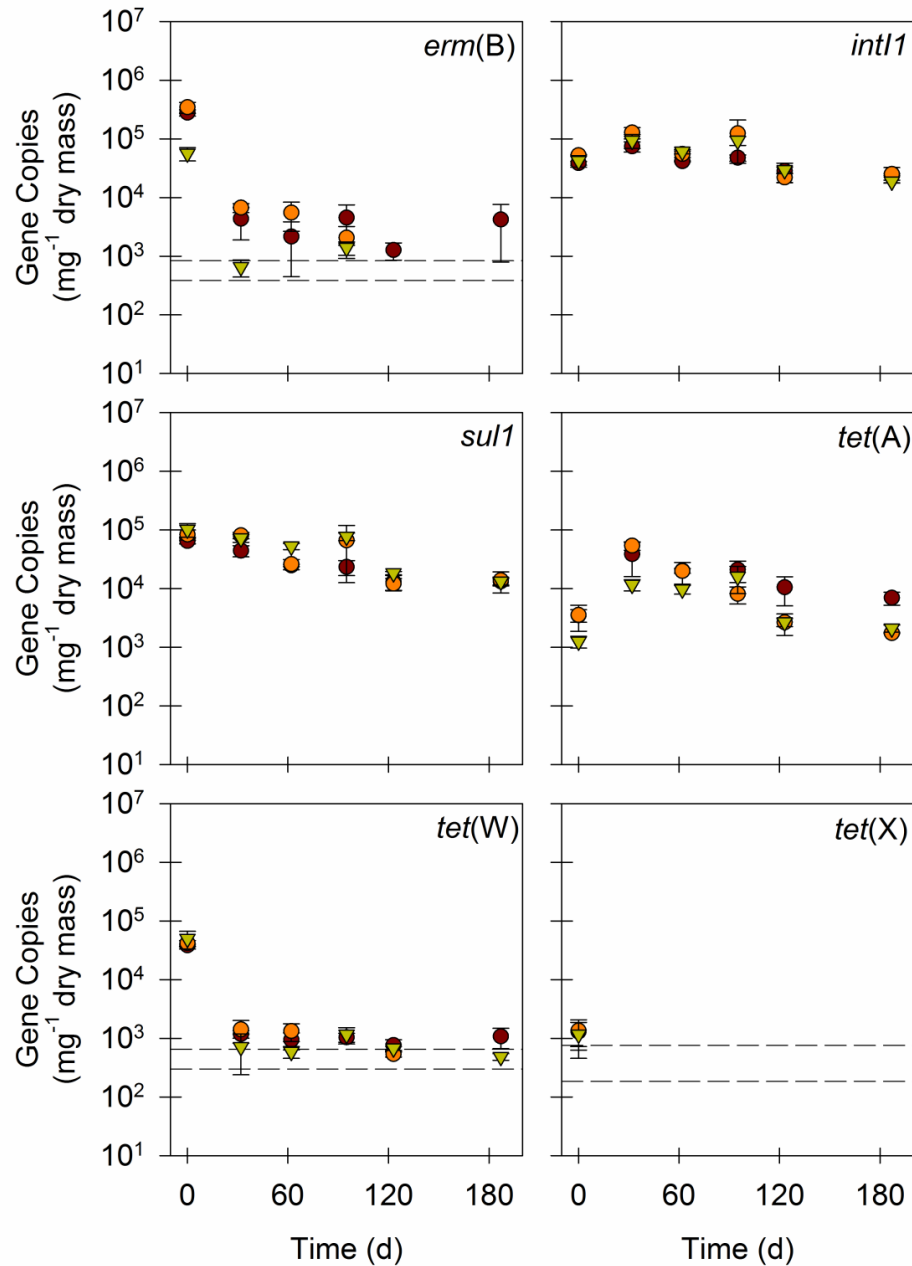


Figure 7.13. Quantities of ARGs and *intI1* in soil microcosms that received anaerobically digested (38°C) residual solids. Values are the arithmetic mean of duplicate or triplicate samples; error bars represent one standard deviation. Dashed lines represent the maximum and minimum limits of quantification for data sets that contain one or more experimental observations below those limits.

For the remaining soil microcosms, ARG and *intII* quantities tended to decline in most microcosms, and the nature of the decline varied based on the experimental treatment (Figure 7.14, Figure 7.15, Figure 7.16, Figure 7.17, Figure 7.18, Figure 7.19, Figure 7.20, and Figure E.3). With some exceptions, ARG and *intII* quantities declined sharply within the first 33 d in soil microcosms that received alkali stabilized residual solids, pasteurized residual solids, and residual solids digested anaerobically at 55°C, 62°C, or 69°C. In these microcosms, initial decreases varied between 53.2% \pm 17.1% (*intII*, anaerobically digested at 65°C) and 99.8% \pm 0.1% (*erm*(B), alkali stabilized) (mean \pm standard deviation), with a median initial decrease of 95.0% (*tet*(W), anaerobically digested at 55°C). Following these initial decreases, ARG and *intII* quantities in these microcosms either did not change ($P > 0.05$) or continued to decrease ($P \leq 0.05$) relatively slowly, with half-lives varying between 44 (*erm*(B), pasteurized) and 330 (*intII*, anaerobically digested at 60°C) d. In contrast, ARG and *intII* quantities in soil microcosms that received aerobically digested or untreated residual solids decreased by between 42.9% \pm 20.8% (*tet*(A), untreated) and 99.2% \pm 0.003% (*erm*(B), untreated), with a median decrease of 65.4% (average of *erm*(B) and *tet*(X), aerobically digested), within the first 33 d. Following these decreases, quantities of all ARGs and *intII* continued to decrease ($P \leq 0.02$), with half-lives varying between 40 (*tet*(X), aerobically digested) and 120 (*tet*(A), aerobically digested) d. Quantities of *qnrA* in soil microcosms that received untreated residual solids were low relative to other ARGs and were mostly below quantification limits (2.5 to 6.3 copies mg⁻¹ dry mass) after 96 d, so *qnrA* was not quantified in the remaining soil microcosms.

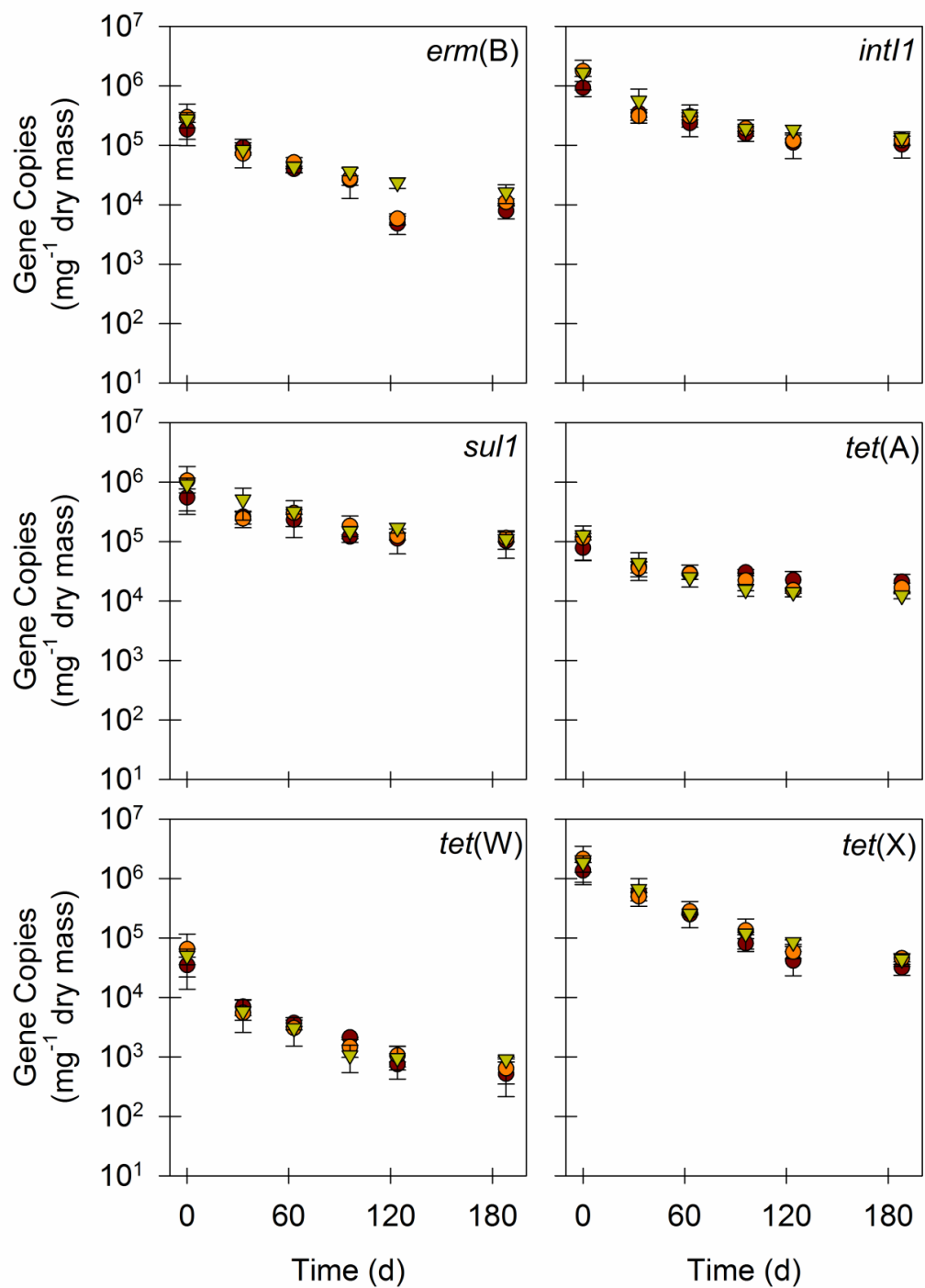


Figure 7.14. Quantities of ARGs and *intI1* in soil microcosms that received aerobically digested residual solids. Values are the arithmetic mean of triplicate samples; error bars represent one standard deviation.

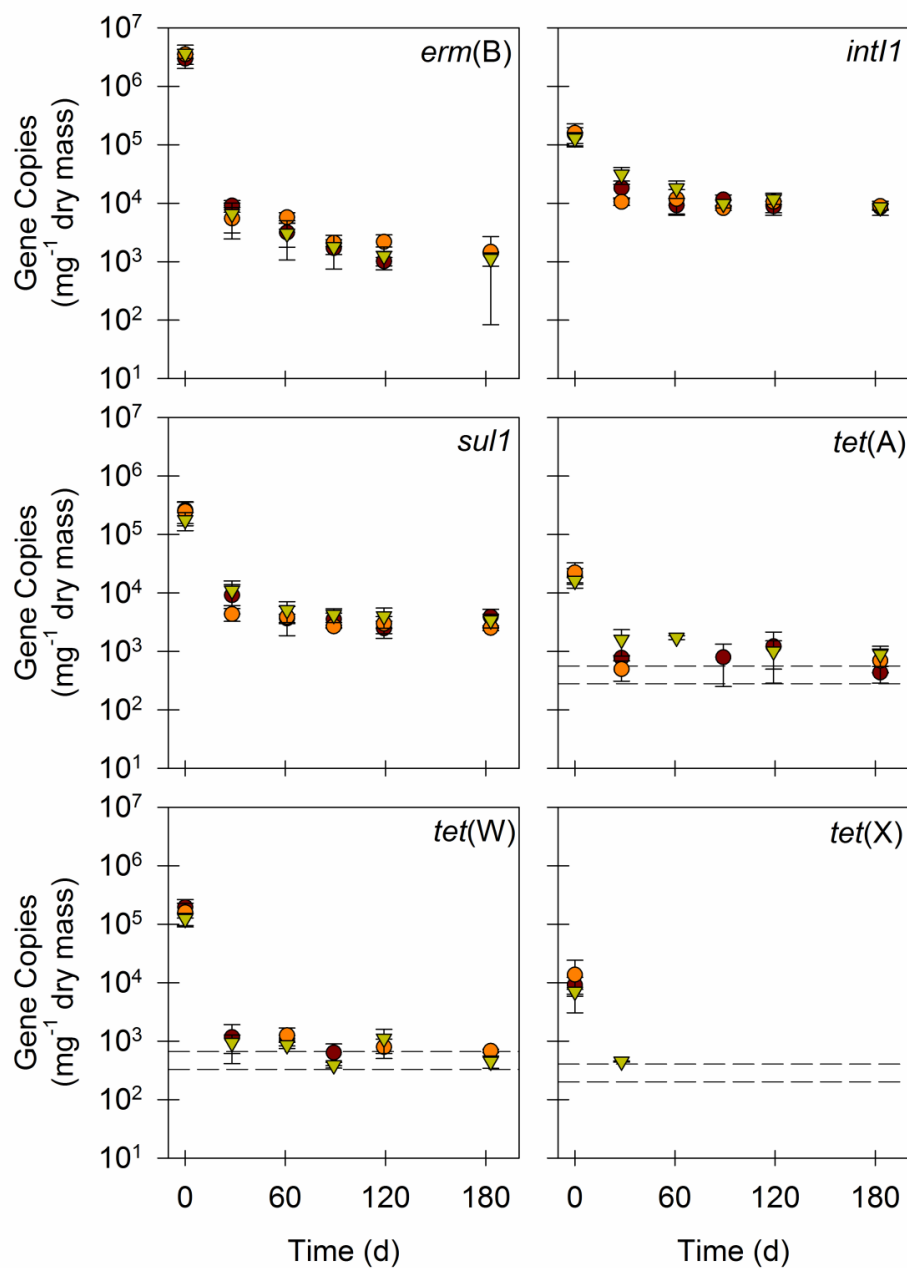


Figure 7.15. Quantities of ARGs and *int11* in soil microcosms that received alkali stabilized residual solids. Values are the arithmetic mean of duplicate or triplicate samples; error bars represent one standard deviation. Dashed lines represent the maximum and minimum limits of quantification for data sets that contain one or more experimental observations below those limits.

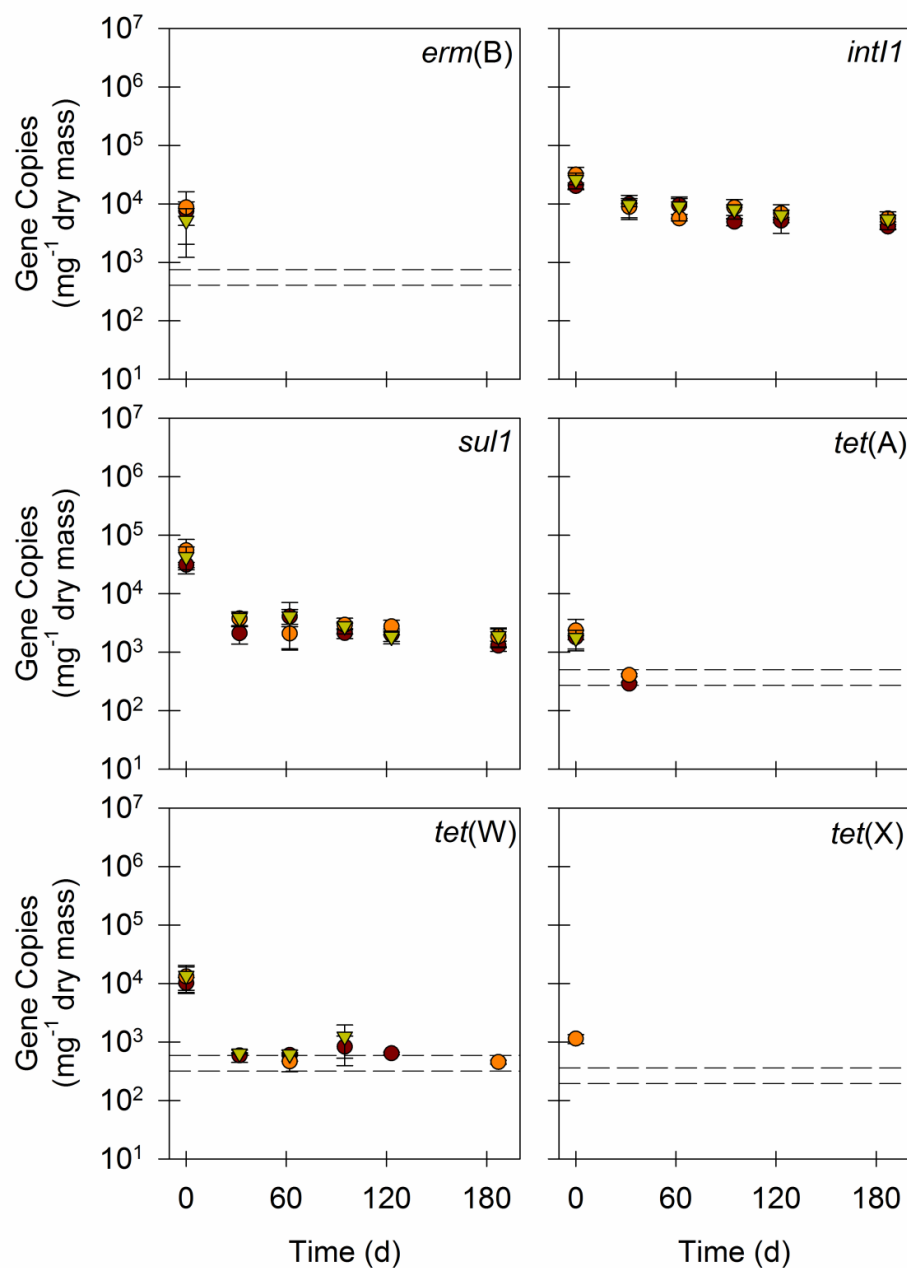


Figure 7.16. Quantities of ARGs and *intI1* in soil microcosms that received anaerobically digested (55°C) residual solids. Values are the arithmetic mean of duplicate or triplicate samples; error bars represent one standard deviation. Dashed lines represent the maximum and minimum limits of quantification for data sets that contain one or more experimental observations below those limits.

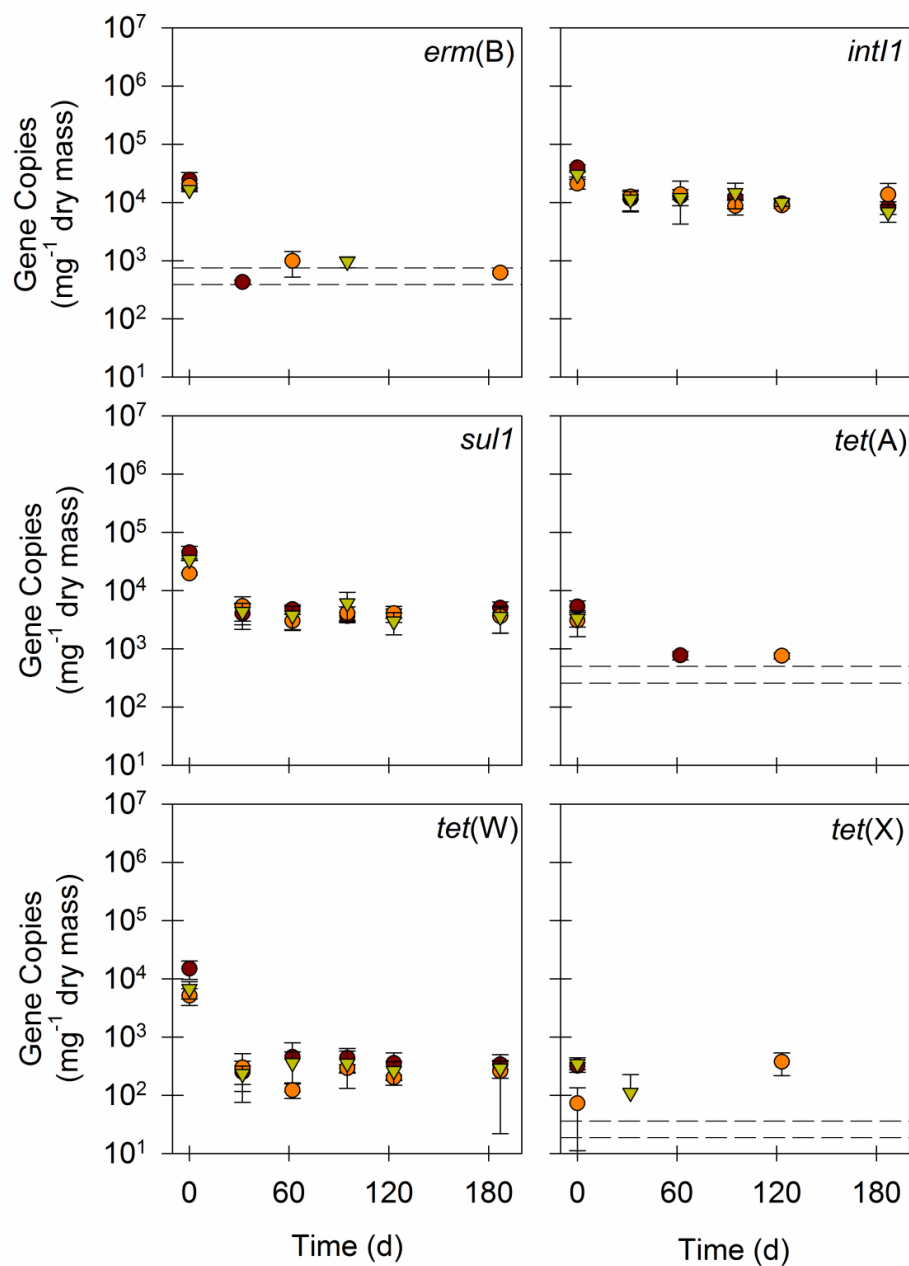


Figure 7.17. Quantities of ARGs and *int11* in soil microcosms that received anaerobically digested (62°C) residual solids. Values are the arithmetic mean of duplicate or triplicate samples; error bars represent one standard deviation. Dashed lines represent the maximum and minimum limits of quantification for data sets that contain one or more experimental observations below those limits.

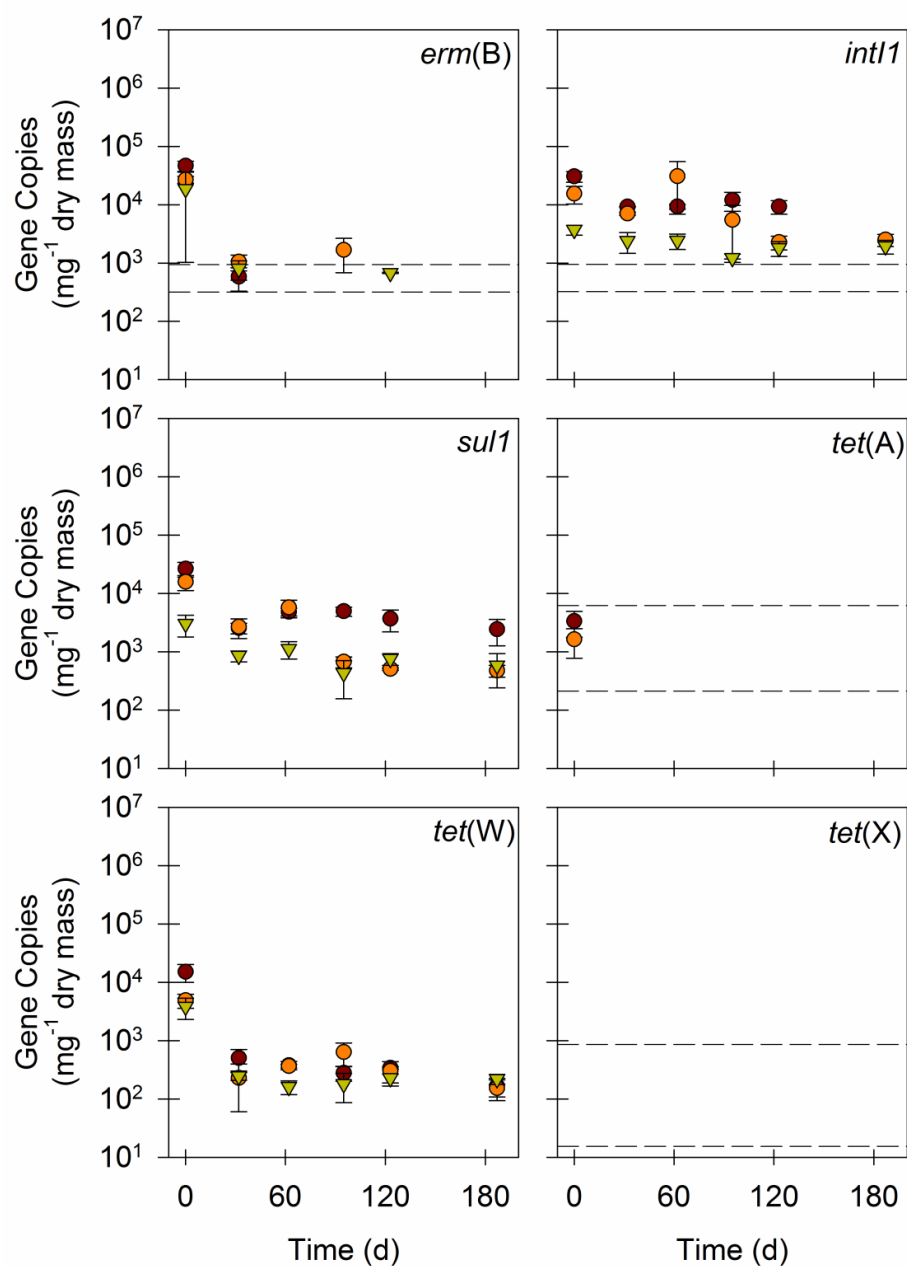


Figure 7.18. Quantities of ARGs and *int11* in soil microcosms that received anaerobically digested (69°C) residual solids. Values are the arithmetic mean of duplicate or triplicate samples; error bars represent one standard deviation. Dashed lines represent the maximum and minimum limits of quantification for data sets that contain one or more experimental observations below those limits.

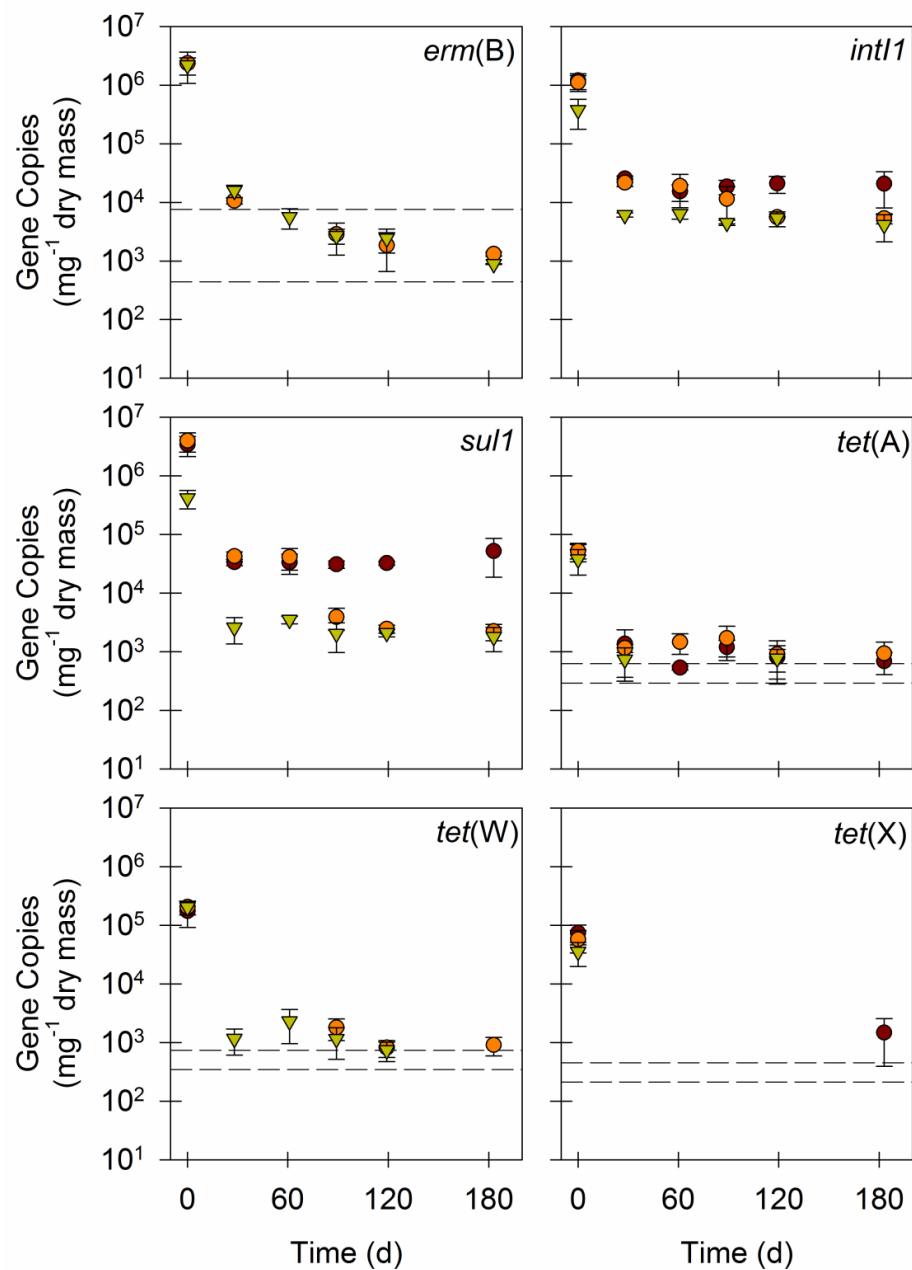


Figure 7.19. Quantities of ARGs and *int11* in soil microcosms that received pasteurized residual solids. Values are the arithmetic mean of duplicate or triplicate samples; error bars represent one standard deviation. Dashed lines represent the maximum and minimum limits of quantification for data sets that contain one or more experimental observations below those limits.

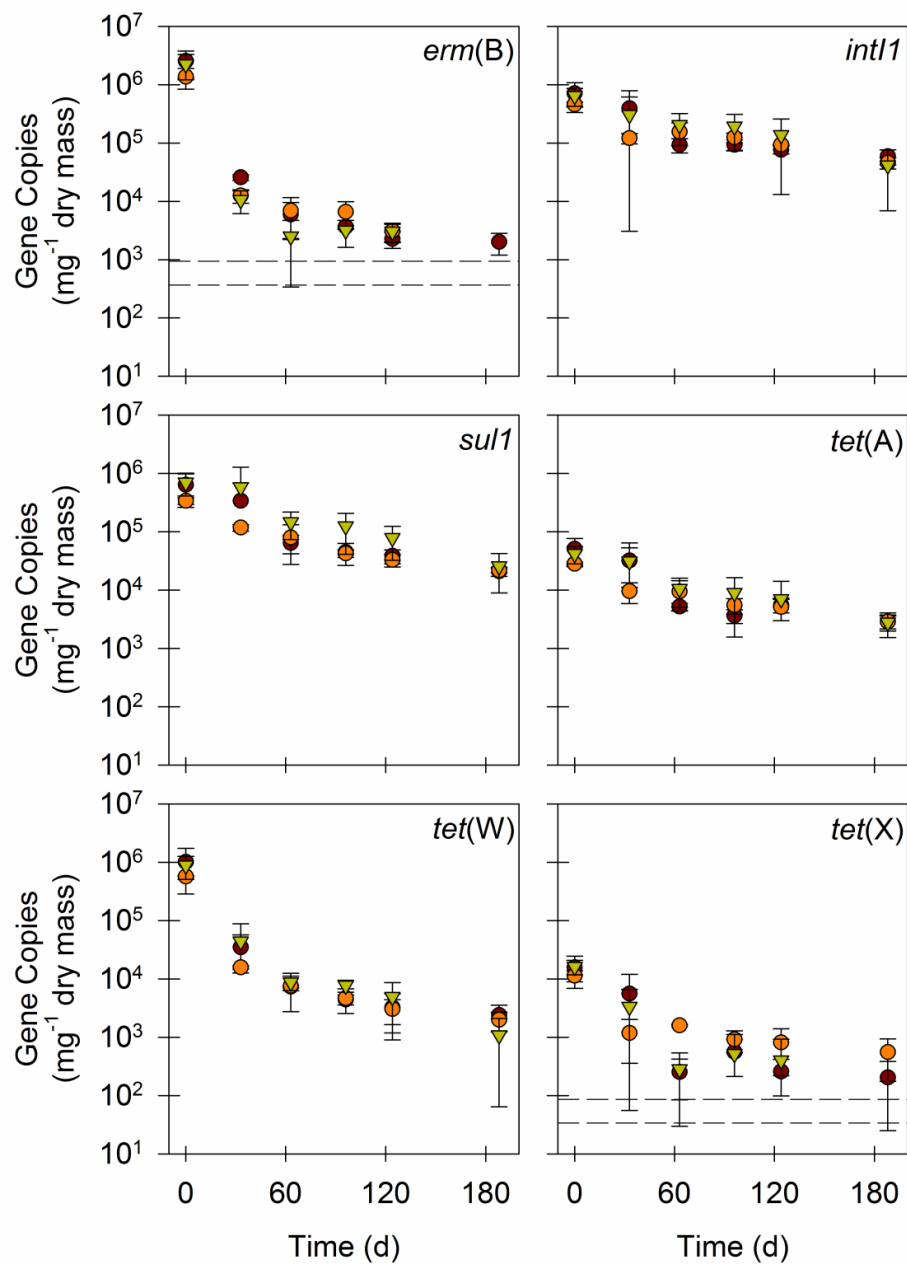


Figure 7.20. Quantities of ARGs and *int11* in soil microcosms that received untreated residual solids. Values are the arithmetic mean of duplicate or triplicate samples; error bars represent one standard deviation. Dashed lines represent the maximum and minimum limits of quantification for data sets that contain one or more experimental observations below those limits.

Quantities of *intII* were relatively persistent compared to those of other gene targets during the first 33 d. In four of the nine sets of microcosms, *intII* had the lowest percentage decrease among all ARGs and *intII*. These four values varied between $53.2\% \pm 17.1\%$ (anaerobically digested at 38°C) and $85.8\% \pm 8.9\%$ (alkali stabilized) (mean \pm standard deviation). Furthermore, *intII* quantities during the first 33 d changed little in soil microcosms that received air-dried residual solids and increased by a factor of 2.2 ± 0.2 (mean \pm standard deviation) in microcosms that received residual solids that were anaerobically digested at 38°C. The only other gene target that had the lowest percentage decrease during the first 33 d in more than one set of soil microcosms was *tet(A)*, which decreased by $97.7\% \pm 0.3\%$ and $42.9\% \pm 20.8\%$ (mean \pm standard deviation) in soil microcosms that received pasteurized and untreated residual solids, respectively. As noted previously, quantities of *tet(A)* also increased during the first 33 d in soil microcosms that received residual solids that were anaerobically digested at 38°C.

7.4 Discussion

Upstream treatment units can have a substantial effect on the fate of ARGs and *intII* in residual municipal wastewater solids applied to soil. Alkali stabilization, pasteurization, and anaerobic digestion at temperatures of 55°C, 62°C, and 69°C all caused sharp initial decreases in ARG and *intII* quantities in land-applied treated residual solids relative to alternative technologies. These sharp decreases are important, because they lead to ARG and *intII* soil concentrations that are up to two orders of magnitude lower than initial concentrations after only approximately 30 d, as opposed to nearly 180 d as has been shown for land-applied residual solids from a typical full-scale treatment

process (i.e. mesophilic anaerobic digestion) (Chapter 6). Achieving lower ARG and *intI1* concentrations in soil sooner should reduce the overall risk for off-site transport of ARGs and, eventually, exposure of ARGs to humans. Thus, residual solids treatment technologies that can produce this effect should be preferable to alternatives that do not, because they hold the capacity to reduce the number of ARGs circulating in the environment.

Future work should explicitly consider the fraction of ARGs present in environmental samples as extracellular DNA. The results presented here demonstrate that at least one technology, alkali stabilization, appeared to produce a large fraction of extracellular DNA (which was separated from the residual solids during centrifugation prior to application to the soil microcosms). This same technology was also among those that consistently produced a time series pattern in which ARG and *intI1* quantities in soil microcosms decreased rapidly over the first 33 d. It would seem likely that the other technologies that produced this effect, which included pasteurization and anaerobic digestion at 55°C, 62°C, and 69°C, also produce a large fraction of extracellular ARGs. This presumably exposes the ARGs to biodegradation and other extracellular DNA fate and transport mechanisms, and it could be a key factor in the fate of ARGs both in soil to which treated residual solids are applied and in the treatment units themselves.

This work adds to a growing body of evidence suggesting that the significance of integrons to the environmental spread of ARGs is in need of further scrutiny (198). Integrons enable both horizontal gene transfer and the accumulation of multiple ARGs in an individual bacterium (82). As a result, they are typically assumed to be significant

with respect to the spread of antibiotic resistance, and, in fact, have been shown to contain multiple ARGs in environmental samples (126,133,145). However, the discrepancy between the initial extents of *intII* removal and the initial extents of removal for many ARGs in this work would seem to suggest that the ARGs considered here are not strongly associated with class 1 integrons. It may be that the integrons in these experiments contain ARGs not targeted in this work, or it may be that these integrons contain very few or no ARGs. Confirmation of either result would be highly informative for efforts intended to mitigate the environmental spread of ARGs, and future work ought to consider the contents of integrons, in addition to the overall quantities, as well as the fate of individual gene cassettes.

The approach used in this work is quantitative, culture-independent, and isolates mixtures of soil and residual solids in closed and reasonably homogenous experimental systems. However, it is also subject to well-known limitations of molecular analytical methods as well as limitations related to the experimental design. The real-time PCR protocol used in this work cannot distinguish gene targets in pathogens from those in non-pathogens, gene targets in living bacteria from those in dead bacteria or present as extracellular DNA in the soil matrix, full-length genes from gene fragments that happen to contain the primer annealing sites, or genes that can be transcribed in their hosts from those that cannot. Also, the soil microcosms did not simulate the effects of direct sunlight, natural fluctuations in moisture content and temperature, or the presence of a full soil ecosystem on the rates at which ARG and *intII* quantities decline in soil. Furthermore, the fact that a large fraction of extracellular DNA from alkali stabilized and

pasteurized residual solids may have been excluded from the soil microcosms might have affected the results observed here. It would be expected, however, that if the initially sharp decrease in gene target concentrations observed in some microcosms was due to the presence of extracellular DNA, that these effects would not be fundamentally different from those that were actually observed. Finally, the work presented in this manuscript investigates only a small fraction of known ARGs. For instance, there are at least 45 genes known to encode resistance to macrolide, lincosamide, and streptogramin B (MLS_B) antibiotics and at least 30 genes known to encode resistance to tetracycline antibiotics (73,74), yet this work considered only one MLS_B resistance gene and three tetracycline resistance genes.

Chapter 8: Conclusions and Recommendations

This work contributes significantly to our ability to optimize treatment and disposal of residual municipal wastewater solids for the removal of ARGs. The primary conclusions can be summarized in seven points:

Aerobic digestion, air drying, and hyperthermophilic ($\geq 60^{\circ}\text{C}$) anaerobic digestion can effectively remove ARGs from residual municipal wastewater solids.

Aerobic digestion, operated under different flow conditions, has been previously demonstrated to be largely ineffective at removing ARGs from residual solids (121), while air drying and hyperthermophilic anaerobic digestion have been previously unconsidered for their effects on ARG quantities in residual solids. The results presented here (204,208) indicate that the many treatment plants already using aerobic digestion and air drying to treat (or dewater) residual municipal wastewater solids (186) could likely optimize their existing treatment systems to achieve significant ARG removal. Furthermore, hyperthermophilic anaerobic digestion was found to be the most effective treatment technology considered in this work based on kinetic analyses (Chapter 5). Future work ought to focus on optimizing this treatment process for removing ARGs from residual municipal wastewater solids, as it may represent the most effective currently available treatment option.

The kinetic analyses presented in this work enable rational selection among alternative treatment technologies and management practices to optimize the entire residual municipal wastewater solids treatment and disposal process. The selection and design of alternative treatment technologies to meet treatment objectives is governed

by operating costs (e.g. energy and chemical inputs and outputs) and capital costs (e.g. tank size). Understanding these costs requires detailed process design, which relies on understanding the kinetics of the underlying biological, chemical, or physical processes. However, only one study prior to this work (121) has considered the kinetics of ARG removal during treatment of residual solids. Thus, the identification of appropriate kinetic models (e.g. modified Collins-Selleck disinfection kinetics) (Chapter 5) and specific kinetic coefficients (Chapter 3, Chapter 4, Chapter 5, and Chapter 6) in this work significantly expands our ability to choose among alternative treatment technologies and management practices (e.g. frequency of land-application of treated residual solids) for optimizing the removal of ARGs from residual municipal wastewater solids.

Batch and semi-batch operation of aerobic and anaerobic digestion may be an effective optimization of those technologies for enhancing ARG removal. The effectiveness of ARG removal achieved by semi-continuous-flow aerobic digestion (121,204) differs considerably from that achieved by batch aerobic digestion (204). Furthermore, the superior performance of thermophilic and hyperthermophilic anaerobic digestion with regard to ARG removal is far more clear for semi-batch (121) (Chapter 5) than semi-continuous-flow (131) treatment systems. Future work should be directed at optimizing the degree to which aerobic and anaerobic digestion can be operated in batch or semi-batch flow configurations while maintaining desirable treatment performance with respect to more traditional objectives (e.g. volatile solids destruction).

The treatment environment imposed by a treatment technology can select for particular ARGs based on their ecological niche. Semi-continuous-flow aerobic

digestion selected for increased quantities, relative to untreated residual solids, of an ARG that requires oxygen to function (*tet(X)*) (Chapter 3). Air-drying beds selected for increased quantities of *tet(X)* as the treatment environment became presumably more aerobic (Chapter 4). Selection of specific ARGs based on the relationship between treatment environment and the ecological niche of the ARG is important to the selection and design of individual treatment units depending on the ARG(s) of concern.

Class 1 integrons are an early, promising candidate for consideration as a design gene. Identification of a design gene or a set of design genes is an important step in formulating reasonable treatment objectives for treatment systems intended to remove ARGs from residual municipal wastewater solids. An ideal design gene would be one that is both relevant to human health and that is relatively persistent in the treatment environments being considered. Class 1 integrons appear to satisfy both of those requirements. They enable both horizontal gene transfer and the accumulation of multiple ARGs (82). They are also among the most persistent gene targets considered in this work (Chapter 3, Chapter 4, Chapter 5, Chapter 6, and Chapter 7). The relationship between class 1 integron quantities (as represented by *intII*) and quantities of the ARGs considered in this work, however, is frequently unclear. Many ARGs considered here decrease in quantity even when *intII* quantities remain relatively constant. Thus, future work should consider the gene cassette content of integrons in addition to their quantities (198). Understanding the distribution of gene cassettes (whether ARGs, metabolic genes, or something else) on integrons in the environment would improve our understanding of the processes that determine their fate in those environments.

ARG quantities in treated residual municipal wastewater solids applied to soil decrease slowly. ARGs in treated residual solids collected from full-scale treatment facilities exhibited half-lives on the order of months following land-application (Chapter 6). ARGs were more persistent in soil than in laboratory-scale residual solids treatment units, and they were more persistent than fecal microorganisms in the same soil (Chapter 6). This result is significant for several reasons. First, it indicates that the best location to control the fate of ARGs in residual municipal wastewater solids may be during residual solids treatment in the treatment plant, because ARGs are relatively persistent once the residual solids are land-applied. Second, the persistence of ARGs in land-applied residual solids in relatively high quantities likely provides the opportunity for their transport through the environment, and ultimately, for human exposure to ARGs. This highlights our current lack of knowledge regarding the fate and transport of ARGs in the environment, and future work should focus on understanding the fate and transport of ARGs on regional or larger scales, the degree to which individuals tend to be exposed to ARGs in pathogens or in forms that permit horizontal gene transfer to pathogens, and the resultant risks associated with varying levels of exposure to ARGs in natural and engineered systems. Finally, the specific kinetic coefficients determined in this work can be used to manage the frequency with which treated residual solids are land-applied at individual sites in order to control their quantities in receiving soils.

Selection of residual solids treatment technology can affect the fate of ARGs in treated residual municipal wastewater solids applied to soil. Approximately half of all treated residual solids in the United States are applied to soil for ultimate disposal

(186). ARGs from these treated residual solids can persist in the soil in high quantities for months (Chapter 6), which likely provides the opportunity for transport of ARGs and human exposure to them. Alkali stabilization, pasteurization, and anaerobic digestion at temperatures in the thermophilic and hyperthermophilic ranges cause ARG quantities to decrease much more rapidly immediately after land-application than alternative technologies. Thus, selection of the residual solids treatment technology used in the treatment plant represents a useful control variable for reducing the quantity of ARGs in soil to which treated residual solids are applied.

Bibliography

1. Armstrong GL, Conn L A, Pinner RW. Trends in infectious disease mortality in the United States during the 20th century. *JAMA*. **1999**, 281(1):61–66.
2. Jabes D. The antibiotic R&D pipeline: an update. *Curr. Opin. Microbiol.* **2011**, 14(5):564–569.
3. Levy SB, Marshall B. Antibacterial resistance worldwide: causes, challenges and responses. *Nat. Med.* **2004**, 10(12):S122–S129.
4. Levy SB. Antibiotic resistance - the problem intensifies. *Adv. Drug Deliv. Rev.* **2005**, 57(10):1446–1450.
5. Pruden A, Pei R, Storteboom H, Carlson KH. Antibiotic resistance genes as emerging contaminants: studies in northern Colorado. *Environ. Sci. Technol.* **2006**, 40(23):7445–7450.
6. Chee-Sanford JC, Aminov RI, Krapac IJ, Garrigues-Jeanjean N, Mackie RI. Occurrence and diversity of tetracycline resistance genes in lagoons and groundwater underlying two swine production facilities. *Appl. Environ. Microbiol.* **2001**, 67(4):1494–1502.
7. Chen J, Jin M, Qiu Z-G, Guo C, Chen Z-L, Shen Z-Q, Wang X-W, Li J-W. A survey of drug resistance *bla* genes originating from synthetic plasmid vectors in six Chinese rivers. *Environ. Sci. Technol.* **2012**, 46(24):13448–13454.
8. Cummings DE, Archer KF, Arriola DJ, Baker PA, Faucett KG, Laroya JB, Pfeil KL, Ryan CR, Ryan KRU, Zuill DE. Broad dissemination of plasmid-mediated quinolone resistance genes in sediments of two urban coastal wetlands. *Environ. Sci. Technol.* **2011**, 45(2):447–454.
9. Graham DW, Olivares-Rieumont S, Knapp CW, Lima L, Werner D, Bowen E. Antibiotic resistance gene abundances associated with waste discharges to the Almendares River near Havana, Cuba. *Environ. Sci. Technol.* **2011**, 45(2):418–424.
10. LaPara TM, Burch TR, McNamara PJ, Tan DT, Yan M, Eichmiller JJ. Tertiary-treated municipal wastewater is a significant point source of antibiotic resistance genes into Duluth-Superior Harbor. *Environ. Sci. Technol.* **2011**, 45(22):9543–9549.

11. Li J, Shao B, Shen J, Wang S, Wu Y. Occurrence of chloramphenicol-resistance genes as environmental pollutants from swine feedlots. *Environ. Sci. Technol.* **2013**, 47(6):2892–2897.
12. Peak N, Knapp CW, Yang RK, Hanfelt MM, Smith MS, Aga DS, Graham DW. Abundance of six tetracycline resistance genes in wastewater lagoons at cattle feedlots with different antibiotic use strategies. *Environ. Microbiol.* **2007**, 9(1):143–151.
13. Pei R, Kim S-C, Carlson KH, Pruden A. Effect of river landscape on the sediment concentrations of antibiotics and corresponding antibiotic resistance genes (ARG). *Water Res.* **2006**, 40(12):2427–2435.
14. Pruden A, Arabi M, Storteboom HN. Correlation between upstream human activities and riverine antibiotic resistance genes. *Environ. Sci. Technol.* **2012**, 46(21):11541–11549.
15. Schwartz T, Kohnen W, Jansen B, Obst U. Detection of antibiotic-resistant bacteria and their resistance genes in wastewater, surface water, and drinking water biofilms. *FEMS Microbiol. Ecol.* **2003**, 43(3):325–335.
16. Seyfried EE, Newton RJ, Rubert KF, Pedersen JA, McMahon KD. Occurrence of tetracycline resistance genes in aquaculture facilities with varying use of oxytetracycline. *Microb. Ecol.* **2010**, 59(4):799–807.
17. Stoll C, Sidhu JPS, Tiehm A, Toze S. Prevalence of clinically relevant antibiotic resistance genes in surface water samples collected from Germany and Australia. *Environ. Sci. Technol.* **2012**, 46(17):9716–9726.
18. Storteboom H, Arabi M, Davis JG, Crimi B, Pruden A. Tracking antibiotic resistance genes in the South Platte River Basin using molecular signatures of urban, agricultural, and pristine sources. *Environ. Sci. Technol.* **2010**, 44(19):7397–7404.
19. Tamminen M, Karkman A, Lõhmus A, Muziasari WI, Takasu H, Wada S, Suzuki S, Virta M. Tetracycline resistance genes persist at aquaculture farms in the absence of selection pressure. *Environ. Sci. Technol.* **2011**, 45(2):386–391.
20. Zhu Y-G, Johnson T a., Su J-Q, Qiao M, Guo G-X, Stedtfeld RD, Hashsham SA, Tiedje JM. Diverse and abundant antibiotic resistance genes in Chinese swine farms. *Proc. Natl. Acad. Sci. U.S.A.* **2013**, 110(9):3435–3440.
21. Auerbach EA, Seyfried EE, McMahon KD. Tetracycline resistance genes in activated sludge wastewater treatment plants. *Water Res.* **2007**, 41(5):1143–1151.

22. Börjesson S, Dienues O, Jarnheimer P-A, Olsen B, Matussek A, Lindgren P-E. Quantification of genes encoding resistance to aminoglycosides, β -lactams and tetracyclines in wastewater environments by real-time PCR. *Int. J. Environ. Heal. Res.* **2009**, 19(3):219–230.
23. Börjesson S, Melin S, Matussek A, Lindgren P-E. A seasonal study of the *mecA* gene and *Staphylococcus aureus* including methicillin-resistant *S. aureus* in a municipal wastewater treatment plant. *Water Res.* **2009**, 43(4):925–932.
24. Ghosh S, Ramsden SJ, LaPara TM. The role of anaerobic digestion in controlling the release of tetracycline resistance genes and class 1 integrons from municipal wastewater treatment plants. *Appl. Microbiol. Biotechnol.* **2009**, 84(4):791–796.
25. Kim S, Park H, Chandran K. Propensity of activated sludge to amplify or attenuate tetracycline resistance genes and tetracycline resistant bacteria: a mathematical modeling approach. *Chemosphere* **2010**, 78(9):1071–1077.
26. Lachmayr KL, Kerkhof LJ, Dirienzo AG, Cavanaugh CM, Ford TE. Quantifying nonspecific TEM β -lactamase (*bla*_{TEM}) genes in a wastewater stream. *Appl. Environ. Microbiol.* **2009**, 75(1):203–211.
27. Munir M, Wong K, Xagorarakis I. Release of antibiotic resistant bacteria and genes in the effluent and biosolids of five wastewater utilities in Michigan. *Water Res.* **2011**, 45(2):681–693.
28. Uyaguari MI, Fichot EB, Scott GI, Norman RS. Characterization and quantitation of a novel β -lactamase gene within a wastewater treatment facility and surrounding coastal ecosystem. *Appl. Environ. Microbiol.* **2011**, 77(23):8226–8233.
29. Volkmann H, Schwartz T, Bischoff P, Kirchen S, Obst U. Detection of clinically relevant antibiotic-resistance genes in municipal wastewater using real-time PCR (TaqMan). *J. Microbiol. Methods* **2004**, 56(2):277–286.
30. Zhang X-X, Zhang T. Occurrence, abundance, and diversity of tetracycline resistance genes in 15 sewage treatment plants across China and other global locations. *Environ. Sci. Technol.* **2011**, 45(7):2598–2604.
31. Zhang T, Zhang M, Zhang X, Fang HH. Tetracycline resistance genes and tetracycline resistant lactose-fermenting *Enterobacteriaceae* in activated sludge of sewage treatment plants. *Environ. Sci. Technol.* **2009**, 43(9):3455–3460.
32. Zhang X-X, Zhang T, Zhang M, Fang HHP, Cheng S-P. Characterization and quantification of class 1 integrons and associated gene cassettes in sewage treatment plants. *Appl. Microbiol. Biotechnol.* **2009**, 82(6):1169–1177.

33. Fleming A. On the antibacterial action of cultures of a *Penicillium*, with special reference to their use in the isolation of *B. influenzae*. *Br. J. Exp. Pathol.* **1929**, 10(3):226–236.
34. Greenwood D. Historical introduction. In: Finch RG, Greenwood D, Norrby SR, Whitley RJ, editors. *Antibiot. Chemother. Anti-Infective Agents Their Use Ther.* 8th ed. New York, NY: Churchill Livingstone; **2003**. p. 3–10.
35. Food and Drug Administration. U.S. Department of Health and Human Services. Systemic antibacterial drug products. **2012**.
36. National Center for Health Statistics. U.S. Department of Health, Education, and Welfare. The change in mortality trend in the United States. **1964**.
37. Madigan MT, Martinko JM. *Brock Biology of Microorganisms*. 11th ed. Upper Saddle River, NJ: Pearson Prentice Hall; **2006**.
38. Kümmerer K. Antibiotics in the aquatic environment--a review--part I. *Chemosphere* **2009**, 75(4):417–434.
39. Davies J. Are antibiotics naturally antibiotics? *J. Ind. Microbiol. Biotechnol.* **2006**, 33(7):496–499.
40. Yim G, Wang HH, Davies J. Antibiotics as signalling molecules. *Philos. Trans. R. Soc. London Ser. B* **2007**, 362(1483):1195–1200.
41. Martínez JL. Antibiotics and antibiotic resistance genes in natural environments. *Science* **2008**, 321(5887):365–367.
42. Fajardo A, Martínez JL. Antibiotics as signals that trigger specific bacterial responses. *Curr. Opin. Microbiol.* **2008**, 11(2):161–167.
43. Waksman SA, Woodruff HB. The soil as a source of microorganisms antagonistic to disease-producing bacteria. *J. Bacteriol.* **1940**, 40(4):581–600.
44. Aminov RI. The role of antibiotics and antibiotic resistance in nature. *Environ. Microbiol.* **2009**, 11(12):2970–2988.
45. Sarmah AK, Meyer MT, Boxall ABA. A global perspective on the use, sales, exposure pathways, occurrence, fate and effects of veterinary antibiotics (VAs) in the environment. *Chemosphere* **2006**, 65(5):725–759.

46. Norrby SR. Principles of chemoprophylaxis. In: Finch RG, Greenwood D, Norrby SR, Whitley RJ, editors. *Antibiot. Chemother. Anti-Infective Agents Their Use Ther.* 8th ed. New York, NY: Churchill Livingstone; **2003**. p. 120–122.
47. Cabello FC. Heavy use of prophylactic antibiotics in aquaculture: a growing problem for human and animal health and for the environment. *Environ. Microbiol.* **2006**, 8(7):1137–1144.
48. Lipsitch M, Singer RS, Levin BR. Antibiotics in agriculture: when is it time to close the barn door? *Proc. Natl. Acad. Sci. U.S.A.* **2002**, 99(9):5752–5754.
49. Food and Drug Administration. U.S. Department of Health and Human Services. Summary report on antimicrobials sold or distributed for use in food-producing animals. **2011**.
50. Greenwood D, Whitley R. Modes of action. In: Finch RG, Greenwood D, Norrby SR, Whitley RJ, editors. *Antibiot. Chemother. Anti-Infective Agents Their Use Ther.* 8th ed. New York, NY: Churchill Livingstone; **2003**. p. 11–24.
51. Walsh C. *Antibiotics: Actions, Origins, Resistance*. Washington, DC: ASM Press; **2003**.
52. Bush K. Beta-lactam antibiotics: penicillins. In: Finch RG, Greenwood D, Norrby SR, Whitley RJ, editors. *Antibiot. Chemother. Anti-Infective Agents Their Use Ther.* 8th ed. New York, NY: Churchill Livingstone; **2003**. p. 224–258.
53. Greenwood D. Sulfonamides. In: Finch RG, Greenwood D, Norrby SR, Whitley RJ, editors. *Antibiot. Chemother. Anti-Infective Agents Their Use Ther.* 8th ed. New York, NY: Churchill Livingstone; **2003**. p. 385–392.
54. Boehr DD, Draker K, Wright GD. Aminoglycosides and aminocyclitols. In: Finch RG, Greenwood D, Norrby SR, Whitley RJ, editors. *Antibiot. Chemother. Anti-Infective Agents Their Use Ther.* 8th ed. New York, NY: Churchill Livingstone; **2003**. p. 155–184.
55. Wilcox MH. Chloramphenicol and thiamphenicol. In: Finch RG, Greenwood D, Norrby SR, Whitley RJ, editors. *Antibiot. Chemother. Anti-Infective Agents Their Use Ther.* 8th ed. New York, NY: Churchill Livingstone; **2003**. p. 279–283.
56. Greenwood D. Beta-lactam antibiotics: cephalosporins. In: Finch RG, Greenwood D, Norrby SR, Whitley RJ, editors. *Antibiot. Chemother. Anti-Infective Agents Their Use Ther.* 8th ed. New York, NY: Churchill Livingstone; **2003**. p. 185–223.

57. Chopra I. Tetracyclines. In: Finch RG, Greenwood D, Norrby SR, Whitley RJ, editors. *Antibiot. Chemother. Anti-Infective Agents Their Use Ther.* 8th ed. New York, NY: Churchill Livingstone; **2003**. p. 393–406.
58. Bryskier A, Butzler J-P. Macrolides. In: Finch RG, Greenwood D, Norrby SR, Whitley RJ, editors. *Antibiot. Chemother. Anti-Infective Agents Their Use Ther.* 8th ed. New York, NY: Churchill Livingstone; **2003**. p. 310–325.
59. Greenwood D. Glycopeptides. In: Finch RG, Greenwood D, Norrby SR, Whitley RJ, editors. *Antibiot. Chemother. Anti-Infective Agents Their Use Ther.* 8th ed. New York, NY: Churchill Livingstone; **2003**. p. 300–304.
60. Parenti F, Lancini G. Rifamycins. In: Finch RG, Greenwood D, Norrby SR, Whitley RJ, editors. *Antibiot. Chemother. Anti-Infective Agents Their Use Ther.* 8th ed. New York, NY: Churchill Livingstone; **2003**. p. 374–381.
61. Palumbi SR. Humans as the world's greatest evolutionary force. *Science* **2001**, 293(5536):1786–1790.
62. Greenwood D. Lincosamides. In: Finch RG, Greenwood D, Norrby SR, Whitley RJ, editors. *Antibiot. Chemother. Anti-Infective Agents Their Use Ther.* 8th ed. New York, NY: Churchill Livingstone; **2003**. p. 305–309.
63. Andriole VT. Quinolones. In: Finch RG, Greenwood D, Norrby SR, Whitley RJ, editors. *Antibiot. Chemother. Anti-Infective Agents Their Use Ther.* 8th ed. New York, NY: Churchill Livingstone; **2003**. p. 349–373.
64. Riain UN, MacGowan AP. Oxazolidinones. In: Finch RG, Greenwood D, Norrby SR, Whitley RJ, editors. *Antibiot. Chemother. Anti-Infective Agents Their Use Ther.* 8th ed. New York, NY: Churchill Livingstone; **2003**. p. 345–348.
65. Centers for Disease Control and Prevention. U.S. Department of Health and Human Services. Antibiotic resistance threats in the United States. **2013**.
66. Murphy SL, Xu J, Kochanek KD. Deaths: final data for 2010. *National Vital Statistics Reports* 61(4). Hyattsville, MD: National Center for Health Statistics. **2013**.
67. Roberts RR, Hota B, Ahmad I, Scott RD, Foster SD, Abbasi F, Schabowski S, Kampe LM, Ciavarella GG, Supino M, Naples J, Cordell R, Levy SB, Weinstein RA. Hospital and societal costs of antimicrobial-resistant infections in a Chicago teaching hospital: implications for antibiotic stewardship. *Clin. Infect. Dis.* **2009**, 49(8):1175–1184.

68. Mazel D, Davies J. Antibiotic resistance in microbes. *Cell. Mol. Life Sci.* **1999**, 56(9–10):742–754.
69. Wright GD. The antibiotic resistome: the nexus of chemical and genetic diversity. *Nat. Rev. Microbiol.* **2007**, 5(3):175–186.
70. Davies J, Spiegelman GB, Yim G. The world of subinhibitory antibiotic concentrations. *Curr. Opin. Microbiol.* **2006**, 9(5):445–453.
71. Then RL. Diaminopyrimidines. In: Finch RG, Greenwood D, Norrby SR, Whitley RJ, editors. *Antibiot. Chemother. Anti-Infective Agents Their Use Ther.* 8th ed. New York, NY: Churchill Livingstone; **2003**. p. 284–293.
72. Dantas G, Sommer MOA, Oluwasegun RD, Church GM. Bacteria subsisting on antibiotics. *Science* **2008**, 320(5872):100–103.
73. Levy SB, McMurry LM, Barbosa TM, Burdett V, Courvalin P, Hillen W, Roberts MC, Rood JI, Taylor DE. Nomenclature for new tetracycline resistance determinants. *Antimicrob. Agents Chemother.* **1999**, 43(6):1523–1524.
74. Roberts MC, Sutcliffe J, Courvalin P, Jensen LB, Rood J, Seppala H. Nomenclature for macrolide and macrolide-lincosamide-streptogramin B resistance determinants. *Antimicrob. Agents Chemother.* **1999**, 43(12):2823–2830.
75. Aminov RI, Mackie RI. Evolution and ecology of antibiotic resistance genes. *FEMS Microbiol. Lett.* **2007**, 271(2):147–161.
76. D’Costa VM, King CE, Kalan L, Morar M, Sung WWL, Schwarz C, Froese D, Zazula G, Calmels F, Debruyne R, Golding GB, Poinar HN, Wright GD. Antibiotic resistance is ancient. *Nature* **2011**, 477(7365):457–461.
77. D’Costa VM, McGrann KM, Hughes DW, Wright GD. Sampling the antibiotic resistome. *Science* **2006**, 311(5759):374–377.
78. Forsberg KJ, Reyes A, Wang B, Selleck EM, Sommer MOA, Dantas G. The shared antibiotic resistome of soil bacteria and human pathogens. *Science* **2012**, 337(6098):1107–1111.
79. Stokes HW, Gillings MR. Gene flow, mobile genetic elements and the recruitment of antibiotic resistance genes into Gram-negative pathogens. *FEMS Microbiol. Rev.* **2011**, 35(5):790–819.
80. Frost LS, Leplae R, Summers AO, Toussaint A. Mobile genetic elements: the agents of open source evolution. *Nat. Rev. Microbiol.* **2005**, 3(9):722–732.

81. Lang AS, Zhaxybayeva O, Beatty JT. Gene transfer agents: phage-like elements of genetic exchange. *Nat. Rev. Microbiol.* **2012**, 10(7):472–482.
82. Mazel D. Integrons: agents of bacterial evolution. *Nat. Rev. Microbiol.* **2006**, 4(8):608–620.
83. Furuya EY, Lowy FD. Antimicrobial-resistant bacteria in the community setting. *Nat. Rev. Microbiol.* **2006**, 4(1):36–45.
84. Wu S, Piscitelli C, de Lencastre H, Tomasz A. Tracking the evolutionary origin of the methicillin resistance gene: cloning and sequencing of a homologue of *mecA* from a methicillin susceptible strain of *Staphylococcus sciuri*. *Microb. Drug Resist.* **1996**, 2(4):435–441.
85. Bloom BR, Murray CJL. Tuberculosis: commentary on a reemergent killer. *Science* **1992**, 257(5073):1055–1064.
86. Alekshun MN, Levy SB. Targeting virulence to prevent infection: to kill or not to kill? *Drug Discov. Today Ther. Strateg.* **2004**, 1(4):483–489.
87. Arnold S, Gassner B, Giger T, Zwahlen R. Banning antimicrobial growth promoters in feedstuffs does not result in increased therapeutic use of antibiotics in medicated feed in pig farming. *Pharmacoepidemiol. Drug Saf.* **2004**, 13(5):323–331.
88. Edgar R, Friedman N, Molshanski-Mor S, Qimron U. Reversing bacterial resistance to antibiotics by phage-mediated delivery of dominant sensitive genes. *Appl. Environ. Microbiol.* **2012**, 78(3):744–751.
89. Kohanski MA, Dwyer DJ, Collins JJ. How antibiotics kill bacteria: from targets to networks. *Nat. Rev. Microbiol.* **2010**, 8(6):423–435.
90. Merril CR, Scholl D, Adhya SL. The prospect for bacteriophage therapy in Western medicine. *Nat. Rev. Drug Discov.* **2003**, 2(June):489–497.
91. Projan SJ. Why is big pharma getting out of antibacterial drug discovery? *Curr. Opin. Microbiol.* **2003**, 6(5):427–430.
92. Smith DL, Harris AD, Johnson JA, Silbergeld EK, Morris JG. Animal antibiotic use has an early but important impact on the emergence of antibiotic resistance in human commensal bacteria. *Proc. Natl. Acad. Sci. U.S.A.* **2002**, 99(9):6434–6439.
93. Klare I, Badstübner D, Konstabel C, Böhme G, Claus H, Witte W. Decreased incidence of VanA-type vancomycin-resistant enterococci isolated from poultry

meat and from fecal samples of humans in the community after discontinuation of avoparcin usage in animal husbandry. *Microb. Drug Resist.* **1999**, 5(1):45–52.

94. Aminov RI, Chee-Sanford JC, Garrigues N, Teferedegne B, Krapac IJ, White BA, Mackie RI. Development, validation, and application of PCR primers for detection of tetracycline efflux genes of Gram-negative bacteria. *Appl. Environ. Microbiol.* **2002**, 68(4):1786–1793.
95. Aminov RI, Garrigues-Jeanjean N, Mackie RI. Molecular ecology of tetracycline resistance: development and validation of primers for detection of tetracycline resistance genes encoding ribosomal protection. *Appl. Environ. Microbiol.* **2001**, 67(1):22–32.
96. Binh CTT, Heuer H, Kaupenjohann M, Smalla K. Piggery manure used for soil fertilization is a reservoir for transferable antibiotic resistance plasmids. *FEMS Microbiol. Ecol.* **2008**, 66(1):25–37.
97. Colomer-Lluch M, Imamovic L, Jofre J, Muniesa M. Bacteriophages carrying antibiotic resistance genes in fecal waste from cattle, pigs, and poultry. *Antimicrob. Agents Chemother.* **2011**, 55(10):4908–4911.
98. Gao P, Mao D, Luo Y, Wang L, Xu B, Xu L. Occurrence of sulfonamide and tetracycline-resistant bacteria and resistance genes in aquaculture environment. *Water Res.* **2012**, 46(7):2355–2364.
99. Heuer H, Krögerrecklenfort E, Wellington EMH, Egan S, van Elsas JD, van Overbeek L, Collard J-M, Guillaume G, Karagouni AD, Nikolakopoulou TL, Smalla K. Gentamicin resistance genes in environmental bacteria: prevalence and transfer. *FEMS Microbiol. Ecol.* **2002**, 42(2):289–302.
100. Joy SR, Bartelt-Hunt SL, Snow DD, Gilley JE, Woodbury BL, Parker DB, Marx DB, Li X. Fate and transport of antimicrobials and antimicrobial resistance genes in soil and runoff following land application of swine manure slurry. *Environ. Sci. Technol.* **2013**, 47(21):7397–7404.
101. Koike S, Krapac IG, Oliver HD, Yannarell AC, Chee-Sanford JC, Aminov RI, Mackie RI. Monitoring and source tracking of tetracycline resistance genes in lagoons and groundwater adjacent to swine production facilities over a 3-year period. *Appl. Environ. Microbiol.* **2007**, 73(15):4813–4823.
102. Koike S, Aminov RI, Yannarell AC, Gans HD, Krapac IG, Chee-Sanford JC, Mackie RI. Molecular ecology of macrolide-lincosamide-streptogramin B methylases in waste lagoons and subsurface waters associated with swine production. *Microb. Ecol.* **2010**, 59(3):487–498.

103. Marti E, Balcázar JL. Real-time PCR assays for quantification of *qnr* genes in environmental water samples and chicken feces. *Appl. Environ. Microbiol.* **2012**, 79(5):17–20.
104. Marti R, Scott A, Tien Y-C, Murray R, Sabourin L, Zhang Y, Topp E. The impact of manure fertilization on the abundance of antibiotic-resistant bacteria and frequency of detection of antibiotic resistance genes in soil, and on vegetables at harvest. *Appl. Environ. Microbiol.* **2013**, 79(18):5701–5709.
105. McKinney CW, Loftin KA, Meyer MT, Davis JG, Pruden A. *tet* and *sul* antibiotic resistance genes in livestock lagoons of various operation type, configuration, and antibiotic occurrence. *Environ. Sci. Technol.* **2010**, 44(16):6102–6109.
106. Nandi S, Maurer JJ, Hofacre C, Summers AO. Gram-positive bacteria are a major reservoir of Class 1 antibiotic resistance integrons in poultry litter. *Proc. Natl. Acad. Sci. U.S.A.* **2004**, 101(18):7118–7122.
107. Pei R, Cha J, Carlson KH, Pruden A. Response of antibiotic resistance genes (ARG) to biological treatment in dairy lagoon water. *Environ. Sci. Technol.* **2007**, 41(14):5108–5113.
108. Phuong Hoa PT, Nonaka L, Hung Viet P, Suzuki S. Detection of the *sul1*, *sul2*, and *sul3* genes in sulfonamide-resistant bacteria from wastewater and shrimp ponds of north Vietnam. *Sci. Total Environ.* **2008**, 405(1-3):377–384.
109. Ponce-Rivas E, Muñoz-Márquez M-E, Khan AA. Identification and molecular characterization of class 1 integrons in multiresistant *Escherichia coli* isolates from poultry litter. *Appl. Environ. Microbiol.* **2012**, 78(15):5444–5447.
110. Shah SQA, Colquhoun DJ, Nikuli HL, Sørum H. Prevalence of antibiotic resistance genes in the bacterial flora of integrated fish farming environments of Pakistan and Tanzania. *Environ. Sci. Technol.* **2012**, 46(16):8672–8679.
111. Smith MS, Yang RK, Knapp CW, Niu Y, Peak N, Hanfelt MM, Galland JC, Graham DW. Quantification of tetracycline resistance genes in feedlot lagoons by real-time PCR. *Appl. Environ. Microbiol.* **2004**, 70(12):7372–7377.
112. Storteboom H, Arabi M. Identification of molecular signatures suitable as tracers of pristine river, urban, and agricultural sources. *Environ. Sci. Technol.* **2010**, 44(6):1947–1953.
113. Storteboom HN, Kim S-C, Doesken KC, Carlson KH, Davis JG, Pruden A. Response of antibiotics and resistance genes to high-intensity and low-intensity manure management. *J. Environ. Qual.* **2002**, 36(6):1695–1703.

114. Tamang MD, Nam H-M, Gurung M, Jang G-C, Kim S-R, Jung S-C, Park YH, Lim S-K. Molecular characterization of CTX-M β -lactamase and associated addiction systems in *Escherichia coli* circulating among cattle, farm workers, and farm environment. *Appl. Environ. Microbiol.* **2013**, 79(13):3898–3905.
115. Zhang W, Sturm BSM, Knapp CW, Graham DW. Accumulation of tetracycline resistance genes in aquatic biofilms due to periodic waste loadings from swine lagoons. *Environ. Sci. Technol.* **2009**, 43(20):7643–7650.
116. Zhang Y, Snow DD, Parker D, Zhou Z, Li X. Intracellular and extracellular antimicrobial resistance genes in the sludge of livestock waste management structures. *Environ. Sci. Technol.* **2013**, 47(18):10206–10213.
117. Castiglioni S, Pomati F, Miller K, Burns BP, Zuccato E, Calamari D, Neilan BA. Novel homologs of the multiple resistance regulator *marA* in antibiotic-contaminated environments. *Water Res.* **2008**, 42(16):4271–4280.
118. Chen H, Zhang M. Effects of advanced treatment systems on the removal of antibiotic resistance genes in wastewater treatment plants from Hangzhou, China. *Environ. Sci. Technol.* **2013**, 47(15):8157–8163.
119. Czekalski N, Berthold T, Caucci S, Egli A, Bürgmann H. Increased levels of multiresistant bacteria and resistance genes after wastewater treatment and their dissemination into Lake Geneva, Switzerland. *Front. Microbiol.* **2012**, 3:Article 106.
120. da Silva MF, Vaz-Moreira I, Gonzalez-Pajuelo M, Nunes OC, Manaia CM. Antimicrobial resistance patterns in *Enterobacteriaceae* isolated from an urban wastewater treatment plant. *FEMS Microbiol. Ecol.* **2007**, 60(1):166–176.
121. Diehl DL, LaPara TM. Effect of temperature on the fate of genes encoding tetracycline resistance and the integrase of class 1 integrons within anaerobic and aerobic digesters treating municipal wastewater solids. *Environ. Sci. Technol.* **2010**, 44(23):9128–9133.
122. Fahrenfeld N, Ma Y, O'Brien M, Pruden A. Reclaimed water as a reservoir of antibiotic resistance genes: distribution system and irrigation implications. *Front. Microbiol.* **2013**, 4:Article 130.
123. Girlich D, Poirel L, Szczepanowski R, Schlüter A, Nordmann P. Carbapenem-hydrolyzing GES-5-encoding gene on different plasmid types recovered from a bacterial community in a sewage treatment plant. *Appl. Environ. Microbiol.* **2012**, 78(4):1292–1295.

124. Guardabassi L, Dalsgaard A. Occurrence, structure, and mobility of Tn1546-like elements in environmental isolates of vancomycin-resistant Enterococci. *Appl. Environ. Microbiol.* **2004**, 70(2):984–990.
125. Guillaume G, Verbrugge D, Chasseur-Libotte M-L, Moens W, Collard J-M. PCR typing of tetracycline resistance determinants (Tet A-E) in *Salmonella enterica* serotype Hadar and in the microbial community of activated sludges from hospital and urban wastewater treatment facilities in Belgium. *FEMS Microbiol. Ecol.* **2000**, 32(1):77–85.
126. Guo X, Xia R, Han N, Xu H. Genetic diversity analyses of class 1 integrons and their associated antimicrobial resistance genes in *Enterobacteriaceae* strains recovered from aquatic habitats in China. *Lett. Appl. Microbiol.* **2011**, 52(6):667–675.
127. Jakobsen L, Sandvang D, Hansen LH, Bagger-Skjøt L, Westh H, Jørgensen C, Hansen DS, Pedersen BM, Monnet DL, Frimodt-Møller N, Sørensen SJ, Hammerum AM. Characterisation, dissemination and persistence of gentamicin resistant *Escherichia coli* from a Danish university hospital to the waste water environment. *Environ. Int.* **2008**, 34(1):108–115.
128. Jung CM, Heinze TM, Strakosha R, Elkins CA, Sutherland JB. Acetylation of fluoroquinolone antimicrobial agents by an *Escherichia coli* strain isolated from a municipal wastewater treatment plant. *J. Appl. Microbiol.* **2009**, 106(2):564–571.
129. Kaplan E, Ofek M, Jurkevitch E, Cytryn E. Characterization of fluoroquinolone resistance and *qnr* diversity in *Enterobacteriaceae* from municipal biosolids. *Front. Microbiol.* **2013**, 4:Article 144.
130. Liu M, Zhang Y, Yang M, Tian Z, Ren L, Zhang S. Abundance and distribution of tetracycline resistance genes and mobile elements in an oxytetracycline production wastewater treatment system. *Environ. Sci. Technol.* **2012**, 46(14):7551–7557.
131. Ma Y, Wilson CA, Novak JT, Riffat R, Aynur S, Murthy S, Pruden A. Effect of various sludge digestion conditions on sulfonamide, macrolide, and tetracycline resistance genes and class I integrons. *Environ. Sci. Technol.* **2011**, 45(18):7855–7861.
132. Miller JH, Novak JT, Knocke WR, Young K, Hong Y, Vikesland PJ, Hull MS, Pruden A. Effect of silver nanoparticles and antibiotics on antibiotic resistance genes in anaerobic digestion. *Water Environ. Res.* **2013**, 85(5):411–421.

133. Mokracka J, Koczura R, Kaznowski A. Multiresistant *Enterobacteriaceae* with class 1 and class 2 integrons in a municipal wastewater treatment plant. *Water Res.* **2012**, 46(10):3353–3363.
134. Moura A, Henriques I, Smalla K, Correia A. Wastewater bacterial communities bring together broad-host range plasmids, integrons and a wide diversity of uncharacterized gene cassettes. *Res. Microbiol.* **2010**, 161(1):58–66.
135. Negreanu Y, Pasternak Z, Jurkevitch E, Cytryn E. Impact of treated wastewater irrigation on antibiotic resistance in agricultural soils. *Environ. Sci. Technol.* **2012**, 46(9):4800–4808.
136. Novais C, Coque TM, Ferreira H, Sousa JC, Peixe L. Environmental contamination with vancomycin-resistant Enterococci from hospital sewage in Portugal. *Appl. Environ. Microbiol.* **2005**, 71(6):3364–3368.
137. Ramsden SJ, Ghosh S, Bohl LJ, LaPara TM. Phenotypic and genotypic analysis of bacteria isolated from three municipal wastewater treatment plants on tetracycline-amended and ciprofloxacin-amended growth media. *J. Appl. Microbiol.* **2010**, 109(5):1609–1618.
138. Schlüter A, Heuer H, Szczepanowski R, Forney LJ, Thomas CM, Pühler A, Top EM. The 64 508 bp IncP-1 β antibiotic multiresistance plasmid pB10 isolated from a waste-water treatment plant provides evidence for recombination between members of different branches of the IncP-1 β group. *Microbiology* **2003**, 149(11):3139–3153.
139. Schlüter A, Szczepanowski R, Kurz N, Schneiker S, Krahn I, Pühler A. Erythromycin resistance-conferring plasmid pRSB105, isolated from a sewage treatment plant, harbors a new macrolide resistance determinant, an integron-containing Tn402-like element, and a large region of unknown function. *Appl. Environ. Microbiol.* **2007**, 73(6):1952–1960.
140. Schwartz T, Volkmann H, Kirchen S, Kohnen W, Schön-Hölz K, Jansen B, Obst U. Real-time PCR detection of *Pseudomonas aeruginosa* in clinical and municipal wastewater and genotyping of the ciprofloxacin-resistant isolates. *FEMS Microbiol. Ecol.* **2006**, 57(1):158–167.
141. Stalder T, Barraud O, Jové T, Casellas M, Gaschet M, Dagot C, Ploy M-C. Quantitative and qualitative impact of hospital effluent on dissemination of the integron pool. *ISME J.* **2013**, 1:1–10.
142. Szczepanowski R, Bekel T, Goesmann A, Krause L, Krömeke H, Kaiser O, Eichler W, Pühler A, Schlüter A. Insight into the plasmid metagenome of

wastewater treatment plant bacteria showing reduced susceptibility to antimicrobial drugs analysed by the 454-pyrosequencing technology. *J. Biotechnol.* **2008**, 136(1-2):54–64.

143. Szczepanowski R, Krahn I, Linke B, Goesmann A, Pühler A, Schlüter A. Antibiotic multiresistance plasmid pRSB101 isolated from a wastewater treatment plant is related to plasmids residing in phytopathogenic bacteria and carries eight different resistance determinants including a multidrug transport system. *Microbiology* **2004**, 150(11):3613–3630.
144. Szczepanowski R, Linke B, Krahn I, Gartemann K-H, Gützkow T, Eichler W, Pühler A, Schlüter A. Detection of 140 clinically relevant antibiotic-resistance genes in the plasmid metagenome of wastewater treatment plant bacteria showing reduced susceptibility to selected antibiotics. *Microbiology* **2009**, 155(7):2306–2319.
145. Tennstedt T, Szczepanowski R, Braun S, Pühler A, Schlüter A. Occurrence of integron-associated resistance gene cassettes located on antibiotic resistance plasmids isolated from a wastewater treatment plant. *FEMS Microbiol. Ecol.* **2003**, 45(3):239–252.
146. Tennstedt T, Szczepanowski R, Krahn I, Pühler A, Schlüter A. Sequence of the 68,869 bp IncP-1 α plasmid pTB11 from a waste-water treatment plant reveals a highly conserved backbone, a Tn402-like integron and other transposable elements. *Plasmid* **2005**, 53(3):218–238.
147. Zhang T, Zhang X-X, Ye L. Plasmid metagenome reveals high levels of antibiotic resistance genes and mobile genetic elements in activated sludge. *PLoS One* **2011**, 6(10):e26041.
148. Agersø Y, Sengeløv G, Jensen LB. Development of a rapid method for direct detection of *tet*(M) genes in soil from Danish farmland. *Environ. Int.* **2004**, 30(1):117–122.
149. Ghosh S, LaPara TM. The effects of subtherapeutic antibiotic use in farm animals on the proliferation and persistence of antibiotic resistance among soil bacteria. *ISME J.* **2007**, 1(3):191–203.
150. Heuer H, Solehati Q, Zimmerling U, Kleineidam K, Schlöter M, Müller T, Focks A, Thiele-Bruhn S, Smalla K. Accumulation of sulfonamide resistance genes in arable soils due to repeated application of manure containing sulfadiazine. *Appl. Environ. Microbiol.* **2011**, 77(7):2527–2530.

151. Heuer H, Smalla K. Manure and sulfadiazine synergistically increased bacterial antibiotic resistance in soil over at least two months. *Environ. Microbiol.* **2007**, 9(3):657–666.
152. Hong P-Y, Yannarell AC, Dai Q, Ekizoglu M, Mackie RI. Monitoring the perturbation of soil and groundwater microbial communities due to pig production activities. *Appl. Environ. Microbiol.* **2013**, 79(8):2620–2629.
153. Jechalke S, Kopmann C, Rosendahl I, Groeneweg J, Weichelt V, Krögerrecklenfort E, Brandes N, Nordwig M, Ding G-C, Siemens J, Heuer H, Smalla K. Field application of manure from sulfadiazine treated pigs increased the abundance and transferability of resistance genes. *Appl. Environ. Microbiol.* **2013**, 79(5):1704–1711.
154. Knapp CW, Dolfing J, Ehlert PAI, Graham DW. Evidence of increasing antibiotic resistance gene abundances in archived soils since 1940. *Environ. Sci. Technol.* **2010**, 44(2):580–587.
155. Kopmann C, Jechalke S, Rosendahl I, Groeneweg J, Krögerrecklenfort E, Zimmerling U, Weichelt V, Siemens J, Amelung W, Heuer H, Smalla K. Abundance and transferability of antibiotic resistance as related to the fate of sulfadiazine in maize rhizosphere and bulk soil. *FEMS Microbiol. Ecol.* **2013**, 83(1):125–134.
156. Malik A, Celik E-K, Bohn C, Böckelmann U, Knobel K, Grohmann E. Detection of conjugative plasmids and antibiotic resistance genes in anthropogenic soils from Germany and India. *FEMS Microbiol. Lett.* **2008**, 279(2):207–216.
157. Popowska M, Rzeczycka M, Miernik A, Krawczyk-Balska A, Walsh F, Duffy B. Influence of soil use on prevalence of tetracycline, streptomycin, and erythromycin resistance and associated resistance genes. *Antimicrob. Agents Chemother.* **2012**, 56(3):1434–1443.
158. You Y, Hilpert M, Ward MJ. Detection of a common and persistent *tet(L)*-carrying plasmid in chicken-waste-impacted farm soil. *Appl. Environ. Microbiol.* **2012**, 78(9):3203–3213.
159. Cattoir V, Poirel L, Aubert C, Soussy C-J, Nordmann P. Unexpected occurrence of plasmid-mediated quinolone resistance determinants in environmental *Aeromonas* spp. *Emerg. Infect. Dis.* **2008**, 14(2):231–237.
160. Drudge CN, Elliott AVC, Plach JM, Ejim LJ, Wright GD, Droppo IG, Warren LA. Diversity of integron- and culture-associated antibiotic resistance genes in freshwater floc. *Appl. Environ. Microbiol.* **2012**, 78(12):4367–4372.

161. Hamelin K, Bruant G, El-Shaarawi A, Hill S, Edge TA, Bekal S, Fairbrother JM, Harel J, Maynard C, Masson L, Brousseau R. A virulence and antimicrobial resistance DNA microarray detects a high frequency of virulence genes in *Escherichia coli* isolates from Great Lakes recreational waters. *Appl. Environ. Microbiol.* **2006**, 72(6):4200–4206.
162. Hamelin K, Bruant G, El-Shaarawi A, Hill S, Edge TA, Fairbrother J, Harel J, Maynard C, Masson L, Brousseau R. Occurrence of virulence and antimicrobial resistance genes in *Escherichia coli* isolates from different aquatic ecosystems within the St. Clair River and Detroit River areas. *Appl. Environ. Microbiol.* **2007**, 73(2):477–484.
163. Hu J, Shi J, Chang H, Li D, Yang M, Kamagata Y. Phenotyping and genotyping of antibiotic-resistant *Escherichia coli* isolated from a natural river basin. *Environ. Sci. Technol.* **2008**, 42(9):3415–3420.
164. Ramírez Castillo FY, Avelar González FJ, Garneau P, Márquez Díaz F, Guerrero Barrera AL, Harel J. Presence of multi-drug resistant pathogenic *Escherichia coli* in the San Pedro River located in the State of Aguascalientes, Mexico. *Front. Microbiol.* **2013**, 4:Article 147.
165. Tao R, Ying G-G, Su H-C, Zhou H-W, Sidhu JPS. Detection of antibiotic resistance and tetracycline resistance genes in *Enterobacteriaceae* isolated from the Pearl rivers in South China. *Environ. Pollut.* **2010**, 158(6):2101–2109.
166. Böckelmann U, Dörries H-H, Ayuso-Gabella MN, Salgot de Marçay M, Tandoi V, Levantesi C, Masciopinto C, Van Houtte E, Szewzyk U, Wintgens T, Grohmann E. Quantitative PCR monitoring of antibiotic resistance genes and bacterial pathogens in three European artificial groundwater recharge systems. *Appl. Environ. Microbiol.* **2009**, 75(1):154–163.
167. Ling AL, Pace NR, Hernandez MT, LaPara TM. Tetracycline resistance and class 1 integron genes associated with indoor and outdoor aerosols. *Environ. Sci. Technol.* **2013**, 47(9):4046–4052.
168. Xi C, Zhang Y, Marrs CF, Ye W, Simon C, Foxman B, Nriagu J. Prevalence of antibiotic resistance in drinking water treatment and distribution systems. *Appl. Environ. Microbiol.* **2009**, 75(17):5714–5718.
169. Schwarzenbach RP, Gschwend PM, Imboden DM. *Environmental Organic Chemistry*. 2nd ed. John Wiley & Sons, Inc.; **2002**.

170. Engemann CA, Keen PL, Knapp CW, Hall KJ, Graham DW. Fate of tetracycline resistance genes in aquatic systems: migration from the water column to peripheral biofilms. *Environ. Sci. Technol.* **2008**, 42(14):5131–5136.
171. Smalla K, Heuer H, Götz A, Niemeyer D, Krögerrecklenfort E, Tietze E. Exogenous isolation of antibiotic resistance plasmids from piggery manure slurries reveals a high prevalence and diversity of IncQ-like plasmids. *Appl. Environ. Microbiol.* **2000**, 66(11):4854–4862.
172. Akiyama T, Asfahl KL, Savin MC. Broad-host-range plasmids in treated wastewater effluent and receiving streams. *J. Environ. Qual.* **2010**, 39(6):2211–2215.
173. Alcaide E, Garay E. R-plasmid transfer in *Salmonella* spp. isolated from wastewater and sewage-contaminated surface waters. *Appl. Environ. Microbiol.* **1984**, 48(2):435–438.
174. Bahl MI, Burmølle M, Meisner A, Hansen LH, Sørensen SJ. All IncP-1 plasmid subgroups, including the novel ϵ subgroup, are prevalent in the influent of a Danish wastewater treatment plant. *Plasmid* **2009**, 62(2):134–139.
175. Dröge M, Pühler A, Selbitschka W. Phenotypic and molecular characterization of conjugative antibiotic resistance plasmids isolated from bacterial communities of activated sludge. *Mol. Gen. Genet.* **2000**, 263(3):471–482.
176. Moura A, Jové T, Ploy M-C, Henriques I, Correia A. Diversity of gene cassette promoters in class 1 integrons from wastewater environments. *Appl. Environ. Microbiol.* **2012**, 78(15):5413–5416.
177. Oberlé K, Capdeville M-J, Berthe T, Budzinski H, Petit F. Evidence for a complex relationship between antibiotics and antibiotic-resistant *Escherichia coli*: from medical center patients to a receiving environment. *Environ. Sci. Technol.* **2012**, 46(3):1859–1868.
178. Tschäpe H, Tietze E, Prager R, Heier H. Occurrence in water and waste water of *E. coli* and coliform bacteria carrying R-plasmids part 3: plasmids encoding gentamicin, trimethoprim or streptothricin. *Acta Hydrochim. Hydrobiol.* **1986**, 14(2):167–174.
179. Nield BS, Holmes AJ, Gillings MR, Recchia GD, Mabbutt BC, Nevalainen KMH, Stokes HW. Recovery of new integron classes from environmental DNA. *FEMS Microbiol. Lett.* **2001**, 195(1):59–65.

180. Alexopoulos A, Voidarou C, Stefanis C, Papadopoulos I, Vavias S, Tsiotsias A, Kalkani E, Charvalos E, Bezirtzoglou E. Antibiotic resistance profiles and integrons in *Enterobacteriaceae* from the riverside of Evros-Arda with respect to chemical and waste pollution. *Microb. Ecol. Health Dis.* **2006**, 18(3-4):170–176.
181. Biyela PT, Lin J, Bezuidenhout CC. The role of aquatic ecosystems as reservoirs of antibiotic resistant bacteria and antibiotic resistance genes. *Water Sci. Technol.* **2004**, 50(1):45–50.
182. Gillings M, Boucher Y, Labbate M, Holmes A, Krishnan S, Holley M, Stokes HW. The evolution of class 1 integrons and the rise of antibiotic resistance. *J. Bacteriol.* **2008**, 190(14):5095–5100.
183. Umaman A, Garaizer J, Cisterna R. Antibiotic resistance and transferable R plasmids in coliforms from a polluted estuary. *Acta Hydrochim. Hydrobiol.* **1989**, 17(5):543–551.
184. Tchobanoglous G, Burton FL, Stensel HD. *Wastewater Engineering: Treatment and Reuse*. 4th ed. Boston, MA: McGraw-Hill; **2003**.
185. Standards for the Use or Disposal of Sewage Sludge. *Code of Federal Regulations*, Part 503, Title 40, **2007**.
186. Beecher N, Crawford K, Goldstein N, Kester G, Lono-Batura M, Dziezyk E, Peckenham J, Cheng T. *Final Report: A National Biosolids Regulation, Quality, End Use, & Disposal Survey*. North East Biosolids and Residuals Association: Tamworth, NH, **2007**.
187. Spellberg B, Blaser M, Guidos RJ, Boucher HW, Bradley JS, Eisenstein BI, Gerding D, Lynfield R, Reller LB, Rex J, Schwartz D, Septimus E, Tenover FC, Gilbert DN. Combating antimicrobial resistance: policy recommendations to save lives. *Clin. Infect. Dis.* **2011**, 52(Suppl 5):S397–S428.
188. Wierup M. The Swedish experience of the 1986 year ban of antimicrobial growth promoters, with special reference to animal health, disease prevention, productivity, and usage of antimicrobials. *Microb. Drug Resist.* **2001**, 7(2):183–190.
189. Galvin S, Boyle F, Hickey P, Vellinga A, Morris D, Cormican M. Enumeration and characterization of antimicrobial-resistant *Escherichia coli* bacteria in effluent from municipal, hospital, and secondary treatment facility sources. *Appl. Environ. Microbiol.* **2010**, 76(14):4772–4779.

190. Bönemann G, Stiens M, Pühler A, Schlüter A. Mobilizable IncQ-related plasmid carrying a new quinolone resistance gene, *qnrS2*, isolated from the bacterial community of a wastewater treatment plant. *Antimicrob. Agents Chemother.* **2006**, 50(9):3075–3080.
191. Schlüter A, Szczepanowski R, Pühler A, Top EM. Genomics of IncP-1 antibiotic resistance plasmids isolated from wastewater treatment plants provides evidence for a widely accessible drug resistance gene pool. *FEMS Microbiol. Rev.* **2007**, 31(4):449–477.
192. da Silva MF, Tiago I, Veríssimo A, Boaventura RAR, Nunes OC, Manaia CM. Antibiotic resistance of enterococci and related bacteria in an urban wastewater treatment plant. *FEMS Microbiol. Ecol.* **2006**, 55(2):322–329.
193. Clesceri LS, Greenberg AE, Eaton AD, editors. *Standard Methods for the Examination of Water and Wastewater*. 20th ed. American Public Health Association; **1999**.
194. Bernhard AE, Field KG. A PCR assay to discriminate human and ruminant feces on the basis of host differences in *Bacteroides-Prevotella* genes encoding 16S rRNA. *Appl. Environ. Microbiol.* **2000**, 66(10):4571–4574.
195. Layton A, McKay L, Williams D, Garrett V, Gentry R, Sayler G. Development of *Bacteroides* 16S rRNA gene TaqMan-based real-time PCR assays for estimation of total, human, and bovine fecal pollution in water. *Appl. Environ. Microbiol.* **2006**, 72(6):4214–4224.
196. Muyzer G, de Waal EC, Uitterlinden AG. Profiling of complex microbial populations by denaturing gradient gel electrophoresis analysis of polymerase chain reaction-amplified genes coding for 16S rRNA. *Appl. Environ. Microbiol.* **1993**, 59(3):695–700.
197. Sambrook J, Fritsch EF, Maniatis T. *Molecular Cloning: A Laboratory Manual*. 2nd ed. Coldspring Harbor, NY: Coldspring Harbor Laboratory; **1989**.
198. Stalder T, Barraud O, Casellas M, Dagot C, Ploy M-C. Integron involvement in environmental spread of antibiotic resistance. *Front. Microbiol.* **2012**, 3:Article 119.
199. Levy SB. *The Antibiotic Paradox: How the Misuse of Antibiotics Destroys Their Curative Powers*. 2nd ed. Cambridge, MA: Perseus Books Group; **2002**.
200. Chen J, Yu Z, Michel FC, Wittum T, Morrison M. Development and application of real-time PCR assays for quantification of *erm* genes conferring resistance to

- macrolides-lincosamides-streptogramin B in livestock manure and manure management systems. *Appl. Environ. Microbiol.* **2007**, 73(14):4407–4416.
201. Goldstein C, Lee MD, Sanchez S, Hudson C, Phillips B, Register B, Grady M, Liebert C, Summers AO, White DG, Maurer JJ. Incidence of class 1 and 2 integrases in clinical and commensal bacteria from livestock , companion animals, and exotics. *Antimicrob. Agents Chemother.* **2001**, 45(3):723–726.
 202. Ng L-K, Martin I, Alfa M, Mulvey M. Multiplex PCR for the detection of tetracycline resistant genes. *Mol. Cell. Probes* **2001**, 15(4):209–215.
 203. Seurinck S, Defoirdt T, Verstraete W, Siciliano SD. Detection and quantification of the human-specific HF183 *Bacteroides* 16S rRNA genetic marker with real-time PCR for assessment of human faecal pollution in freshwater. *Environ. Microbiol.* **2005**, 7(2):249–259.
 204. Burch TR, Sadowsky MJ, LaPara TM. Aerobic digestion reduces the quantity of antibiotic resistance genes in residual municipal wastewater solids. *Front. Microbiol.* **2013**, 4:Article 17.
 205. Cook RD, Weisberg S. *Applied Regression Including Computing and Graphics*. Hoboken, NJ: John Wiley & Sons; **1999**.
 206. Engemann CA, Adams L, Knapp CW, Graham DW. Disappearance of oxytetracycline resistance genes in aquatic systems. *FEMS Microbiol. Lett.* **2006**, 263(2):176–182.
 207. Rogers SW, Donnelly M, Peed L, Kelty CA, Mondal S, Zhong Z, Shanks OC. Decay of bacterial pathogens, fecal indicators, and real-time quantitative PCR genetic markers in manure-amended soils. *Appl. Environ. Microbiol.* **2011**, 77(14):4839–4848.
 208. Burch TR, Sadowsky MJ, LaPara TM. Air-drying beds reduce the quantities of antibiotic resistance genes and class 1 integrons in residual municipal wastewater solids. *Environ. Sci. Technol.* **2013**, 47(17):9965–9971.
 209. Nelson DK, LaPara TM, Novak PJ. Effects of ethanol-based fuel contamination: microbial community changes, production of regulated compounds, and methane generation. *Environ. Sci. Technol.* **2010**, 44(12):4525–4530.
 210. Guiney DG, Hasegawa P, Davis CE. Expression in *Escherichia coli* of cryptic tetracycline resistance genes from bacteroides R plasmids. *Plasmid* **1984**, 11(3):248–252.

211. Speer BS, Bedzyk L, Salyers AA. Evidence that a novel tetracycline resistance gene found on two *Bacteroides* transposons encodes an NADP-requiring oxidoreductase. *J. Bacteriol.* **1991**, 173(1):176–183.
212. Roberts MC. Update on acquired tetracycline resistance genes. *FEMS Microbiol. Lett.* **2005**, 245(2):195–203.
213. Hook SE, Northwood KS, Wright A-DG, McBride BW. Long-term monensin supplementation does not significantly affect the quantity or diversity of methanogens in the rumen of the lactating dairy cow. *Appl. Environ. Microbiol.* **2009**, 75(2):374–380.
214. Crittenden JC, Trussell RR, Hand DW, Howe KJ, Tchobanoglous G. *Water Treatment: Principles and Design*. 2nd ed. Hoboken, NJ: John Wiley & Sons, Inc.; **2005**.
215. Selleck RE, Collins HF, Saunier BM. Kinetics of bacterial deactivation with chlorine. *J. Environ. Eng. Div. ASCE.* **1978**, 104(6):1197–1212.
216. Reddy KR, Khaleel R, Overcash MR. Behavior and transport of microbial pathogens and indicator organisms in soils treated with organic wastes. *J. Environ. Qual.* **1981**, 10(3):255–266.
217. Baertsch C, Paez-Rubio T, Viau E, Peccia J. Source tracking aerosols released from land-applied class B biosolids during high-wind events. *Appl. Environ. Microbiol.* **2007**, 73(14):4522–4531.
218. Low SY, Paez-Rubio T, Baertsch C, Kucharski M, Peccia J. Off-site exposure to respirable aerosols produced during the disk-incorporation of class B biosolids. *J. Environ. Eng.* **2007**, 133(10):987–994.
219. Sánchez de la Campa A, García-Salamanca A, Solano J, de la Rosa J, Ramos J-L. Chemical and microbiological characterization of atmospheric particulate matter during an intense African dust event in southern Spain. *Environ. Sci. Technol.* **2013**, 47(8):3630–3638.
220. Smith DJ, Griffin DW, Schuerger AC. Stratospheric microbiology at 20 km over the Pacific Ocean. *Aerobiologia.* **2010**, 26(1):35–46.
221. Smith DJ, Timonen HJ, Jaffe DA, Griffin DW, Birmele MN, Perry KD, Ward PD, Roberts MS. Intercontinental dispersal of bacteria and archaea by transpacific winds. *Appl. Environ. Microbiol.* **2013**, 79(4):1134–1139.

222. Fricke WF, Welch TJ, McDermott PF, Mammel MK, LeClerc JE, White DG, Cebula TA, Ravel J. Comparative genomics of the IncA/C multidrug resistance plasmid family. *J. Bacteriol.* **2009**, 191(15):4750–4757.
223. Torsvik V, Øvreås L, Thingstad TF. Prokaryotic diversity--magnitude, dynamics, and controlling factors. *Science* **2002**, 296(5570):1064–1066.
224. Viau E, Bibby K, Paez-Rubio T, Peccia J. Toward a consensus view on the infectious risks associated with land application of sewage sludge. *Environ. Sci. Technol.* **2011**, 45(13):5459–5469.

Appendix A: Supporting Information for Chapter 3

Table A.1. Gene targets, resistance mechanisms, primer sequences, amplicon sizes, and annealing temperatures for real-time PCR assays.

Gene Target	Resistance Mechanism	Primer Sequence (5'→3')	Size (bp)	Annealing Temp (°C)	Reference
16S rRNA gene	NA	F: CCT ACG GGA GGC AGC AG	202	60	(196)
		R: ATT ACC GCG GCT GCT GG			
<i>All Bacteroides</i> spp.	NA	F: GAG AGG AAG GTC CCC CAC	116	60	(195)
		R: CGC TAC TTG GCT GGT			

		TCA G			
		F: ATC ATG AGT TCA CAT			
Human-specific		GTC CG			
<i>Bacteroides</i> spp.	NA		82	56	(194,203)
		R: TAC CCC GCC TAC TAT			
		CTA ATG			
		F: GAT ACC GTT TAC GAA			
<i>erm</i> (B)	Ribosomal	ATT GG			
	protection		364	58	(200)
		R: GAA TCG AGA CTT GAG			
		TGT GC			
		F: CCT CCC GCA CGA TGA TC			
<i>intII</i>	Class 1 integron		280	60	(201)
		R: TCC ACG CAT CGT CAG			
		GC			

		F: CCG TTG GCC TTC CTG TAA AG			
<i>sulI</i>	Target modification	R: TTG CCG ATC GCG TGA AGT	67	60	(151)
		F: GCT ACA TCC TGC TTG CCT TC			
<i>tet(A)</i>	Efflux	R: CAT AGA TCG CCG TGA AGA GG	210	60	(202)
		F: GAG AGC CTG CTA TAT GCC AGC			
<i>tet(W)</i>	Ribosomal protection	R: GGG CGT ATC CAC AAT GTT AAC	168	60	(95)

		F: AGC CTT ACC AAT GGG			
	Enzymatic	TGT AAA			
<i>tet</i> (X)	modification	R: TTC TTA CCT TGG ACA	278	60	(24)
		TCC CG			

Table A.2. Values of P for comparing the relative statistical significance of different kinetic coefficients determined using Welch's t-test for unequal n and unequal sample variance.

Gene	All		Human-specific						
	16S rRNA gene		<i>erm</i> (B)	<i>intI1</i>	<i>sulI</i>	<i>tet</i> (A)	<i>tet</i> (W)	<i>tet</i> (X)	
		<i>Bacteroides</i> spp.	<i>Bacteroides</i> spp.						
16S rRNA gene	1	3×10^{-5}	0.6	0.02	0.3	0.06	0.03	7×10^{-4}	0.8
All									
<i>Bacteroides</i> spp.		1	2×10^{-4}	1×10^{-4}	2×10^{-5}	5×10^{-5}	6×10^{-5}	6×10^{-4}	3×10^{-5}
Human-specific									
<i>Bacteroides</i> spp.			1	0.4	0.4	1	0.9	0.1	0.6
<i>erm</i> (B)									
				1	9×10^{-3}	0.1	0.2	0.1	0.02

<i>intI1</i>						1	0.01	5×10^{-3}	2×10^{-4}	0.3
<i>sulI</i>							1	0.6	4×10^{-3}	0.02
<i>tet(A)</i>								1	6×10^{-3}	0.01
<i>tet(W)</i>									1	6×10^{-4}
<i>tet(X)</i>										1

Appendix B: Supporting Information for Chapter 4

Table B.1. The primer sequences, expected amplicon size, and annealing temperature for each gene target considered in this work.

Gene Target	Primer Sequence (5'→3')	Size (bp)	Annealing Temp (°C)	Reference
16S rRNA gene (338F, 518R)	F: CCT ACG GGA GGC AGC AG R: ATT ACC GCG GCT GCT GG	202	60	(196)
all <i>Bacteroides</i> spp. 16S rRNA gene (AllBac)	F: GAG AGG AAG GTC CCC CAC R: CGC TAC TTG GCT GGT TCA G	116	60	(195)
human-specific <i>Bacteroides</i> spp. 16S rRNA gene (HF183)	F: ATC ATG AGT TCA CAT GTC CG R: TAC CCC GCC TAC TAT CTA ATG	82	56	(194,203)

<i>erm(B)</i>	F: GAT ACC GTT TAC GAA ATT GG	364	58	(200)
	R: GAA TCG AGA CTT GAG TGT GC			
<i>intI1</i>	F: CCT CCC GCA CGA TGA TC	280	60	(201)
	R: TCC ACG CAT CGT CAG GC			
<i>sul1</i>	F: CCG TTG GCC TTC CTG TAA AG	67	60	(151)
	R: TTG CCG ATC GCG TGA AGT			
<i>tet(A)</i>	F: GCT ACA TCC TGC TTG CCT TC	210	60	(202)
	R: CAT AGA TCG CCG TGA AGA GG			
<i>tet(W)</i>	F: GAG AGC CTG CTA TAT GCC AGC	168	60	(95)
	R: GGG CGT ATC CAC AAT GTT AAC			

<i>tet</i> (X)	F: AGC CTT ACC AAT GGG TGT AAA	278	60	(24)
	R: TTC TTA CCT TGG ACA TCC CG			

Appendix C: Supporting Information for Chapter 5

Table C.1. The primer sequences, expected amplicon size, and annealing temperature for each real-time PCR method used in this work.

Gene Target	Primer Sequence (5'→3')	Size (bp)	Ann. Temp. (°C)	Reference
16S rRNA gene (338F, 518R)	F: CCT ACG GGA GGC AGC AG R: ATT ACC GCG GCT GCT GG	202	60	(196)
AllBac	F: GAG AGG AAG GTC CCC CAC R: CGC TAC TTG GCT GGT TCA G	116	60	(195)
16S rRNA gene of methanogens (Met630F, Met803R)	F: GGA TTA GAT ACC CSG GTA GT R: GTT GAR TCC AAT TAA ACC GCA	82	56	(213)

<i>intII</i>	F: CCT CCC GCA CGA TGA TC	280	60	(201)
	R: TCC ACG CAT CGT CAG GC			
<i>qnrA</i>	F: AGG ATT TCT CAC GCC AGG ATT	124	57	(8)
	R: CCG CTT TCA ATG AAA CTG CA			
<i>repA</i>	F: TTC ATC AGC TCC AGC TTC TT	126	60	This Study
	R: CAG ATT CAT GAT CGA TTC GTT T			
<i>tet(W)</i>	F: GAG AGC CTG CTA TAT GCC AGC	168	60	(95)
	R: GGG CGT ATC CAC AAT GTT AAC			
<i>tet(X)</i>	F: AGC CTT ACC AAT GGG TGT AAA	278	60	(24)
	R: TTC TTA CCT TGG ACA TCC CG			

Table C.2. The number of standards (n), slope, intercept, amplification efficiency determined from a dilution series of standards, r^2 , and quantification limit (QL, copies μL^{-1} template) for each real-time PCR assay conducted to generate the data presented in this work.

Assay Name	n	Slope	Intercept	Amp. Eff.	r^2	QL
qPCR An Dig Plate 1 (37C) 16S 091613	6	-3.21	36.72	105%	0.992	64,000
qPCR An Dig Plate 1 (37C) AllBac 091713	8	-3.10	39.97	110%	0.993	520
qPCR An Dig Plate 1 (37C) incAC 091613	8	-3.80	44.76	83%	0.988	630
qPCR An Dig Plate 1 (37C) intI1 091613	7	-3.79	43.14	83%	0.999	2,300
qPCR An Dig Plate 1 (37C) Methanogens 091813	9	-3.26	39.53	103%	0.993	230
qPCR An Dig Plate 1 (37C) qnrA 091813	9	-3.48	39.88	94%	0.993	89
qPCR An Dig Plate 1 (37C) tetW 091813	9	-3.33	40.37	100%	0.999	170

qPCR An Dig Plate 1 (37C) tetX 091613	9	-3.86	42.50	81%	0.995	71
qPCR An Dig Plate 2 (55C) 16S 092413	7	-3.22	37.50	104%	0.991	6,400
qPCR An Dig Plate 2 (55C) AllBac 092413	8	-3.00	39.10	115%	0.993	520
qPCR An Dig Plate 2 (55C) incAC 092313	9	-3.74	42.65	85%	0.995	63
qPCR An Dig Plate 2 (55C) intI1 092313	9	-3.51	40.70	93%	0.996	230
qPCR An Dig Plate 2 (55C) Methanogens 091913	10	-3.14	38.08	108%	0.999	23
qPCR An Dig Plate 2 (55C) qnrA 092313	10	-3.41	38.18	96%	0.993	8.9
qPCR An Dig Plate 2 (55C) tetW 092313.Drift Corrected	10	-3.05	39.54	113%	0.997	17
qPCR An Dig Plate 2 (55C) tetX 091913	9	-3.78	41.55	84%	0.996	71
qPCR An Dig Plate 3 (60C) 16S 092613	7	-3.15	36.36	108%	0.989	6,400

qPCR An Dig Plate 3 (60C) AllBac 092713	9	-3.00	39.24	116%	0.992	52
qPCR An Dig Plate 3 (60C) incAC 093013	9	-3.70	41.41	86%	0.998	63
qPCR An Dig Plate 3 (60C) intI1 093013	8	-3.47	40.70	94%	0.999	2,300
qPCR An Dig Plate 3 (60C) Methanogens 092713	10	-3.02	37.42	114%	0.992	23
qPCR An Dig Plate 3 (60C) qnrA 093013	10	-3.39	38.33	97%	0.994	8.9
qPCR An Dig Plate 3 (60C) tetW 092713.Drift Corrected	10	-3.06	39.29	112%	0.996	17
qPCR An Dig Plate 3 (60C) tetX 092613	10	-3.38	39.03	98%	0.991	7.1
qPCR An Dig Plate 4 (65C) 16S 091113	6	-3.32	38.31	100%	0.985	64,000
qPCR An Dig Plate 4 (65C) AllBac 091313	8	-3.11	39.93	110%	0.997	520
qPCR An Dig Plate 4 (65C) incAC 091213	8	-3.54	41.04	92%	0.991	630

qPCR An Dig Plate 4 (65C) intI1 091313	8	-3.60	41.49	89%	0.989	2,300
qPCR An Dig Plate 4 (65C) Methanogens 091713	10	-3.12	38.12	109%	0.998	23
qPCR An Dig Plate 4 (65C) qnrA 091113	9	-3.45	39.96	95%	0.995	89
qPCR An Dig Plate 4 (65C) tetW 091113.Drift Corrected	8	-3.10	37.89	110%	0.998	1,700
qPCR An Dig Plate 4 (65C) tetX 091113	9	-3.63	40.76	88%	0.996	71

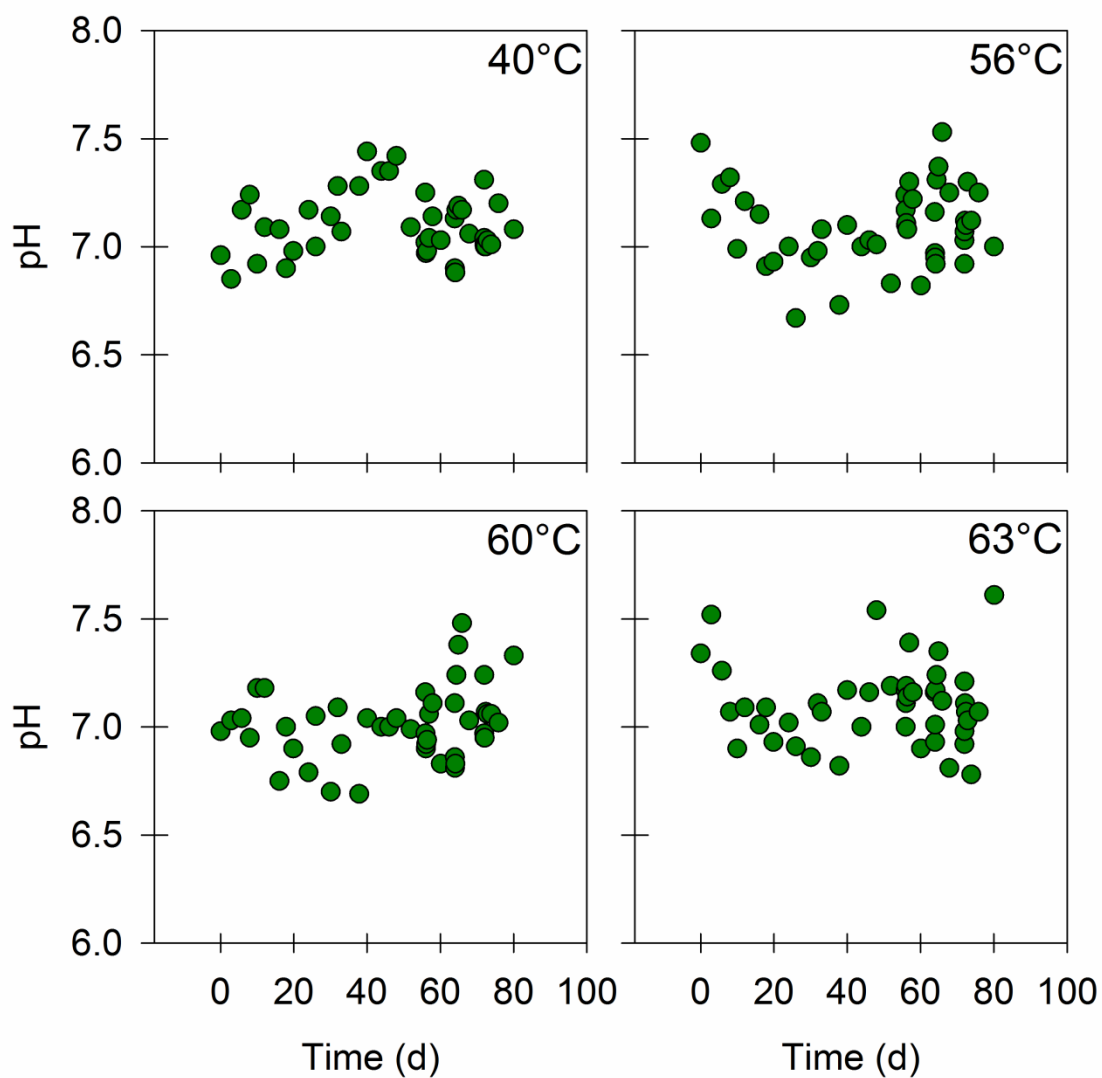


Figure C.1. The pH of anaerobic digesters operated at nominal temperatures of 40°C, 56°C, 60°C, and 63°C.

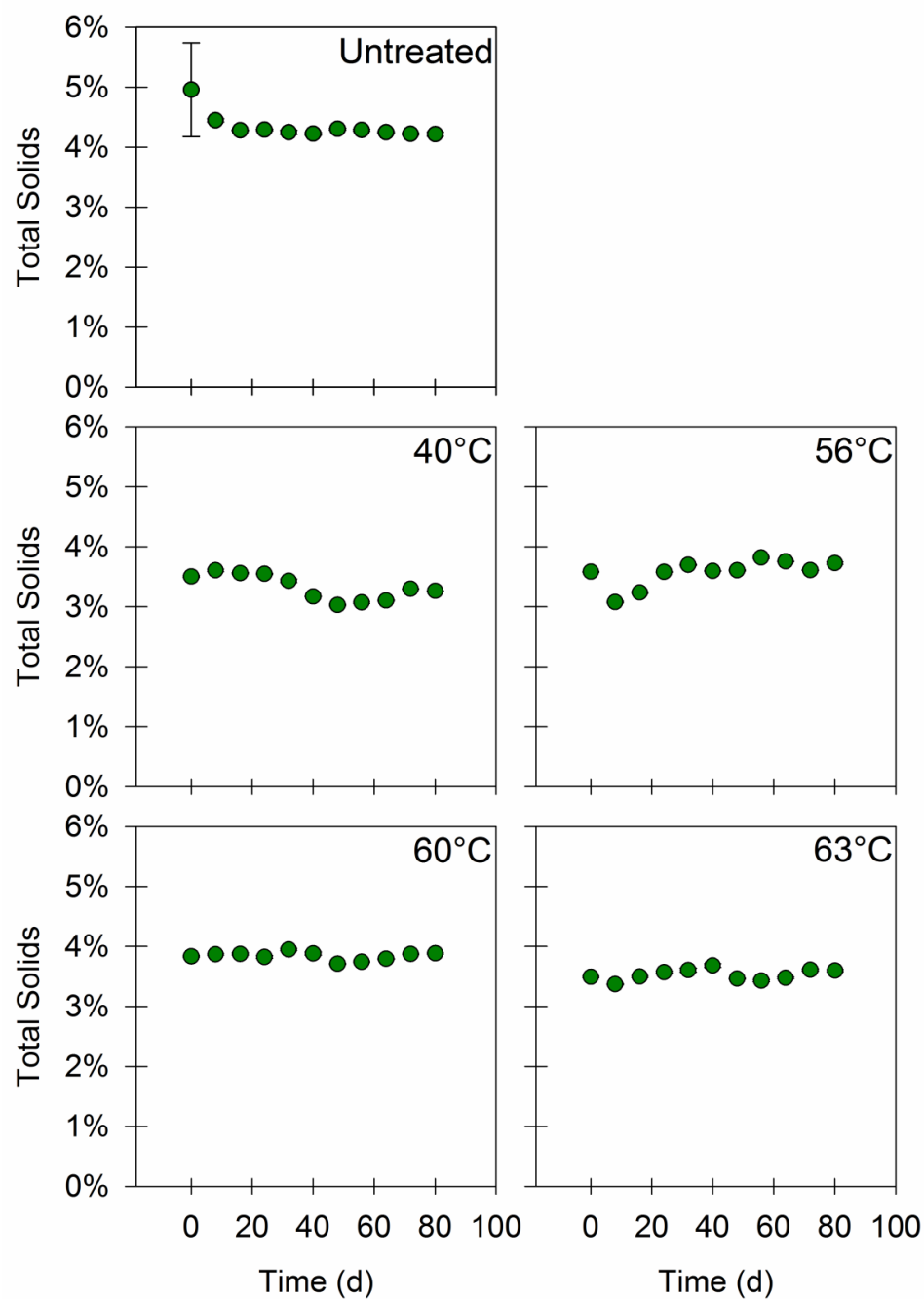


Figure C.2. The total solids content of untreated residual municipal wastewater solids and four anaerobic digesters operated at nominal temperatures of 40°C, 56°C, 60°C, and 63°C. Values are the arithmetic mean of triplicate samples; error bars represent one standard deviation.

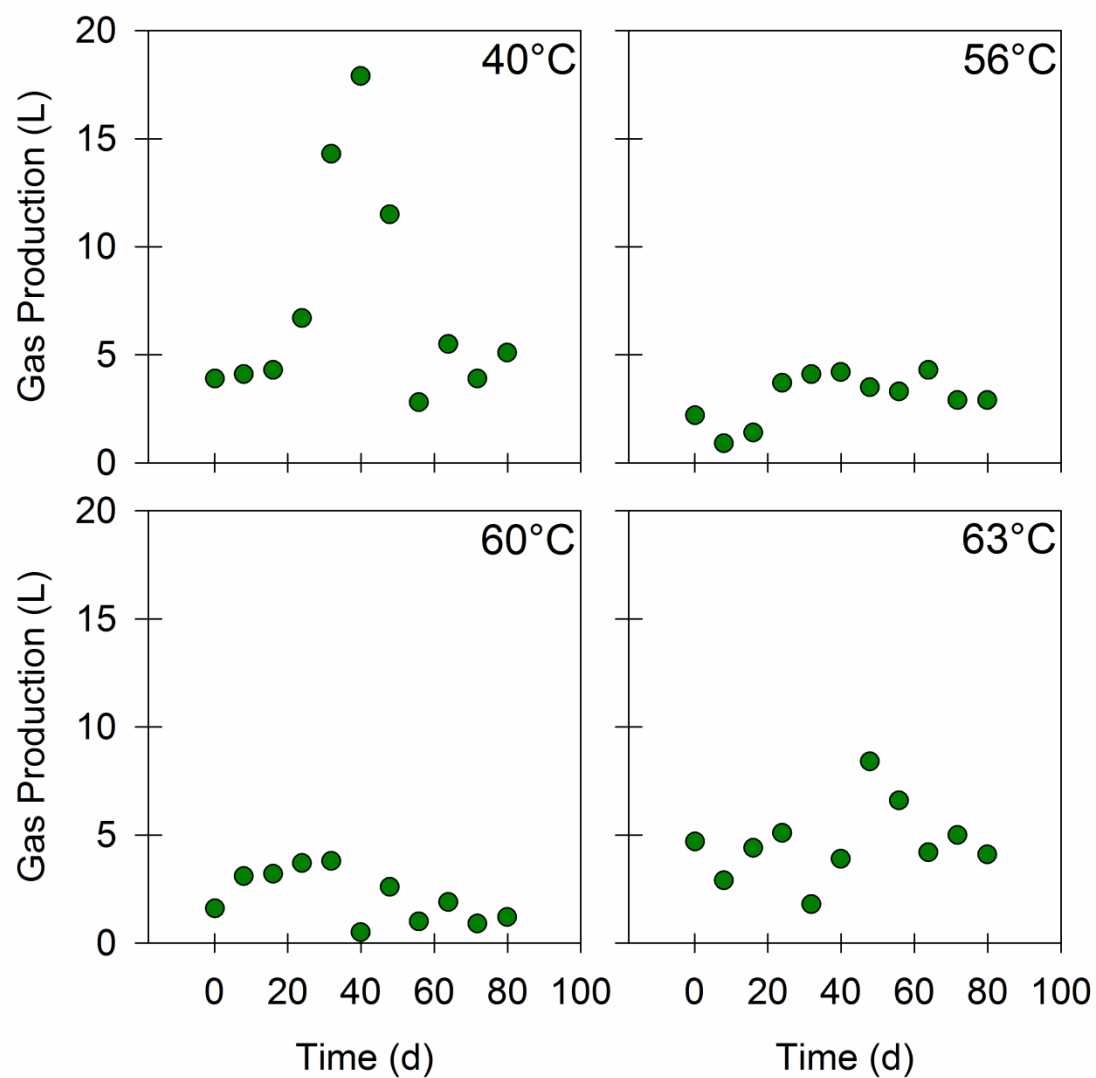


Figure C.3. The volume of gas produced during eight-day batch cycles by anaerobic digesters operated at nominal temperatures of 40°C, 56°C, 60°C, and 63°C.

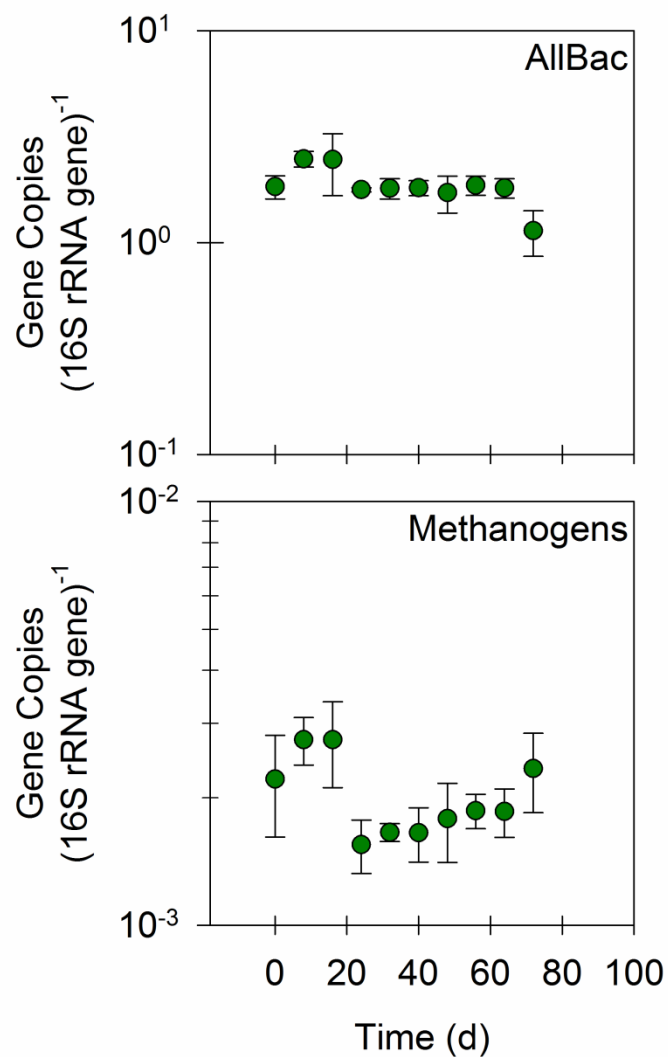


Figure C.4. The ratios of AllBac and methanogen 16S rRNA genes to 16S rRNA genes in untreated residual municipal wastewater solids. Values are the arithmetic mean of triplicate samples; error bars represent one standard deviation.

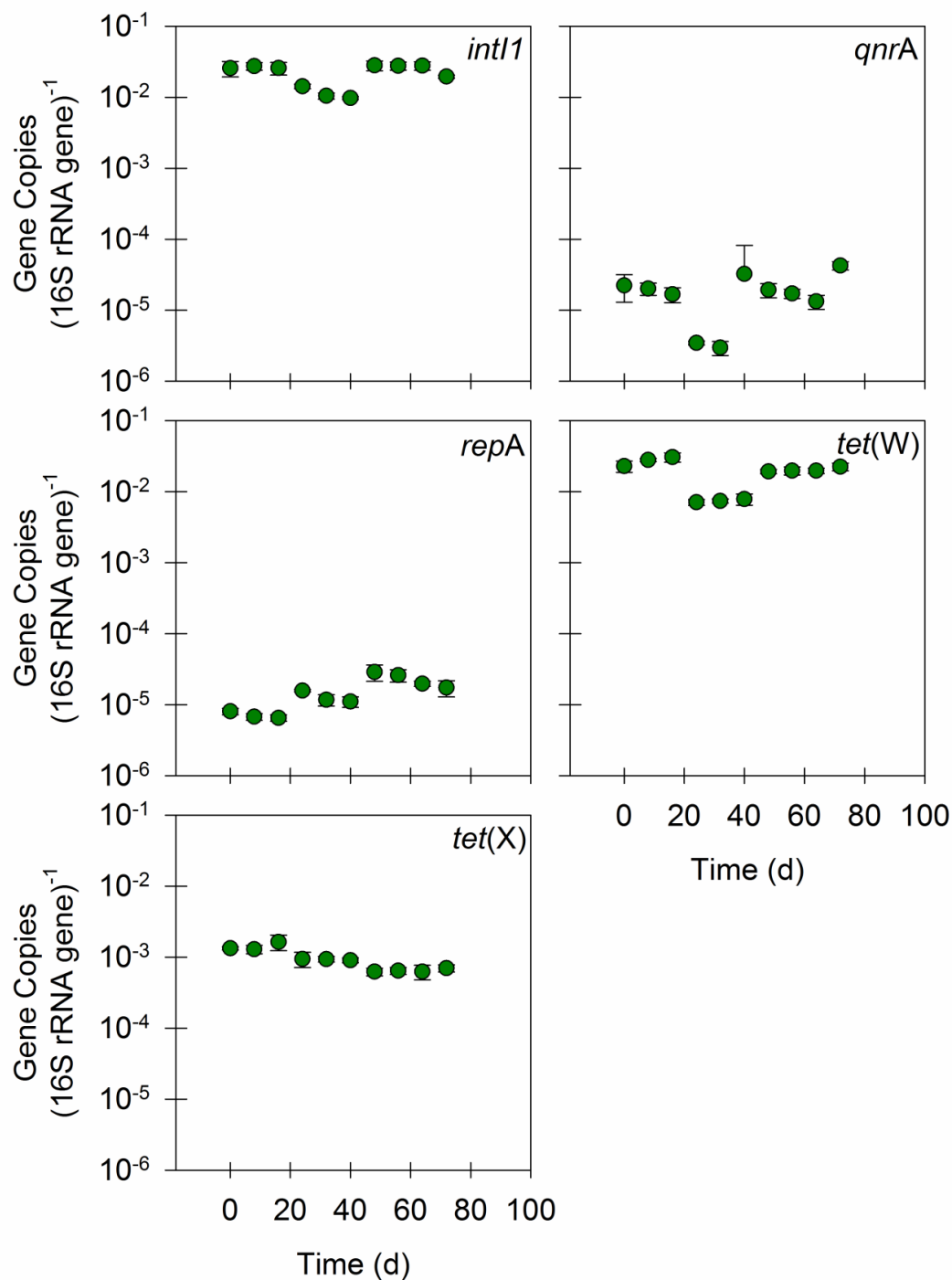


Figure C.5. The ratios of ARGs, *intI1*, and *repA* to 16S rRNA genes in untreated residual municipal wastewater solids. Values are the arithmetic mean of duplicate or triplicate samples; error bars represent one standard deviation.

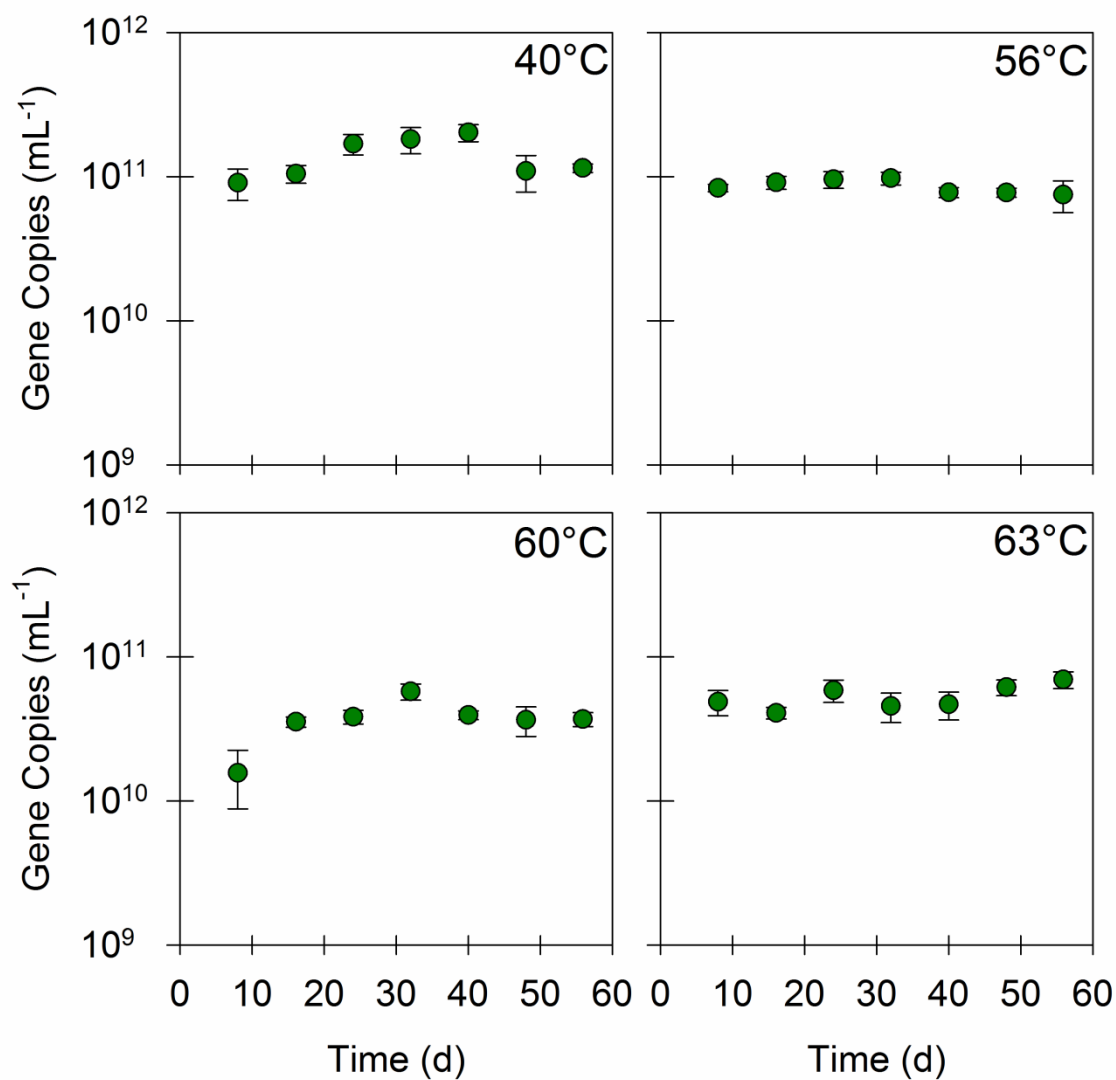


Figure C.6. Quantities of 16S rRNA genes at the end of each of the first seven batches in anaerobic digesters operated at nominal temperatures of 40°C, 56°C, 60°C, and 63°C. Values are the arithmetic mean of triplicate samples; error bars represent one standard deviation.

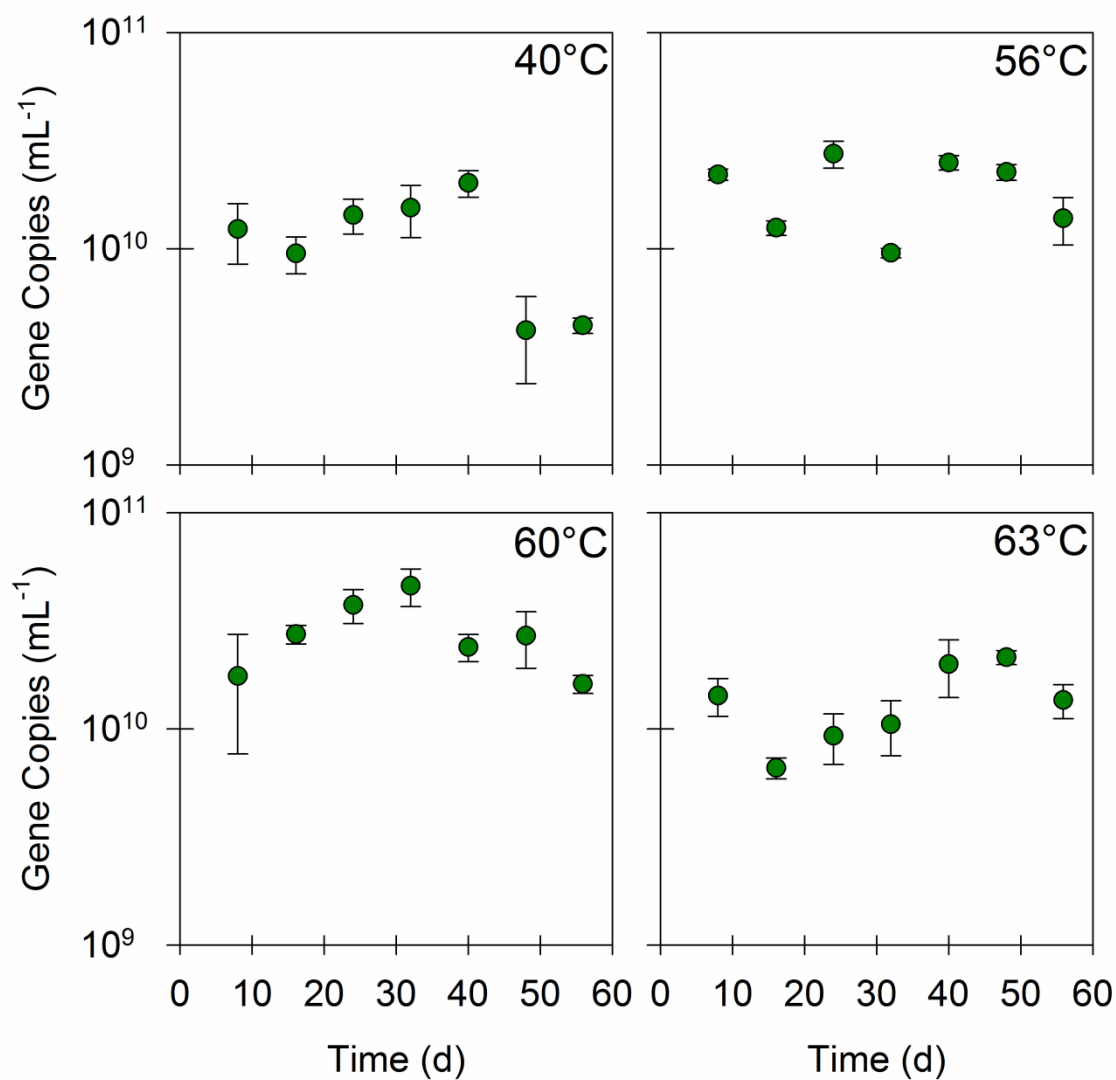


Figure C.7. Quantities of AllBac at the end of each of the first seven batches in anaerobic digesters operated at nominal temperatures of 40°C, 56°C, 60°C, and 63°C. Values are the arithmetic mean of triplicate samples; error bars represent one standard deviation.

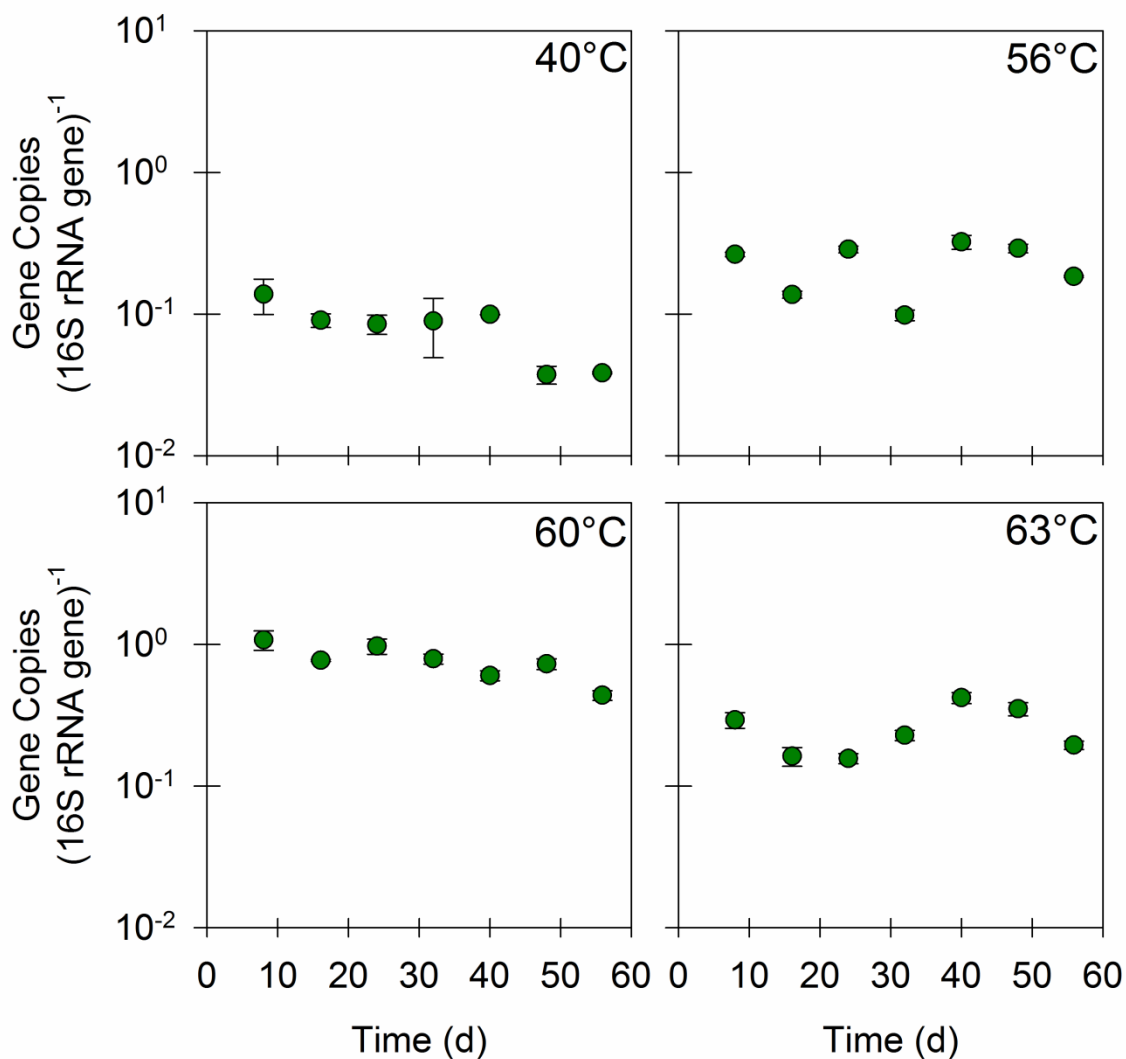


Figure C.8. The ratios of AllBac to 16S rRNA genes at the end of each of the first seven batches in anaerobic digesters operated at nominal temperatures of 40°C, 56°C, 60°C, and 63°C. Values are the arithmetic mean of triplicate samples; error bars represent one standard deviation.

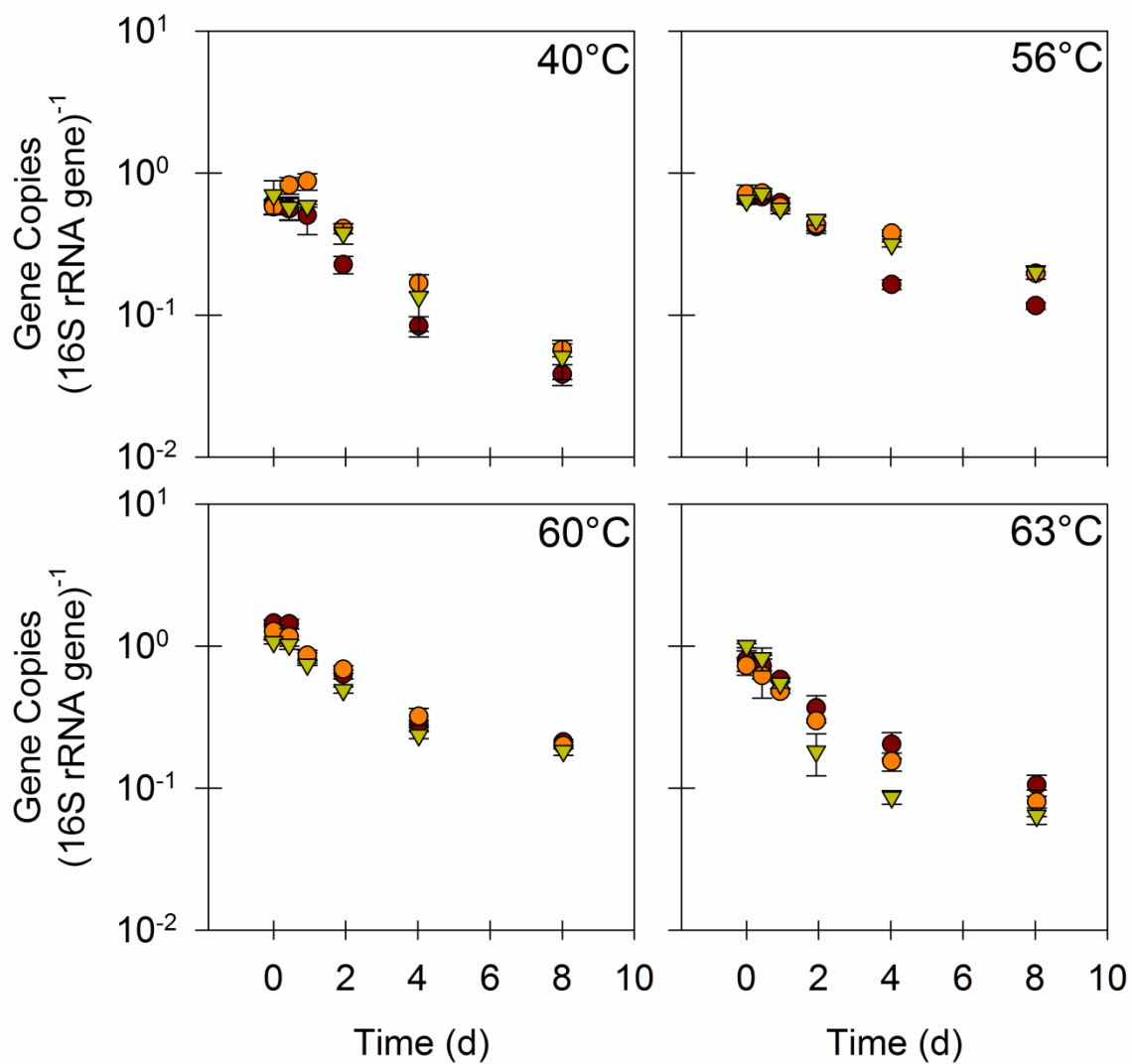


Figure C.9. The ratios of AllBac to 16S rRNA genes during the final three batches (green, orange, and red symbols represent unique batches) in anaerobic digesters operated at nominal temperatures of 40°C, 56°C, 60°C, and 63°C. Values are the arithmetic mean of triplicate samples; error bars represent one standard deviation.

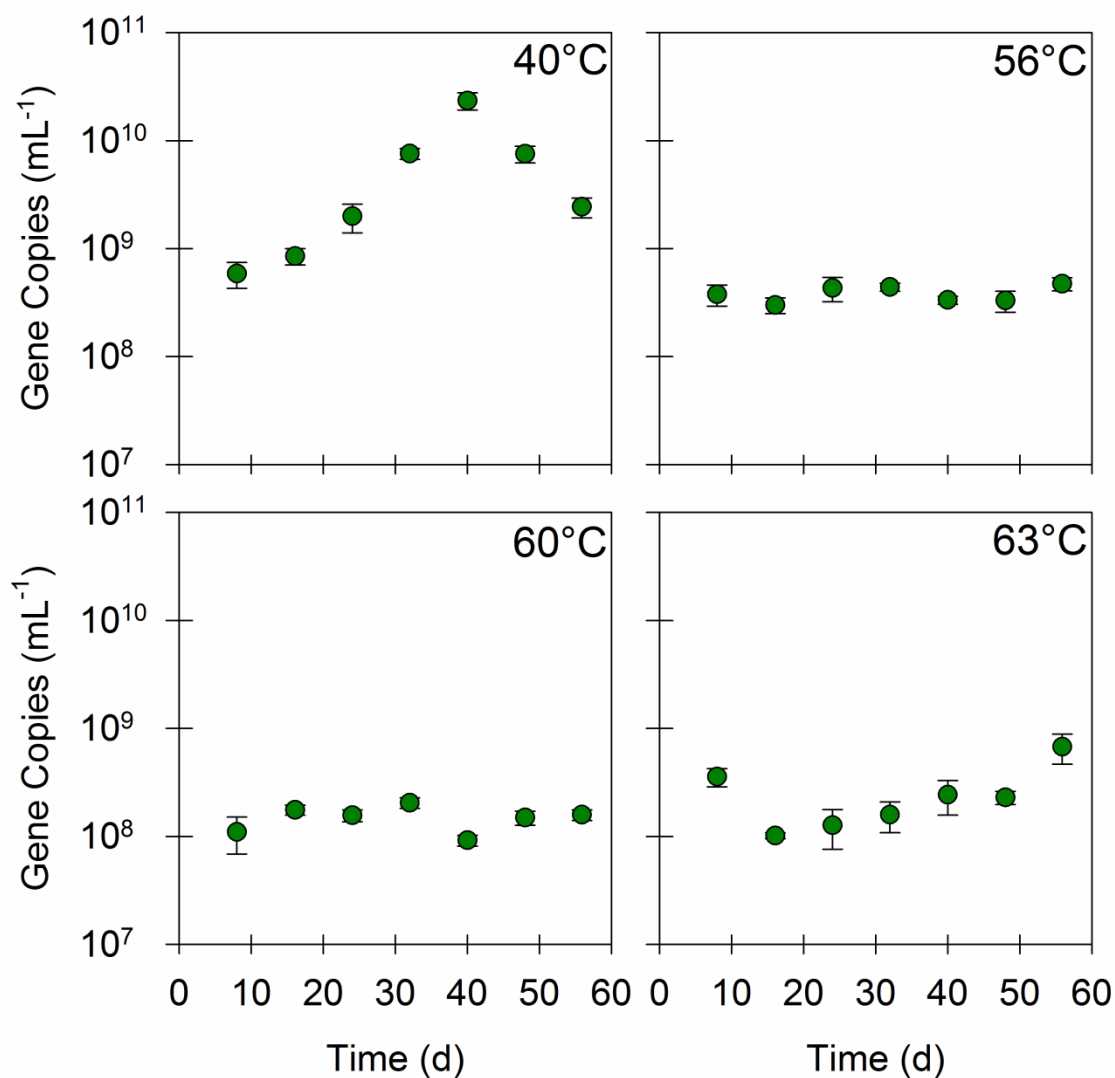


Figure C.10. Quantities of methanogen 16S rRNA genes at the end of each of the first seven batches in anaerobic digesters operated at nominal temperatures of 40°C, 56°C, 60°C, and 63°C. Values are the arithmetic mean of triplicate samples; error bars represent one standard deviation.

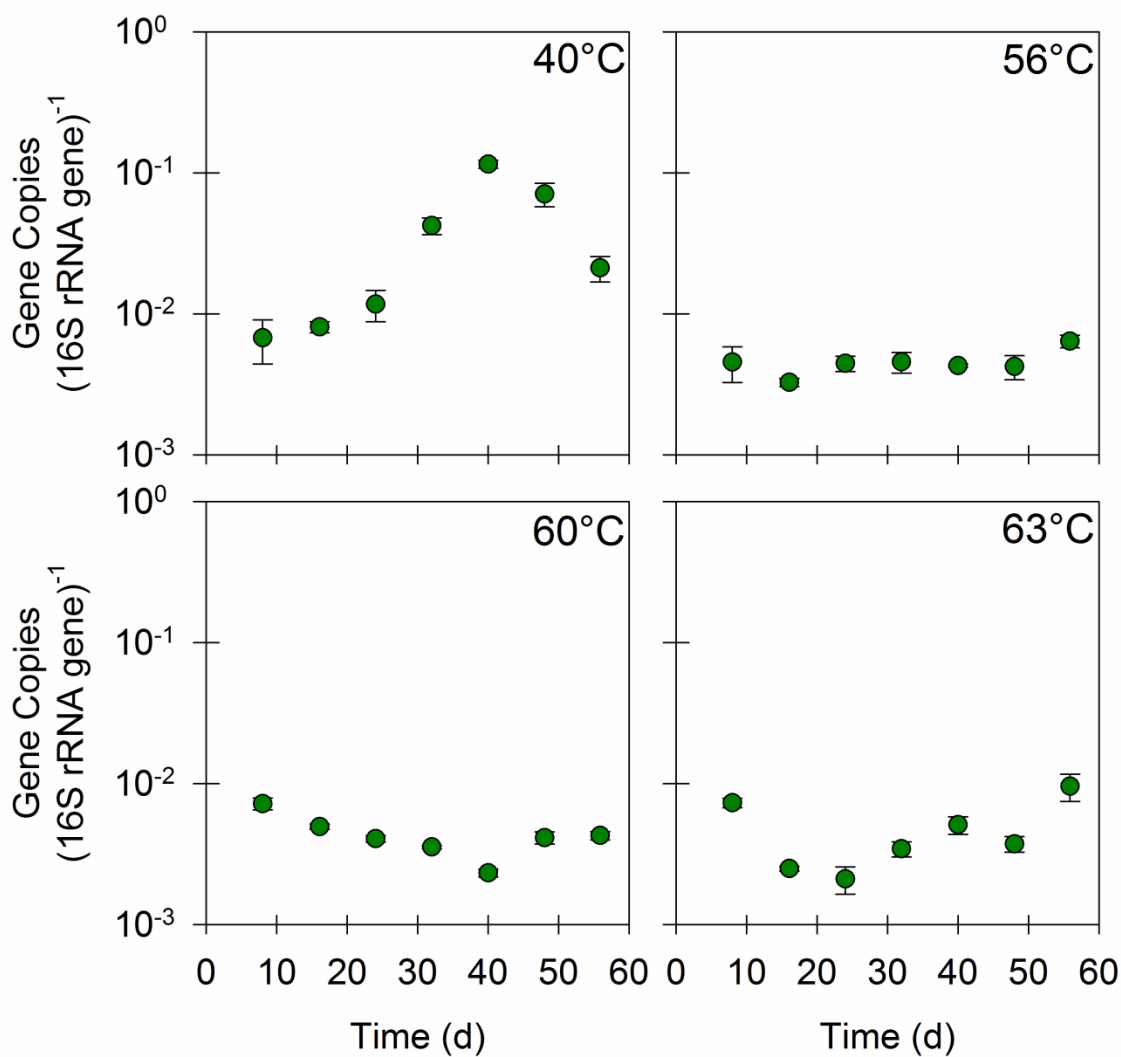


Figure C.11. The ratios of methanogen 16S rRNA genes to 16S rRNA genes at the end of each of the first seven batches in anaerobic digesters operated at nominal temperatures of 40°C, 56°C, 60°C, and 63°C. Values are the arithmetic mean of triplicate samples; error bars represent one standard deviation.

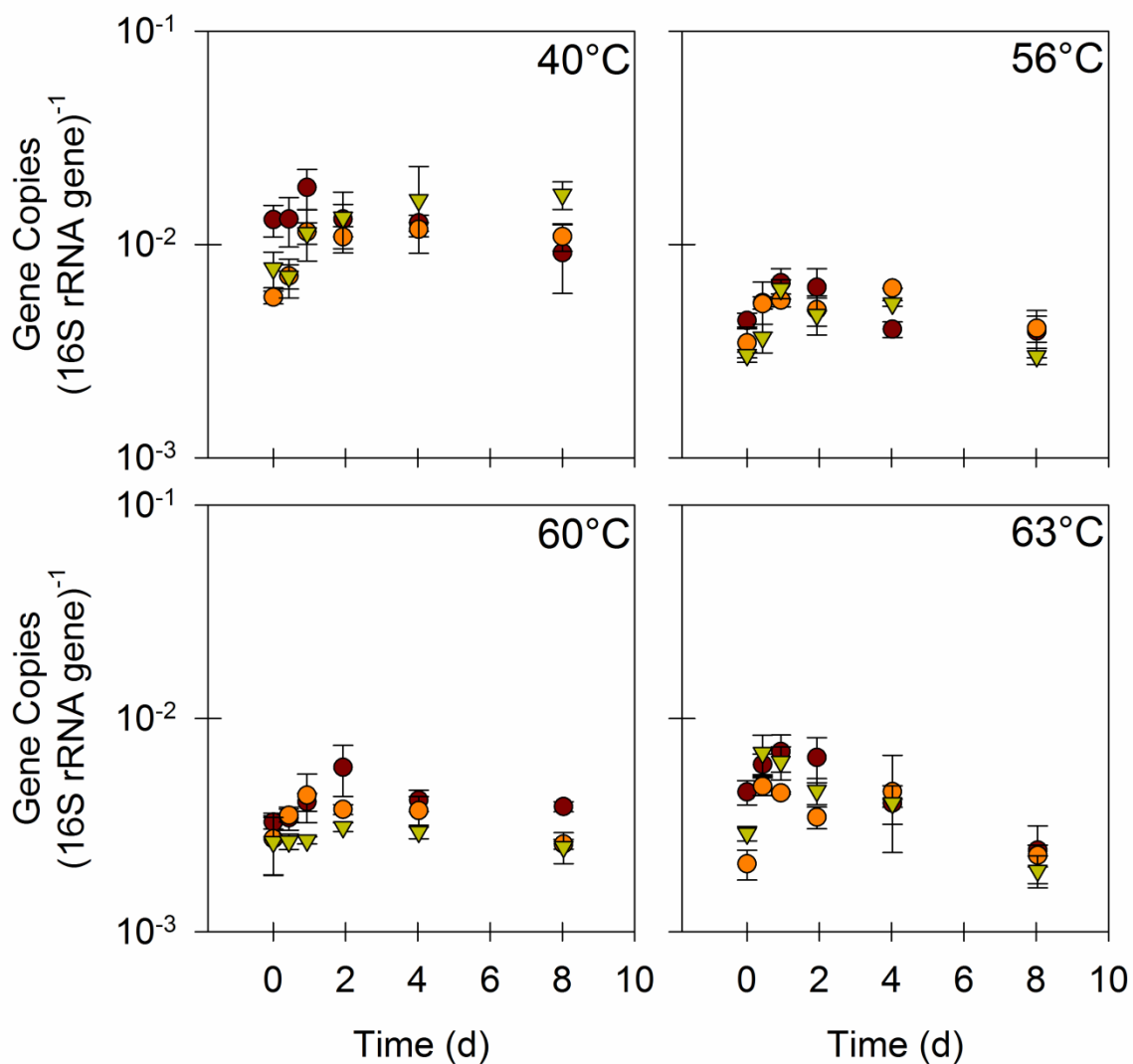


Figure C.12. The ratios of methanogen 16S rRNA genes to 16S rRNA genes during the final three batches (green, orange, and red symbols represent unique batches) in anaerobic digesters operated at nominal temperatures of 40°C, 56°C, 60°C, and 63°C. Values are the arithmetic mean of triplicate samples; error bars represent one standard deviation.

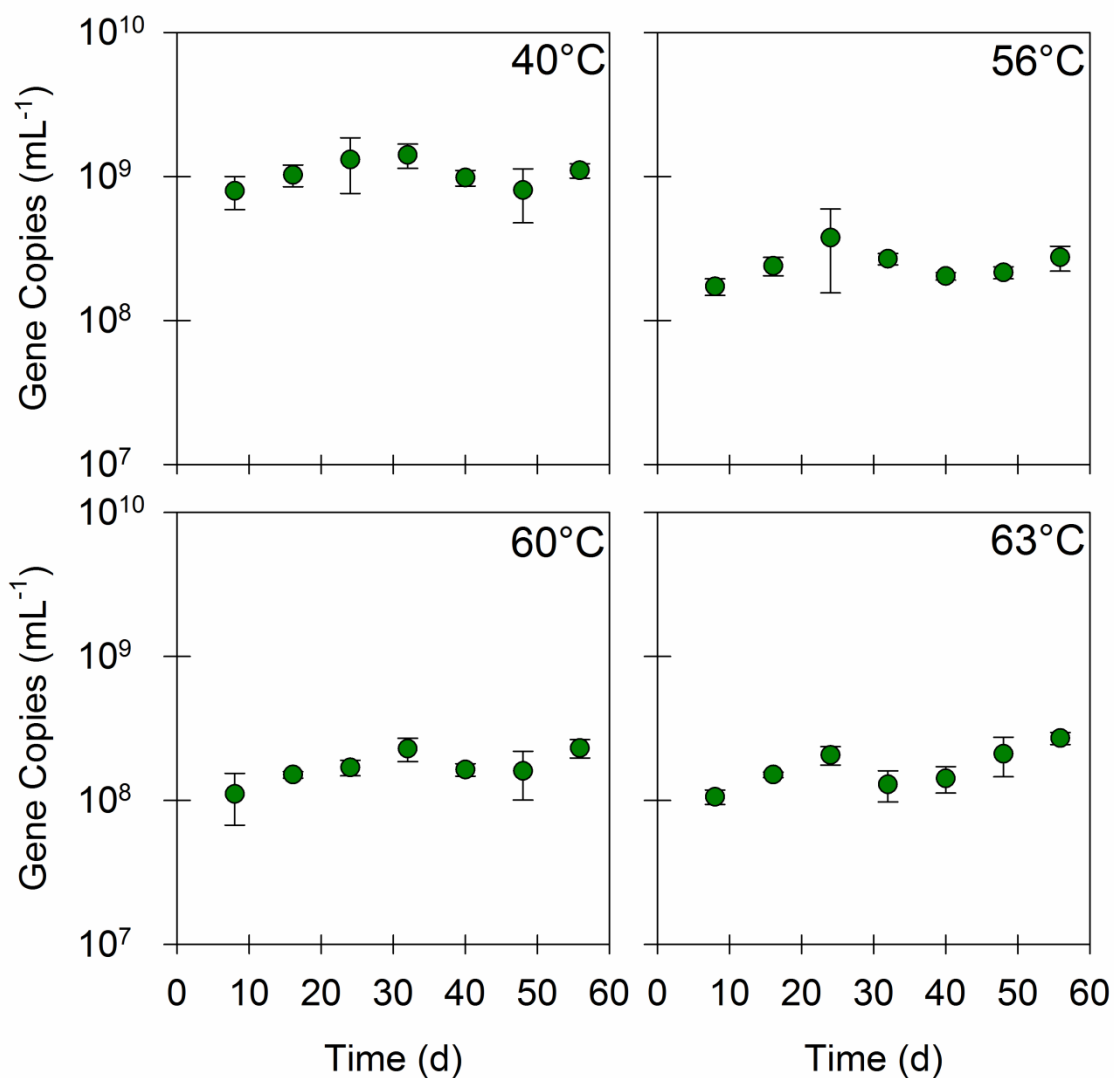


Figure C.13. Quantities of *int11* at the end of each of the first seven batches in anaerobic digesters operated at nominal temperatures of 40°C, 56°C, 60°C, and 63°C. Values are the arithmetic mean of triplicate samples; error bars represent one standard deviation.

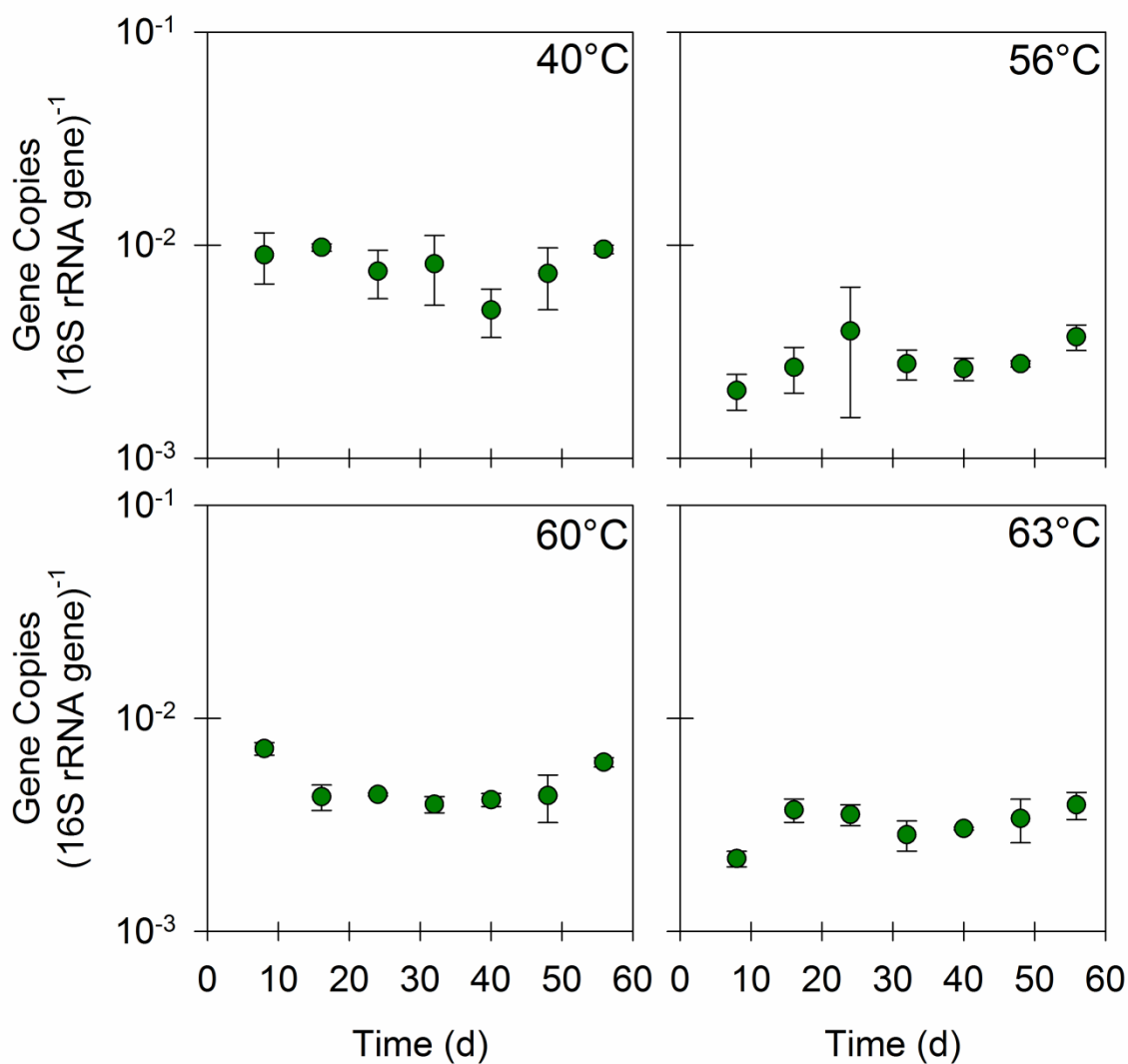


Figure C.14. The ratios of *intII* to 16S rRNA genes at the end of each of the first seven batches in anaerobic digesters operated at nominal temperatures of 40°C, 56°C, 60°C, and 63°C. Values are the arithmetic mean of triplicate samples; error bars represent one standard deviation.

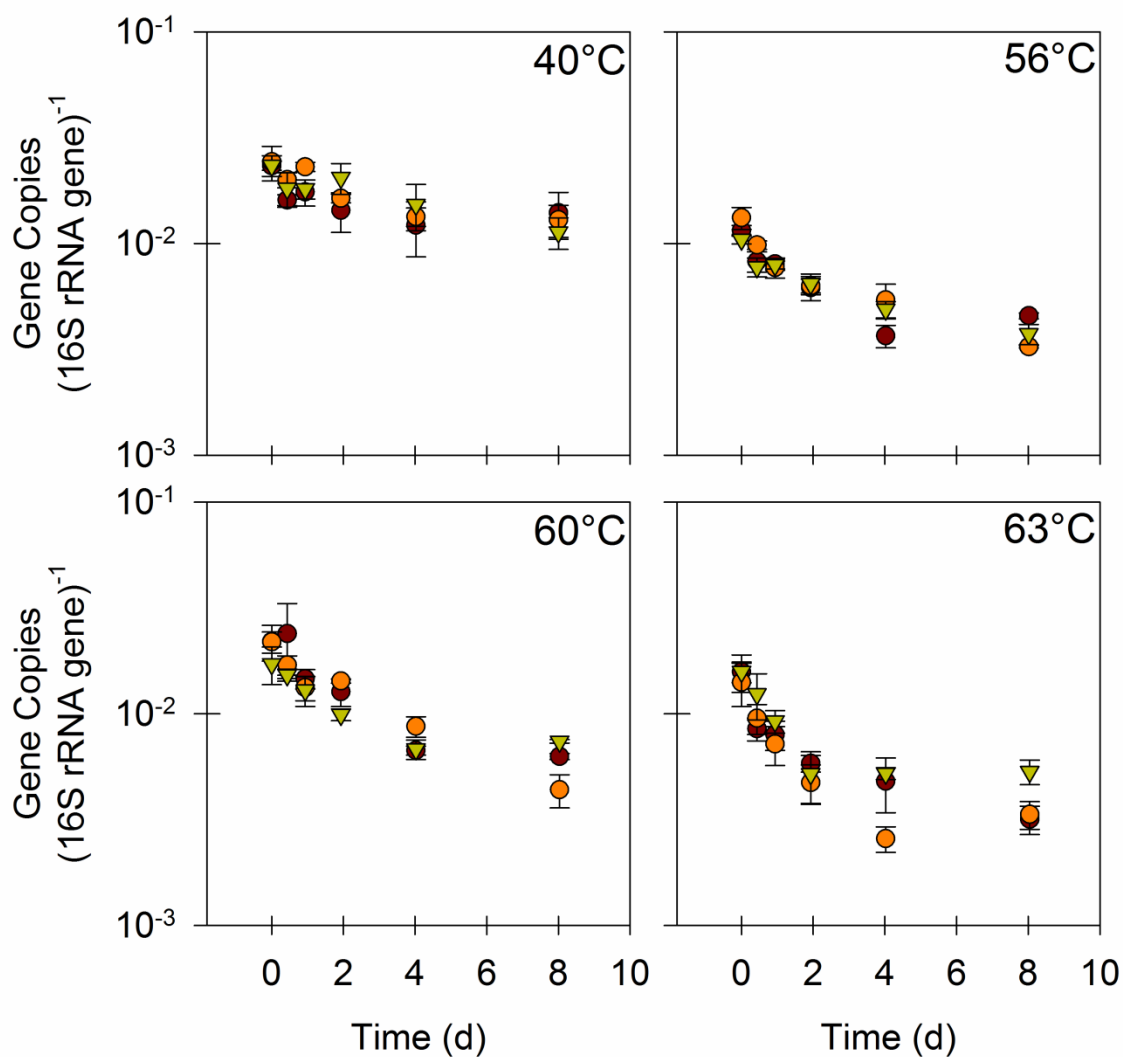


Figure C.15. The ratios of *int11* to 16S rRNA genes during the final three batches (green, orange, and red symbols represent unique batches) in anaerobic digesters operated at nominal temperatures of 40°C, 56°C, 60°C, and 63°C. Values are the arithmetic mean of triplicate samples; error bars represent one standard deviation.

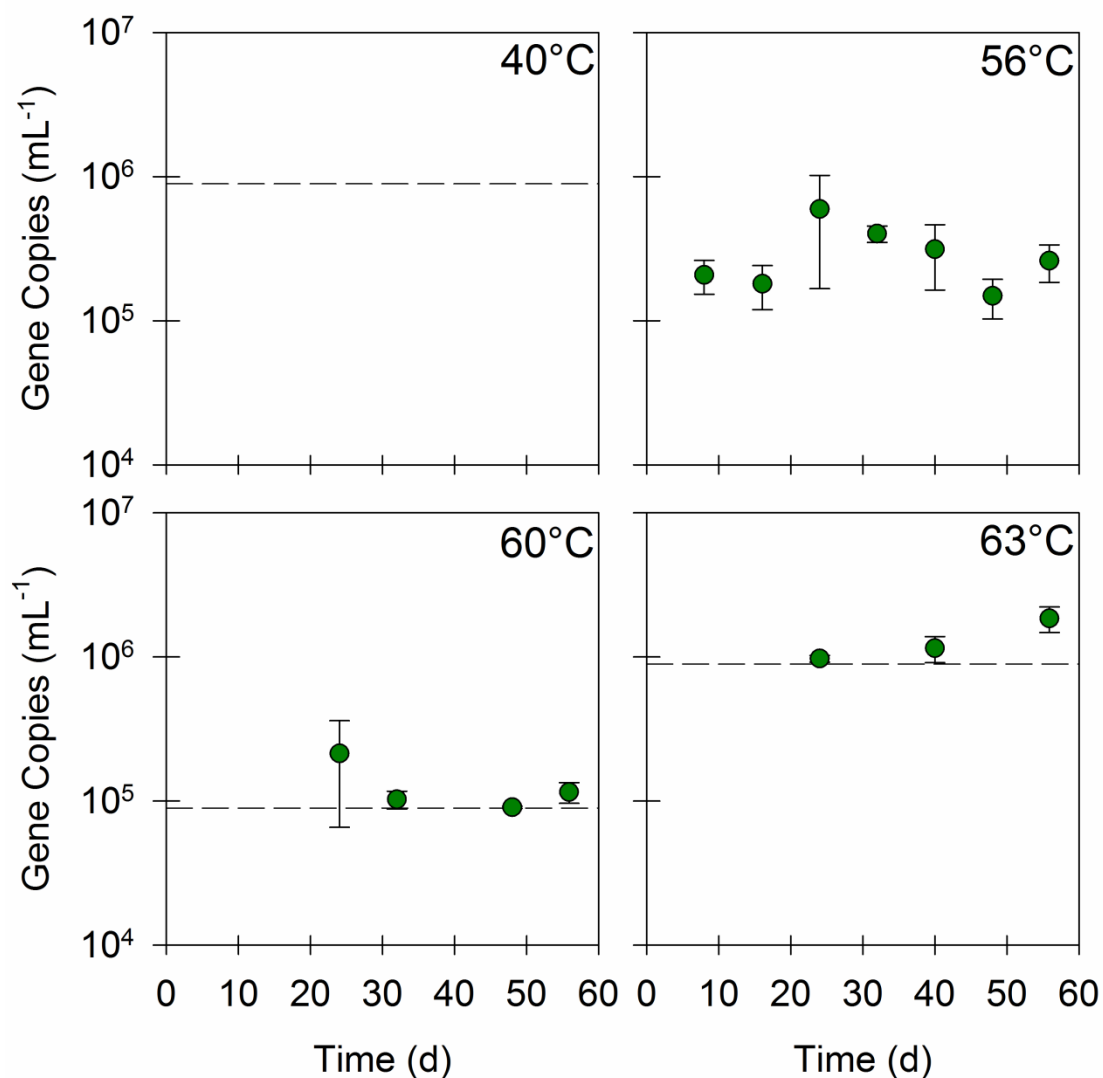


Figure C.16. Quantities of *qnrA* at the end of each of the first seven batches in anaerobic digesters operated at nominal temperatures of 40°C, 56°C, 60°C, and 63°C. Values are the arithmetic mean of duplicate or triplicate samples; error bars represent one standard deviation. Dashed lines represent the limit of quantification for data sets that contain one or more experimental values below that limit.

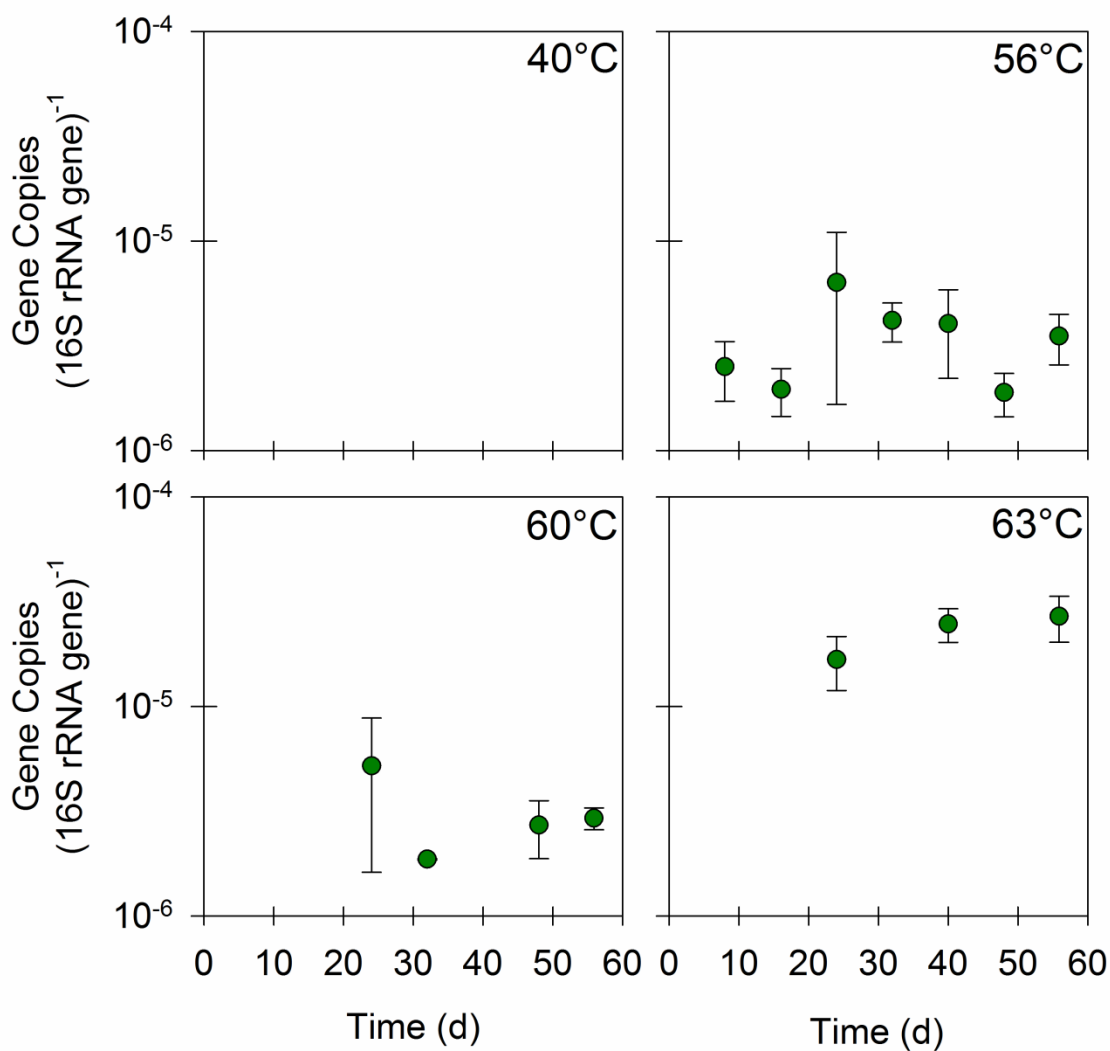


Figure C.17. The ratios of *qnrA* to 16S rRNA genes at the end of each of the first seven batches in anaerobic digesters operated at nominal temperatures of 40°C, 56°C, 60°C, and 63°C. Values are the arithmetic mean of duplicate or triplicate samples; error bars represent one standard deviation.

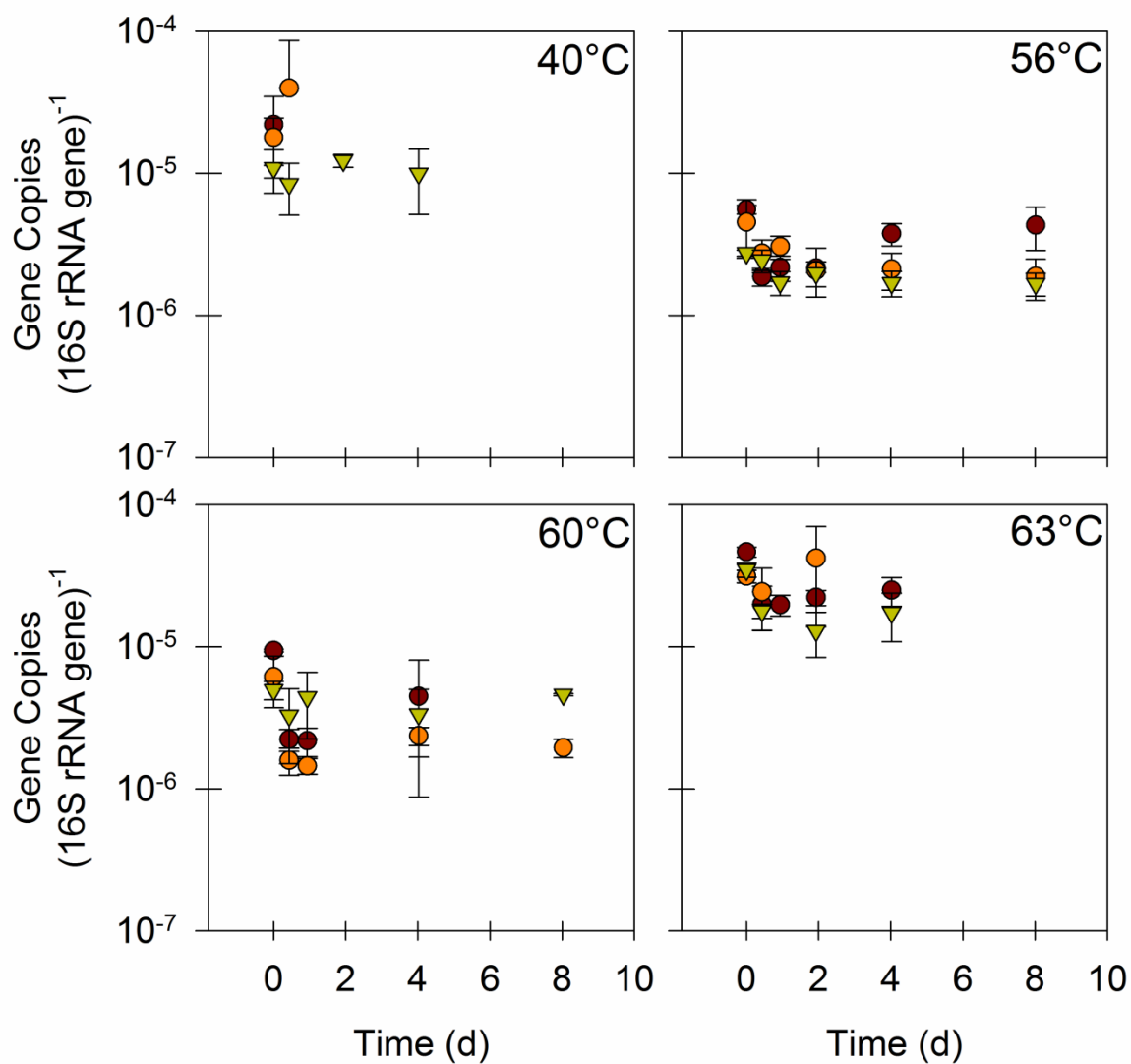


Figure C.18. The ratios of *qnrA* to 16S rRNA genes during the final three batches (green, orange, and red symbols represent unique batches) in anaerobic digesters operated at nominal temperatures of 40°C, 56°C, 60°C, and 63°C. Values are the arithmetic mean of duplicate or triplicate samples; error bars represent one standard deviation.

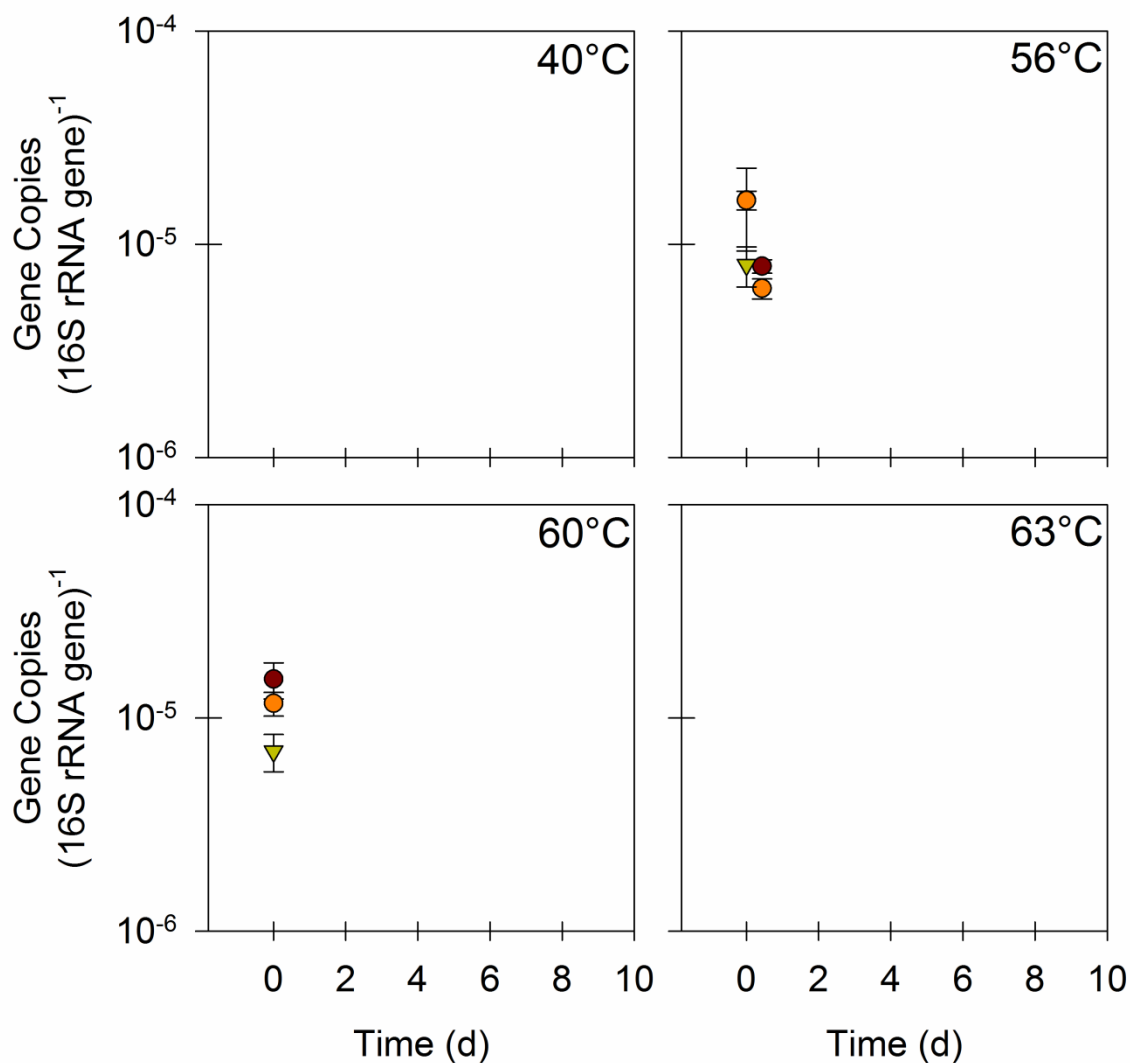


Figure C.19. The ratios of *repA* to 16S rRNA genes during the final three batches (green, orange, and red symbols represent unique batches) in anaerobic digesters operated at nominal temperatures of 40°C, 56°C, 60°C, and 63°C. Values are the arithmetic mean of duplicate or triplicate samples; error bars represent one standard deviation.

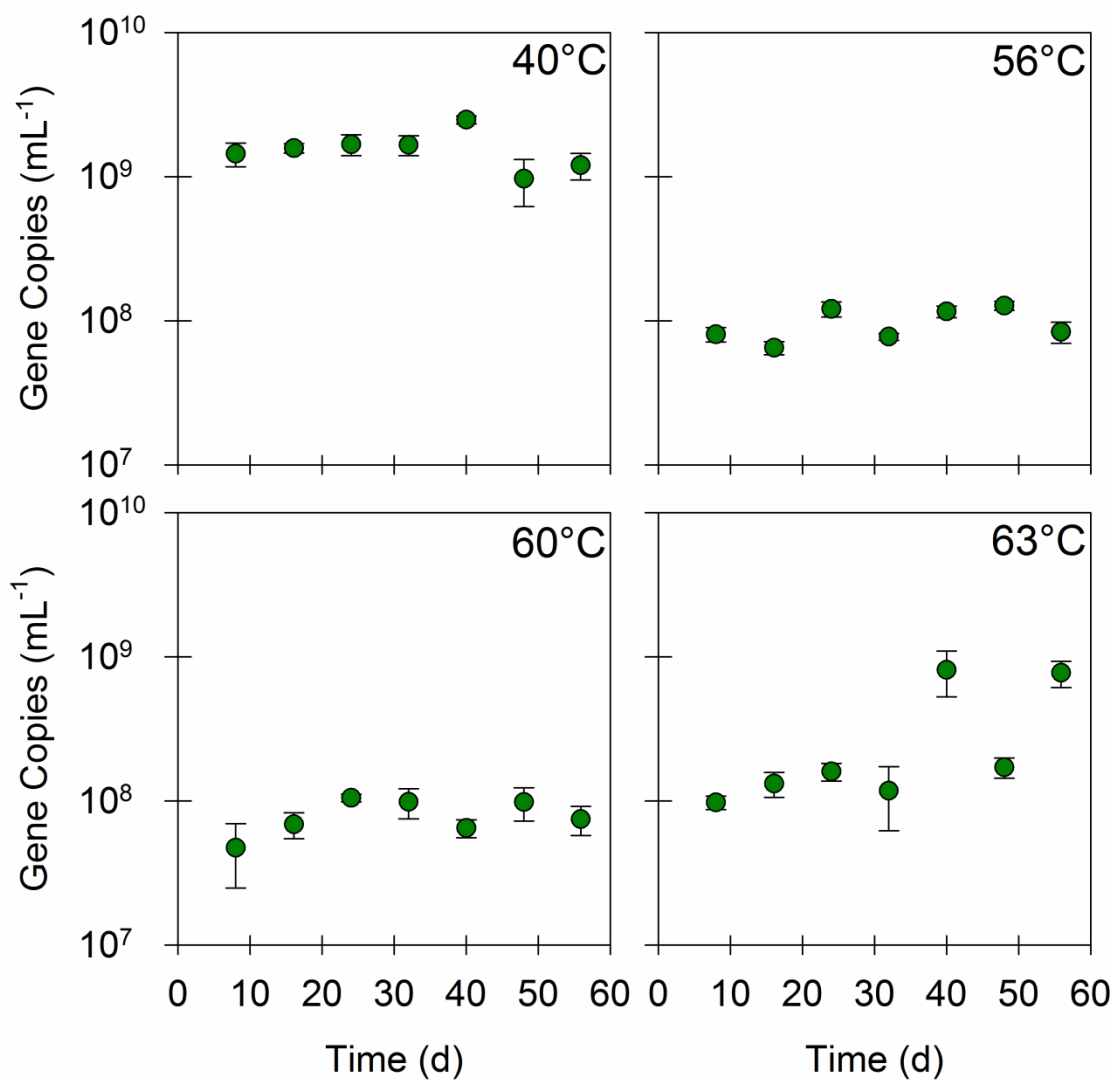


Figure C.20. Quantities of *tet(W)* at the end of each of the first seven batches in anaerobic digesters operated at nominal temperatures of 40°C, 56°C, 60°C, and 63°C. Values are the arithmetic mean of triplicate samples; error bars represent one standard deviation.

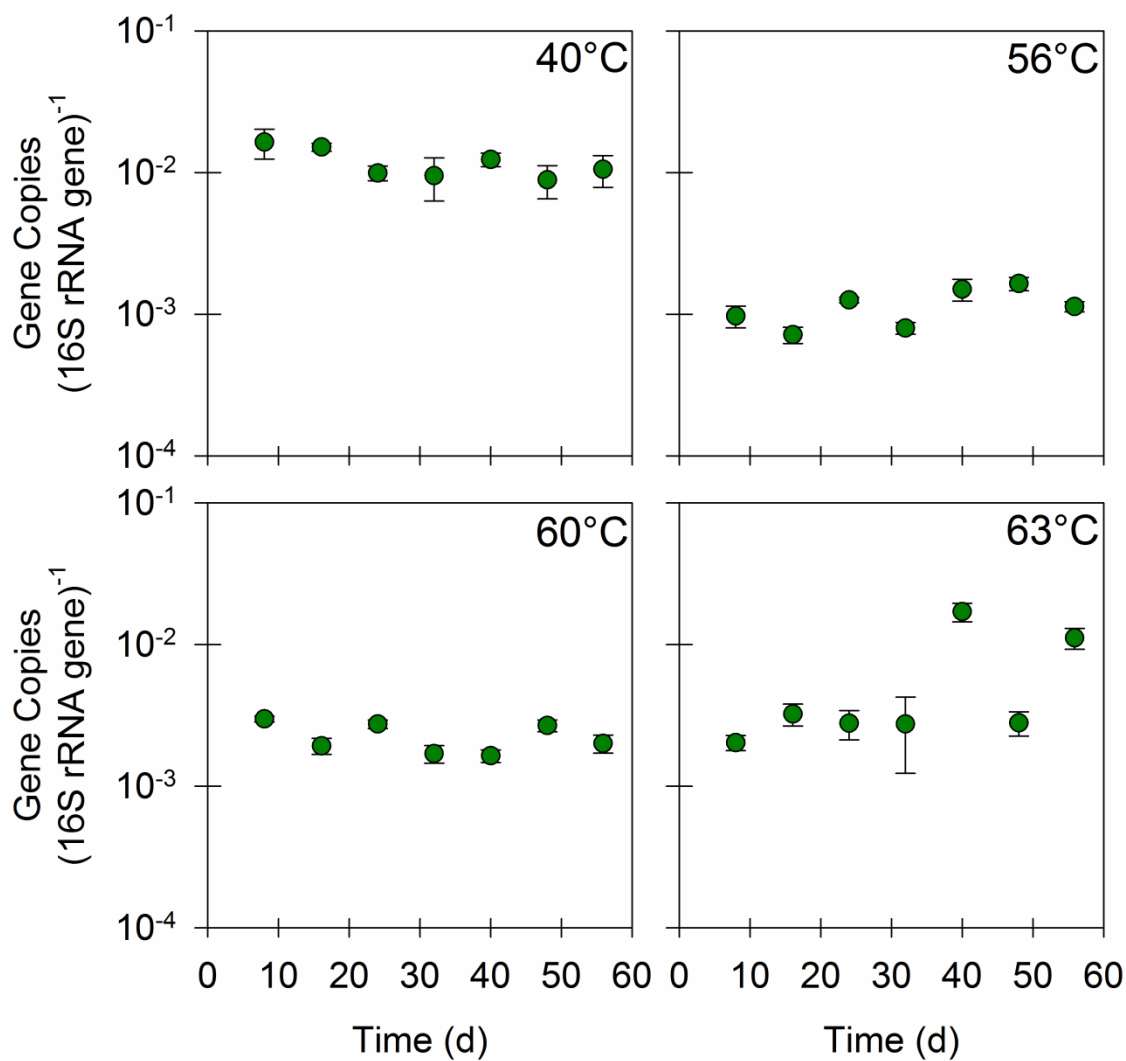


Figure C.21. The ratios of *tet(W)* to 16S rRNA genes at the end of each of the first seven batches in anaerobic digesters operated at nominal temperatures of 40°C, 56°C, 60°C, and 63°C. Values are the arithmetic mean of triplicate samples; error bars represent one standard deviation.

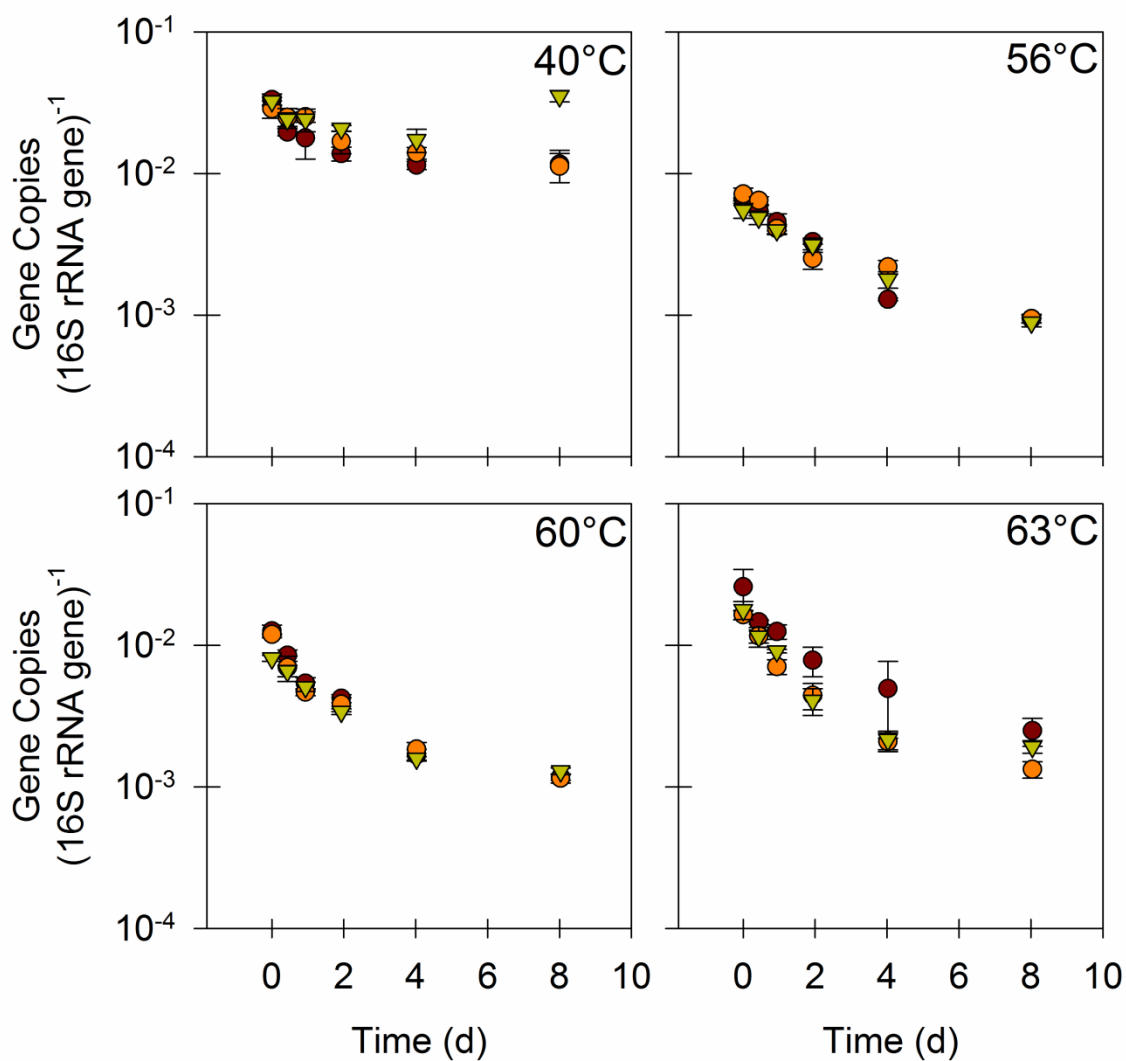


Figure C.22. The ratios of *tet(W)* to 16S rRNA genes during the final three batches (green, orange, and red symbols represent unique batches) in anaerobic digesters operated at nominal temperatures of 40°C, 56°C, 60°C, and 63°C. Values are the arithmetic mean of triplicate samples; error bars represent one standard deviation.

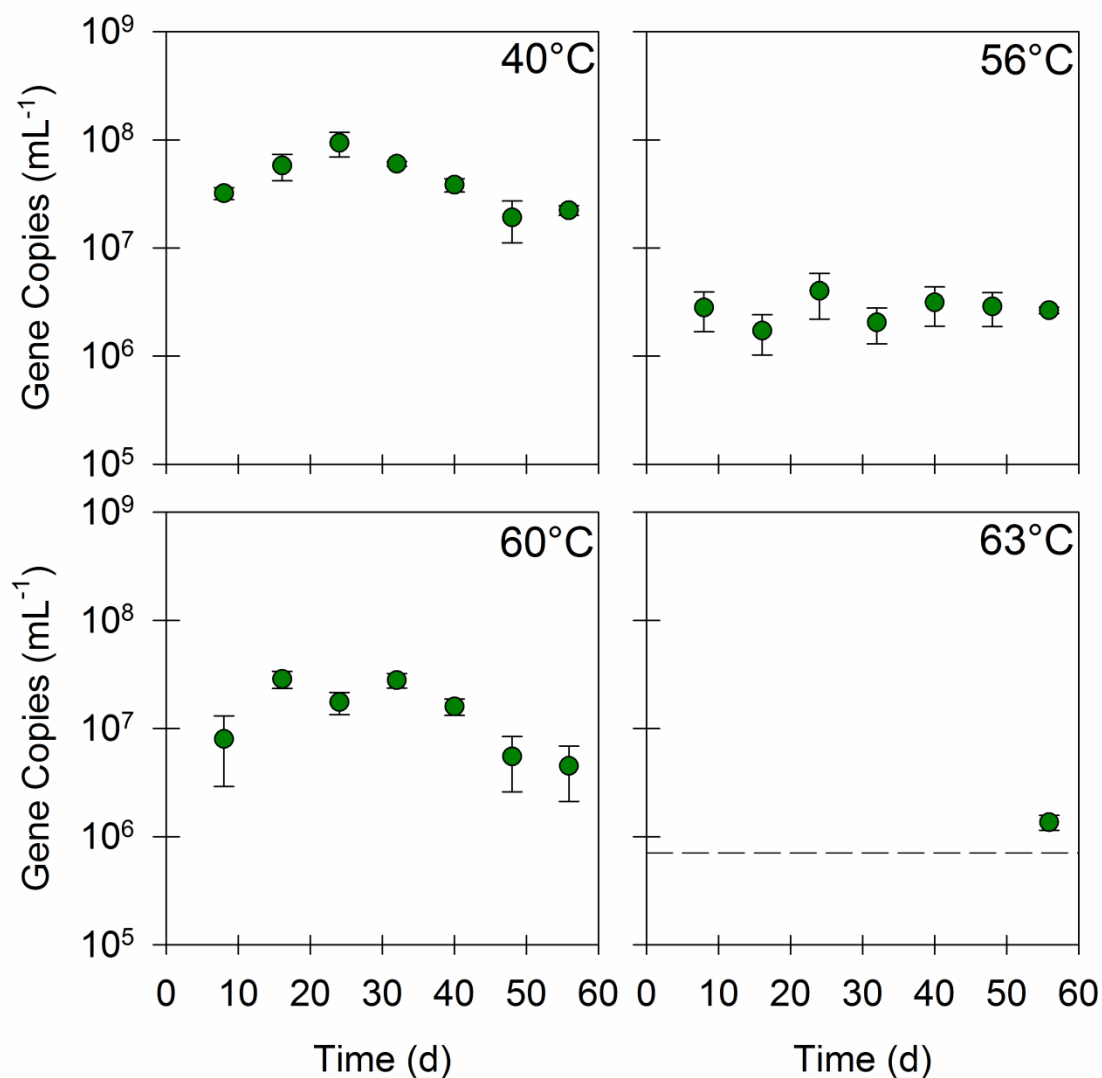


Figure C.23. Quantities of *tet(X)* at the end of each of the first seven batches in anaerobic digesters operated at nominal temperatures of 40°C, 56°C, 60°C, and 63°C. Values are the arithmetic mean of duplicate or triplicate samples; error bars represent one standard deviation. Dashed lines represent the limit of quantification for data sets that contain one or more experimental values below that limit.

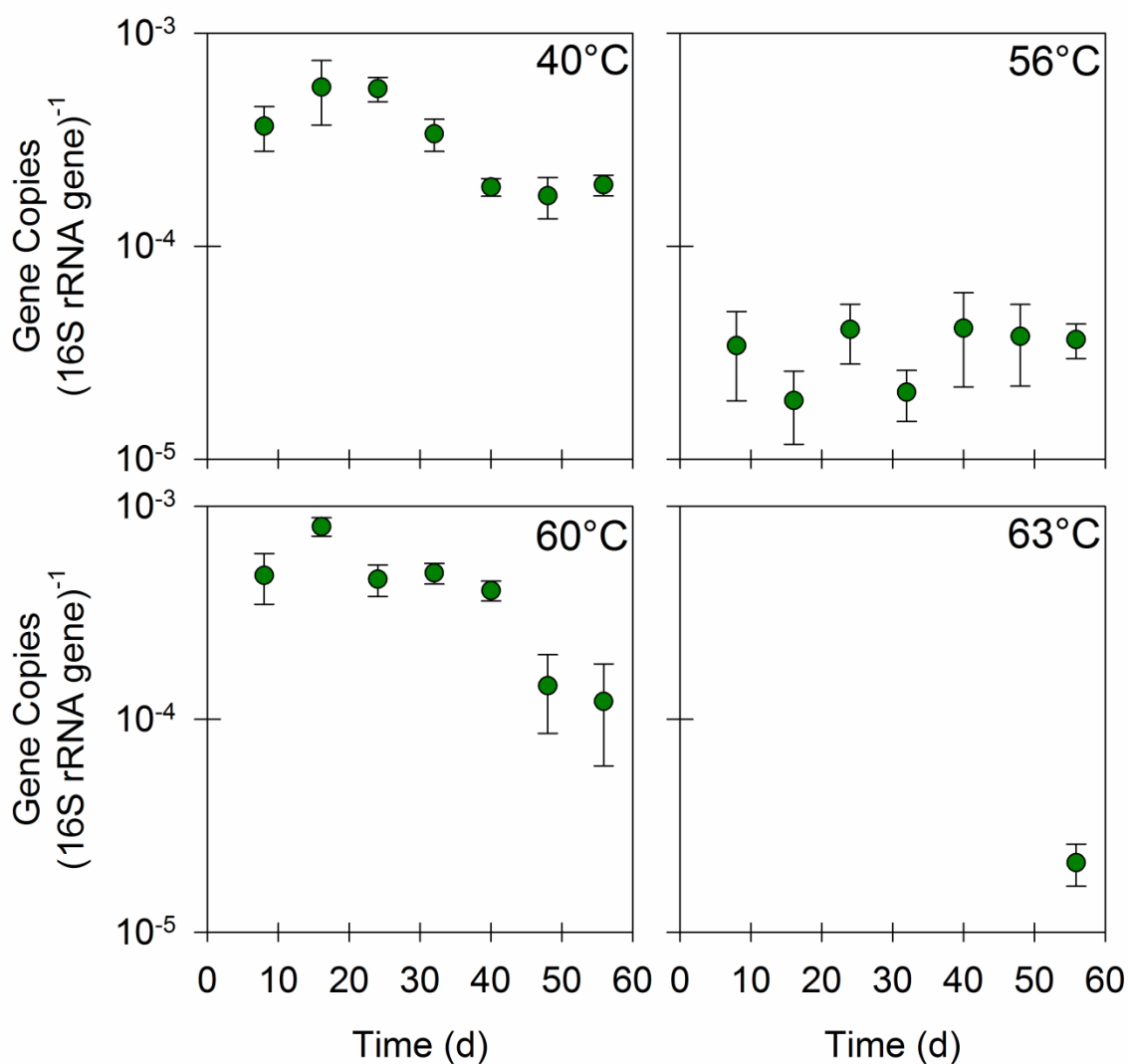


Figure C.24. The ratios of *tet(X)* to 16S rRNA genes at the end of each of the first seven batches in anaerobic digesters operated at nominal temperatures of 40°C, 56°C, 60°C, and 63°C. Values are the arithmetic mean of duplicate or triplicate samples; error bars represent one standard deviation.

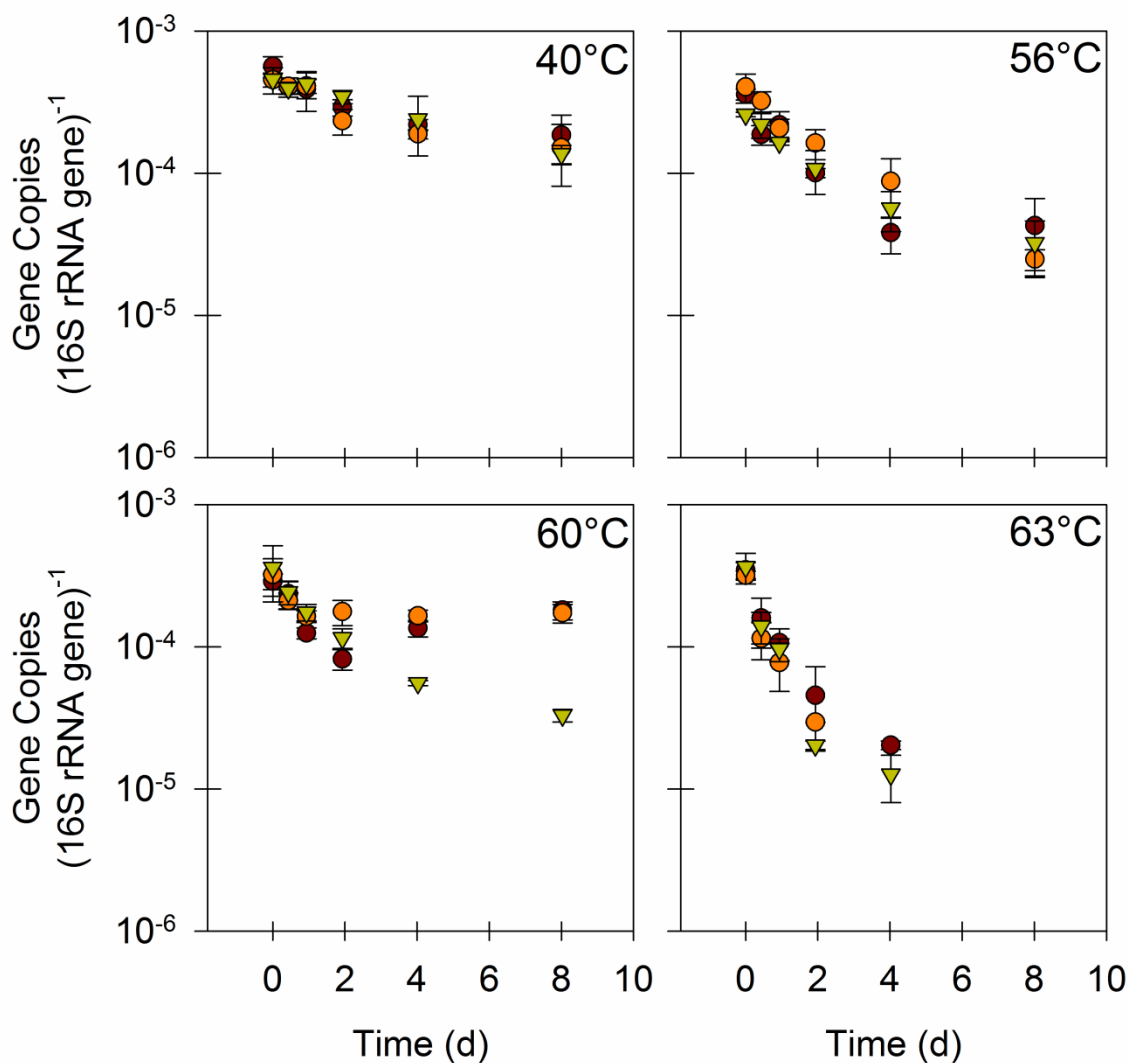


Figure C.25. The ratios of *tet(X)* to 16S rRNA genes during the final three batches (green, orange, and red symbols represent unique batches) in anaerobic digesters operated at nominal temperatures of 40°C, 56°C, 60°C, and 63°C. Values are the arithmetic mean of duplicate or triplicate samples; error bars represent one standard deviation.

Table C.3. The number of data points (n), r^2 , analysis of variance (ANOVA) P , lack-of-fit (LOF) P , and non-constant variance (NCV) P for an ordinary least squares fit of the first-order kinetic model to each time series of gene target quantities or ratios of gene target quantities to 16S rRNA gene quantities.

Target	Units (copies)	Temperature	n	r^2	ANOVA P	LOF P	NCV P
16S rRNA gene	mL ⁻¹	40°C	18	0.40	4.5×10 ⁻³	0.04	0.47
16S rRNA gene	mL ⁻¹	56°C	18	0.37	0.01	0.02	0.75
16S rRNA gene	mL ⁻¹	60°C	18	0.38	0.01	0.01	0.27
16S rRNA gene	mL ⁻¹	63°C	18	0.40	5.0×10 ⁻³	0.01	0.10
AllBac	mL ⁻¹	40°C	18	0.93	7.1×10 ⁻¹¹	0.16	0.16
AllBac	mL ⁻¹	56°C	18	0.84	9.1×10 ⁻⁸	0.10	0.07
AllBac	mL ⁻¹	60°C	18	0.83	1.4×10 ⁻⁷	2.2×10 ⁻⁸	0.80

AllBac	mL ⁻¹	63°C	18	0.82	2.1×10 ⁻⁷	1.6×10 ⁻³	0.55
AllBac	(16S rRNA gene) ⁻¹	40°C	18	0.92	2.4×10 ⁻¹⁰	0.14	0.67
AllBac	(16S rRNA gene) ⁻¹	56°C	18	0.86	2.7×10 ⁻⁸	0.50	0.01
AllBac	(16S rRNA gene) ⁻¹	60°C	18	0.88	1.0×10 ⁻⁸	5.2×10 ⁻⁴	0.42
AllBac	(16S rRNA gene) ⁻¹	63°C	18	0.85	5.8×10 ⁻⁸	0.02	0.39
Methanogen 16S rRNA genes	mL ⁻¹	40°C	18	0.01	0.78	0.72	0.60
Methanogen 16S rRNA genes	mL ⁻¹	56°C	18	0.70	1.6×10 ⁻⁵	0.25	0.57
Methanogen 16S rRNA genes	mL ⁻¹	60°C	18	0.57	2.7×10 ⁻⁴	0.34	0.30
Methanogen 16S rRNA genes	mL ⁻¹	63°C	18	0.68	2.5×10 ⁻⁵	0.93	0.20
Methanogen 16S rRNA genes	(16S rRNA gene) ⁻¹	40°C	18	0.09	0.23	0.26	0.48

Methanogen 16S rRNA genes	(16S rRNA gene) ⁻¹	56°C	18	0.07	0.27	0.02	0.40
Methanogen 16S rRNA genes	(16S rRNA gene) ⁻¹	60°C	18	0.01	0.67	0.30	0.98
Methanogen 16S rRNA genes	(16S rRNA gene) ⁻¹	63°C	18	0.35	0.01	0.01	0.08
<i>intII</i>	mL ⁻¹	40°C	18	0.74	5.2×10 ⁻⁶	2.1×10 ⁻³	0.31
<i>intII</i>	mL ⁻¹	56°C	18	0.74	5.5×10 ⁻⁶	6.6×10 ⁻⁶	0.27
<i>intII</i>	mL ⁻¹	60°C	18	0.76	2.1×10 ⁻⁶	7.3×10 ⁻⁶	0.64
<i>intII</i>	mL ⁻¹	63°C	18	0.59	2.0×10 ⁻⁴	1.1×10 ⁻³	0.35
<i>intII</i>	(16S rRNA gene) ⁻¹	40°C	18	0.64	7.3×10 ⁻⁵	0.07	0.79
<i>intII</i>	(16S rRNA gene) ⁻¹	56°C	18	0.79	8.9×10 ⁻⁷	0.01	0.67
<i>intII</i>	(16S rRNA gene) ⁻¹	60°C	18	0.80	5.9×10 ⁻⁷	0.07	0.33

<i>intI1</i>	(16S rRNA gene) ⁻¹	63°C	18	0.60	1.5×10 ⁻⁴	3.6×10 ⁻³	0.67
<i>qnrA</i>	mL ⁻¹	40°C	4	0.61	0.22	ND ^a	0.41
<i>qnrA</i>	mL ⁻¹	56°C	18	0.20	0.06	0.01	0.23
<i>qnrA</i>	mL ⁻¹	60°C	8	0.25	0.20	0.01	0.27
<i>qnrA</i>	mL ⁻¹	63°C	9	0.37	0.08	0.03	0.54
<i>qnrA</i>	(16S rRNA gene) ⁻¹	40°C	4	0.56	0.25	ND ^a	0.41
<i>qnrA</i>	(16S rRNA gene) ⁻¹	56°C	18	0.04	0.45	0.20	0.73
<i>qnrA</i>	(16S rRNA gene) ⁻¹	60°C	8	0.03	0.67	0.08	0.29
<i>qnrA</i>	(16S rRNA gene) ⁻¹	63°C	9	0.18	0.25	0.13	0.68
<i>repA</i>	mL ⁻¹	40°C	0			ND ^b	

<i>repA</i>	mL ⁻¹	56°C	4	0.69	0.17	ND ^a	0.41
<i>repA</i>	mL ⁻¹	60°C	4			ND ^b	
<i>repA</i>	mL ⁻¹	63°C	0			ND ^b	
<i>repA</i>	(16S rRNA gene) ⁻¹	40°C	0			ND ^b	
<i>repA</i>	(16S rRNA gene) ⁻¹	56°C	4	0.35	0.41	ND ^a	0.41
<i>repA</i>	(16S rRNA gene) ⁻¹	60°C	4			ND ^b	
<i>repA</i>	(16S rRNA gene) ⁻¹	63°C	0			ND ^b	
<i>tet</i> (W)	mL ⁻¹	40°C	18	0.38	0.01	0.08	0.03
<i>tet</i> (W)	mL ⁻¹	56°C	18	0.88	9.0×10 ⁻⁹	1.8×10 ⁻⁴	0.51
<i>tet</i> (W)	mL ⁻¹	60°C	18	0.79	6.8×10 ⁻⁷	1.1×10 ⁻⁷	0.60

<i>tet</i> (W)	mL ⁻¹	63°C	18	0.73	6.4×10 ⁻⁶	0.01	0.48
<i>tet</i> (W)	(16S rRNA gene) ⁻¹	40°C	18	0.25	0.04	0.21	0.01
<i>tet</i> (W)	(16S rRNA gene) ⁻¹	56°C	18	0.92	2.1×10 ⁻¹⁰	0.03	0.78
<i>tet</i> (W)	(16S rRNA gene) ⁻¹	60°C	18	0.86	3.7×10 ⁻⁸	3.2×10 ⁻⁵	0.82
<i>tet</i> (W)	(16S rRNA gene) ⁻¹	63°C	18	0.78	1.2×10 ⁻⁶	0.02	0.65
<i>tet</i> (X)	mL ⁻¹	40°C	18	0.86	2.4×10 ⁻⁸	1.1×10 ⁻³	0.35
<i>tet</i> (X)	mL ⁻¹	56°C	18	0.86	2.4×10 ⁻⁸	2.1×10 ⁻⁴	0.56
<i>tet</i> (X)	mL ⁻¹	60°C	18	0.42	3.4×10 ⁻³	0.01	0.54
<i>tet</i> (X)	mL ⁻¹	63°C	11	0.75	6.0×10 ⁻⁴	0.01	0.58
<i>tet</i> (X)	(16S rRNA gene) ⁻¹	40°C	18	0.87	2.0×10 ⁻⁸	0.04	0.55

<i>tet</i> (X)	(16S rRNA gene) ⁻¹	56°C	18	0.86	3.1×10 ⁻⁸	0.08	0.48
<i>tet</i> (X)	(16S rRNA gene) ⁻¹	60°C	18	0.31	0.02	0.30	0.01
<i>tet</i> (X)	(16S rRNA gene) ⁻¹	63°C	11	0.90	6.8×10 ⁻⁶	4.5×10 ⁻³	0.55

^aSome time series lacked sufficient experimental replication to conduct a lack-of-fit test, and so LOF *P* was not determined (ND).

^bQuantities of some gene targets were above quantification limits for only $n \leq 2$ time points, so ordinary least squares fits of the model to the data were not determined (ND).

Table C.4. The number of data points (n), r^2 , analysis of variance (ANOVA) P , lack-of-fit (LOF) P , and non-constant variance (NCV) P for an ordinary least squares fit of the second-order kinetic model to each time series of gene target quantities or ratios of gene target quantities to 16S rRNA gene quantities.

Target	Units (copies)	Temperature	n	r^2	ANOVA P	LOF P	NCV P
16S rRNA gene	mL ⁻¹	40°C	18	0.40	4.7×10 ⁻³	0.08	0.74
16S rRNA gene	mL ⁻¹	56°C	18	0.39	0.01	0.11	0.41
16S rRNA gene	mL ⁻¹	60°C	18	0.38	0.01	0.02	0.61
16S rRNA gene	mL ⁻¹	63°C	18	0.46	2.1×10 ⁻³	0.11	0.62
AllBac	mL ⁻¹	40°C	18	0.84	1.0×10 ⁻⁷	0.51	1.5×10 ⁻⁵
AllBac	mL ⁻¹	56°C	18	0.69	1.9×10 ⁻⁵	0.99	3.8×10 ⁻⁸
AllBac	mL ⁻¹	60°C	18	0.98	7.0×10 ⁻¹⁵	0.47	4.0×10 ⁻⁴

AllBac	mL ⁻¹	63°C	18	0.88	1.2×10 ⁻⁸	0.88	4.7×10 ⁻⁶
AllBac	(16S rRNA gene) ⁻¹	40°C	18	0.91	1.2×10 ⁻⁹	0.30	3.6×10 ⁻³
AllBac	(16S rRNA gene) ⁻¹	56°C	18	0.77	1.5×10 ⁻⁶	0.98	1.3×10 ⁻⁴
AllBac	(16S rRNA gene) ⁻¹	60°C	18	0.95	1.4×10 ⁻¹¹	0.04	0.06
AllBac	(16S rRNA gene) ⁻¹	63°C	18	0.86	3.5×10 ⁻⁸	0.95	3.0×10 ⁻³
Methanogen 16S rRNA genes	mL ⁻¹	40°C	18	0.01	0.67	0.67	0.23
Methanogen 16S rRNA genes	mL ⁻¹	56°C	18	0.71	1.2×10 ⁻⁵	0.17	0.04
Methanogen 16S rRNA genes	mL ⁻¹	60°C	18	0.62	1.1×10 ⁻⁴	0.44	0.79
Methanogen 16S rRNA genes	mL ⁻¹	63°C	18	0.75	3.5×10 ⁻⁶	0.30	0.14
Methanogen 16S rRNA genes	(16S rRNA gene) ⁻¹	40°C	18	0.10	0.19	0.21	0.23

Methanogen 16S rRNA genes	(16S rRNA gene) ⁻¹	56°C	18	0.07	0.28	0.02	0.49
Methanogen 16S rRNA genes	(16S rRNA gene) ⁻¹	60°C	18	0.02	0.61	0.31	0.84
Methanogen 16S rRNA genes	(16S rRNA gene) ⁻¹	63°C	18	0.36	0.01	0.01	0.17
<i>intII</i>	mL ⁻¹	40°C	18	0.83	1.3×10 ⁻⁷	0.05	0.83
<i>intII</i>	mL ⁻¹	56°C	18	0.89	4.1×10 ⁻⁹	0.09	0.20
<i>intII</i>	mL ⁻¹	60°C	18	0.89	3.3×10 ⁻⁹	0.36	7.8×10 ⁻⁴
<i>intII</i>	mL ⁻¹	63°C	18	0.70	1.3×10 ⁻⁵	0.76	0.01
<i>intII</i>	(16S rRNA gene) ⁻¹	40°C	18	0.67	3.0×10 ⁻⁵	0.15	0.65
<i>intII</i>	(16S rRNA gene) ⁻¹	56°C	18	0.83	1.6×10 ⁻⁷	0.25	0.02
<i>intII</i>	(16S rRNA gene) ⁻¹	60°C	18	0.82	2.7×10 ⁻⁷	0.62	1.4×10 ⁻⁴

<i>intI1</i>	(16S rRNA gene) ⁻¹	63°C	18	0.59	2.2×10 ⁻⁴	0.15	0.06
<i>qnrA</i>	mL ⁻¹	40°C	4	0.70	0.17	ND ^a	0.41
<i>qnrA</i>	mL ⁻¹	56°C	18	0.21	0.06	0.06	0.67
<i>qnrA</i>	mL ⁻¹	60°C	8	0.15	0.35	0.06	0.28
<i>qnrA</i>	mL ⁻¹	63°C	9	0.39	0.07	0.02	0.74
<i>qnrA</i>	(16S rRNA gene) ⁻¹	40°C	4	0.66	0.19	ND ^a	0.41
<i>qnrA</i>	(16S rRNA gene) ⁻¹	56°C	18	0.05	0.35	0.32	0.47
<i>qnrA</i>	(16S rRNA gene) ⁻¹	60°C	8	0.00	0.95	0.12	0.31
<i>qnrA</i>	(16S rRNA gene) ⁻¹	63°C	9	0.15	0.31	0.20	0.31
<i>repA</i>	mL ⁻¹	40°C	0			ND ^b	

<i>repA</i>	mL ⁻¹	56°C	4	0.81	0.10	ND ^a	0.41
<i>repA</i>	mL ⁻¹	60°C	4			ND ^b	
<i>repA</i>	mL ⁻¹	63°C	0			ND ^b	
<i>repA</i>	(16S rRNA gene) ⁻¹	40°C	0			ND ^b	
<i>repA</i>	(16S rRNA gene) ⁻¹	56°C	4	0.35	0.40	ND ^a	0.41
<i>repA</i>	(16S rRNA gene) ⁻¹	60°C	4			ND ^b	
<i>repA</i>	(16S rRNA gene) ⁻¹	63°C	0			ND ^b	
<i>tet</i> (W)	mL ⁻¹	40°C	18	0.46	1.9×10 ⁻³	0.47	2.4×10 ⁻⁴
<i>tet</i> (W)	mL ⁻¹	56°C	18	0.93	1.6×10 ⁻¹⁰	0.61	1.5×10 ⁻⁵
<i>tet</i> (W)	mL ⁻¹	60°C	18	0.96	2.8×10 ⁻¹²	0.82	1.8×10 ⁻⁴

<i>tet</i> (W)	mL ⁻¹	63°C	18	0.75	3.7×10 ⁻⁶	1.00	2.6×10 ⁻⁷
<i>tet</i> (W)	(16S rRNA gene) ⁻¹	40°C	18	0.33	0.01	0.37	1.6×10 ⁻³
<i>tet</i> (W)	(16S rRNA gene) ⁻¹	56°C	18	0.97	3.5×10 ⁻¹³	0.97	0.18
<i>tet</i> (W)	(16S rRNA gene) ⁻¹	60°C	18	0.96	8.6×10 ⁻¹³	1.6×10 ⁻³	0.05
<i>tet</i> (W)	(16S rRNA gene) ⁻¹	63°C	18	0.81	3.4×10 ⁻⁷	0.85	5.8×10 ⁻⁴
<i>tet</i> (X)	mL ⁻¹	40°C	18	0.95	1.6×10 ⁻¹¹	0.13	0.81
<i>tet</i> (X)	mL ⁻¹	56°C	18	0.94	2.2×10 ⁻¹¹	0.85	1.3×10 ⁻⁵
<i>tet</i> (X)	mL ⁻¹	60°C	18	0.37	0.01	0.84	3.1×10 ⁻⁶
<i>tet</i> (X)	mL ⁻¹	63°C	11	0.94	8.4×10 ⁻⁷	0.02	0.09
<i>tet</i> (X)	(16S rRNA gene) ⁻¹	40°C	18	0.90	1.7×10 ⁻⁹	0.62	0.01

<i>tet</i> (X)	(16S rRNA gene) ⁻¹	56°C	18	0.87	1.8×10 ⁻⁸	0.97	2.8×10 ⁻⁴
<i>tet</i> (X)	(16S rRNA gene) ⁻¹	60°C	18	0.29	0.02	0.96	3.7×10 ⁻⁶
<i>tet</i> (X)	(16S rRNA gene) ⁻¹	63°C	11	0.94	1.1×10 ⁻⁶	7.0×10 ⁻⁵	0.07

^aSome time series lacked sufficient experimental replication to conduct a lack-of-fit test, and so LOF *P* was not determined (ND).

^bQuantities of some gene targets were above quantification limits for only $n \leq 2$ time points, so ordinary least squares fits of the model to the data were not determined (ND).

Table C.5. The number of data points (n), r^2 , analysis of variance (ANOVA) P , lack-of-fit (LOF) P , and non-constant variance (NCV) P for an ordinary least squares fit of the modified Collins-Selleck kinetic model to each time series of gene target quantities or ratios of gene target quantities to 16S rRNA gene quantities.

Target	Units (copies)	Temperature	n	r^2	ANOVA P	LOF P	NCV P
16S rRNA gene	mL ⁻¹	40°C	15	0.34	0.02	0.35	0.46
16S rRNA gene	mL ⁻¹	56°C	15	0.35	0.02	0.41	0.24
16S rRNA gene	mL ⁻¹	60°C	15	0.45	0.01	0.17	1.00
16S rRNA gene	mL ⁻¹	63°C	15	0.24	0.07	0.55	0.96
AllBac	mL ⁻¹	40°C	15	0.90	6.0×10 ⁻⁸	0.03	0.90
AllBac	mL ⁻¹	56°C	15	0.85	1.1×10 ⁻⁶	0.61	0.01
AllBac	mL ⁻¹	60°C	15	0.98	2.0×10 ⁻¹²	1.00	0.75

AllBac	mL ⁻¹	63°C	15	0.94	2.4×10 ⁻⁹	0.30	0.39
AllBac	(16S rRNA gene) ⁻¹	40°C	15	0.85	9.8×10 ⁻⁷	0.03	0.48
AllBac	(16S rRNA gene) ⁻¹	56°C	15	0.84	1.7×10 ⁻⁶	0.41	0.09
AllBac	(16S rRNA gene) ⁻¹	60°C	15	0.96	1.5×10 ⁻¹⁰	0.01	0.83
AllBac	(16S rRNA gene) ⁻¹	63°C	15	0.85	1.1×10 ⁻⁶	0.77	0.25
Methanogen 16S rRNA genes	mL ⁻¹	40°C	15	0.00	0.94	0.70	0.01
Methanogen 16S rRNA genes	mL ⁻¹	56°C	15	0.41	0.01	0.16	0.10
Methanogen 16S rRNA genes	mL ⁻¹	60°C	15	0.34	0.02	0.79	0.60
Methanogen 16S rRNA genes	mL ⁻¹	63°C	15	0.55	1.5×10 ⁻³	0.25	0.31
Methanogen 16S rRNA genes	(16S rRNA gene) ⁻¹	40°C	15	0.07	0.35	0.67	0.09

Methanogen 16S rRNA genes	(16S rRNA gene) ⁻¹	56°C	15	0.15	0.15	0.13	0.60
Methanogen 16S rRNA genes	(16S rRNA gene) ⁻¹	60°C	15	0.02	0.65	0.14	0.82
Methanogen 16S rRNA genes	(16S rRNA gene) ⁻¹	63°C	15	0.53	2.1×10 ⁻³	0.31	0.31
<i>intII</i>	mL ⁻¹	40°C	15	0.90	8.3×10 ⁻⁸	0.70	0.77
<i>intII</i>	mL ⁻¹	56°C	15	0.90	6.1×10 ⁻⁸	0.75	0.10
<i>intII</i>	mL ⁻¹	60°C	15	0.96	2.3×10 ⁻¹⁰	0.61	0.35
<i>intII</i>	mL ⁻¹	63°C	15	0.74	3.4×10 ⁻⁵	0.99	0.44
<i>intII</i>	(16S rRNA gene) ⁻¹	40°C	15	0.58	9.9×10 ⁻⁴	0.28	0.65
<i>intII</i>	(16S rRNA gene) ⁻¹	56°C	15	0.81	5.1×10 ⁻⁶	0.60	0.15
<i>intII</i>	(16S rRNA gene) ⁻¹	60°C	15	0.83	2.5×10 ⁻⁶	0.58	0.07

<i>intII</i>	(16S rRNA gene) ⁻¹	63°C	15	0.79	9.1×10 ⁻⁶	0.52	0.16
<i>qnrA</i>	mL ⁻¹	40°C	2			ND ^a	
<i>qnrA</i>	mL ⁻¹	56°C	15	0.07	0.34	0.76	0.24
<i>qnrA</i>	mL ⁻¹	60°C	5	0.01	0.90	0.41	0.45
<i>qnrA</i>	mL ⁻¹	63°C	6	0.28	0.28	0.54	0.90
<i>qnrA</i>	(16S rRNA gene) ⁻¹	40°C	2			ND ^a	
<i>qnrA</i>	(16S rRNA gene) ⁻¹	56°C	15	0.00	0.85	0.95	0.26
<i>qnrA</i>	(16S rRNA gene) ⁻¹	60°C	5	0.06	0.68	0.37	0.35
<i>qnrA</i>	(16S rRNA gene) ⁻¹	63°C	6	0.08	0.59	0.68	0.39
<i>repA</i>	mL ⁻¹	40°C	0			ND ^a	

<i>repA</i>	mL ⁻¹	56°C	2					ND ^a
<i>repA</i>	mL ⁻¹	60°C	0					ND ^a
<i>repA</i>	mL ⁻¹	63°C	0					ND ^a
<i>repA</i>	(16S rRNA gene) ⁻¹	40°C	0					ND ^a
<i>repA</i>	(16S rRNA gene) ⁻¹	56°C	2					ND ^a
<i>repA</i>	(16S rRNA gene) ⁻¹	60°C	0					ND ^a
<i>repA</i>	(16S rRNA gene) ⁻¹	63°C	0					ND ^a
<i>tet</i> (W)	mL ⁻¹	40°C	15	0.44	0.01	0.79	3.6×10 ⁻³	
<i>tet</i> (W)	mL ⁻¹	56°C	15	0.92	1.2×10 ⁻⁸	0.22	0.11	
<i>tet</i> (W)	mL ⁻¹	60°C	15	0.98	1.4×10 ⁻¹²	0.99	0.19	

<i>tet</i> (W)	mL ⁻¹	63°C	15	0.93	8.9×10 ⁻⁹	0.51	0.69
<i>tet</i> (W)	(16S rRNA gene) ⁻¹	40°C	15	0.21	0.09	0.74	0.03
<i>tet</i> (W)	(16S rRNA gene) ⁻¹	56°C	15	0.91	2.6×10 ⁻⁸	0.16	0.54
<i>tet</i> (W)	(16S rRNA gene) ⁻¹	60°C	15	0.90	5.7×10 ⁻⁸	0.26	0.62
<i>tet</i> (W)	(16S rRNA gene) ⁻¹	63°C	15	0.95	4.6×10 ⁻¹⁰	0.27	0.87
<i>tet</i> (X)	mL ⁻¹	40°C	15	0.92	1.9×10 ⁻⁸	0.13	0.81
<i>tet</i> (X)	mL ⁻¹	56°C	15	0.92	2.2×10 ⁻⁸	0.39	0.66
<i>tet</i> (X)	mL ⁻¹	60°C	15	0.38	0.01	0.73	0.01
<i>tet</i> (X)	mL ⁻¹	63°C	8	0.92	1.8×10 ⁻⁴	0.54	0.46
<i>tet</i> (X)	(16S rRNA gene) ⁻¹	40°C	15	0.83	2.2×10 ⁻⁶	0.17	0.34

<i>tet</i> (X)	(16S rRNA gene) ⁻¹	56°C	15	0.86	6.2×10 ⁻⁷	0.31	0.53
<i>tet</i> (X)	(16S rRNA gene) ⁻¹	60°C	15	0.25	0.06	0.94	4.5×10 ⁻³
<i>tet</i> (X)	(16S rRNA gene) ⁻¹	63°C	8	0.90	3.4×10 ⁻⁴	0.01	0.35

^aQuantities of some gene targets were above quantification limits for only $n \leq 2$ time points, so ordinary least squares fits of the model to the data were not determined (ND).

Table C.6. Fitted values of k and calculated initial half-lives ($t_{1/2}$) from an ordinary least squares fit of the second-order kinetic model to each time series of gene target quantities or ratios of gene target quantities to 16S rRNA genes. Error terms represent the standard error of the mean.

Target	Units (copies)	Temperature	$k^{a,b}$ (mL copy ⁻¹ day ⁻¹)	Initial $t_{1/2}^c$ (days)
16S rRNA gene	mL ⁻¹	40°C	$-2.4 \times 10^{-13} \pm 7.2 \times 10^{-14}$	22.8
16S rRNA gene	mL ⁻¹	56°C	$-5.2 \times 10^{-13} \pm 1.6 \times 10^{-13}$	14.0
16S rRNA gene	mL ⁻¹	60°C	$-1.2 \times 10^{-12} \pm 3.7 \times 10^{-13}$	11.3
16S rRNA gene	mL ⁻¹	63°C	$-1.4 \times 10^{-12} \pm 3.9 \times 10^{-13}$	7.9
AllBac	mL ⁻¹	40°C	$-1.9 \times 10^{-11} \pm 2.1 \times 10^{-12}$	-0.3
AllBac	mL ⁻¹	56°C	$-8.0 \times 10^{-12} \pm 1.3 \times 10^{-12}$	0.9
AllBac	mL ⁻¹	60°C	$-1.3 \times 10^{-11} \pm 4.6 \times 10^{-13}$	0.6

AllBac	mL ⁻¹	63°C	$-3.4 \times 10^{-11} \pm 3.2 \times 10^{-12}$	0.0
AllBac	(16S rRNA gene) ⁻¹	40°C	$-2.5 \times 10^0 \pm 2.0 \times 10^{-1}$	0.0
AllBac	(16S rRNA gene) ⁻¹	56°C	$-6.3 \times 10^{-1} \pm 8.5 \times 10^{-2}$	2.0
AllBac	(16S rRNA gene) ⁻¹	60°C	$-5.7 \times 10^{-1} \pm 3.4 \times 10^{-2}$	1.4
AllBac	(16S rRNA gene) ⁻¹	63°C	$-1.5 \times 10^0 \pm 1.5 \times 10^{-1}$	0.7
Methanogen 16S rRNA genes	mL ⁻¹	40°C	$-6.3 \times 10^{-12} \pm 1.4 \times 10^{-11}$	85.9
Methanogen 16S rRNA genes	mL ⁻¹	56°C	$-1.9 \times 10^{-10} \pm 3.0 \times 10^{-11}$	7.5
Methanogen 16S rRNA genes	mL ⁻¹	60°C	$-4.3 \times 10^{-10} \pm 8.5 \times 10^{-11}$	8.5
Methanogen 16S rRNA genes	mL ⁻¹	63°C	$-9.5 \times 10^{-10} \pm 1.4 \times 10^{-10}$	1.9
Methanogen 16S rRNA genes	(16S rRNA gene) ⁻¹	40°C	$3.7 \times 10^0 \pm 2.7 \times 10^0$	-28.0

Methanogen 16S rRNA genes	(16S rRNA gene) ⁻¹	56°C	-5.4×10 ⁰ ± 4.8×10 ⁰	38.9
Methanogen 16S rRNA genes	(16S rRNA gene) ⁻¹	60°C	-2.9×10 ⁰ ± 5.7×10 ⁰	101.2
Methanogen 16S rRNA genes	(16S rRNA gene) ⁻¹	63°C	-2.5×10 ¹ ± 8.4×10 ⁰	8.1
<i>intII</i>	mL ⁻¹	40°C	-4.1×10 ⁻¹¹ ± 4.6×10 ⁻¹²	6.5
<i>intII</i>	mL ⁻¹	56°C	-2.8×10 ⁻¹⁰ ± 2.5×10 ⁻¹¹	2.8
<i>intII</i>	mL ⁻¹	60°C	-3.9×10 ⁻¹⁰ ± 3.4×10 ⁻¹¹	1.7
<i>intII</i>	mL ⁻¹	63°C	-6.7×10 ⁻¹⁰ ± 1.1×10 ⁻¹⁰	1.7
<i>intII</i>	(16S rRNA gene) ⁻¹	40°C	-4.2×10 ⁰ ± 7.3×10 ⁻¹	12.0
<i>intII</i>	(16S rRNA gene) ⁻¹	56°C	-2.2×10 ¹ ± 2.5×10 ⁰	5.0
<i>intII</i>	(16S rRNA gene) ⁻¹	60°C	-1.6×10 ¹ ± 1.9×10 ⁰	3.4

<i>intI1</i>	(16S rRNA gene) ⁻¹	63°C	-2.5×10 ¹ ± 5.2×10 ⁰	4.3
<i>qnrA</i>	mL ⁻¹	40°C	-6.2×10 ⁻⁷ ± 2.9×10 ⁻⁷	0.5
<i>qnrA</i>	mL ⁻¹	56°C	-2.5×10 ⁻⁷ ± 1.2×10 ⁻⁷	12.3
<i>qnrA</i>	mL ⁻¹	60°C	-4.1×10 ⁻⁷ ± 4.1×10 ⁻⁷	6.5
<i>qnrA</i>	mL ⁻¹	63°C	-1.3×10 ⁻⁷ ± 5.9×10 ⁻⁸	3.0
<i>qnrA</i>	(16S rRNA gene) ⁻¹	40°C	-1.4×10 ⁵ ± 6.9×10 ⁴	0.5
<i>qnrA</i>	(16S rRNA gene) ⁻¹	56°C	-1.1×10 ⁴ ± 1.1×10 ⁴	36.3
<i>qnrA</i>	(16S rRNA gene) ⁻¹	60°C	-2.6×10 ³ ± 3.7×10 ⁴	101.1
<i>qnrA</i>	(16S rRNA gene) ⁻¹	63°C	-4.6×10 ³ ± 4.2×10 ³	8.2
<i>repA</i>	mL ⁻¹	40°C	ND ^d	

<i>repA</i>	mL ⁻¹	56°C	-1.3×10 ⁻⁶ ± 4.6×10 ⁻⁷	0.3
<i>repA</i>	mL ⁻¹	60°C	ND ^d	
<i>repA</i>	mL ⁻¹	63°C	ND ^d	
<i>repA</i>	(16S rRNA gene) ⁻¹	40°C	ND ^d	
<i>repA</i>	(16S rRNA gene) ⁻¹	56°C	-1.1×10 ⁵ ± 1.0×10 ⁵	0.8
<i>repA</i>	(16S rRNA gene) ⁻¹	60°C	ND ^d	
<i>repA</i>	(16S rRNA gene) ⁻¹	63°C	ND ^d	
<i>tet(W)</i>	mL ⁻¹	40°C	-3.9×10 ⁻¹¹ ± 1.1×10 ⁻¹¹	5.9
<i>tet(W)</i>	mL ⁻¹	56°C	-1.4×10 ⁻⁹ ± 9.6×10 ⁻¹¹	0.5
<i>tet(W)</i>	mL ⁻¹	60°C	-2.1×10 ⁻⁹ ± 1.1×10 ⁻¹⁰	0.6

<i>tet</i> (W)	mL ⁻¹	63°C	$-1.6 \times 10^{-9} \pm 2.3 \times 10^{-10}$	0.2
<i>tet</i> (W)	(16S rRNA gene) ⁻¹	40°C	$-4.1 \times 10^0 \pm 1.4 \times 10^0$	10.6
<i>tet</i> (W)	(16S rRNA gene) ⁻¹	56°C	$-1.2 \times 10^2 \pm 5.5 \times 10^0$	1.2
<i>tet</i> (W)	(16S rRNA gene) ⁻¹	60°C	$-9.5 \times 10^1 \pm 4.7 \times 10^0$	1.2
<i>tet</i> (W)	(16S rRNA gene) ⁻¹	63°C	$-6.5 \times 10^1 \pm 7.8 \times 10^0$	1.0
<i>tet</i> (X)	mL ⁻¹	40°C	$-4.4 \times 10^{-9} \pm 2.6 \times 10^{-10}$	2.6
<i>tet</i> (X)	mL ⁻¹	56°C	$-4.1 \times 10^{-8} \pm 2.5 \times 10^{-9}$	0.2
<i>tet</i> (X)	mL ⁻¹	60°C	$-2.9 \times 10^{-8} \pm 9.4 \times 10^{-9}$	2.2
<i>tet</i> (X)	mL ⁻¹	63°C	$-3.0 \times 10^{-7} \pm 2.5 \times 10^{-8}$	-0.1
<i>tet</i> (X)	(16S rRNA gene) ⁻¹	40°C	$-5.5 \times 10^2 \pm 4.5 \times 10^1$	4.0

<i>tet</i> (X)	(16S rRNA gene) ⁻¹	56°C	-3.7×10 ³ ± 3.5×10 ²	0.7
<i>tet</i> (X)	(16S rRNA gene) ⁻¹	60°C	-1.3×10 ³ ± 4.9×10 ²	3.8
<i>tet</i> (X)	(16S rRNA gene) ⁻¹	63°C	-1.8×10 ⁴ ± 1.6×10 ³	-0.1

^aSee Table C.4 for ANOVA *P* values, which are equal to values of *P* for *k*, as well as other summary metrics that describe the quality of fit of the model to the data.

^bAlternatively, units may be 16S rRNA genes copy⁻¹ day⁻¹.

^cInitial half-lives (*t*_{1/2}) were calculated using fitted values of *k* and *C*₀.

^dQuantities of some gene targets were above quantification limits for only *n* ≤ 2 time points, so *k* was not determined (ND).

Appendix D: Supporting Information for Chapter 6

Table D.1. The primer sequences, expected amplicon size, and annealing temperature for each real-time PCR method used in this work.

Gene Target	Primer Sequence (5'→3')	Size (bp)	Ann. Temp. (°C)	Reference
16S rRNA gene (338F, 518R)	F: CCT ACG GGA GGC AGC AG R: ATT ACC GCG GCT GCT GG	202	60	(196)
all <i>Bacteroides</i> spp. 16S rRNA gene (AllBac)	F: GAG AGG AAG GTC CCC CAC R: CGC TAC TTG GCT GGT TCA G	116	60	(195)
human-specific <i>Bacteroides</i> spp. 16S rRNA gene (HF183)	F: ATC ATG AGT TCA CAT GTC CG R: TAC CCC GCC TAC TAT CTA ATG	82	56	(194,203)

<i>erm(B)</i>	F: GAT ACC GTT TAC GAA ATT GG	364	58	(200)
	R: GAA TCG AGA CTT GAG TGT GC			
<i>intI1</i>	F: CCT CCC GCA CGA TGA TC	280	60	(201)
	R: TCC ACG CAT CGT CAG GC			
<i>qnrA</i>	F: AGG ATT TCT CAC GCC AGG ATT	124	57	(8)
	R: CCG CTT TCA ATG AAA CTG CA			
<i>repA</i>	F: TTC ATC AGC TCC AGC TTC TT	126	60	This Study
	R: CAG ATT CAT GAT CGA TTC GTT T			
<i>sul1</i>	F: CCG TTG GCC TTC CTG TAA AG	67	60	(151)
	R: TTG CCG ATC GCG TGA AGT			

<i>tet</i> (A)	F: GCT ACA TCC TGC TTG CCT TC R: CAT AGA TCG CCG TGA AGA GG	210	60	(202)
<i>tet</i> (W)	F: GAG AGC CTG CTA TAT GCC AGC R: GGG CGT ATC CAC AAT GTT AAC	168	60	(95)
<i>tet</i> (X)	F: AGC CTT ACC AAT GGG TGT AAA R: TTC TTA CCT TGG ACA TCC CG	278	60	(24)

Table D.2. The number of standards (n), slope, intercept, amplification efficiency determined from a dilution series of standards, r^2 , and quantification limit (QL, copies μL^{-1} template) for each real-time PCR assay conducted to generate the data presented in this work.

Assay Name	n	Slope	Intercept	Amp. Eff.	r^2	QL
qPCR Soil Microcosms 13-16 16S 061313	7	-3.06	35.86	112%	0.994	23,000
qPCR Soil Microcosms 17-20 16S 061413	5	-3.10	37.28	110%	0.998	23,000
TRB 16S rRNA Gene qPCR 21-24 and C 040111	7	-3.09	36.14	111%	0.999	16,000
qPCR Soil Microcosms A1-A3 16S rRNA gene 010313	5	-3.32	38.67	100%	0.997	69,000
qPCR Soil Microcosms B1-C2-3.122911 16S 012913	5	-3.52	41.28	92%	0.999	690,000
qPCR Soil Microcosms 13-15 AllBac 071112	8	-2.95	37.47	118%	0.995	630
qPCR Soil Microcosms 16-18 AllBac 071812	8	-3.51	42.52	93%	0.976	630

qPCR Soil Microcosms 19-21 AllBac 062812	8	-3.16	40.25	107%	0.995	630
qPCR Soil Microcosms 22-24 AllBac 080112	8	-2.99	38.36	116%	0.999	630
qPCR Soil Microcosms A1-A3 AllBac 122712	9	-3.09	38.62	111%	0.998	63
qPCR Soil Microcosms B1-C2.122911 AllBac 121212	9	-3.16	39.53	107%	0.997	63
qPCR Soil Microcosms 13-15 HF183 071112	8	-3.18	38.83	106%	0.998	730
qPCR Soil Microcosms 16-18 HF183 071812	8	-3.22	39.32	104%	0.994	730
qPCR Soil Microcosms 19-21 HF183 062812	8	-3.35	40.82	99%	0.995	730
qPCR Soil Microcosms 22-24 HF183 080112	7	-3.50	40.82	93%	0.993	730
qPCR Soil Microcosms B1-C2-3.122911 HF183 121812	8	-3.21	38.90	105%	0.999	730
qPCR Soil Microcosms 13-15 ermB 071012	9	-3.59	43.47	90%	0.992	220

qPCR Soil Microcosms 16-18 ermB 071212	10	-3.58	42.90	90%	0.996	22
qPCR Soil Microcosms 19-21 ermB 062512	8	-3.50	42.24	93%	0.994	220
qPCR Soil Microcosms 22-24 ermB 073112	9	-3.50	41.87	93%	0.993	22
qPCR Soil Microcosms A1-A3 ermB 122712	9	-3.88	45.30	81%	0.998	220
qPCR Soil Microcosms B1-C2.122912 ermB 121112	9	-3.62	43.95	89%	0.996	220
qPCR Soil Microcosms B1-C2.122911 IncAC 121212	9	-3.56	41.86	91%	0.994	63
qPCR Soil Microcosms K1-Startups incAC 012513	8	-3.80	46.01	83%	0.992	630
TRB IntI1 qPCR 13-16 051611	9	-3.03	32.36	114%	0.992	10
TRB IntI1 qPCR 17-20 041311	8	-3.13	34.62	109%	0.994	980
TRB IntI1 qPCR 21-24 and C 041811	9	-3.40	38.09	97%	0.998	98

qPCR Soil Microcosms A1-A3 intI1 122012	9	-3.17	37.54	107%	0.998	190
qPCR Soil Microcosms B1-C2.122912 intI1 121012	9	-3.49	39.78	93%	0.991	190
qPCR Soil Microcosms B1-C2.122911 qnrA 121112	8	-3.25	36.88	103%	0.993	150
qPCR Soil Microcosms K1-Startups qnrA 012513	10	-3.06	35.85	112%	0.995	1.5
qPCR Soil Microcosms 13-15 sul1 071012	9	-2.98	36.92	117%	0.994	25
qPCR Soil Microcosms 16-18 sul1 071812	8	-3.05	38.21	113%	0.993	250
qPCR Soil Microcosms 19-21 sul1 062512	7	-3.17	39.14	107%	0.993	25
qPCR Soil Microcosms 22-24 sul1 080112	7	-3.22	40.09	104%	0.995	2,500
qPCR Soil Microcosms A1-A3 sul1 122712	10	-3.07	38.33	112%	0.996	25
qPCR Soil Microcosms B1-C2.122912 sul1 121112	8	-3.19	39.01	106%	0.998	250

qPCR Soil Microcosms 13-15 tetA 071012	9	-3.15	36.45	108%	0.994	17
qPCR Soil Microcosms 16-18 tetA 071212	8	-3.13	36.85	109%	0.992	170
qPCR Soil Microcosms 19-21 tetA 062212	9	-3.14	37.26	108%	0.994	17
qPCR Soil Microcosms 22-24 tetA 073112	9	-3.20	37.55	105%	0.997	17
qPCR Soil Microcosms A1-A3 tetA 122612	10	-3.12	37.78	109%	0.999	17
qPCR Soil Microcosms B1-C2.122912 tetA 121012	9	-3.28	39.17	102%	0.998	170
TRB tetW qPCR 13-16 042711	9	-3.16	36.83	107%	0.996	110
TRB tetW qPCR 17-20 042911	8	-3.21	36.36	105%	0.995	11
TRB tetW qPCR 21-24 and C 050611	8	-2.90	34.48	121%	0.996	1,100
qPCR Soil Microcosms A1-A3 tetW 122612	9	-3.14	37.82	108%	0.998	170

qPCR Soil Microcosms B1-C2-3.122911 tetW 010313	9	-3.22	38.30	104%	0.993	170
TRB tetx qPCR 13-16 040211	10	-3.38	37.55	98%	0.993	13
TRB tetx qPCR 17-20 040411	10	-3.49	39.73	93%	0.993	13
TRB tetx qPCR 21-24 and C 040511	9	-3.68	40.52	87%	0.996	130
qPCR Soil Microcosms A1-A3 tetX 122112	10	-3.44	40.09	95%	0.997	20
qPCR Soil Microcosms B1-C2.122912 tetX 121012	9	-3.57	41.06	91%	0.996	200

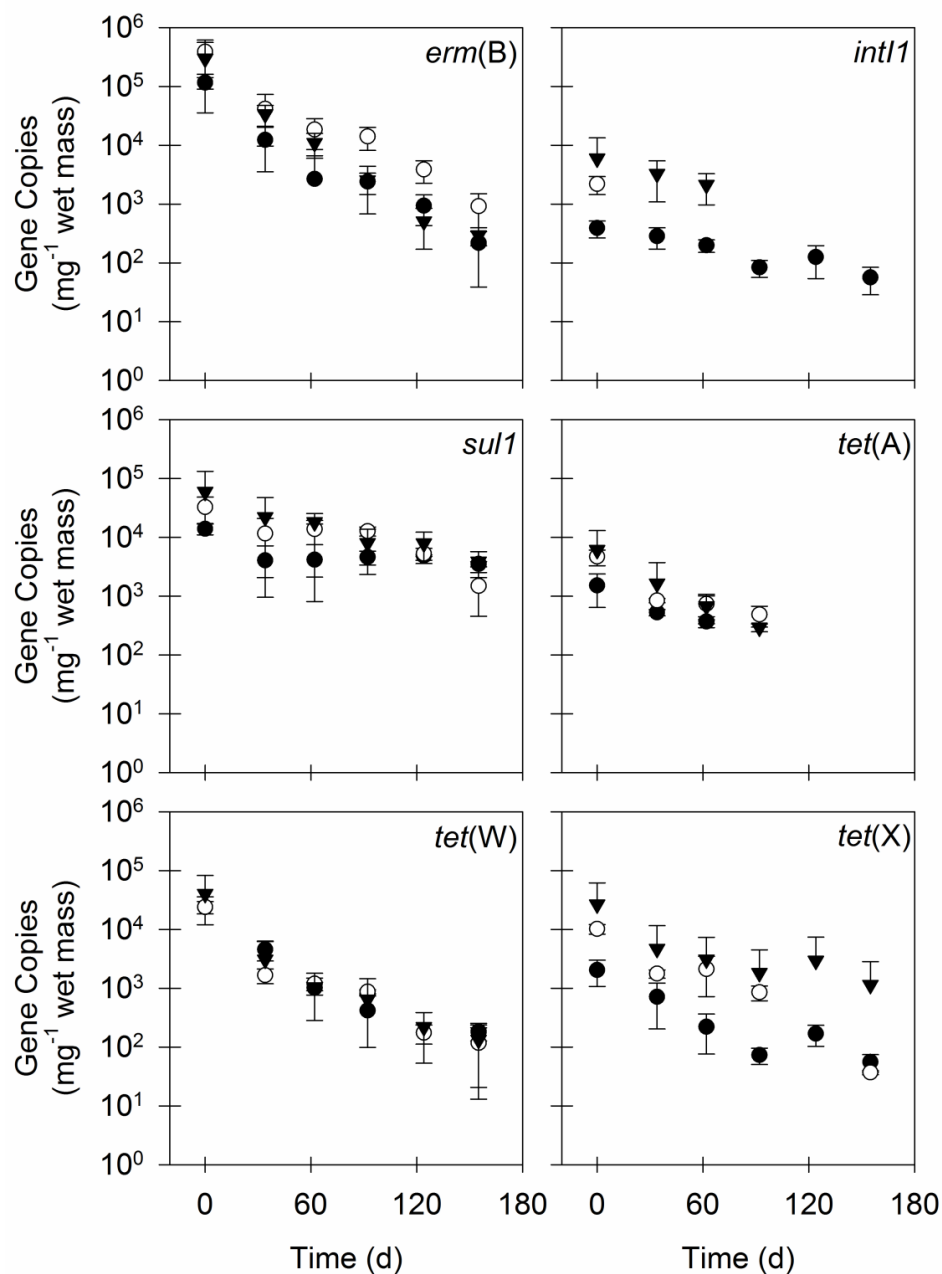


Figure D.1. The quantities of ARGs and *int11* in three replicate soil microcosms (closed circles, open circles, and closed triangles represent unique experimental units) at a loading rate of 20 g residual solids kg⁻¹ soil for Experiment 1. Values are the arithmetic mean of duplicate or triplicate samples; error bars represent one standard deviation.

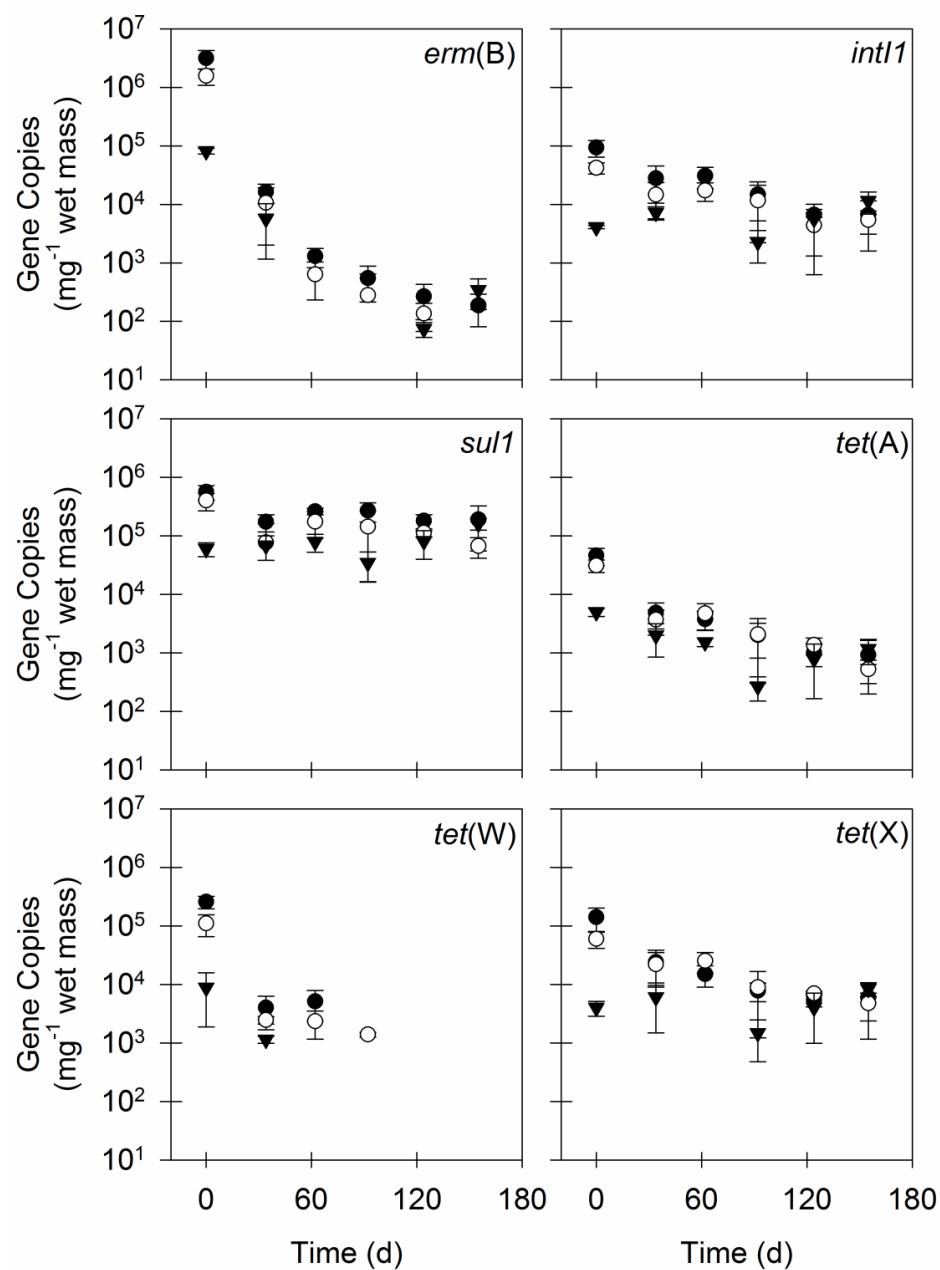


Figure D.2. The quantities of ARGs and *int11* in three replicate soil microcosms (closed circles, open circles, and closed triangles represent unique experimental units) at a loading rate of 100 g residual solids kg⁻¹ soil for Experiment 1. Values are the arithmetic mean of duplicate or triplicate samples; error bars represent one standard deviation.

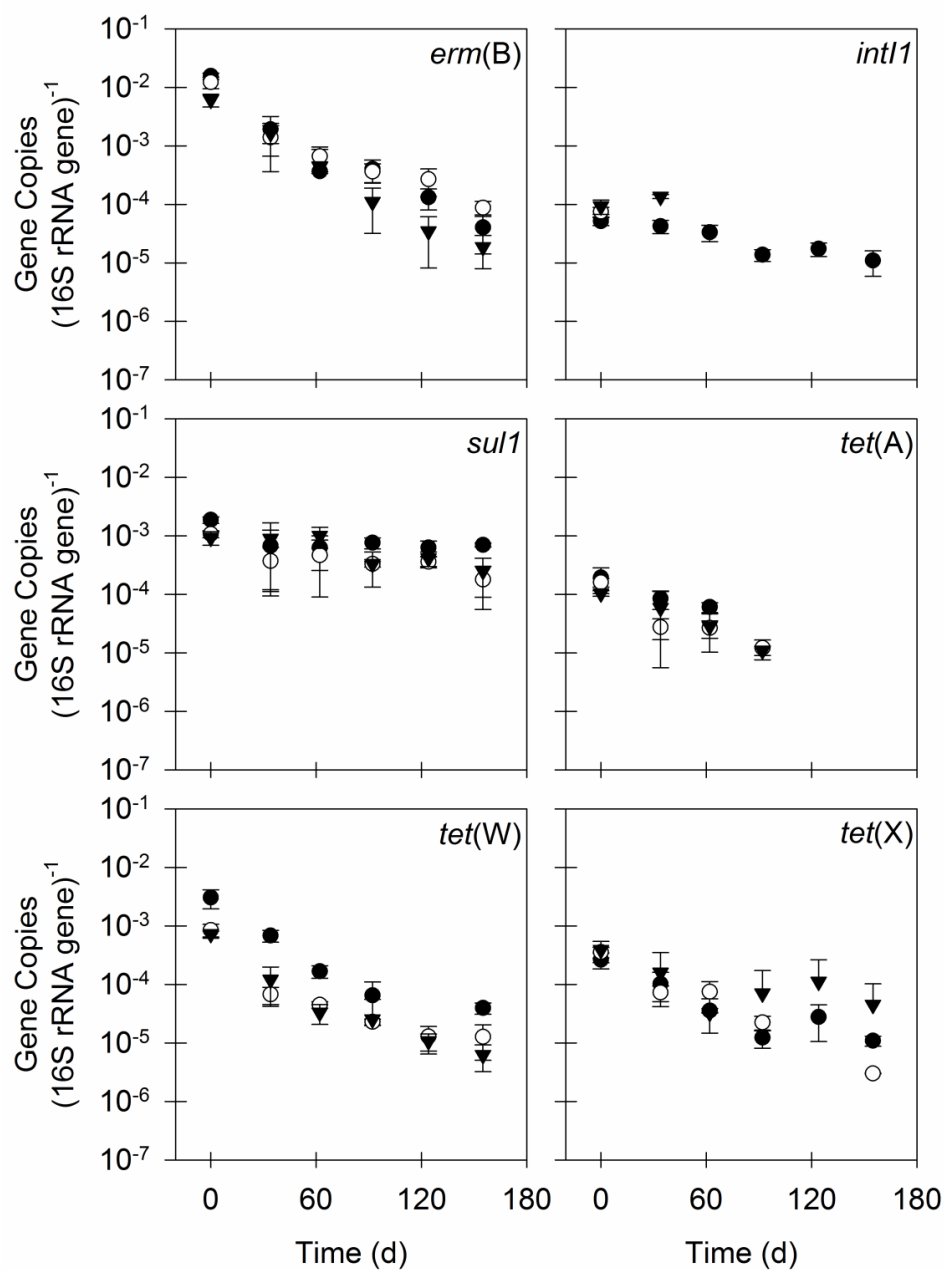


Figure D.3. The ratios of ARGs and *intI1* to 16S rRNA genes in three replicate soil microcosms (closed circles, open circles, and closed triangles represent unique experimental units) at a loading rate of 20 g residual solids kg⁻¹ soil for Experiment 1. Values are the arithmetic mean of duplicate or triplicate samples; error bars represent one standard deviation.

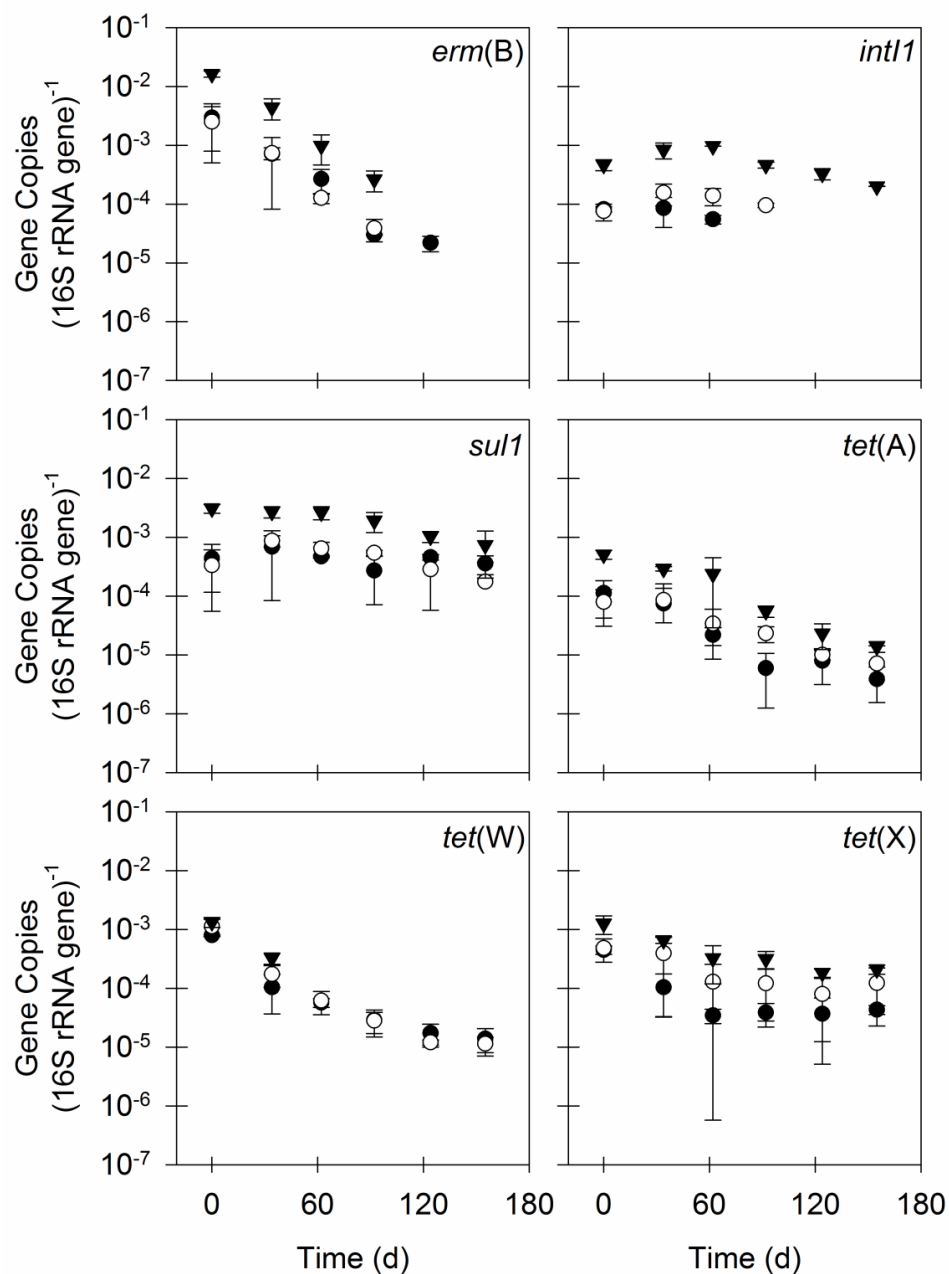


Figure D.4. The ratios of ARGs and *intI1* to 16S rRNA genes in three replicate soil microcosms (closed circles, open circles, and closed triangles represent unique experimental units) at a loading rate of 40 g residual solids kg⁻¹ soil for Experiment 1. Values are the arithmetic mean of duplicate or triplicate samples; error bars represent one standard deviation.

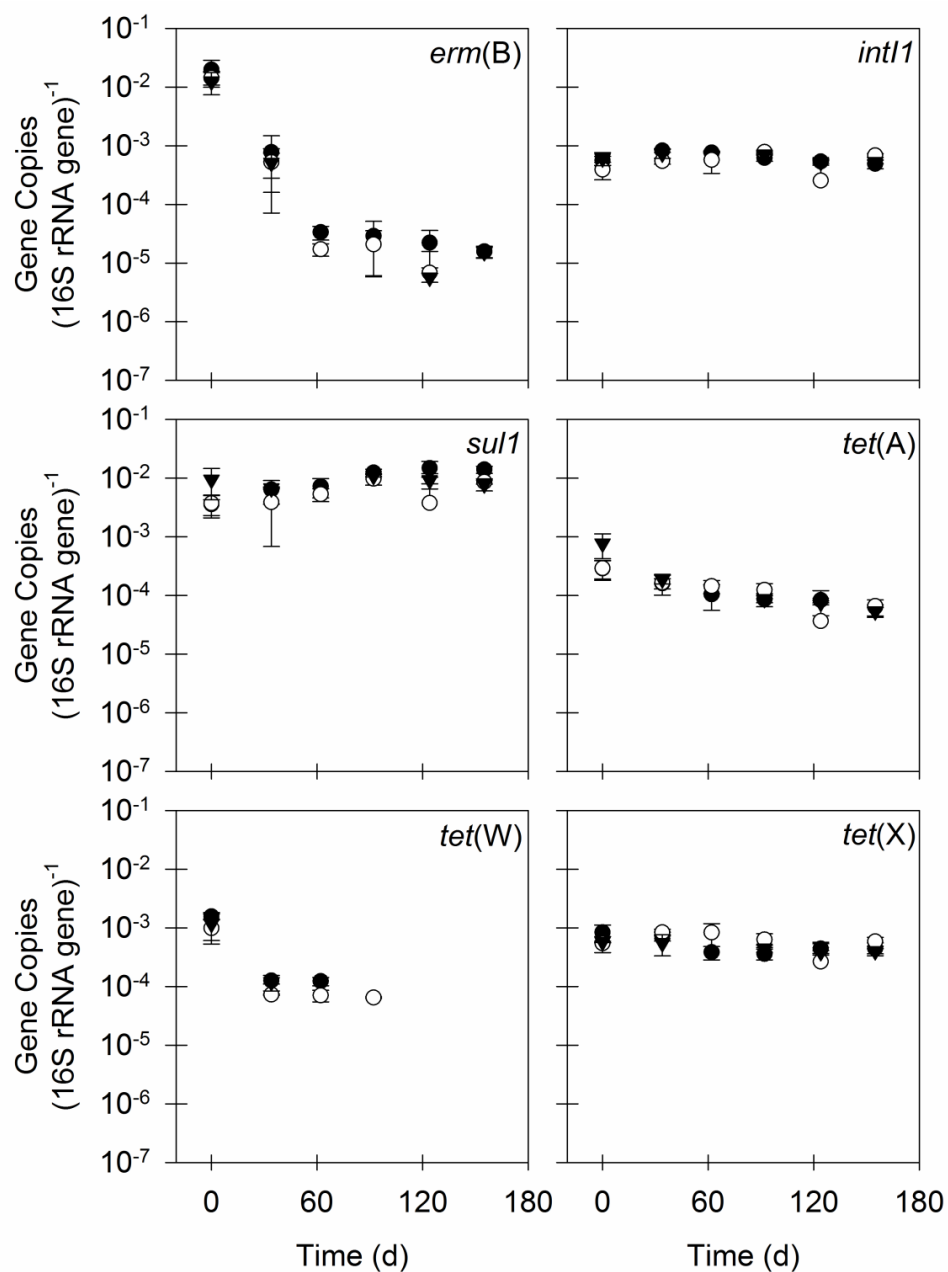


Figure D.5. The ratios of ARGs and *intI1* to 16S rRNA genes in three replicate soil microcosms (closed circles, open circles, and closed triangles represent unique experimental units) at a loading rate of 100 g residual solids kg⁻¹ soil for Experiment 1. Values are the arithmetic mean of duplicate or triplicate samples; error bars represent one standard deviation.

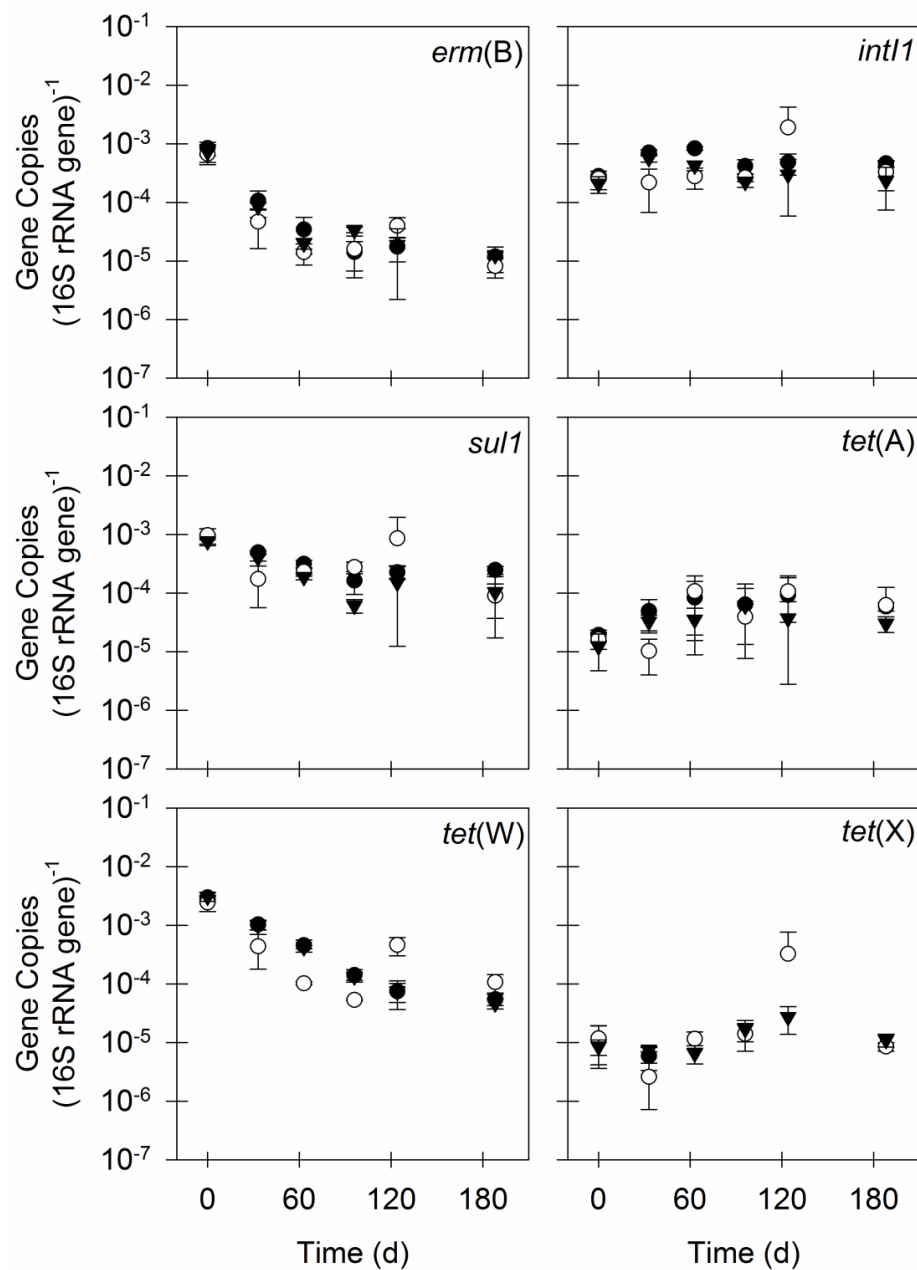


Figure D.6. The ratios of ARGs and *intI1* to 16S rRNA genes in three replicate soil microcosms (closed circles, open circles, and closed triangles represent unique experimental units) at a loading rate of 40 g residual solids kg⁻¹ soil for Experiment 2. Values are the arithmetic mean of duplicate or triplicate samples; error bars represent one standard deviation.

Appendix E: Supporting Information for Chapter 7

Table E.1. The temperatures, hydraulic residence times (HRT), total solids (TS) destruction, volatile solids (VS) destruction, gas methane content, and dissolved oxygen (DO) concentrations in an aerobic digester and anaerobic digesters operated at four temperatures during the 70 days prior to sampling for residual solids. Values are arithmetic means; error terms represent one standard deviation.

Digester	Temperature (°C)	HRT (days)	TS Destruction	VS Destruction	Gas Methane Content	DO (mg L ⁻¹)
Aerobic	14.8 ± 1.0	12.4 ± 0.8	35%	45%	NA ^a	5.6 ± 1.7
Anaerobic, 38°C	38.1 ± 2.4	16.2 ± 1.3	25%	39%	36.8% ± 8.9%	NA ^a
Anaerobic, 55°C	54.7 ± 2.1	15.3 ± 1.6	28%	41%	24.1% ± 10.9%	NA ^a
Anaerobic, 62°C	61.5 ± 1.7	16.3 ± 1.1	27%	43%	20.0% ± 10.2%	NA ^a

Anaerobic, 69°C	69.0 ± 1.8	16.1 ± 1.2	23%	36%	7.6% ± 2.0%	NA ^a
-----------------	------------	------------	-----	-----	-------------	-----------------

^aSome operating variables are not applicable (NA) depending on digester operating conditions.

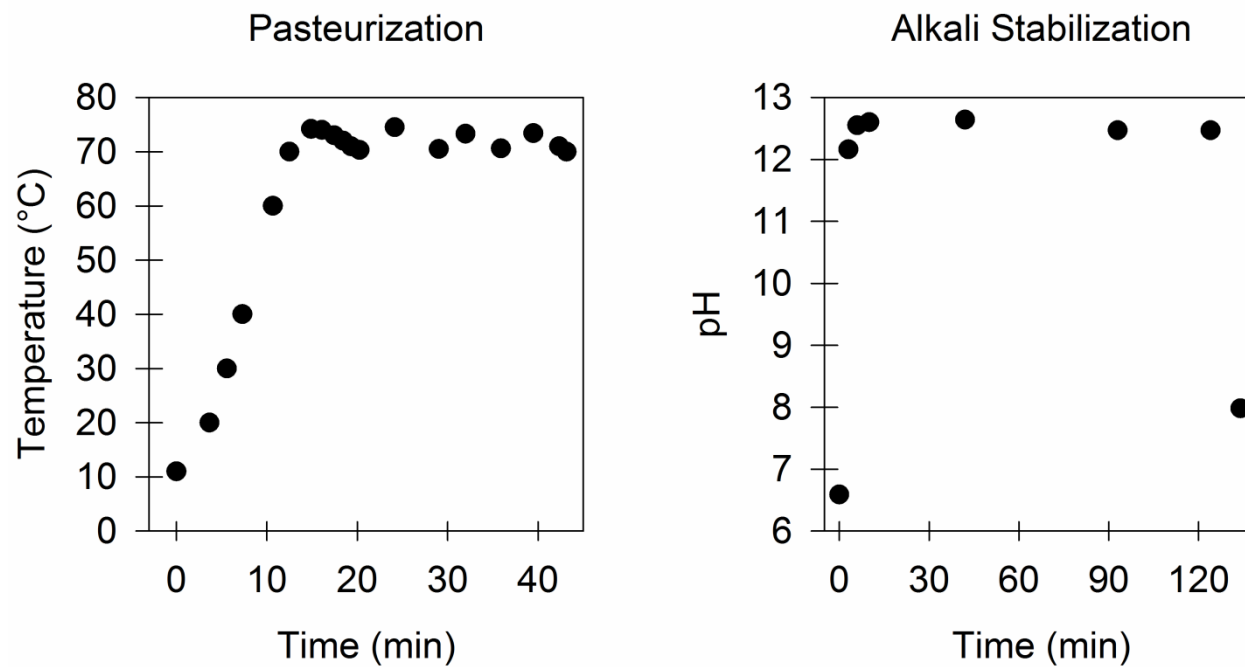


Figure E.1. The temperature of untreated residual solids undergoing pasteurization and the pH of untreated residual solids undergoing alkali stabilization prior to application to soil microcosms.

Table E.2. The number of standards (n), slope, intercept, amplification efficiency determined from a dilution series of standards, r^2 , and quantification limit (QL, copies μL^{-1} template) for each real-time PCR assay conducted to generate the data presented in this work. Assays for “Soil Microcosms A1-A3” are also listed in Table D.2.

Assay Name	n	Slope	Intercept	Amp. Eff.	r^2	QL
qPCR Soil Microcosms A1-A3 16S rRNA gene 010313	5	-3.32	38.67	100%	0.997	69,000
qPCR Soil Microcosms A1-A3 AllBac 122712	9	-3.09	38.62	111%	0.998	63
qPCR Soil Microcosms A1-A3 ermB 122712	9	-3.88	45.30	81%	0.998	220
qPCR Soil Microcosms A1-A3 intI1 122012	9	-3.17	37.54	107%	0.998	190
qPCR Soil Microcosms A1-A3 sul1 122712	10	-3.07	38.33	112%	0.996	25
qPCR Soil Microcosms A1-A3 tetA 122612	10	-3.12	37.78	109%	0.999	17
qPCR Soil Microcosms A1-A3 tetW 122612	9	-3.14	37.82	108%	0.998	170

qPCR Soil Microcosms A1-A3 tetX 122112	10	-3.44	40.09	95%	0.997	20
qPCR Soil Microcosms C2.013112-D3 16S 032713	6	-3.07	36.01	112%	0.997	23,000
qPCR Soil Microcosms C2.013112-D3 AllBac 032713	8	-3.02	38.47	114%	0.991	520
qPCR Soil Microcosms C2.013112-D3 ermB 032713	8	-3.54	43.40	92%	0.998	220
qPCR Soil Microcosms C2.013112-D3 intI1 032513	9	-3.59	40.59	90%	0.993	23
qPCR Soil Microcosms C2.013112-D3 sul1 032713	9	-3.15	39.35	108%	0.998	25
qPCR Soil Microcosms C2.013112-D3 tetA 032513	9	-3.65	39.32	88%	0.980	150
qPCR Soil Microcosms C2.013112-D3 tetW 040213	9	-3.13	38.11	109%	0.998	170
qPCR Soil Microcosms C2.013112-D3 tetX 031813	9	-3.70	42.46	86%	0.997	110
qPCR Soil Microcosms E1-F2.122911 16S 041113	5	-3.23	37.83	104%	0.996	230,000

qPCR Soil Microcosms E1-F2.122911 AllBac 041613	11	-2.93	36.99	119%	0.994	5.2
qPCR Soil Microcosms E1-F2.122911 ermB 043013	8	-3.87	43.84	81%	0.998	220
qPCR Soil Microcosms E1-F2.122911 intI1 041613	10	-3.66	41.51	88%	0.998	230
qPCR Soil Microcosms E1-F2.122911 sul1 041113	10	-3.42	40.83	96%	0.992	25
qPCR Soil Microcosms E1-F2.122911 tetA 040913	9	-3.64	40.95	88%	0.990	150
qPCR Soil Microcosms E1-F2.122911 tetW 040913	11	-3.03	37.48	114%	0.994	17
qPCR Soil Microcosms E1-F2.122911 tetX 041613	10	-3.51	40.83	93%	0.985	11
qPCR Soil Microcosms F2.013112-G3 16S 041713	5	-3.21	37.66	105%	0.999	230,000
qPCR Soil Microcosms F2.013112-G3 AllBac 041713	10	-2.80	36.39	127%	0.997	5.2
qPCR Soil Microcosms F2.013112-G3 ermB 042913	8	-3.95	45.06	79%	0.995	220

qPCR Soil Microcosms F2.013112-G3 intI1 050113	8	-3.50	39.12	93%	0.995	230
qPCR Soil Microcosms F2.013112-G3 sul1 042913	9	-3.00	37.75	115%	0.997	25
qPCR Soil Microcosms F2.013112-G3 tetA 042413	7	-4.10	42.51	75%	0.980	1,500
qPCR Soil Microcosms F2.013112-G3 tetW 042413	10	-3.13	37.74	109%	0.996	17
qPCR Soil Microcosms F2.013112-G3 tetX 050113	8	-3.46	39.45	94%	0.994	200
qPCR Soil Microcosms H1-I2.013112 16S 031213	6	-3.01	35.39	115%	0.998	23,000
qPCR Soil Microcosms H1-I2.013112 AllBac 040213	8	-2.95	37.93	118%	0.991	520
qPCR Soil Microcosms H1-I2.013112 ermB 031113	8	-3.87	45.12	81%	0.999	2,200
qPCR Soil Microcosms H1-I2.013112 intI1 031113	9	-3.67	42.05	87%	0.997	230
qPCR Soil Microcosms H1-I2.013112 sul1 031213	9	-3.62	43.78	89%	0.989	250

qPCR Soil Microcosms H1-I2.013112 tetA 031113	8	-3.44	39.32	95%	0.993	150
qPCR Soil Microcosms H1-I2.013112 tetW 030713	9	-3.00	36.89	116%	0.998	170
qPCR Soil Microcosms H1-I2.013112 tetX 030713	9	-3.87	43.44	81%	0.990	110
qPCR Soil Microcosms I2.022812-J3 16S 030613	6	-3.01	34.83	115%	0.991	23,000
qPCR Soil Microcosms I2.022812-J3 AllBac 030613	9	-3.04	38.84	113%	0.998	63
qPCR Soil Microcosms I2.022812-J3 ermB 021913	8	-4.07	46.49	76%	1.000	220
qPCR Soil Microcosms I2.022812-J3 intI1 022213	8	-3.31	39.08	101%	0.998	230
qPCR Soil Microcosms I2.022812-J3 sul1 021913	10	-3.02	38.12	115%	0.998	25
qPCR Soil Microcosms I2.022812-J3 tetA 022013	8	-3.38	39.64	98%	0.999	150
qPCR Soil Microcosms I2.022812-J3 tetW 021213	9	-3.23	38.97	104%	0.996	170

qPCR Soil Microcosms I2.022812-J3 tetX 021213	9	-3.71	42.71	86%	0.999	110
qPCR Soil Microcosms K1-Startups 16S gene 020413	5	-3.77	43.34	84%	0.998	690,000
qPCR Soil Microcosms K1-Startups AllBac 012813	8	-3.12	40.04	109%	0.997	630
qPCR Soil Microcosms K1-Startups HF183 012813	8	-3.21	38.96	105%	0.995	730
qPCR Soil Microcosms K1-Startups ermB 012313	8	-4.07	47.21	76%	0.996	220
qPCR Soil Microcosms K1-Startups intI1 012313	9	-3.61	41.48	89%	0.994	230
qPCR Soil Microcosms K1-Startups qnrA 012513	10	-3.06	35.85	112%	0.995	1.5
qPCR Soil Microcosms K1-Startups sul1 012813	10	-3.11	39.26	110%	0.999	25.0
qPCR Soil Microcosms K1-Startups tetA 012313	9	-3.34	39.82	99%	0.999	170
qPCR Soil Microcosms K1-Startups tetW 012213	8	-3.45	40.40	95%	0.996	170

qPCR Soil Microcosms K1-Startups tetX 012213	10	-3.41	40.19	96%	0.997	20
--	----	-------	-------	-----	-------	----

Table E.3. The quantities of 16S rRNA genes, *intII*, and *sulI* in soil used to initiate microcosms that received aerobically digested, air-dried, anaerobically digested, or untreated residual solids (10/27/11) vs. alkali stabilized or pasteurized residual solids (12/1/11). Values are the arithmetic mean of at least five of nine positive samples (for 10/27/11) or two of three positive samples (for 12/1/11); error terms represent one standard deviation. All other gene targets were below quantification limits in at least six of nine samples (for 10/27/11) or in all three samples (for 12/1/11).

Gene Target	Gene Copies (mg ⁻¹ dry mass)						<i>P</i> ^a
	10/27/11			12/1/11			
16S rRNA gene	4.2×10 ⁷	±	2×10 ⁷	1.0×10 ⁸	±	1×10 ⁷	1×10 ⁻³
<i>intII</i>	1.0×10 ³	±	4×10 ²	5.0×10 ³	±	4×10 ²	9×10 ⁻⁵
<i>sulI</i>	4.8×10 ²	±	3×10 ²	1.2×10 ³	±	2×10 ²	2×10 ⁻³

^aWelch's t-test (two-sample, unequal variance)

Table E.4. First-order kinetic coefficients (k), P , r^2 , and half-lives ($t_{1/2}$) from first-order kinetic models of gene target quantities in residual municipal wastewater solids undergoing pasteurization or alkali stabilization. Error terms for k represent one standard error; all values of k were regressed from eight data points.

Gene Target	Treatment	k (min ⁻¹)	P	r^2	$t_{1/2}$ (min)
16S rRNA gene	Pasteurization	$-4.5 \times 10^{-3} \pm 3 \times 10^{-3}$	0.21	0.25	160
<i>intII</i>	Pasteurization	$-3.4 \times 10^{-3} \pm 3 \times 10^{-3}$	0.35	0.15	200
<i>tet(X)</i>	Pasteurization	$-1.0 \times 10^{-2} \pm 3 \times 10^{-3}$	0.02	0.60	68
<i>intII</i> /16S rRNA gene	Pasteurization	$1.3 \times 10^{-3} \pm 2 \times 10^{-3}$	0.48	0.09	-540
<i>tet(X)</i> /16S rRNA gene	Pasteurization	$-5.7 \times 10^{-3} \pm 2 \times 10^{-3}$	0.01	0.68	120
16S rRNA gene	Alkali Stabilization	$-3.6 \times 10^{-3} \pm 1 \times 10^{-3}$	0.02	0.61	190

<i>intI1</i>	Alkali Stabilization	$-2.7 \times 10^{-3} \pm 1 \times 10^{-3}$	0.12	0.36	260
<i>tet(X)</i>	Alkali Stabilization	$-2.8 \times 10^{-3} \pm 1 \times 10^{-3}$	0.03	0.58	250
<i>intI1</i> /16S rRNA gene	Alkali Stabilization	$9.1 \times 10^{-4} \pm 5 \times 10^{-4}$	0.14	0.32	-760
<i>tet(X)</i> /16S rRNA gene	Alkali Stabilization	$8.6 \times 10^{-4} \pm 4 \times 10^{-4}$	0.10	0.38	-810

Table E.5. Evaporation rates and cumulative evaporation in all sets of soil microcosms. Error terms for evaporation rates represent one standard error. Error terms for fraction of initial microcosm mass lost to evaporation and final moisture content represent one standard deviation.

Residual Solids	Evaporation Rate^a (mm H₂O day⁻¹)	Fraction of Initial Microcosm Mass Lost to Evaporation	Final Moisture Content
Aerobically Digested	1×10 ⁻³ ± 1×10 ⁻⁴	4.1% ± 1.0%	10.0% ± 1.6%
Air-dried	2×10 ⁻³ ± 2×10 ⁻⁴	6.9% ± 1.7%	4.5% ± 1.5%
Alkali Stabilized	2×10 ⁻³ ± 2×10 ⁻⁴	6.2% ± 1.0%	7.6% ± 0.8%
Anaerobically Digested, 38°C	2×10 ⁻³ ± 2×10 ⁻⁴	8.1% ± 1.6%	5.2% ± 1.1%
Anaerobically Digested, 55°C	2×10 ⁻³ ± 1×10 ⁻⁴	7.0% ± 0.6%	7.0% ± 0.5%

Anaerobically Digested, 62°C	2×10^{-3}	±	2×10^{-4}	7.4%	±	2.3%	6.2%	±	2.2%
Anaerobically Digested, 69°C	2×10^{-3}	±	3×10^{-4}	7.3%	±	2.4%	5.7%	±	1.6%
Pasteurized	2×10^{-3}	±	3×10^{-4}	5.9%	±	2.0%	7.8%	±	2.2%
Untreated	2×10^{-3}	±	8×10^{-5}	6.0%	±	0.7%	8.5%	±	0.5%

“Evaporation rates were determined using linear regression (R 2.15.0). The predictor was time, and the cumulative mass of water lost from each group of replicate soil microcosms (i.e. three values at each time point) was used as the response variable. All evaporation rates are statistically significant ($P < 0.05$).

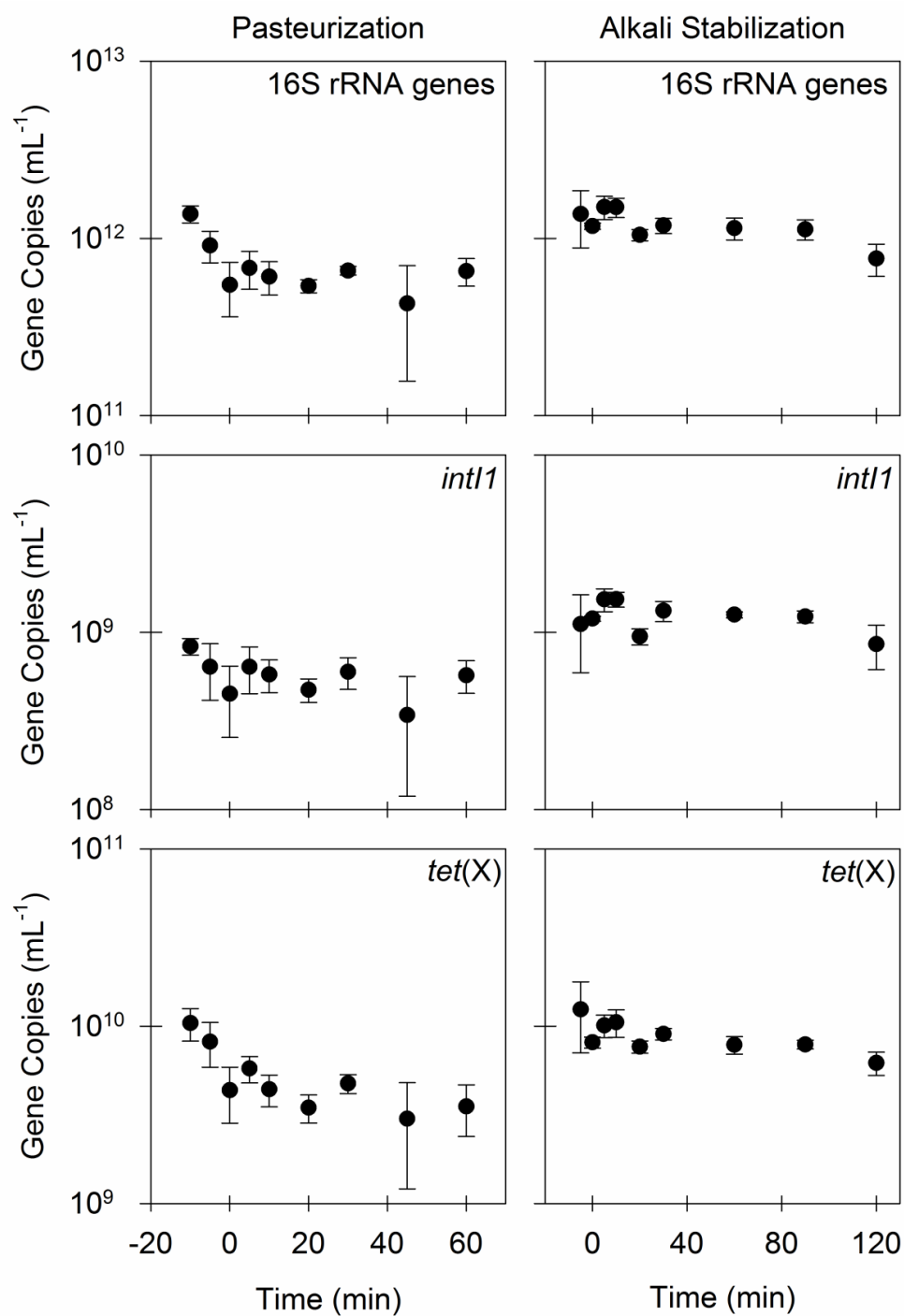


Figure E.2. The quantities of 16S rRNA genes, *int11*, and *tet(X)* in residual solids undergoing pasteurization or alkali stabilization. Values are the arithmetic mean of triplicate samples; error bars represent one standard deviation.

Table E.6. First-order kinetic coefficients (k), number of data points (n), r^2 , P , lack-of-fit P (LOF P), and half-lives ($t_{1/2}$) from first-order kinetic models applied to full time series of gene target quantities in triplicate soil microcosms that received different residual municipal wastewater solids. Error terms for k represent the standard error of the mean.

Residual Solids	Target	k (day ⁻¹)	n	r^2	P	LOF P	$t_{1/2}$ (days)
Aerobically Digested	16S rRNA genes	-6.0×10 ⁻³ ± 8×10 ⁻⁴	18	0.77	2×10 ⁻⁶	4×10 ⁻⁴	120
Aerobically Digested	AllBac	-2.6×10 ⁻² ± 4×10 ⁻³	18	0.72	9×10 ⁻⁶	2×10 ⁻⁸	26
Aerobically Digested	<i>erm</i> (B)	-1.7×10 ⁻² ± 2×10 ⁻³	18	0.78	1×10 ⁻⁶	0.01	40
Aerobically Digested	<i>intI1</i>	-1.2×10 ⁻² ± 2×10 ⁻³	18	0.77	2×10 ⁻⁶	1×10 ⁻³	57
Aerobically Digested	<i>sulI</i>	-1.0×10 ⁻² ± 1×10 ⁻³	18	0.78	1×10 ⁻⁶	0.02	68
Aerobically Digested	<i>tet</i> (A)	-9.1×10 ⁻³ ± 1×10 ⁻³	18	0.71	1×10 ⁻⁵	3×10 ⁻³	76
Aerobically Digested	<i>tet</i> (W)	-2.1×10 ⁻² ± 3×10 ⁻³	18	0.82	3×10 ⁻⁷	8×10 ⁻⁶	32

Aerobically Digested	<i>tet(X)</i>	-2.1×10^{-2}	\pm	2×10^{-3}	18	0.91	1×10^{-9}	5×10^{-4}	34
Air-dried	16S rRNA genes	2.7×10^{-4}	\pm	1×10^{-3}	18	0.00	0.78	0.18	-2,500
Air-dried	AllBac					ND ^a			
Air-dried	<i>erm(B)</i>					ND ^a			
Air-dried	<i>intI1</i>	-7.2×10^{-3}	\pm	3×10^{-3}	18	0.29	0.02	0.95	96
Air-dried	<i>sulI</i>	-7.1×10^{-3}	\pm	3×10^{-3}	18	0.23	0.04	0.87	97
Air-dried	<i>tet(A)</i>	-4.6×10^{-3}	\pm	4×10^{-3}	11	0.11	0.33	0.90	150
Air-dried	<i>tet(W)</i>					ND ^a			
Air-dried	<i>tet(X)</i>	-6.5×10^{-3}	\pm	4×10^{-3}	18	0.15	0.11	0.85	110
Alkali Stabilized	16S rRNA genes	-1.2×10^{-3}	\pm	7×10^{-4}	18	0.17	0.09	0.02	560

Alkali Stabilized	AllBac	-3.8×10^{-2}	\pm	1×10^{-2}	18	0.45	2×10^{-3}	1×10^{-11}	18
Alkali Stabilized	<i>erm(B)</i>	-3.4×10^{-2}	\pm	8×10^{-3}	18	0.53	6×10^{-4}	2×10^{-11}	21
Alkali Stabilized	<i>intI1</i>	-1.2×10^{-2}	\pm	3×10^{-3}	18	0.53	6×10^{-4}	1×10^{-5}	57
Alkali Stabilized	<i>sulI</i>	-1.8×10^{-2}	\pm	5×10^{-3}	18	0.49	1×10^{-3}	5×10^{-8}	38
Alkali Stabilized	<i>tet(A)</i>	-1.3×10^{-2}	\pm	4×10^{-3}	13	0.44	0.01	5×10^{-4}	53
Alkali Stabilized	<i>tet(W)</i>	-2.6×10^{-2}	\pm	8×10^{-3}	14	0.49	0.01	2×10^{-7}	27
Alkali Stabilized	<i>tet(X)</i>	-1.1×10^{-1}	\pm	1×10^{-2}	4	0.97	0.02	ND ^b	6.3
Anaerobically Digested, 38°C	16S rRNA genes	-3.4×10^{-3}	\pm	3×10^{-3}	18	0.06	0.31	0.89	200
Anaerobically Digested, 38°C	AllBac	-2.3×10^{-2}	\pm	3×10^{-3}	18	0.77	2×10^{-6}	4×10^{-4}	30
Anaerobically Digested, 38°C	<i>erm(B)</i>	-2.1×10^{-2}	\pm	9×10^{-3}	13	0.35	0.03	0.01	32

Anaerobically Digested, 38°C	<i>intI1</i>	-5.6×10^{-3}	$\pm 2 \times 10^{-3}$	18	0.35	0.01	7×10^{-4}	120
Anaerobically Digested, 38°C	<i>sulI</i>	-1.0×10^{-2}	$\pm 2 \times 10^{-3}$	18	0.69	2×10^{-5}	0.06	67
Anaerobically Digested, 38°C	<i>tet(A)</i>	-4.7×10^{-3}	$\pm 4 \times 10^{-3}$	18	0.07	0.28	2×10^{-3}	150
Anaerobically Digested, 38°C	<i>tet(W)</i>	-1.8×10^{-2}	$\pm 5 \times 10^{-3}$	16	0.45	4×10^{-3}	1×10^{-6}	39
Anaerobically Digested, 38°C	<i>tet(X)</i>				ND ^a			
Anaerobically Digested, 55°C	16S rRNA genes	-7.9×10^{-4}	$\pm 8 \times 10^{-4}$	18	0.05	0.36	0.47	880
Anaerobically Digested, 55°C	AllBac	-2.4×10^{-2}	$\pm 6 \times 10^{-3}$	18	0.50	1×10^{-3}	8×10^{-8}	29
Anaerobically Digested, 55°C	<i>erm(B)</i>				ND ^a			
Anaerobically Digested, 55°C	<i>intI1</i>	-7.3×10^{-3}	$\pm 1 \times 10^{-3}$	18	0.66	4×10^{-5}	5×10^{-3}	94
Anaerobically Digested, 55°C	<i>sulI</i>	-1.3×10^{-2}	$\pm 3 \times 10^{-3}$	18	0.55	4×10^{-4}	5×10^{-6}	52

Anaerobically Digested, 55°C	<i>tet(A)</i>	-5.4×10^{-2}	\pm	5×10^{-3}	5	0.97	2×10^{-3}	ND ^b	13
Anaerobically Digested, 55°C	<i>tet(W)</i>	-1.6×10^{-2}	\pm	6×10^{-3}	12	0.45	0.02	2×10^{-5}	43
Anaerobically Digested, 55°C	<i>tet(X)</i>					ND ^a			
Anaerobically Digested, 62°C	16S rRNA genes	1.2×10^{-3}	\pm	6×10^{-4}	18	0.19	0.07	2×10^{-3}	-560
Anaerobically Digested, 62°C	AllBac	-2.0×10^{-2}	\pm	5×10^{-3}	16	0.48	3×10^{-3}	1×10^{-6}	35
Anaerobically Digested, 62°C	<i>erm(B)</i>	-1.8×10^{-2}	\pm	8×10^{-3}	7	0.50	0.08	0.01	38
Anaerobically Digested, 62°C	<i>intI1</i>	-5.0×10^{-3}	\pm	1×10^{-3}	18	0.51	9×10^{-4}	0.01	140
Anaerobically Digested, 62°C	<i>sulI</i>	-7.9×10^{-3}	\pm	3×10^{-3}	18	0.37	0.01	1×10^{-5}	88
Anaerobically Digested, 62°C	<i>tet(A)</i>	-1.5×10^{-2}	\pm	4×10^{-3}	5	0.81	0.04	0.15	47
Anaerobically Digested, 62°C	<i>tet(W)</i>	-1.2×10^{-2}	\pm	4×10^{-3}	18	0.32	0.01	5×10^{-6}	58

Anaerobically Digested, 62°C	<i>tet(X)</i>	5.1×10^{-3}	±	8×10^{-3}	5	0.13	0.55	0.52	-140
Anaerobically Digested, 69°C	16S rRNA genes	1.3×10^{-3}	±	9×10^{-4}	18	0.10	0.20	0.03	-550
Anaerobically Digested, 69°C	AllBac	-2.0×10^{-2}	±	6×10^{-3}	17	0.45	3×10^{-3}	8×10^{-6}	35
Anaerobically Digested, 69°C	<i>erm(B)</i>	-2.6×10^{-2}	±	1×10^{-2}	8	0.44	0.07	2×10^{-3}	26
Anaerobically Digested, 69°C	<i>intI1</i>	-8.6×10^{-3}	±	4×10^{-3}	17	0.26	0.04	0.91	81
Anaerobically Digested, 69°C	<i>sulI</i>	-1.2×10^{-2}	±	4×10^{-3}	18	0.35	0.01	0.43	60
Anaerobically Digested, 69°C	<i>tet(A)</i>					ND ^a			
Anaerobically Digested, 69°C	<i>tet(W)</i>	-1.4×10^{-2}	±	4×10^{-3}	18	0.45	2×10^{-3}	2×10^{-4}	50
Anaerobically Digested, 69°C	<i>tet(X)</i>					ND ^a			
Pasteurized	16S rRNA gene	-4.4×10^{-3}	±	2×10^{-3}	18	0.34	0.01	0.79	160

Pasteurized	AllBac	-4.4×10^{-2}	\pm	1×10^{-2}	11	0.60	0.01	4×10^{-5}	16
Pasteurized	<i>erm(B)</i>	-3.5×10^{-2}	\pm	8×10^{-3}	11	0.66	2×10^{-3}	2×10^{-5}	20
Pasteurized	<i>intI1</i>	-1.9×10^{-2}	\pm	5×10^{-3}	18	0.42	3×10^{-3}	4×10^{-4}	37
Pasteurized	<i>sulI</i>	-2.4×10^{-2}	\pm	8×10^{-3}	18	0.38	0.01	0.03	28
Pasteurized	<i>tet(A)</i>	-1.7×10^{-2}	\pm	6×10^{-3}	15	0.42	0.01	3×10^{-6}	40
Pasteurized	<i>tet(W)</i>	-3.2×10^{-2}	\pm	8×10^{-3}	10	0.65	0.01	1×10^{-4}	22
Pasteurized	<i>tet(X)</i>	-2.0×10^{-2}	\pm	2×10^{-3}	4	0.97	0.01	ND ^b	35
Untreated	16S rRNA gene	-3.0×10^{-3}	\pm	8×10^{-4}	18	0.46	2×10^{-3}	0.22	230
Untreated	AllBac	-3.6×10^{-2}	\pm	5×10^{-3}	18	0.78	1×10^{-6}	8×10^{-5}	19
Untreated	<i>erm(B)</i>	-3.7×10^{-2}	\pm	8×10^{-3}	16	0.63	2×10^{-4}	1×10^{-6}	19

Untreated	<i>intI1</i>	-1.2×10^{-2}	$\pm 2 \times 10^{-3}$	18	0.80	5×10^{-7}	0.31	57
Untreated	<i>sulI</i>	-1.7×10^{-2}	$\pm 2 \times 10^{-3}$	18	0.81	4×10^{-7}	0.32	41
Untreated	<i>tet(A)</i>	-1.4×10^{-2}	$\pm 2 \times 10^{-3}$	18	0.79	7×10^{-7}	0.13	51
Untreated	<i>tet(W)</i>	-2.9×10^{-2}	$\pm 4 \times 10^{-3}$	18	0.75	4×10^{-6}	1×10^{-6}	24
Untreated	<i>tet(X)</i>	-2.0×10^{-2}	$\pm 4 \times 10^{-3}$	17	0.61	2×10^{-4}	0.01	35

^aQuantities of some gene targets were above quantification limits for only $n \leq 2$ time points, so k was not determined (ND).

^bQuantities of some gene targets did not provide sufficient experimental replication to conduct the lack-of-fit test, so LOF P was not determined (ND).

Table E.7. First-order kinetic coefficients (k), number of data points (n), r^2 , P , lack-of-fit P (LOF P), and half-lives ($t_{1/2}$) from first-order kinetic models applied to time series of gene target quantities with time zero values removed in triplicate soil microcosms that received different residual municipal wastewater solids. Error terms for k represent the standard error of the mean.

Residual Solids	Target	k (day ⁻¹)	n	r^2	P	LOF P	$t_{1/2}$ (days)
Aerobically Digested	16S rRNA gene	$-3.9 \times 10^{-3} \pm 5 \times 10^{-4}$	15	0.81	6×10^{-6}	0.01	180
Aerobically Digested	AllBac	$-1.5 \times 10^{-2} \pm 3 \times 10^{-3}$	15	0.70	1×10^{-4}	4×10^{-5}	45
Aerobically Digested	<i>erm</i> (B)	$-1.4 \times 10^{-2} \pm 3 \times 10^{-3}$	15	0.66	2×10^{-4}	0.04	50
Aerobically Digested	<i>intI1</i>	$-8.0 \times 10^{-3} \pm 1 \times 10^{-3}$	15	0.77	2×10^{-5}	0.12	87
Aerobically Digested	<i>sul1</i>	$-7.5 \times 10^{-3} \pm 1 \times 10^{-3}$	15	0.72	7×10^{-5}	0.17	93
Aerobically Digested	<i>tet</i> (A)	$-5.6 \times 10^{-3} \pm 1 \times 10^{-3}$	15	0.64	4×10^{-4}	0.26	120

Aerobically Digested	<i>tet</i> (W)	-1.5×10^{-2}	$\pm 2 \times 10^{-3}$	15	0.86	7×10^{-7}	0.01	48
Aerobically Digested	<i>tet</i> (X)	-1.8×10^{-2}	$\pm 2 \times 10^{-3}$	15	0.88	3×10^{-7}	5×10^{-3}	40
Air-dried	16S rRNA gene	-1.4×10^{-3}	$\pm 1 \times 10^{-3}$	15	0.12	0.20	0.60	510
Air-dried	AllBac				ND ^a			
Air-dried	<i>erm</i> (B)				ND ^a			
Air-dried	<i>intI1</i>	-7.4×10^{-3}	$\pm 4 \times 10^{-3}$	15	0.25	0.06	0.88	93
Air-dried	<i>sulI</i>	-7.4×10^{-3}	$\pm 4 \times 10^{-3}$	15	0.19	0.11	0.77	94
Air-dried	<i>tet</i> (A)	-4.6×10^{-3}	$\pm 5 \times 10^{-3}$	9	0.12	0.37	0.67	150
Air-dried	<i>tet</i> (W)				ND ^a			
Air-dried	<i>tet</i> (X)	-9.7×10^{-3}	$\pm 4 \times 10^{-3}$	15	0.27	0.04	0.95	71

Alkali Stabilized	16S rRNA gene	-2.5×10 ⁻³	± 7×10 ⁻⁴	15	0.46	0.01	0.16	280
Alkali Stabilized	AllBac	-6.8×10 ⁻³	± 1×10 ⁻³	15	0.63	4×10 ⁻⁴	1.00	100
Alkali Stabilized	<i>erm</i> (B)	-1.1×10 ⁻²	± 2×10 ⁻³	15	0.71	8×10 ⁻⁵	0.02	64
Alkali Stabilized	<i>intI1</i>	-4.3×10 ⁻³	± 1×10 ⁻³	15	0.40	0.01	0.50	160
Alkali Stabilized	<i>sulI</i>	-4.9×10 ⁻³	± 2×10 ⁻³	15	0.40	0.01	0.13	140
Alkali Stabilized	<i>tet</i> (A)	-2.2×10 ⁻³	± 2×10 ⁻³	10	0.11	0.36	0.41	310
Alkali Stabilized	<i>tet</i> (W)	-4.0×10 ⁻³	± 2×10 ⁻³	11	0.31	0.08	0.08	170
Alkali Stabilized	<i>tet</i> (X)	ND ^a						
Anaerobically Digested, 38°C	16S rRNA gene	-5.2×10 ⁻³	± 4×10 ⁻³	15	0.10	0.24	0.88	130
Anaerobically Digested, 38°C	AllBac	-1.5×10 ⁻²	± 2×10 ⁻³	15	0.74	3×10 ⁻⁵	0.23	46

Anaerobically Digested, 38°C	<i>erm(B)</i>	9.3×10^{-5}	$\pm 5 \times 10^{-3}$	10	0.00	0.99	0.78	-7,500
Anaerobically Digested, 38°C	<i>intI1</i>	-9.3×10^{-3}	$\pm 2 \times 10^{-3}$	15	0.62	5×10^{-4}	0.01	75
Anaerobically Digested, 38°C	<i>sulI</i>	-1.0×10^{-2}	$\pm 2 \times 10^{-3}$	15	0.58	1×10^{-3}	0.05	68
Anaerobically Digested, 38°C	<i>tet(A)</i>	-1.5×10^{-2}	$\pm 3 \times 10^{-3}$	15	0.64	3×10^{-4}	0.54	45
Anaerobically Digested, 38°C	<i>tet(W)</i>	-2.9×10^{-3}	$\pm 2 \times 10^{-3}$	13	0.19	0.14	0.57	240
Anaerobically Digested, 38°C	<i>tet(X)</i>				ND ^a			
Anaerobically Digested, 55°C	16S rRNA gene	-1.9×10^{-3}	$\pm 9 \times 10^{-4}$	15	0.23	0.07	0.78	370
Anaerobically Digested, 55°C	AllBac	-6.0×10^{-3}	$\pm 2 \times 10^{-3}$	15	0.47	5×10^{-3}	0.89	120
Anaerobically Digested, 55°C	<i>erm(B)</i>				ND ^a			
Anaerobically Digested, 55°C	<i>intI1</i>	-4.0×10^{-3}	$\pm 9 \times 10^{-4}$	15	0.59	9×10^{-4}	0.96	170

Anaerobically Digested, 55°C	<i>sulI</i>	-4.6×10^{-3}	$\pm 1 \times 10^{-3}$	15	0.51	3×10^{-3}	0.89	150
Anaerobically Digested, 55°C	<i>tet(A)</i>				ND ^a			
Anaerobically Digested, 55°C	<i>tet(W)</i>	-5.9×10^{-4}	$\pm 2 \times 10^{-3}$	9	0.01	0.81	0.06	1,200
Anaerobically Digested, 55°C	<i>tet(X)</i>				ND ^a			
Anaerobically Digested, 62°C	16S rRNA gene	-3.6×10^{-4}	$\pm 5 \times 10^{-4}$	15	0.04	0.47	0.30	1,900
Anaerobically Digested, 62°C	AllBac	-4.1×10^{-3}	$\pm 2 \times 10^{-3}$	13	0.30	0.05	0.19	170
Anaerobically Digested, 62°C	<i>erm(B)</i>	5.9×10^{-4}	$\pm 4 \times 10^{-3}$	4	0.01	0.90	ND ^b	-1,200
Anaerobically Digested, 62°C	<i>intI1</i>	-2.1×10^{-3}	$\pm 9 \times 10^{-4}$	15	0.28	0.04	0.67	330
Anaerobically Digested, 62°C	<i>sulI</i>	-6.1×10^{-4}	$\pm 1 \times 10^{-3}$	15	0.03	0.55	0.53	1,100
Anaerobically Digested, 62°C	<i>tet(A)</i>				ND ^a			

Anaerobically Digested, 62°C	<i>tet(W)</i>	5.8×10^{-4}	±	2×10^{-3}	15	0.01	0.73	0.71	-1,200
Anaerobically Digested, 62°C	<i>tet(X)</i>					ND ^a			
Anaerobically Digested, 69°C	16S rRNA gene	-5.7×10^{-4}	±	1×10^{-3}	15	0.02	0.58	0.32	1,200
Anaerobically Digested, 69°C	AllBac	-3.8×10^{-3}	±	3×10^{-3}	14	0.12	0.22	0.14	180
Anaerobically Digested, 69°C	<i>erm(B)</i>	2.0×10^{-3}	±	5×10^{-3}	5	0.04	0.73	0.14	-350
Anaerobically Digested, 69°C	<i>intII</i>	-7.4×10^{-3}	±	5×10^{-3}	14	0.17	0.14	0.83	93
Anaerobically Digested, 69°C	<i>sulI</i>	-6.5×10^{-3}	±	4×10^{-3}	15	0.14	0.17	0.73	110
Anaerobically Digested, 69°C	<i>tet(A)</i>					ND ^a			
Anaerobically Digested, 69°C	<i>tet(W)</i>	-3.2×10^{-3}	±	2×10^{-3}	15	0.18	0.12	0.75	210
Anaerobically Digested, 69°C	<i>tet(X)</i>					ND ^a			

Pasteurized	16S rRNA gene	-3.1×10^{-3}	$\pm 2 \times 10^{-3}$	15	0.19	0.11	0.90	220
Pasteurized	AllBac	-3.9×10^{-3}	$\pm 2 \times 10^{-3}$	8	0.33	0.14	0.64	180
Pasteurized	<i>erm(B)</i>	-1.6×10^{-2}	$\pm 2 \times 10^{-3}$	9	0.91	7×10^{-5}	0.15	44
Pasteurized	<i>intI1</i>	-4.4×10^{-3}	$\pm 3 \times 10^{-3}$	15	0.12	0.20	0.99	160
Pasteurized	<i>sulI</i>	-7.4×10^{-3}	$\pm 7 \times 10^{-3}$	15	0.08	0.30	0.90	93
Pasteurized	<i>tet(A)</i>	-1.8×10^{-3}	$\pm 2 \times 10^{-3}$	12	0.08	0.36	0.43	380
Pasteurized	<i>tet(W)</i>	-4.6×10^{-3}	$\pm 3 \times 10^{-3}$	7	0.30	0.21	0.20	150
Pasteurized	<i>tet(X)</i>	ND ^a						
Untreated	16S rRNA gene	-2.5×10^{-3}	$\pm 1 \times 10^{-3}$	15	0.28	0.04	0.21	280
Untreated	AllBac	-2.4×10^{-2}	$\pm 4 \times 10^{-3}$	15	0.77	2×10^{-5}	0.05	29

Untreated	<i>erm(B)</i>	-1.3×10^{-2}	$\pm 3 \times 10^{-3}$	13	0.64	1×10^{-3}	0.18	52
Untreated	<i>intI1</i>	-9.8×10^{-3}	$\pm 2 \times 10^{-3}$	15	0.70	9×10^{-5}	0.86	71
Untreated	<i>sulI</i>	-1.5×10^{-2}	$\pm 3 \times 10^{-3}$	15	0.71	7×10^{-5}	0.39	46
Untreated	<i>tet(A)</i>	-1.1×10^{-2}	$\pm 2 \times 10^{-3}$	15	0.68	1×10^{-4}	0.23	61
Untreated	<i>tet(W)</i>	-1.7×10^{-2}	$\pm 2 \times 10^{-3}$	15	0.83	3×10^{-6}	0.07	42
Untreated	<i>tet(X)</i>	-1.2×10^{-2}	$\pm 4 \times 10^{-3}$	14	0.37	0.02	0.17	60

^aQuantities of some gene targets were above quantification limits for only $n \leq 2$ time points, so k was not determined (ND).

^bQuantities of some gene targets did not provide sufficient experimental replication to conduct the lack-of-fit test, so LOF P was not determined (ND).

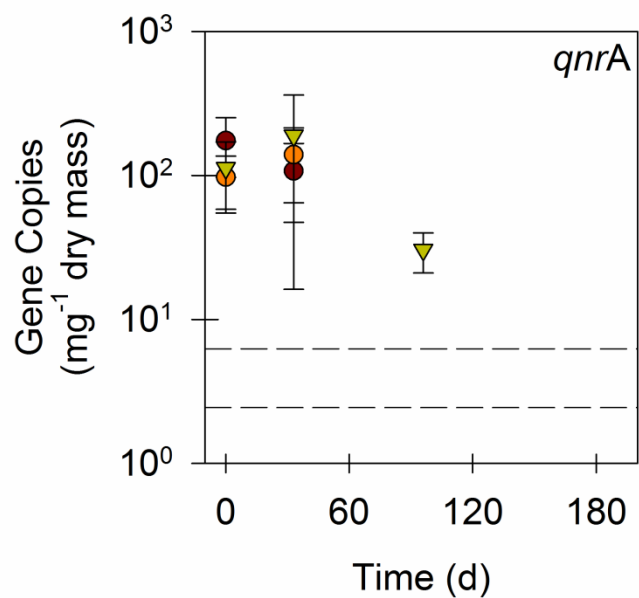


Figure E.3. Quantities of *qnrA* in soil microcosms that received untreated residual solids. Values are the arithmetic mean of duplicate or triplicate samples; error bars represent one standard deviation. Dashed lines represent the maximum and minimum limits of quantification for data sets that contain one or more experimental observations below those limits.